ZooKeys 718: 1–33 (2017)
doi: 10.3897/zookeys.718.13700
http://zookeys.pensoft.net

RESEARCH ARTICLE

A peer-reviewed open-access journal
ZooKeys
Launched to accelerate biodiversity research

New *Mesopsyllus* species from the Bohai Sea, China, re-evaluation of the validity of *Vibriopsyllus* Kornev & Chertoprud, 2008 and proposal of *Sympodella* gen. n. (Copepoda, Harpacticoida, Canthocamptidae)

Fang-hong Mu[1], Rony Huys[2]

1 *College of Marine Life Sciences, Ocean University of China, 5 Yushan Road, Qingdao 266003, China*
2 *Department of Life Sciences, The Natural History Museum, Cromwell Road, London SW7 5BD, United Kingdom*

Corresponding author: *Rony Huys* (r.huys@nhm.ac.uk)

Academic editor: *K.H. George* | Received 16 May 2017 | Accepted 7 November 2017 | Published 4 December 2017

http://zoobank.org/924EC9A3-EA54-4703-9D91-CAF58736DE15

Citation: Mu F-h, Huys R (2017) New *Mesopsyllus* species from the Bohai Sea, China, re-evaluation of the validity of *Vibriopsyllus* Kornev & Chertoprud, 2008 and proposal of *Sympodella* gen. n. (Copepoda, Harpacticoida, Canthocamptidae). ZooKeys 718: 1–33. https://doi.org/10.3897/zookeys.718.13700

Abstract

Two new species of the genus *Mesopsyllus* Por, 1960 (Canthocamptidae) are described from the Bohai Sea, eastern China. *Mesopsyllus dimorphus* **sp. n.** and *M. spiniferus* **sp. n.** differ from their congeners by the presence of two instead of three outer spines on P2–P3 exp-3. They can be differentiated from each other by (1) number of inner setae on P3–P4 enp-2; (2) anterior margin of antennulary segment 7 of male; (3) ornamentation of male abdomen; (4) sexual dimorphism on P2 endopod and P3–P4 exp-3; and (5) differences in length of setae on male P5. Some observations in the original description of *M. atargatis* Por, 1960 are reinterpreted and the type material of *M. secundus* (Wells, 1965) is re-examined. Comparison between the type species of *Vibriopsyllus* Kornev & Chertoprud, 2008 and the four known species of *Mesopsyllus* shows the former as a junior subjective synonym of the latter. Consequently, *Vibriopsyllus curviseta* Kornev & Chertoprud, 2008 is formally transferred to *Mesopsyllus* as *M. curvisetus* (Kornev & Chertoprud, 2008), **comb. n.** A key to species and an updated generic diagnosis of *Mesopsyllus* are presented.

The taxonomic status of the genus *Carolinicola* Huys & Thistle, 1989 is re-evaluated. The characters of its type species, *C. trisetosa* (Coull, 1973), indicate that the latter (and – by inference – the genus *Carolinicola*) should remain in the Danielsseniinae. *Carolinicola galapagoensis* Mielke, 1997 is fixed as the type species of a new genus *Sympodella* **gen. n.** and placed in the Hemimesochrinae (Canthocamptidae) as the putative sistertaxon of *Pusillargillus* Huys & Thistle, 1989. The relationships and potential synonymy of the genera *Pyrocletodes* Coull, 1973, *Perucamptus* Huys & Thistle, 1989 and *Isthmiocaris* George & Schminke, 2003 are briefly discussed.

Keywords
Carolinicola, Hemimesochrinae, *Isthmiocaris*, *Mesopsyllus dimorphus* sp. n., *M. spiniferus* sp. n., *Perucamptus*, *Pyrocletodes*, *Sympodella* gen. n.

Introduction

Sars (1920) proposed the monotypic genus *Hemimesochra* Sars, 1920 in the family Canthocamptidae for *H. clavularis* Sars, 1920. The species is extremely rare, being known from only five females collected from deepwater (91–101 m) muddy sediments off Risør, southern Norway (Sars 1920) and Loch Nevis, western Scotland (Wells 1965). Baguley (2004) recorded five specimens from the northern Gulf of Mexico deep sea which he assigned to *Hemimesochra* aff. *clavularis*. Monard (1927) continued to list *Hemimesochra* as a member of the Canthocamptidae in his *Synopsis universalis generum harpacticoidarum* while Lang (1936) transferred it to the family Cletodidae which he subdivided in a number of lineages ("Reihen"). *Hemimesochra* was initially placed in the *Heteropsyllus*-Reihe, together with *Heteropsyllus* T. Scott, 1894 and *Pontopolites* T. Scott, 1894. However, the Reihe concept was subsequently abandoned by Lang (1944, 1948).

Por (1960) established the genus *Mesopsyllus* Por, 1960 in the family Cletodidae for the type and only species, *M. atargatis* Por, 1960, from the Black Sea basin. In a later paper, Por (1964a) considered *Mesopsyllus* a junior subjective synonym of *Hemimesochra* in which was included a third, newly described, species, *H. derketo* Por, 1964a, from the Israeli Levantine coast. Lang (1965) rejected Por's revised diagnosis of *Hemimesochra*, claiming the three species represented three monotypic genera and *H. derketo* (which he consistently misspelled as *dekerto*) should be placed in a new genus *Poria* Lang, 1965 (= *Hanikraia* Huys, 2009). Meanwhile and unbeknown to Lang (1965), Por (1964b) had further expanded the generic concept of *Hemimesochra* by adding two new species from the Swedish west coast, *H. nixe* Por, 1964b and *H. nympha* Por, 1964b, while Wells (1965) had described *H. secunda* Wells, 1965 from Loch Nevis. Additional, but radically divergent, species were subsequently included from the deep sea off North Carolina (*H. trisetosa* Coull, 1973a) and the Peru–Chile (Atacama) Trench (*H. rapiens* Becker, 1979) (Coull 1973a, Becker 1979). Finally, *Leimia dubia* Wells, 1965, originally described from the Scottish west coast, was transferred to *Hemimesochra* by Becker (1972, 1979), raising the number of species to seven.

Por (1986) removed the genera *Hemimesochra*, *Mesopsyllus* and *Poria* from the Cletodidae and placed them in a new subfamily Hemimesochrinae in the Canthocamptidae without making a proper recommendation for this course of action. Likewise, *Hemimesochra rapiens* was transferred as *species incertae sedis* to the Canthocamptidae without any justification. Huys and Thistle (1989) reviewed the relationships within the heterogeneous genus *Hemimesochra* and redistributed the seven species over six genera, four of which proposed as new. Following this revision, *Hemimesochra* remained monotypic with *H. clavularis* as its only member. *Hemimesochra secunda* was

transferred as *M. secundus* to the genus *Mesopsyllus* while the new genera *Boreolimella* Huys & Thistle, 1989 (*H. dubia*, *H. nympha*), *Carolinicola* Huys & Thistle, 1989 (*H. trisetosa*), *Perucamptus* Huys & Thistle, 1989 (*H. rapiens*) and *Pusillargillus* Huys & Thistle, 1989 (*H. nixe*) accommodated the remaining species (Huys and Thistle 1989).

Karaytuğ and Huys (2004) recognized within the primarily freshwater Canthocamptidae a core complex of genera confined to marine and brackish water habitats which they called the *Mesochra*-group. This group, which is fundamentally different from Por's (1986) taxonomic concept of the Hemimesochrinae, comprises the genera *Mesochra* Boeck, 1865, *Parepactophanes* Kunz, 1935, *Mesopsyllus*, *Psammocamptus* Mielke, 1975, *Taurocletodes* Kunz, 1975, *Amphibiperita* Fiers & Rutledge, 1990, *Bathycamptus* Huys & Thistle, 1989, and *Isthmiocaris* George & Schminke, 2003. Members of this group share the reduced morphology of the male sixth legs (unconfirmed in *Parepactophanes*), being represented by membranous flaps completely lacking in armature elements. In the females the sixth legs closing off the genital apertures bear 1–3 setae, indicating a different ontogenetic trajectory between the sexes. The genera *Hemimesochra*, *Poria*, *Boreolimella*, *Perucamptus* and *Pusillargillus* which are known from females only, were also regarded as representatives of the *Mesochra*-group based on their close similarity in mouthpart morphology with *Bathycamptus*, *Mesopsyllus* and *Psammocamptus*. The current understanding of relationships within this group is insufficient since many species are incompletely described or known from only one sex. The discovery of two new species of *Mesopsyllus* from the Bohai Sea (one of which was cited as *Mesopsyllus* sp. 2 in Mu et al. (2001)) provides us with an opportunity to update its generic diagnosis, including new information about the male. In this paper we present descriptions of both species, provide a key to species of *Mesopsyllus*, assess the validity of a recently established genus, *Vibriopsyllus* Kornev & Chertoprud, 2008, from the White Sea, and re-evaluate the taxonomic position of *Carolinicola*.

Materials and methods

Specimens were collected during 1998–1999 from the central region and the strait of the Bohai Sea (Fig. 1) in eastern China. Sediments ranged from muddy sand to pure mud. Samples were collected with a 0.1 m^2 box corer at an average depth of 20 m (range 11–70 m). Standard subsamples were taken from the box corer by three 26 mm diameter plastic tubes inserted to a depth of 5 cm and were subsequently fixed in 10% formalin. Meiofauna was extracted by Ludox centrifugation flotation. Harpacticoids were sorted and preserved in 4% formalin. Prior to dissection the habitus was drawn from whole specimens temporarily mounted in lactophenol. Specimens were dissected in lactic acid and the parts individually mounted in lactophenol under coverslips which were subsequently sealed with transparent nail varnish.

All drawings were prepared using a camera lucida on a Zeiss Axioskop differential interference contrast microscope. The terminology for body and appendage morphology follows that of Huys and Boxshall (1991) and Huys et al. (1996). Abbreviations used

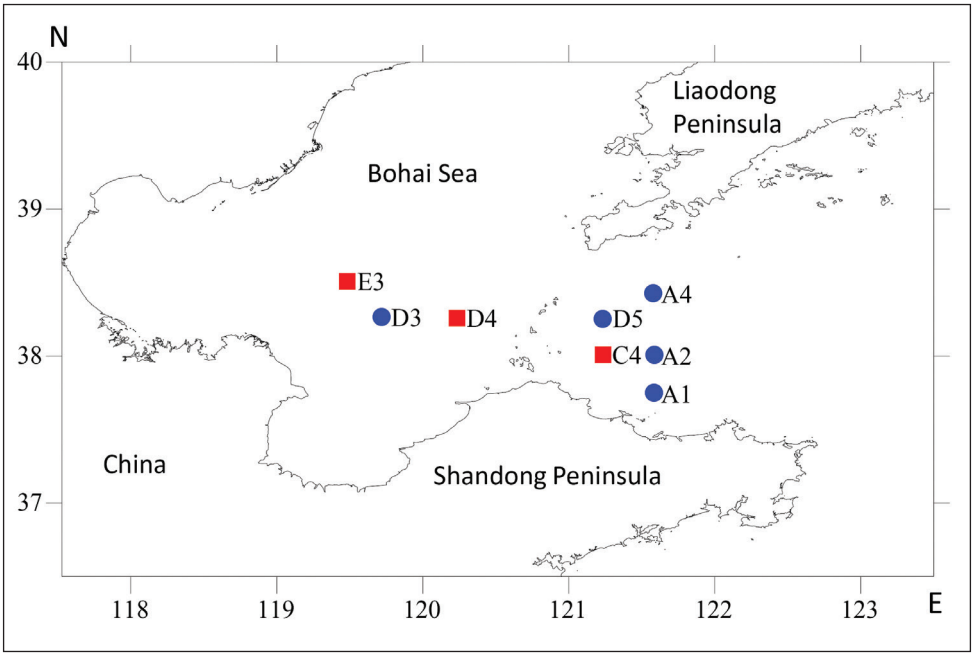

Figure 1. Location of sampling stations in the Bohai Sea, China where *Mesopsyllus spiniferus* sp. n. and *M. dimorphus* sp. n. were observed, indicated by red squares and blue circles, respectively.

in the text and Tables 2 and 4 are A1 for antennule, A2 for antenna, P1–P6 for thoracopods 1–6, exp for exopod, enp for endopod, benp for baseoendopod, exp(enp)-1(2, 3) to denote the proximal (middle, distal) segment of a ramus; apo for apohysis, and ae for aesthetasc. The setae on P5 are counted from the innermost on each ramus (as in P1–P4). Body length was measured from the anterior margin of the cephalic shield to the posterior margin of the anal somite. Scale bars in all illustrations are in μm. Type material is deposited in The Natural History Museum, London (NHMUK).

Systematics

Order Harpacticoida Sars, 1903
Family Canthocamptidae Brady, 1880
Subfamily Hemimesochrinae Por, 1986

Genus *Mesopsyllus* Por, 1960

Diagnosis. Rostrum not defined at base; triangular. Antennule 6-segmented in ♀, with aesthetasc on segments 4 and 6; 8-segmented, haplocer with geniculation between segments 6 and 7 in ♂; with enlarged modified spines on segments 2–3 and 6 in ♀, and segments 2–4 in ♂. Antenna with one abexopodal seta on allobasis; exopod

1-segmented, with 2–3 setae. Mandibular palp with short basis (with one seta), 1-segmented endopod (with four setae) and vestigial unisetose exopod. Maxillule with rami incorporated into basis. Maxilla with two endites on syncoxa; endopod discrete. Maxilliped with well developed seta on syncoxa. Swimming legs of ♀ with 3-segmented exopods and 3- (typical condition in P1) or 2-segmented endopods (P2–P4, unusual condition in P1). Setal formulae of P1–P4 as follows:

Thoracopod	Exopod	Endopod
P1	0.1.022	1.1.111 or 1.111
P2	0.1.12[2–3]	1.[1–2]21
P3	0.1.22[2–3]	1.[1–2]21 (♀) or 1.1+apo.020 (♂)
P4	0.1.[1–2]2[2–3]	1.[1–2]21

Inner seta of P1 enp-1 short, not recurved backwardly and dorsally; outer spine of P1 exp-1 not enlarged; outer exopodal spines of P1–P4 sparsely bipinnate, in P2–P4 without elongate pinnules in proximal half. P2 endopod occasionally with sexual dimorphism (inner seta of enp-1 distinctly shorter in ♀; enp-2 with additional inner seta in ♀). P3 endopod 3-segmented in ♂; enp-2 with inner seta and slender terminal apophysis; enp-3 with two apical setae. P4 enp-1 and sometimes enp-2 and exp-3 with slight sexual dimorphism (setal lengths). P4 exp-3 occasionally sexually dimorphic (length of proximal inner seta). P5 with discrete exopod and baseoendopod; exopod small, with 3–5 and 4–5 elements in ♀ and ♂, respectively; endopodal lobe with four and two elements in ♀ and ♂, respectively. Sixth pair of legs asymmetrical in ♂, unarmed. Caudal ramus short, with six setae.

Type species. *Mesopsyllus atargatis* Por, 1960 (by monotypy).

Other species. *Mesopsyllus secundus* (Wells, 1965), *M. curvisetus* (Kornev & Chertoprud, 2008), comb. n., *M. dimorphus* sp. n., *M. spiniferus* sp. n.

Mesopsyllus dimorphus sp. n.

http://zoobank.org/EF350CF9-712C-4BD0-8301-1134C452CBD6

Figures 2–7

Type locality. Eastern China, Strait of the Bohai Sea, sampling locality D5 (38°15'N, 121°15'E); 37.0 m depth; very fine sand (Fig. 1; Table 1).

Material examined. Holotype: adult ♂ dissected on 13 slides (NHMUK reg. no. 2013.1033). Paratypes are 1 ♀ dissected on 17 slides (NHMUK reg. no. 2013.1034), and 10 ♀♀ and 2 ♂♂ preserved in ethanol (NHMUK reg. nos 2013.1035–1044); all paratypes were collected from the type locality. Additional material was collected from stations A1 (37°44'N, 121°35'E), A2 (38°N, 121°35'E), A4 (38°25'N, 121°35'E) and D3 (38°15'N, 119°44'E) in the central part and the strait of the Bohai Sea, eastern China (Fig. 1; Table 1). Collected by F.-h. Mu and Y.-q. Guo in September 1998.

Description of male. Body length 220–280 μm (n = 3, mean = 250 μm). Body slightly tapering posteriorly as in ♀ (compare Fig. 7B–C). P1-bearing somite fused with cephalothorax. Pleural margins of cephalic shield furnished with long hair-like setules

Table 1. Location and environmental characteristics of sampling stations in the Bohai Sea (Md = median grain size).

Station	Latitude	Longitude	Depth (m)	Sediment type	Md
A1	37°44'N	121°35'E	20.5	coarse silt	5.42
A2	38°00'N	121°35'E	42.8	sandy silt	5.4
A4	38°25'N	121°35'E	50.8	very fine sand	3.87
C4	38°00'N	121°15'E	23.8	sandy silt	5.19
D3	38°15'N	119°44'E	22.9	coarse silt	5.73
D4	38°15'N	120°15'E	24.3	silty sand	4.96
D5	38°15'N	121°15'E	37.0	very fine sand	3.94
E3	38°30'N	119°30'E	26.0	clayey silt	7.63

(as shown for female in Fig. 7B). Body covered with pattern of minute pimples (not figured). Hyaline frills plain (as shown for female in Fig. 7B–C). Posterior margin of anal operculum straight and with fine denticles (as figured for ♀ in Fig. 2H); anus terminal.

Body ornamentation (Fig. 2A–C). All somites with integumental sensilla, except for penultimate one. Pores present on all somites (positions on urosomites indicated in Fig. 2A–C). Prosome without spinular ornamentation. Pattern of spinular rows on urosome as follows: urosomite-1 with short paired dorsal rows; urosomite-2 with pairs of short rows dorsally and dorsolaterally; urosomite-3 with a pair of short rows dorsally and a long, continuous row stretching ventrally and laterally; urosomite-4 without dorsal spinules but with a long, continuous row ventrally and laterally; urosomite-5 without dorsal spinules but with an interrupted row ventrally and laterally; anal somite with lateral and ventral spinules at base of caudal rami.

Rostrum (Fig. 2F) not defined at base; triangular with a round apex; with a pair of lateral sensilla subapically and a median pore dorsally.

Antennule (Fig. 3A–B) 8-segmented, haplocer with geniculation located between segments 6 and 7. Segment 1 with spinules along anterior and subdistal margins and one minute seta. Segment 2 with two stout spinulose spines and six smooth setae. Segment 3 with one stout spinulose spine, two long and three minute, naked setae. Segment 4 moderately swollen, with one stout pinnate spine, three short, naked setae (one of which arising from minute cylindrical process) and one small spiniform process near anterior distal corner; ventral surface of segment 4 with a sub-cylindrical setophore carrying one slender seta and one large aesthetasc. Segment 5 with two naked setae. Segment 6 with two slender setae and two conical elements (modified setae). Segment 7 with three conical elements and one anterodistal seta. Segment 8 with seven naked setae and apical acrothek consisting of two setae and short aesthetasc.

Antenna (Fig. 4A). Coxa well developed, bearing row of spinules. Allobasis without trace of original segmentation; with row of spinules and short smooth seta in proximal half of abexopodal margin. Exopod 1-segmented, about twice as long as wide; with two apical naked setae. Free endopod 1-segmented, bearing two surface rows of stout

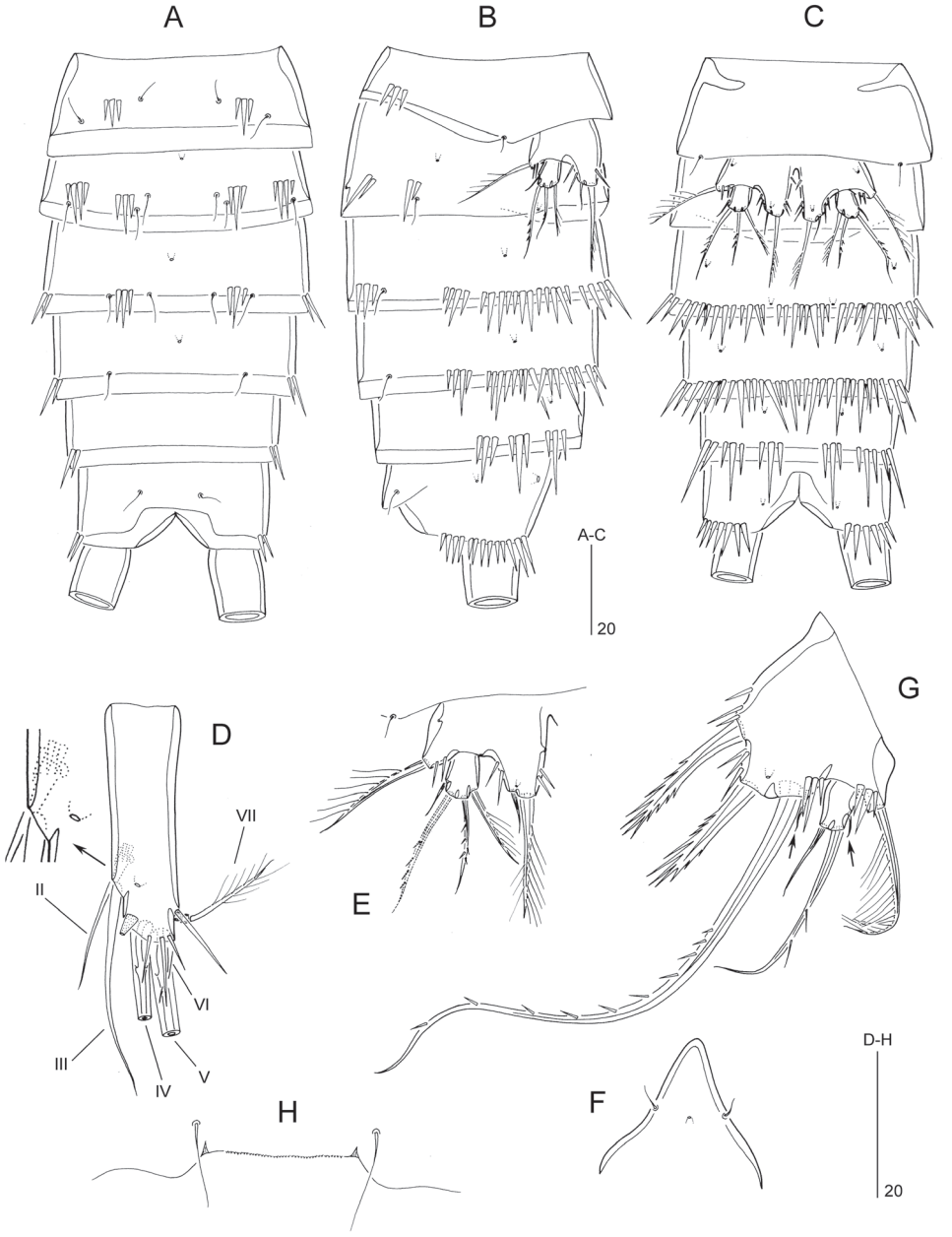

Figure 2. *Mesopsyllus dimorphus* sp. n.: **A** urosome ♂, dorsal **B** urosome ♂, lateral **C** urosome ♂, ventral **D** caudal ramus ♂, ventral (inset showing spinules around base of seta II) **E** P5 ♂, anterior **F** rostrum ♂, dorsal **G** P5 ♀, anterior (minute setae on exopod and endopodal lobe indicated by arrow) **H** anal operculum ♀. [Caudal rami in A–C not drawn at full length]. **A–F** based on holotype (NHMUK reg. no. 2013.1033), **G–H** based on paratype (NHMUK reg. no. 2013.1034).

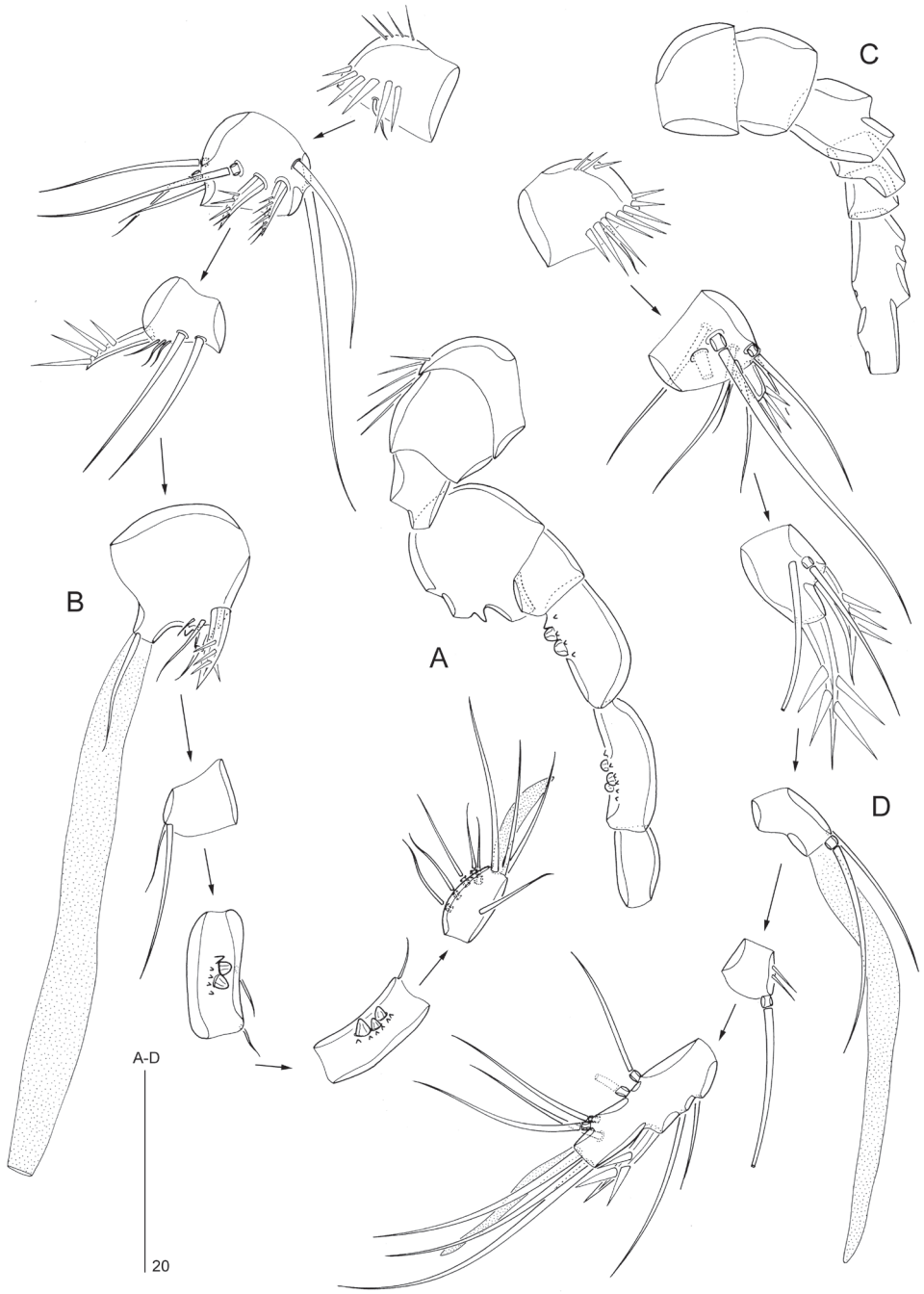

Figure 3. *Mesopsyllus dimorphus* sp. n.: **A** antennule ♂ (armature omitted), ventral **B** antennule ♂ (disarticulated), ventral **C** antennule ♀ (armature omitted), ventral **D** antennule ♀ (disarticulated), ventral **A–B** based on holotype (NHMUK reg. no. 2013.1033) **C–D** based on paratype (NHMUK reg. no. 2013.1034).

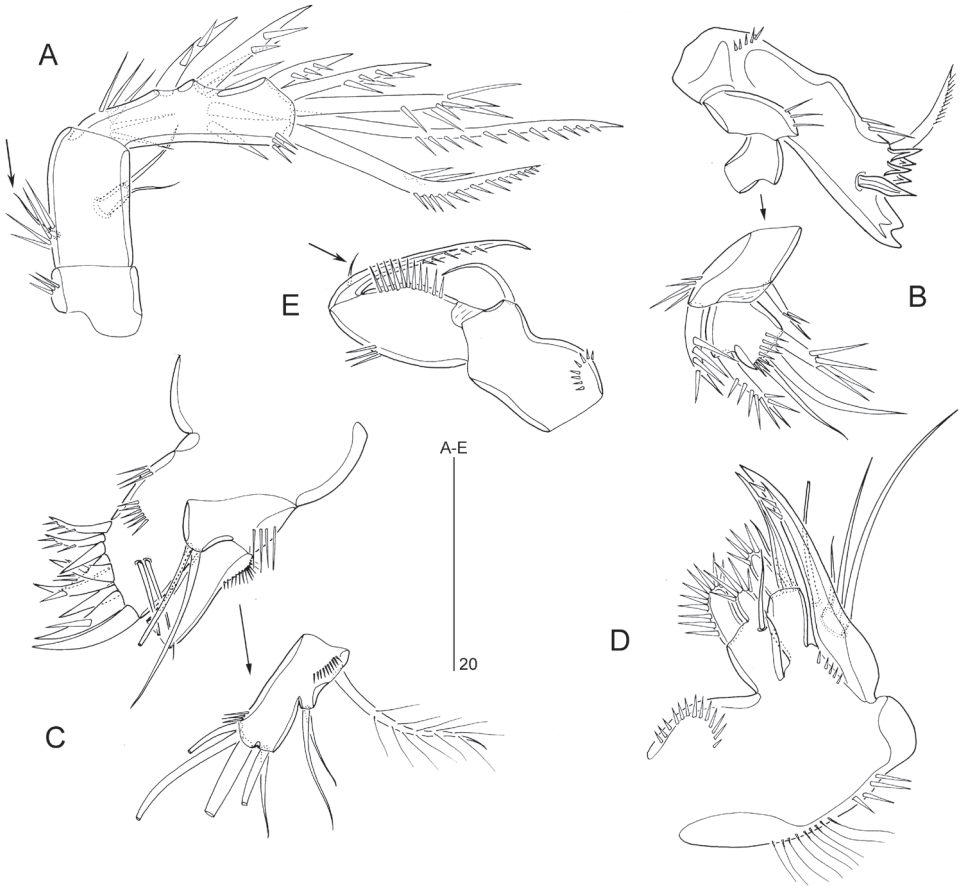

Figure 4. *Mesopsyllus dimorphus* sp. n. (♂): **A** antenna (abexopodal seta on allobasis indicated by arrow) **B** mandible (with palp disarticulated) **C** maxillule (with palp disarticulated) **D** maxilla **E** maxilliped (vestigial seta on endopod indicated by arrow). All drawings based on holotype (NHMUK reg. no. 2013.1033).

spinules and two stout pinnate spines along lateral margin; apical armature consisting of five pinnate spines; outer distal corner with few spinules.

Mandible (Fig. 4B). Gnathobase with strong teeth and unipinnate seta at dorsal corner, with spinular ornamentation as illustrated. Palp consisting of basis, 1-segmented endopod and vestigial exopod. Basis short, with few spinules and strong pinnate spine near inner distal corner. Endopod with one pinnate inner spine; apical margin with one pinnate spine, two naked setae and transverse spinular row. Exopod represented by a short pinnate spine.

Maxillule (Fig. 4C). Praecoxa with well-developed arthrite bearing two setae and two spinular rows on anterior surface, and nine spines along distal margin. Coxa with long spinules along outer margin; with cylindrical endite bearing two apical setae. Basis and rami fused, forming elongate palp; with spinules on inner and outer margins as

figured; basal armature presumably consisting of five naked setae; endopod represented by small cylindrical outgrowth with two distal setae; exopod represented by one long plumose seta.

Maxilla (Fig. 4D). Syncoxa with three rows of spinules, a row of setules and two (coxal) endites; proximal endite with a fused spinulose process, one spinulose spine and one short naked seta; distal endite with one spinulose spine, one naked spine and one naked seta. Allobasis drawn into slightly curved claw, bearing few spinules near apex and naked seta halfway down the claw. Exopod a minute segment with three naked setae.

Maxilliped (Fig. 4E) subchelate. Syncoxa with row of small spinules near base and naked seta at inner distal corner. Basis with spinular row along most of palmar (inner) margin and few spinules halfway along outer margin; unarmed. Endopod represented by a strong, acutely curved claw, spinulose along inner distal half and with one minute seta near base.

Swimming legs with 3-segmented exopods and 3- (P1, P3) or 2-segmented endopods (P2, P4).

P1 (Fig. 5A). Praecoxa (not illustrated) a well-developed U-shaped. Coxa with two rows of long spinules and additional small spinules on anterior surface as figured; outer distal corner produced into a round bulge, bearing spinules posteriorly. Basis bearing short outer seta (indicated by arrow in inset of Fig. 5A) and stout bipinnate inner spine; anterior surface with pore and three spinule rows; additional spinules along inner margin. Exopodal and endopodal segments with spinules along outer and distal margins, and with sparse setules along inner margin (except exp-3). Exp-1 with pinnate outer spine; exp-2 with plumose inner seta and pinnate outer spine; exp-3 with two outer and one apical pinnate spines, and one subdistal plumose seta. Enp-1 and enp-2 each with plumose inner seta and small spinous process at outer distal corner; enp-3 with plumose inner seta subdistally and two pinnate elements apically.

P2 (Fig. 5B). Praecoxa (not illustrated) a well-developed U-shaped sclerite with spinules along its distal margin. Coxa with a row of long spinules along outer margin and few long setules near outer distal corner; anterior surface with a pore and rows of tiny spinules as figured. Basis with short outer seta; with spinules along inner, distal and outer margins; inner margin also with hair-like setules; with pore on anterior surface; inner distal corner produced into sharp spinous process; distal margin between exopod and endopod with spinous process. Exopodal segments with spinules along outer margin; exp-1 and -2 with setules along inner margin and spinous process at outer distal corner; exp-2 with plumose inner seta and pinnate outer spine; exp-3 with one plumose inner seta, two pinnate spines (with setules on inner and spinules on outer margin) distally and two pinnate outer spines; exp-3 with pore on anterior surface and spinules along distal margin. Endopodal segments with spinules along outer, inner and distal margins; enp-1 with short, plumose inner seta and spinous process at outer distal corner; enp-2 with one short, plumose inner seta, one plumose seta subdistally, one long pinnate spiniform seta distally and one unipinnate outer spine; outer margin of enp-2 with small spike halfway down the segment length, possibly indicating ancestral segmentation boundary. Intersegmental hyaline frills of segments well developed, serrate.

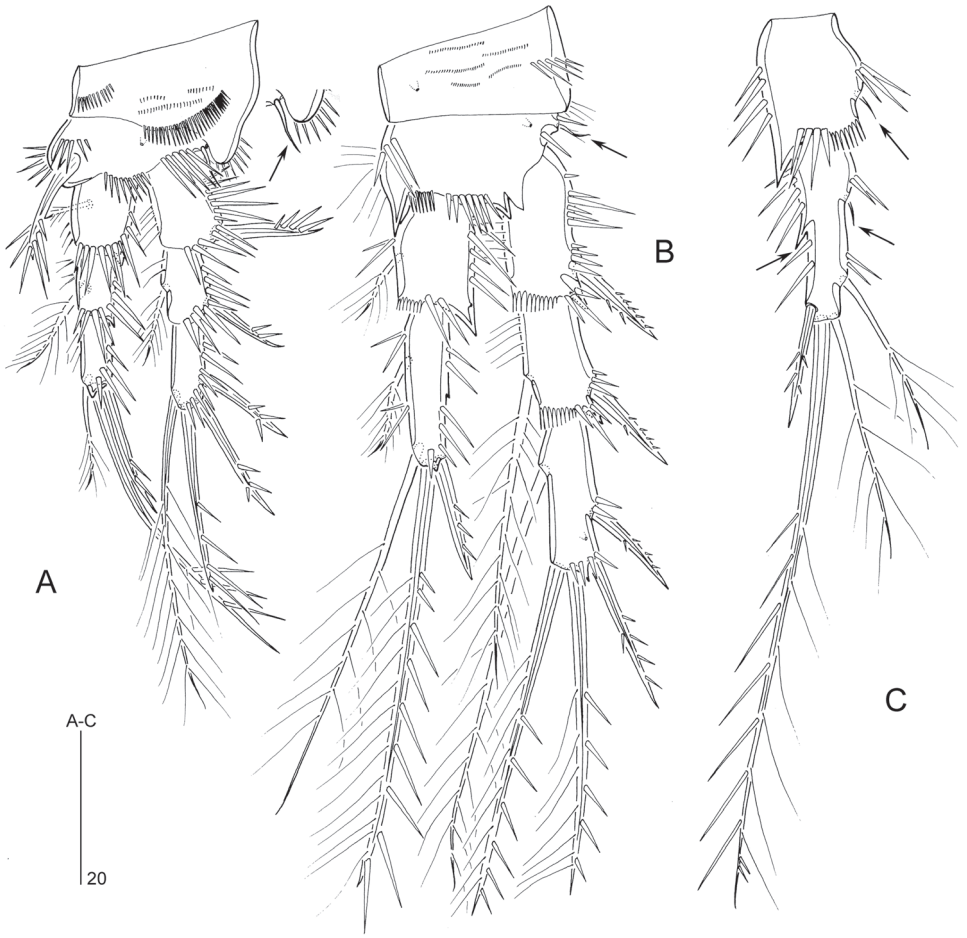

Figure 5. *Mesopsyllus dimorphus* sp. n.: **A** P1 ♂, anterior (outer basal seta indicated by arrow in inset) **B** P2 ♂, anterior (outer basal seta indicated by arrow) **C** P2 endopod ♀, anterior (vestigial setae along inner margin and hook-like process along outer margin indicated by arrows) **A–B** based on holotype (NHMUK reg. no. 2013.1033), **C** based on paratype (NHMUK reg. no. 2013.1034).

P3 (Fig. 6A). Praecoxa a well-developed U-shaped sclerite with spinules along its distal margin. Coxa and basis as in P2, except for presence of setules along inner margin of basis. Proximal and middle exopodal segments as in P2; distal segment with two plumose inner setae, two pinnate spines apically and two pinnate outer spines. Endopod 3-segmented; enp-1 and -2 with spinules along outer and inner margins; enp-1 with long, plumose inner seta, a row of short spinules along distal margin, and a spinous process at outer distal corner; enp-2 with one short, plumose inner seta; distal margin of enp-2 with outer spinous process and long anterior apophysis extending beyond enp-3; enp-3 (pseudosegment originating from secondary subdivision of ancestral enp-2) with two plumose setae apically.

P4 (Fig. 6B). Praecoxa, coxa and basis as in P2–P3, except spinous process at inner distal corner of basis absent; inner margin of basis without setular ornamentation. Exopod as in P3. Endopod short, reaching just beyond distal margin of exp-1; enp-1 with plumose inner seta and few spinules along outer and inner margins; enp-2 with one plumose inner seta, two plumose setae apically and one short, pinnate outer spine; with sparse spinular ornamentation along outer margin and pore on anterior surface.

P5 (Fig. 2E). Baseoendopods of fifth pair of legs fused medially forming deeply incised plate. Baseoendopod and exopod not fused, the former with outer basal seta. Endopodal lobe conical, reaching to apical margin of exopod; with one plumose inner spine and one short, naked outer seta; with sparse spinules along outer and inner margins. Exopod small, slightly longer than wide; with four elements: one plumose inner seta, two pinnate apical setae and one small, naked outer seta.

P6 (Fig. 2C). Fused to genital somite; represented by a median lobe without armature.

Caudal ramus (Fig. 2D). About 3.1 times as long as maximum width; with long spinules around insertion sites of setae IV–VII and short spinules around base of seta II. Ventral surface with pore near seta III and tube-pore near distal outer corner. Armature consisting of six setae (seta I apparently absent); setae II–III slender and bare, positioned along distal half of outer margin; seta IV–V well developed, pinnate; seta V about twice as long as seta VI and about half as long as the body length; seta VI small and naked; seta VII tri-articulated at base, laterally displaced and inserting near distal inner corner.

Description of female. Body length 240–330 μm (n = 10, mean = 292 μm). General body shape (Fig. 7B–C) as in male. Body covered with pattern of minute pimples (not figured). Sexual dimorphism in antennule, P2–P6, and urosomal segmentation and ornamentation.

Urosome (Fig. 7A–C). Genital and first abdominal somites fused forming genital double-somite; original segmentation marked by internal, transverse chitinous ribs laterodorsally, laterally and ventrally. Spinular ornamentation as follows: urosomite-1 with short paired dorsolateral rows; genital double-somite with short, paired lateral rows in anterior half (urosomite-2) and paired lateral rows extending laterodorsally and lateroventrally in posterior half (urosomite-3); urosomite-4 and urosomite-5 each with a long row, extending ventrally and ventrolaterally; anal somite with lateral and ventral rows around bases of caudal rami. Gonopores (Fig. 7D) fused, forming common median genital slit. P6 represented by two minute setae. Copulatory pore large, located in centre of genital double-somite; anterior half of genital double-somite with paired rows of minute spinules either side of genital slit.

Antennule (Fig. 3C–D) short, 6-segmented. Segment 1 with two spinule rows and one minute seta; segment 2 with eight naked setae (two with bi-articulated base) and one spinulose spine; segment 3 with two stout spinulose spines and two slender setae (one with bi-articulated base); segment 4 with large aesthetasc fused basally to short seta and one slender bi-articulated seta; segment 5 with few spinules and one bi-articulated naked seta along anterior margin; distal segment with one stout spinulose

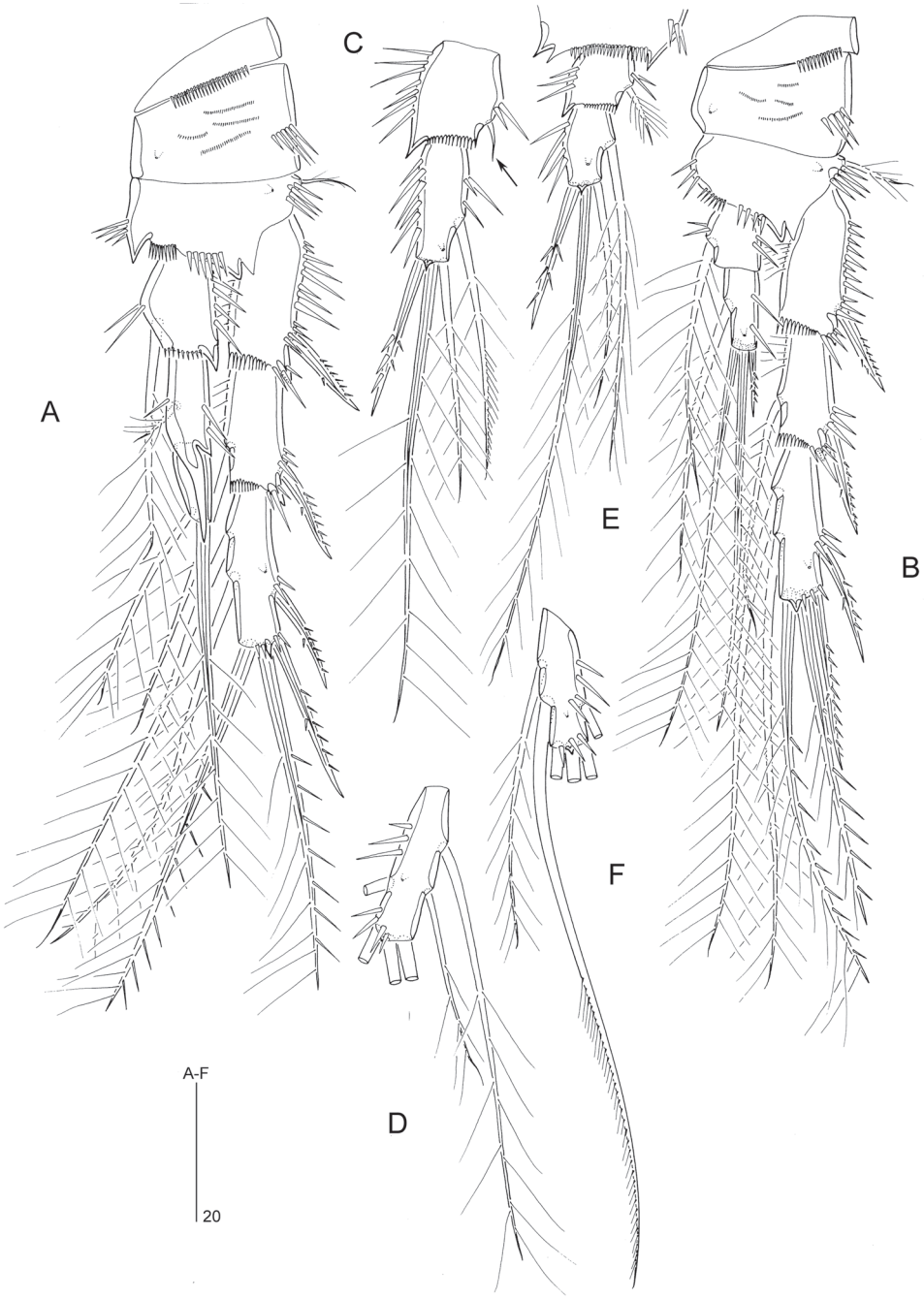

Figure 6. *Mesopsyllus dimorphus* sp. n.: **A** P3 ♂, anterior **B** P4 ♂, anterior **C** P3 endopod ♀, anterior (vestigial seta indicated by arrow) **D** P3 exp-3 ♀ (apical and outer elements not drawn at full length), anterior **E** P4 endopod and distal portion of basis ♀, anterior **F** P4 exp-3 ♀ (apical and outer elements not drawn at full length), anterior **A–B** based on holotype (NHMUK reg. no. 2013.1033) **C–F** based on paratype (NHMUK reg. no. 2013.1034).

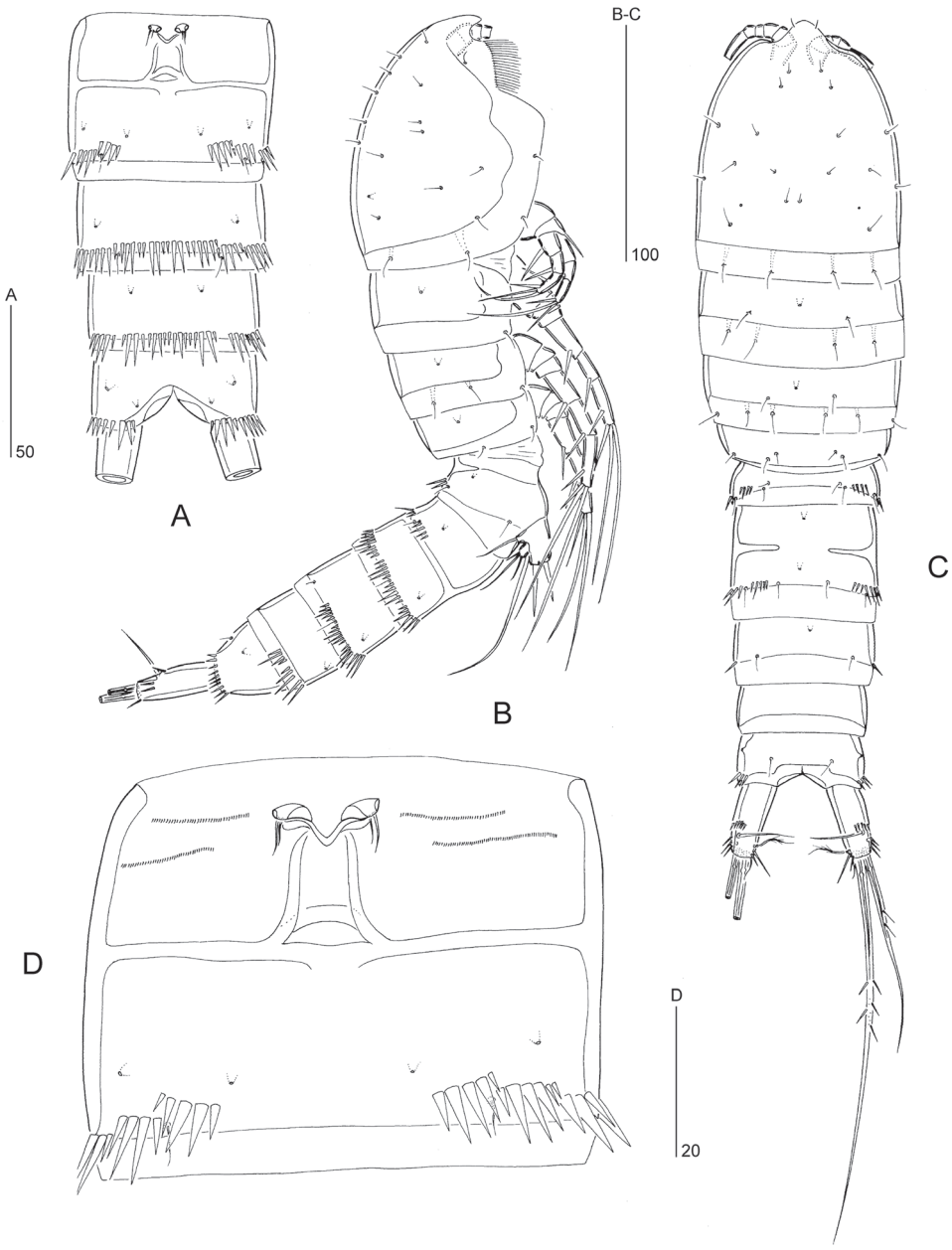

Figure 7. *Mesopsyllus dimorphus* sp. n. (♀): **A** urosome (excluding P5-bearing somite; distal portion of caudal rami omitted), ventral **B** habitus, lateral **C** habitus, dorsal **D** genital double-somite, ventral (copulatory pore indicated by arrow). All drawings based on paratype (NHMUK reg. no. 2013.1034).

spine, nine naked setae (four bi-articulated at base) and apical acrothek consisting of slender seta and short aesthetasc.

P2 (Fig. 5C). Coxa, basis and exopod as in ♂. Endopod 2-segmented. Enp-1 with one minute inner seta (indicated by arrow) and spinules along outer, distal and inner margins; outer distal corner produced into spinous process. Enp-2 with spinules along inner and outer margins and a sharp hook halfway along outer margin (indicating ancestral segmentation); inner margin with two setae, proximal one (homologue of inner seta in ♂) minute (indicated by arrow); armature around distal margin as in ♂ except for plumose inner distal seta distinctly shorter.

P3 (Fig 6C–D). Coxa, basis and first two segments of exopod as in ♂. Exp-3 with two plumose inner setae as in ♂ but distal one markedly shorter. Endopod 2-segmented, with spinules along inner and outer margins of both segments. Enp-1 with minute inner seta (indicated by arrow) and outer distal corner produced into spinous process. Enp-2 with one plumose inner seta, two plumose distal setae and one pinnate outer spine; distal margin with small spinous process; anterior surface with pore.

P4 (Fig. 6E–F). Coxa and first two segments of exopod as in ♂. Basis inner distal corner and distal margin between exopod and endopod with spinous process. Exp-3 (Fig. 6F) with two inner setae; proximal one considerably shorter than in ♂, distal one long and thick, unipinnate (rather than plumose as in ♂) in distal half. Endopod (Fig. 6E) 2-segmented, with spinules along outer margin of both segments and inner margin of enp-1. Enp-1 with small, plumose inner seta and spinous process at outer distal corner. Enp-2 with one plumose inner seta, two plumose distal setae and one pinnate outer spine, the latter much longer than in ♂; anterior surface with pore.

Seta and spine formulae of P1–P4 as follows:

Thoracopod	**Exopod**	**Endopod**
P1	0.1.022	1.1.111
P2	0.1.122	1.121 (1.221)
P3	0.1.222	1.1+apo.020 (1.121)
P4	0.1.222	1.121

Formulae in parentheses denote female condition.

P5 (Fig. 2G). Fifth pair of legs not fused medially. Baseoendopod and exopod discrete. Endopodal lobe trapezoid with stepped distal margin; with spinules as figured and pore on anterior surface; armature consisting of four elements: innermost two spiniform, serrate and subequal in length, 3rd one very long, pinnate and typically bent medially, and innermost one (indicated by arrow) minute, naked and setiform. Exopod small, longer than wide; with three setae: outermost one (indicated by arrow) minute and naked, middle one longest and unipinnate, and outermost short and naked.

Variability. One female specimen shows an asymmetrical armature pattern on P4 exp-3, having one inner seta on one side and two on the other.

Etymology. The species name is derived from the Greek *dis*, meaning twice, and *morphe*, meaning form, and alludes to the sexual dimorphism on P2–P4.

***Mesopsyllus spiniferus* sp. n.**
http://zoobank.org/CE004F59-6DAC-4B88-B63D-C3A524A05AFB
Figures 8–10

Type locality. Eastern China, strait of Bohai Sea, sampling locality C4 (38°00'N, 121°15'E); 23.8 m depth; sandy silt (Fig. 1; Table 1).

Material examined. Holotype: adult ♂ dissected on 16 slides (NHMUK reg. no. 2013.1045). Paratypes are 2 ♀♀ dissected on 15 and 17 slides, respectively (NHMUK reg. nos 2013.1046–1047), and 1 ♂ preserved in alcohol (NHMUK reg. no. 2013.1048); one paratype collected from type locality, others from the central Bohai Sea, localities D4 (38°15'N, 120°15'E) and E3 (38°30'N, 119°30'E), respectively (Fig. 1; Table 1). Collected by F.-h. Mu and Y.-q. Guo in September 1998 and April 1999.

Since the new species is very similar to *M. dimorphus* its description is largely restricted to those features which are different.

Description of male. Body length 280–320 μm (n = 2, mean = 300 μm). Body covered with pattern of minute pimples (not figured). Urosomal ornamentation (Fig. 8A–C) very similar to that of *M. dimorphus* except for presence of one additional pair of dorsal spinule rows on urosomite-4.

Antennae, mouthparts, P6, caudal rami and rostrum as in *M. dimorphus*.

Antennule (Fig. 9A–B) 8-segmented. Anterior margin of segment 7 with two spiniform elements (modified setae) instead of three conical elements in *M. dimorphus*.

P1 with different spinular ornamentation on coxa, as figured for ♀ (Fig. 9D). Endopod shorter and inner seta on enp-2 distinctly shorter than in *M. dimorphus*.

P2 (Fig. 9C). Coxa with a row of long spinules on anterior surface. Inner seta of exp-2 shorter than in *M. dimorphus*, only extending to distal margin of exp-3. Endopod 2-segmented. Enp-1 with 1 minute inner seta and spinules along outer, inner and distal margins; outer distal corner produced into spinous process. Enp-2 with spinules along inner and outer margins and a sharp spinous process halfway down outer margin; inner margin with two setae, proximal of which minute and plumose; distal margin with two apical setae and one outer spine.

P3 (Fig. 10A). Coxa, basis and exopod as in *M. dimorphus*. Inner seta of enp-1 much shorter than in *M. dimorphus*.

P4 (Fig. 10B). Coxa as in *M. dimorphus*. Basis with a spinous process at inner distal corner and between insertion sites of exopod and endopod. Distal inner seta of exp-3 thicker than proximal one. Inner seta of enp-1 much shorter than in *M. dimorphus*, only reaching distal margin of enp-2; enp-2 longer than in *M. dimorphus*, with two (instead of one) inner setae.

Seta and spine formula of P1–P4 as follows:

Thoracopod	Exopod	Endopod
P1	0.1.022	1.1.111
P2	0.1.122	1.221
P3	0.1.222	1.1+apo.020 (1.221)
P4	0.1.222	1.221

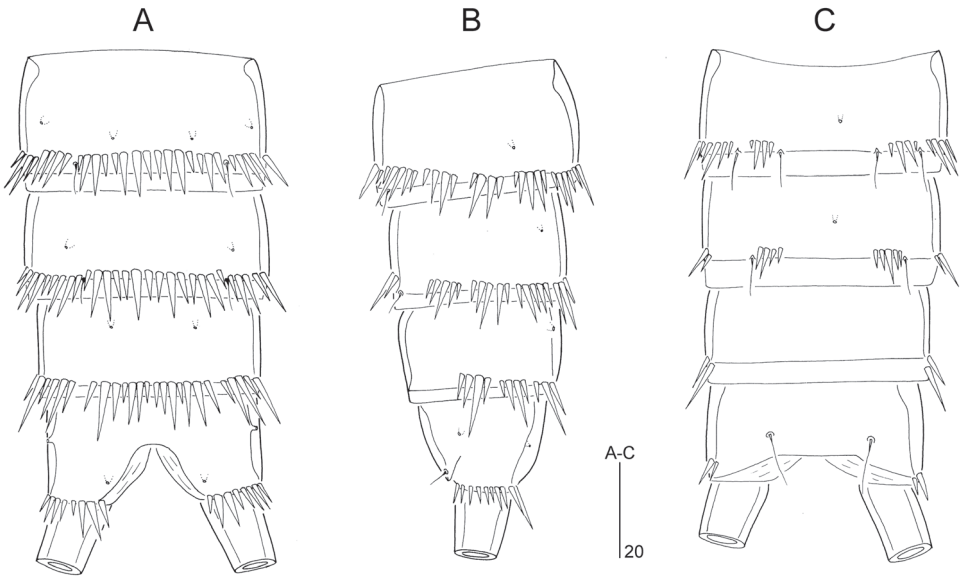

Figure 8. *Mesopsyllus spiniferus* sp. n. (♂): **A** abdomen, ventral **B** abdomen, lateral **C** abdomen, dorsal [Caudal rami in **A–C** not drawn at full length]. All drawings based on holotype (NHMUK reg. no. 2013.1045).

Formulae in parentheses denote female condition.

P5 (Fig. 10E). Number of armature elements as in *M. dimorphus*. Endopodal lobe slightly wider and inner spine more spiniform and shorter than in *M. dimorphus*. Exopodal setae 1–2 relatively shorter compared to seta 3.

Description of female. Body length 340–350 μm (n = 2, mean = 345 μm). Body covered with pattern of minute pimples (not figured). Sexual dimorphism in antennule, P3–P5, and urosomal segmentation and ornamentation.

Antennule, P5, and urosomal segmentation and ornamentation as in *M. dimorphus*.

P3 (Fig. 10C). Coxa, basis and exopod as in ♂. Enp-1 with minute inner seta and spinous process at outer distal corner; enp-2 with two inner setae.

P4 (Fig. 10D). Coxa, basis and exopod as in ♂. Enp-1 with minute, plumose inner seta (indicated by arrow).

Variability. Both female specimens display right-left asymmetrical setal formulae on one pair of swimming legs. In the first specimen P3 enp-2 displays only one inner seta on one side and two on the other; in the second specimen P4 exp-3 exhibits one inner seta on one side but two on the other. The male holotype is aberrant in leg 1 with one side represented by a single segment with two distal setae and one outer spine (compare typical condition observed in dissected ♀ paratype: Fig. 9D).

Etymology. The species name alludes to the two spiniform elements on segment 7 of the male antennule.

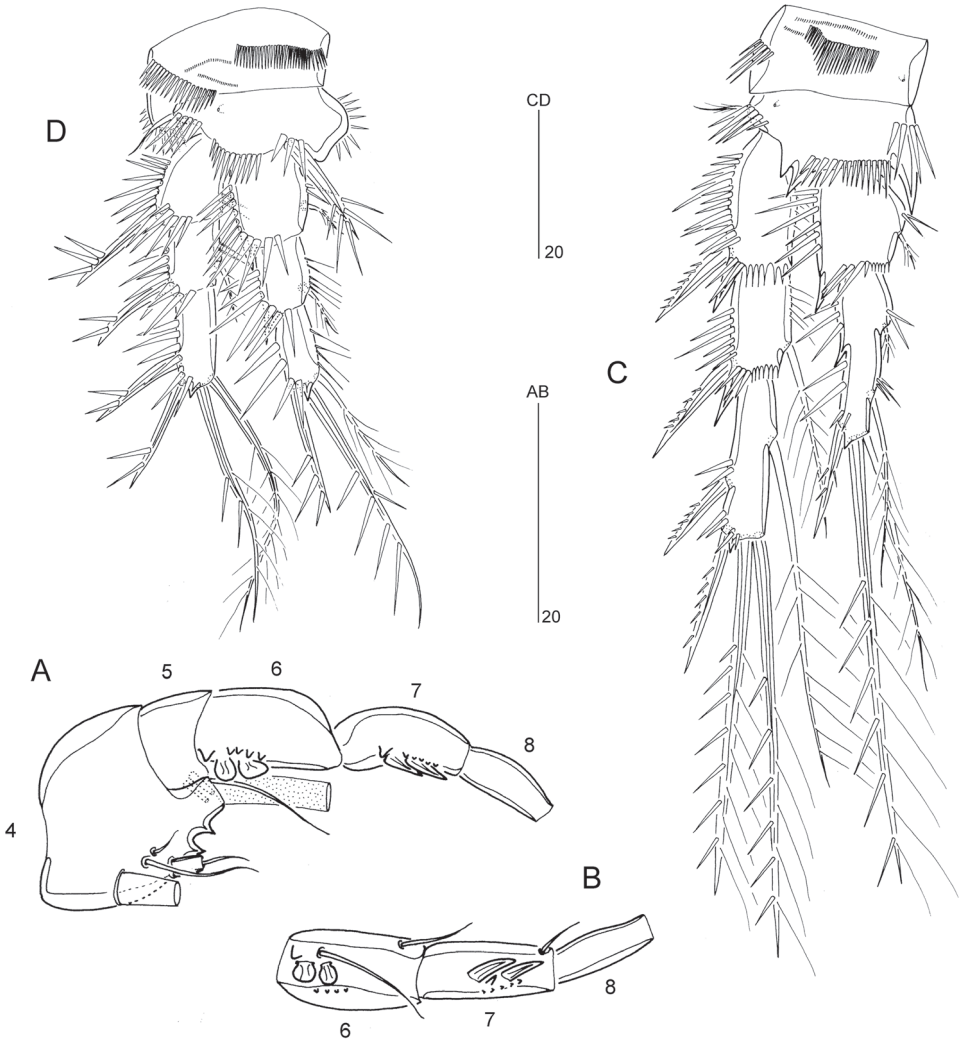

Figure 9. *Mesopsyllus spiniferus* sp. n.: **A** antennule ♂, distal five segments, showing modified elements on segments 6–7 (armature elements on other segments omitted or not drawn at full length), ventral **B** antennule ♂, distal three segments, showing modified elements on segments 6–7 (elements on segment 8 omitted), anterior **C** P2 ♂, anterior **D** P1 ♀, anterior **A–C** based on holotype (NHMUK reg. no. 2013.1045), **D** based on paratype (NHMUK reg. no. 2013.1046).

Discussion

Species differentiation and validity of *Vibriopsyllus* Kornev & Chertoprud, 2008

Por (1960) proposed the monotypic genus *Mesopsyllus* for a new species, *M. atargatis*, based on four females collected from muddy substrates at 51–82 m depth off the Romanian Black Sea coast. The species has only been recorded twice since its original

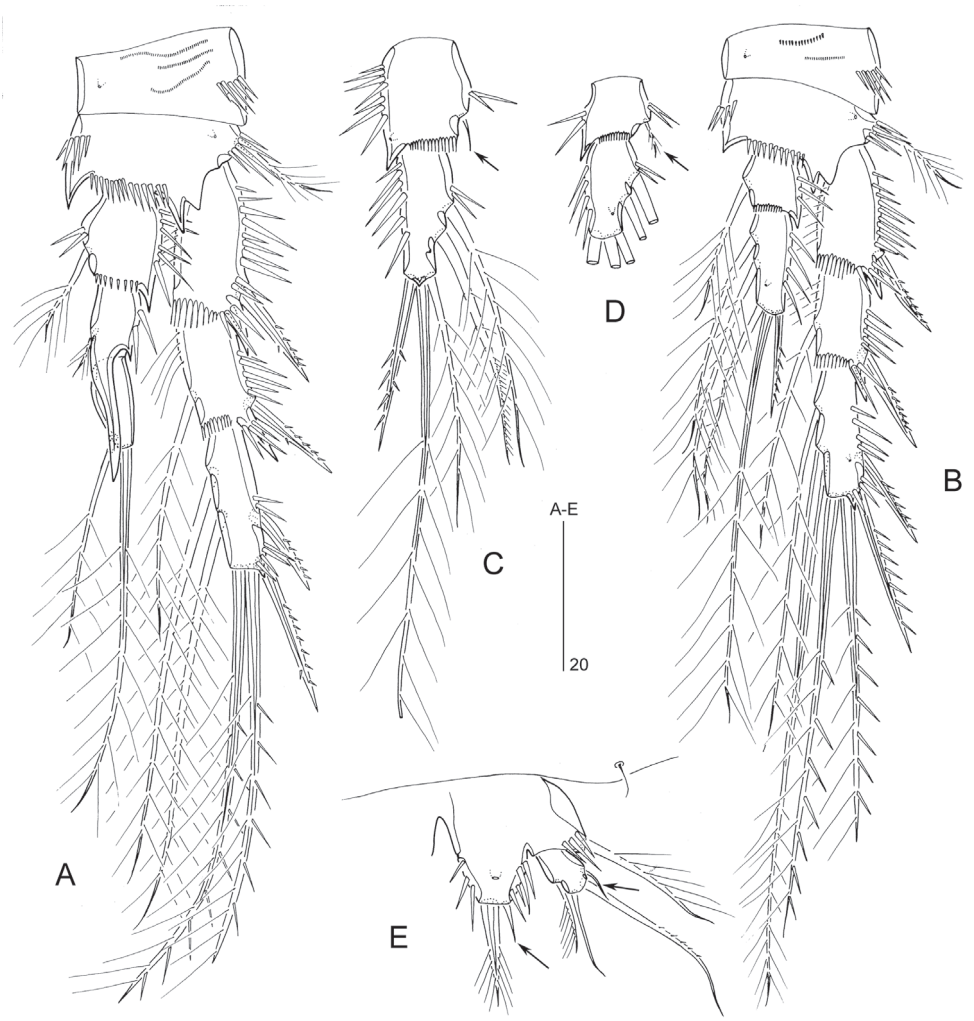

Figure 10. *Mesopsyllus spiniferus* sp. n.: **A** P3 ♂, anterior **B** P4 ♂, anterior **C** P3 endopod ♀, anterior (vestigial seta on enp-1 indicated by arrow) **D** P4 endopod ♀ (reduced seta on enp-1 indicated by arrow; setae on enp-2 not drawn at full length), anterior **E** P5 ♂, anterior (minute setae on exopod and endopodal lobe indicated by arrow) **A–B, E** based on holotype (NHMUK reg. no. 2013.1045) **C–D** based on paratype (NHMUK reg. no. 2013.1046).

description. Marinov and Apostolov (1981) recorded three females at 15 m depth in the Gulf of Piran (Slovenia) in the northern Adriatic. Bodin and Le Guellec (1992) found *M. atargatis* at 8.7–11 m depth in the Bay of Saint-Brieux, northern Brittany (France). Por's (1960) description contains deficiencies and some of them, such as the doubtful armature pattern on the P2 endopod (cf. Table 2), have been pointed out by Lang (1965). *Mesopsyllus* females typically display one and two enlarged spinulose spines on antennulary segments 2–3, respectively (Fig. 3D); however, Por (1960) shows a diver-

gent (and probably incorrect) pattern in *M. atargatis*, with segments 2–4 each bearing a single spine. His claim that the antennary exopod is absent is almost certainly false (the antenna was not illustrated) since this condition is not found in any of the other four congeners, all of which display a 1-segmented bisetose or trisetose exopod. Note that the antennary exopod of *M. atargatis* was therefore probably incorrectly scored as completely absent in Wells' (2007) tabular key to the Canthocamptidae (his codon KG0; p. 203). According to Por's (1960) text the armature formula for the distal exopodal segment of P4 is 223 but this is contradicted by his illustration which shows only one inner seta; this error was adopted by Por (1964a: 116) but subsequently corrected by Por (1964b: 252). *Mesopsyllus atargatis* is the only member of the genus that was described as having five elements on the endopodal lobe of the female leg 5. Morphological comparison with other species (all of which possess four elements) lends support to the assumption that the innermost element in reality represents one of the spinules typically found in this position (cf. Fig. 2D). His statement that the anal operculum is fringed with fine spinules is based on an observational error; the alleged spinular ornamentation in reality refers to the underlying incised frill bordering the anal opening.

Por (1964a) transferred *M. atargatis* to a more inclusive genus, *Hemimesochra*, effectively rendering *Mesopsyllus* a junior subjective synonym of the latter. Lang (1965) dismissed Por's heterogeneous concept of *Hemimesochra* and restricted the genus to its type species *H. clavularis*, resurrected the monotypic *Mesopsyllus*, and transferred the third species, *H. derketo*, to a new genus *Poria*. The new replacement name *Hanikraia* was substituted for *Poria*, the latter being preoccupied by a genus of Coleoptera (Huys 2009). Wells (1965) described *Hemimesochra secunda* based on one female and one male collected at 101 m depth in Loch Nevis, a sea loch on the west coast of Scotland where it co-occurs with *H. clavularis*; the species has not been recorded again. Although no factual justification for its generic assignment was given it appears that Wells (1965) based his course of action primarily on the 2-segmented condition of the P1 endopod, a character shared with the type species *H. clavularis*. Huys and Thistle (1989) reviewed the genus *Hemimesochra* and transferred *H. secunda* to *Mesopsyllus* based on similarities with the type species in the morphology of the rostrum, female antennule and legs 2–4. Re-examination of the types (NHMUK reg. nos 1965.3.26.10–11) not only confirmed the 2-segmented P1 endopod (3-segmented in all other *Mesopsyllus* species) but also revealed minor errors in the original description of legs 1–2 (Table 2). *Mesopsyllus atargatis* and *M. secundus* differ from their congeners by the setulose anterior margin of the rostrum (*vs* naked), the presence of only one inner seta on P2 enp-2 (*vs* two) and of three outer spines on P4 exp-3 (*vs* two). They can be differentiated from each other by the segmentation of the P1 endopod, the number of inner setae on P4 exp-3, and the number of elements on the exopod of leg 5 in the female.

Kornev and Chertoprud (2008) described a new genus and species, *Vibriopsyllus curviseta* Kornev & Chertoprud, 2008, from shell gravel at 10 m depth in Rugozorskaya, an inlet of the Kandalaksha Gulf in the White Sea. The species was recently recorded from silty sand at 39 m depth in the Kara Sea (Garlitska and Azovsky 2016). Kornev and Chertoprud (2008) assigned *V. curviseta* to the Hemimesochrinae and considered

it closest to *Hemimesochra clavularis* because of the morphological similarities in the antennule (6-segmented in ♀; although in *H. clavularis* it is only 5-segmented!), antenna ("conspicuous" allobasis with 1-segmented trisetose exopod; but note, however, that the antenna in *H. clavularis* has a genuine basis), maxillule (unisetose exopod, bisetose endopod), maxilla (syncoxa with two endites) and the female P5 (exopod small, with four setae; baseoendopod with four setae, seta III being very long). Despite these similarities Kornev and Chertoprud (2008) refrained from including their new species in *Hemimesochra* and considered the proposal of *Vibriopsyllus* warranted based on three differences, i.e. (a) P1 endopod 3-segmented (*vs* 2-segmented in *Hemimesochra*), (b) caudal ramus shape, and (c) P3 enp-2 with six elements (*vs* seven in *Hemimesochra*). Note that the last character must be an inadvertent slip of the pen since *V. curviseta* has in reality five while *H. clavularis* displays only six elements on this segment (cf. Sars, 1920: Plate XLV; Kornev and Chertoprud 2008: Fig. 5.123B). Kornev and Chertoprud (2008) regarded the distinctive morphology of the female leg 5 as a synapomorphy supporting the sistergroup relationship between both genera. Presumably this statement referred to the armature rather than the segmentation since re-examination by Por (1964b: 254) revealed that the baseoendopod and exopod are fused in *H. clavularis* while they remain separate in *V. curviseta*. Although Kornev and Chertoprud (2008) cited Huys and Thistle's (1989) revision of *Hemimesochra* and related genera they surprisingly did not compare *V. curviseta* with other members of the Hemimesochrinae. Within the latter, a lineage consisting of the genera *Mesopsyllus*, *Psammocamptus* and *Bathycamptus* shares with *V. curviseta* two antennulary characters, i.e. the position of the proximal aesthetasc (on segment 4 rather than segment 3) and the spinulose spine pattern (one on segment 2, two on segment 3 and one on the apical segment) (Table 2), the reduction of the inner seta on P1 enp-1, and the elongate caudal rami. *Psammocamptus* and *Bathycamptus* are closely related to each other since both display the same sexual dimorphism on leg 4 endopod (the presence of an additional inner seta on enp-2 in the ♂); based on this synapomorphy and the fused condition of leg 5 in both sexes the two genera can be considered sister taxa. Members of the genus *Mesopsyllus* all exhibit a 6-segmented antennule in the female, an apomorphic condition derived by failure of separation of the two apicalmost segments that is also shared by *V. curviseta*; see Huys and Thistle (1989: Fig. 3A) and Mielke (1997: Fig. 15A) for the ancestral 7-segmented condition in *Bathycamptus eckmani* Huys & Thistle, 1898 and *Psammocamptus galapagoensis* Mielke, 1997, respectively. Both *Hanikraia derketo* (Por, 1964a) and *Carolinicola galapagoensis* Mielke, 1997 also display a 6-segmented antennule, however, this condition is not homologous to the *Mesopsyllus* segmentation pattern since it originated from failure of separation of segments 3 and 4 (as indicated by the armature pattern and the position of the aesthetasc). Comparison between the type species of *Vibriopsyllus* and the four known species of *Mesopsyllus* (Table 2) shows that there are no grounds for maintaining the former as a distinct genus and hence it should be relegated to a junior subjective synonym of the latter. *Vibriopsyllus curviseta* is here formally transferred to *Mesopsyllus* as *M. curvisetus* (Kornev & Chertoprud, 2008), comb. n. The species is characterized by the presence of four elements on the female P5 exopod, and five elements on the male P5 exopod, a condition so far unique in the genus (Table 2).

Table 2. Antennulary characters (# = number of segments; ae = segment on which proximal aesthetasc is located; sp = presence/absence of enlarged spinulose spines on segments 2–3) and P1–P5 armature formulae of species of *Mesopsyllus* Por, 1960 (*M.*) and related genera (*Ba.* = *Bathycamptus* Huys & Thistle, 1989; *Bo.* = *Boreolimella* Huys & Thistle, 1989; *Ha.* = *Hanikraia* Huys, 2009; *He.* = *Hemimesochra* Sars, 1920; *Ps.* = *Psammocamptus* Mielke, 1975; *Pu.* = *Pusillargillus* Huys & Thistle, 1989; *S.* = *Sympodella* gen. n.; ? = condition unknown).

	A1 ♀			P1		P2		P3		P4		P5 ♀			P5 ♂	
	#	ae	sp	exp	enp	exp	enp	exp	enp	exp	enp	rami	exp	benp	exp	benp
M. atargatis	6	4	+	0.1.022[a]	1.1.111	0.1.123	1.121[b]	0.1.223	1.121	0.1.123[c]	1.121	free	3	4[d]	?	?
M. curvisetus	6	4	+	0.1.022	1.1.111[e]	0.1.123	1?.221[f]	0.1.223	1.221	0.1.222	1.121	free	4	4	5	2
M. dimorphus	6	4	+	0.1.022	1.1.111	0.1.122	1.221	0.1.222	1.121	0.1.222	1.121	free	3	4	4	2
M. secundus	6	4	+	0.1.022[g]	1.111[h]	0.1.123[i]	1.121	0.1.223	1.121	0.1.223	1.121	free	5	4	4	2
M. spiniferus	6	4	+	0.1.022	1.1.111	0.1.122	1.221	0.1.222	1.221	0.1.222	1.221	free	3	4	4	2
Ba. minutus	?	?	+	0.1.022	1.1.111	0.1.122	1.121	0.1.222	?	0.1.222	?	?	?	?	5	2
Ba. eckmani	7	4	+	0.1.022	1.1.111	0.1.122	1.121	0.1.223	1.121	0.1.223	1.121	fused	4	4	5	2
Ps. axi	(7)[j]	4	+	0.1.022[k]	1.1.111[k]	0.0.022	(1).111[l]	0.0.122	(1).121[l]	0.(1).122[l]	1.121	fused	3	4	4	2
Ps. galapagoensis	7	4	+	0.1.022	1.1.111	0.1.122	1.111	1.1.122	1.121	0.1.122	1.121	fused	3	4	4	2
He. clavularis	5	3	+	0.0.022[m]	1.111	0.1.123	1.221	0.1.223	1.321	unknown[n]	unknown[n]	fused[o]	4	4	?	?
Bo. dubia	5[p]	3	+	0.1.022[q]	1.211[q]	0.1.122	1.121	0.1.122	1.121	0.1.122	1.121	fused	4	4	?	?
Bo. nympha	5	3	+	0.1.022	1.211[r]	0.1.122	1.221	0.1.222	1.221	0.1.222	1.221	fused	4	4	?	?
Ha. derketo	6[s]	3	–	0.0.022[m]	1.1.111	0.1.123[t]	1.1.111	0.1.223[t]	1.1.121	0.1.223	1.221	free	4	4	?	?
Pu. nixe	5	3	–	0.1.022	1.211	0.1.122	1.221	0.1.222	1.221	0.1.222	1.221	free	5	4	5	2
S. galapagoensis	6	3	–	0.1.022[m]	1.1.111	0.1.122	1.111	0.1.222	1.121	0.1.222	1.121	fused	5	4	6	2

[a] Por erroneously tabulates the formula as 0.1.121 (1964a: 116) or 0.1.120 (1964b: 252).

[b] According to Por's (1960, 1964a, 1964b) illustrations and text the formula appears to be 0.111; the notches illustrated along the inner margin of both endopodal segments were interpreted by Lang (1965: 423) as insertion sites of setae which had been dislodged prior or during dissection, suggesting that the correct armature formula is 1.121 which is adopted here.

[c] Por (1960) illustrates only one inner seta on exp-3 but lists the setal formula as 223; this error was adopted by Por (1964a: 116) but subsequently corrected by Por (1964b: 252).

[d] According to Por's (1960) text the endopodal lobe bears five elements; comparison with other species lends support to the assumption that the innermost element in reality represents one of the spinules typically found in this position.

[e] Kornev and Chertoprud (2008) give the setal formula as 1.1.220, erroneously interpreting the long proximal spinule along the inner margin as an additional seta.

[f] It is questionable whether Kornev and Chertoprud's (2008) setal formula (0.221) is correct. Their illustration of leg 2 (fig. 5.123Б) shows a setule-like element on enp-1 in exactly the same position as the vestigial inner seta in *M. dimorphus* (Fig. 5C) and *M. spiniferus* (Fig. 9C), suggesting that the real setal formula is 1.221 as in the Chinese species.

[g] Wells (1965) interprets the armature pattern of exp-3 as 121.

[h] Although Wells (1965: Text-fig. 56) does not illustrate an inner seta on enp-1, its presence (as indicated by his setal formula 1.121) was confirmed by examination of the holotype (NHMUK reg. no. 1965.3.26.10); confirmation of the armature pattern on enp-2 is more problematic due to the bad preservation of the type slides, however, it appears that the short proximal outer element figured by Wells is in reality a spinule and that the distal formula is 111 as in other species of the genus; the outer distal element is spiniform rather than setiform and only half the size of that illustrated in the original description.

[i] Wells (1965: Text-Fig. 57) gives the correct setal formula for exp-3 but the slender seta figured at the inner distal corner is distinctly longer and originates from the proximal half of the inner margin.

[j] Mielke (1975) described the antennule as 6-segmented; his re-examination (Mielke 1997: 187) revealed the distal segment to be weakly subdivided.

[k] Contrary to Mielke's (1975) original description P1 exp-2 and enp-1–3 have a minute inner seta.

[l] The rudimentary setules indicated as (1) in Mielke's (1975) armature formula are genuine armature elements.

[m] Mielke's (1997: Fig. 11A) description of *Carolinicola galapagoensis* showed that the inner seta on exp-2 can attain vestigial proportions. The absence of this element in *Ha. derketo* and *He. clavularis* therefore requires confirmation.

[n] Sars' (1920) description was based on two ♀♀ from Risør, southern Norway and illustrated only P1–P3 without giving any information about the armature pattern of leg 4. The only other record of the species is that by Wells (1965) who obtained three ♀♀ from Loch Nevis but refrained from making additional observations. Lang (1948: 1249) listed the formula for leg 4 as 0.1.223 for the exopod and 1.221 for the endopod. Since he did not collect material of the species nor re-examined the type material the armature pattern is probably based on Sars's (1920) statement that the legs are "… of a structure similar to that in *Mesochra*" and should therefore be considered unconfirmed. Unfortunately this unverified fact has been perpetuated in the literature (Por 1964a, 1964b, Wells 1965, Coull 1973a).

[o] According to Sars (1920) the exopod is discrete but Por (1964b: 254) claims that it is fused to the baseoendopod.

[p] Wells (1965: Text-Fig. 93) shows a 6-segmented condition but claims in the text that the antennule is 5-segmented; the proximal "segment" represents a pedestal with which the antennule articulates.

[q] There is controversy over the correct armature of leg 1 since there is a discrepancy between Wells' (1965) text and illustration (his Fig. 96 shows no inner seta on exp-2 and four elements on enp-2) (Becker 1972, Huys and Thistle 1989). Re-examination of the holotype (NHMUK reg. no. 1965.3.26.15) confirmed the presence of the inner seta on exp-2 and one inner and three apical elements on enp-2.

[r] According to Por's (1964b) text and illustration (Fig. X-111) the armature formula of the distal segment is 120. The inner seta on this compound segment is derived from the ancestral enp-2 segment while the two distal elements are derived from ancestral enp-3; it is assumed here that the short inner apical seta on the latter segment was overlooked by Por (cf. *M. spiniferus*, Fig. 9D for ancestral 1.1.111 condition).

[s] Por (1964a: Plate 21, fig. 243) shows a 7-segmented condition but states in the text that the antennule is 6-segmented with the proximal aesthetasc arising from the fourth segment; the armature of the proximal section of the antennule shows that the first unarmed "segment" is in reality the pedestal.

[t] According to Por's (1964a: Plate 21, figs 246–247) illustrations the inner seta on P2–P3 exp-2 is absent but the notches along the inner margin of both segments suggest that the setae were dislodged prior or during dissection; Por's (1964a: 116) setal formulae indicate that the inner setae are present.

The two Chinese species described herein, *M. dimorphus* and *M. spiniferus*, differ from their congeners by the presence of two instead of three outer spines on P2–P3 exp-3. They can be differentiated from each other by the following combination of characters: (1) number of inner setae on P3–P4 enp-2 (one in *M. dimorphus*, two in *M. spiniferus*); (2) anterior margin of antennulary segment 7 of male (with two spiniform elements in *M. spiniferus*; with three conical elements in *M. dimorphus*); (3) ornamentation of male urosome (second abdominal somite with paired dorsal spinular patches in *M. spiniferus*; absent in *M. dimorphus*); (4) presence/absence of sexual dimorphism on P2 endopod, P3–P4 exp-3 (present in *M. dimorphus*; absent in *M. spiniferus*); and (5) differences in length of setae on male P5.

The genus *Mesopsyllus* is so far restricted to the Northern Hemisphere. Soyer (1971) listed an as yet undescribed species as *Hemimesochra* sp. from Banyuls-sur-Mer, France. Baguley (2004) recorded eight undescribed species of *Mesopsyllus* from the deep sea in the Northern Gulf of Mexico. George (2013) listed an unidentified species from the Sedlo Seamount in the North Atlantic. An as yet undescribed *Mesopsyllus* species, possibly conspecific with *M. secundus*, was collected from a muddy substrate at 11 m depth in Loch Creran, Argyll in Scotland (E. Ólafsson, pers. commn). Grego et al. (2014) recently recorded an unnamed species of *Vibriopsyllus* during a field experiment on a silty sand bottom at 24 m depth in the northern Adriatic Sea. Undescribed species of the closely related genera *Psammocamptus* and *Bathycamptus* have been reported from the Gulf of Mexico (Baguley 2004, Brooks et al. 2009, Plum et al. 2015), the Porcupine Seabight (Gheerardyn et al. 2009), the Seine Seamount (Büntzow in George 2013), French Polynesia (Villiers and Bodiou 1996), Svalbard (Kotwicki 2002), and Kuwait (R. Huys, unpublished data).

Key to species of *Mesopsyllus*

Caution must be exercised while attempting to identify species since some original descriptions contain inaccuracies and anomalous setation patterns in legs 1–5 are known to exist in some species so that observations based on a single specimen may not always reveal the usual (typical) condition. Members of the genus *Mesopsyllus* are typically small to very small and most original descriptions were based on very few specimens (Table 3). The swimming leg armature formulae of all species – with reinterpretations where required – are tabulated in Table 2. The key below is applicable to both sexes.

Table 3. Body length (in μm) and number of specimens (#) used in original descriptions of *Mesopsyllus* species.

Species	♀ (μm)	♂ (μm)	# ♀♀	# ♂♂
M. atargatis	470	?	4	?
M. secundus	400	340	1	1
M. dimorphus	240–330	220–280	11	3
M. spiniferus	340–350	280–320	2	2
M. curvisetus	405	not given	1	1

1 Rostrum with setulose anterior margin; P2 enp-2 with one inner seta; P4 exp-3 with three outer spines **2**

– Rostrum with smooth anterior margin; P2 enp-2 with two inner setae; P4 exp-3 with two outer spines **3**

2 P1 endopod 3-segmented; P4 exp-3 with one inner seta ..... ***M. atargatis* Por, 1960**

– P1 endopod 2-segmented; P4 exp-3 with two inner setae ..... ***M. secundus* (Wells, 1965)**

3 P2–P3 exp-3 with two outer spines; P5 ♀ exopod with three elements; P5 ♂ exopod with four elements **4**

– P2–P3 exp-3 with three outer spines; P5 ♀ exopod with four elements; P5 ♂ exopod with five elements ..... ***M. curvisetus* (Kornev & Chertoprud, 2008), comb. n.**

4 P3–P4 enp-2 ♀ with one inner seta; P2 endopod and P3–P4 exp-3 displaying sexual dimorphism as illustrated in Fig. 5A–B and Fig. 6A, B, D, F, respectively; second abdominal somite without paired dorsal spinular patches in ♂ ..... ***M. dimorphus* sp. n.**

– P3–P4 enp-2 ♀ with two inner setae; P2 endopod and P3–P4 exp-3 without such sexual dimorphism; second abdominal somite with paired dorsal spinular patches in ♂ ..... ***M. spiniferus* sp. n.**

Taxonomic position of *Carolinicola* Huys & Thistle, 1989 and proposal of *Sympodella* gen. n.

Coull (1973a) described *Hemimesochra trisetosa* based exclusively on females obtained from deep sea sediments off North Carolina. Huys and Thistle (1989) pointed out that the species was radically different from the species included in *Hemimesochra* at that time and established the genus *Carolinicola* to accommodate it. Mielke (1997) described both sexes of a second species, *C. galapagoensis*, from a sandy beach in the Galápagos archipelago, which he provisionally assigned to the genus. Additional, as yet undescribed, species have been reported from the Straits of Magellan and the Beagle Channel (George 1999, 2005), the abyssal plain of the Kuril Trench (Kitahashi et al. 2013) and from a marine cave near Marseille, France (Janssen et al. 2013).

Based on irreconcilable differences in the morphology of the rostrum, antenna, mandible and caudal rami, Huys and Thistle (1989) removed *Carolinicola trisetosa* (Coull, 1973a) from the Hemimesochrinae (Canthocamptidae) and placed it as an "advanced member" in the "Paranannopidae" (= Danielsseniidae; see Huys (2009: 11) for a discussion on the availability of these family-group names). Willen (2000) likewise listed *Carolinicola* as a member of the subfamily Paranannopinae (= Danielsseniinae) in the Pseudotachidiidae, a view that was adopted by Wells (2007). However, the discovery of the male of *C. galapagoensis* led Mielke (1997) to suggest that both species of *Carolinicola* should remain in the same family as the former *Hemimesochra* species. Kim et

al. (2011) endorsed Mielke's (1997) view that *Carolinicola* has canthocamptid affinities (e.g., sexual dimorphism of P3 endopod), showing similarities with *Boreolimella* and *Poria* (= *Hanikraia*), and consequently removed the genus from the Danielsseniinae to the Hemimesochrinae. Unfortunately, Kim et al. (2011) neglected to address the heterogeneity of the genus. While the morphology of *C. galapagoensis* lends support to their course of action, the characters of the type species, *C. trisetosa*, clearly indicate that the latter (and – by inference – the genus *Carolinicola*) should remain in the Danielsseniinae as initially advocated by Huys and Thistle (1989). Within the Hemimesochrinae *C. galapagoensis* belongs to a lineage that is characterised by (1) proximal aesthetasc positioned on third antennulary segment due to failure of separation of ancestral segments 3–4, and (2) inner seta of P1 enp-1 long, pectinate and recurved both dorsally and backwardly. This combination of characters is expressed in members of the genera *Hemimesochra* (the presence of the posteriorly directed seta in *H. clavularis* was confirmed by Por (1964b: 254)), *Boreolimella*, *Hanikraia* and *Pusillargillus*. Both *Hanikraia derketo* and *Pusillargillus nixe* (Por, 1964b) share with *C. galapagoensis* the absence of enlarged spinulose spines on the antennule (typically one on second and apical segments, two on third segment) and the short caudal rami. *Hanikraia derketo* displays the most plesiomorphic swimming leg segmentation and armature, having 3-segmented endopods on legs 1–3 and three outer spines on P2–P4 exp-3 (Table 2). Both *P. nixe* and *C. galapagoensis* display the 2-segmented condition in the endopods of legs 1–4 and have only two outer spines on P2–P4 exp-3; based on these synapomorphies these species cannot be placed in *Hanikraia*. *Pusillargillus nixe* differs from *C. galapagoensis* in the segmentation of the P1 endopod, the presence of an enlarged outer spine on P1 exp-3, the unipinnate nature (with very long pinnules in distal half) of the outer exopodal spines on legs 2–4 and the separation of leg 5 exopod and baseoendopod in both sexes. *Carolinicola galapagoensis* has retained the 3-segmented condition of the P1 endopod but displays a more reduced armature on the endopods of legs 2–4 (Table 2). Based on this combination of mutually exclusive characters states, *C. galapagoensis* and *P. nixe* cannot be considered congeneric and consequently the former is here fixed as the type species of a new genus, *Sympodella* gen. n. whose diagnosis is given below.

Family Canthocamptidae Brady, 1880
Subfamily Hemimesochrinae Por, 1986

Genus *Sympodella* gen. n.

http://zoobank.org/3D8C3AAA-42DC-4D11-AE0F-0EB5F870F134

Diagnosis. Rostrum defined at base; triangular. Antennule 6-segmented in ♀, with aesthetasc on segments 3 and 6; 9-segmented, haplocer with geniculation between segments 7 and 8 in ♂; without enlarged modified spines in both sexes. Antenna with two abexopodal setae on allobasis; exopod 1-segmented, with three setae. Mandibular palp with elongate basis (with one seta), 1-segmented endopod (with four setae) and ves-

tigial unisetose exopod. Maxillule with rami incorporated into basis. Maxilla with two endites on syncoxa; endopod fused to allobasis. Maxilliped with well developed seta on syncoxa. Swimming legs of ♀ with 3-segmented exopods and 3- (P1) or 2-segmented endopods (P2–P4); armature formulae as in Table 2. Inner seta of P1 enp-1 recurved backwardly and dorsally; outer spine of P1 exp-1 not enlarged; outer exopodal spines of P1–P4 bipinnate, without elongate pinnules in proximal half. Inner distal seta of P2 enp-2 and outer distal seta of P4 enp-2 longer in ♂. P3 endopod 3-segmented in ♂; enp-2 with inner seta and slender terminal apophysis; enp-3 with two apical setae. P5 with fused exopod and baseoendopod, forming weakly bilobate plate in both sexes; exopodal lobe with five and six elements in ♀ and ♂, respectively; endopodal lobe with four and two elements in ♀ and ♂, respectively. Sixth pair of legs asymmetrical in ♂, each with two tiny setae. Caudal ramus short, with six setae.

Type and only species. *Carolinicola galapagoensis* Mielke, 1997 = *Sympodella galapagoensis* (Mielke, 1997) (by original designation).

Etymology. The name is derived from the Greek *syn*, *sym*, meaning together, and *pous* (genitive *podos*), meaning foot, and refers to the fused condition of leg 5 in both sexes. Gender: feminine.

A note on *Isthmiocaris* George & Schminke, 2003 and related genera

George and Schminke (2003) proposed the monotypic genus *Isthmiocaris* for a deepwater species, *I. longitelson* George & Schminke, 2003, from the Patagonian continental slope, and considered it most closely related to *Itunella* Brady, 1896 and *Bathycamptus*, primarily on account of the sexual dimorphism expressed in the endopods of P3–P4. Bruch et al. (2011) added a second species, *I. laurae* Bruch, Glatzel & Veit-Köhler, 2011 from the Angola Basin, which differed substantially from the type species in the segmentation and armature of the swimming legs (Table 4) and in the absence of the postcephalothoracic collar (or "isthmion" — the primary diagnostic of the genus). While endorsing George and Schminke's (2003) view on its relationships within the Canthocamptidae, they also recognized a close affinity (and potential synonymy) with the genus *Pyrocletodes* Coull, 1973b. The latter currently accommodates two deepwater species, *P. desuramus* Coull, 1973b from the deep sea off North Carolina and *P. coulli* Dinet, 1976 from the Angola Basin, both known exclusively from females (Coull 1973b, Dinet 1976) (Table 4). Coull (1973b) assigned *Pyrocletodes* to the Cletodidae but this course of action was disputed by Dinet (1976) who preferred to view its position as uncertain. For some inexplicable reason Por (1986) claimed that *Pyrocletodes* is a member of the Tetragonicipitidae, erroneously citing Dinet (1976) as the source for this familial assignment. This claim was considered a slip of the pen by several authors (Kunz 1994, Fiers 1995, Huys 1995). Huys et al. (1996) transferred the genus to the Canthocamptidae but gave no formal justification for this action while others continued to consider it as a *genus incertae sedis*, either in the Cletodidae (Wells 2007), the Podogennonta (Seifried 2003), the Syngnatharthra (Seifried and Schminke 2003) or the Harpacticoida (Bodin

Table 4. Salient characters of members of *Pyrocletodes* Coull, 1973b, *Perucamptus* Huys & Thisle, 1989 and *Isthmiocaris* George & Schminke, 2003. [A1 ♀: number of segments and position of aesthetasc (ae); A2 exp = number of setae on antennary exopod; P3 enp: apo = apophysis; P5: b = outer basal setae, sp = spine(s); — = absent].

Species	sex	A1 ♀	A2	P1		P2		P3		P4		P5
			exp	exp	enp	exp	enp	exp	enp	exp	enp	
Pyrocletodes desuramus	♀	5 (ae on 3)	2	0.1.022	1.020	0.1.122	—	0.1.122	—	0.1.122	—	b + 2
Pyrocletodes coulli	♀	5 (ae on 3)	3	0.0.021	1.020	0.1.122	—	0.1.122	—	0.1.122	—	b + 2
Perucamptus rapiens	?†	5 (ae on 3)	3	0.0.022	1.121	0.1.122	0.121	0.1.122	0.020	0.1.122	—	b+2 + 2
Isthmiocaris longitelson	♀	6 (ae on 4)	3	0.021	010	0.020	—	0.1.021	—	0.021	—	1
	♂		3	0.021	010	0.021	—	0.1.021	0.apo.020	0.0.021	0.021	b + 2 + sp
Isthmiocaris laurae	♀	6 (ae on 3)	3	0.0.022	0.011	0.0.022	020	0.0.022	020	0.0.022	010	b + 2
	♂		3	0.0.022	0.021	0.1.122	1.321	0.1.222	1.apo.020	0.1.222	0.221	b + 5 + 2sp
	CV♀	?	?	0.0.022	0.021	0.0.022	0.020	0.0.022	0.020	0.0.022	010	?
	CV♂	?	?	0.0.022	0.021	0.1.122	0.121	0.1.122	0.0.021	0.1.022	0.011	?

† Becker's (1979) dorsal habitus drawing of the holotype suggests that he was dealing with a copepodid V stage, presumably a CV♀.

1997). Based on the elongate, cylindrical habitus, caudal ramus shape, mouthpart morphology, and strongly reduced leg 5 there is no doubt that *Isthmiocaris* and *Pyrocletodes* are closely related and should be placed in the same family. Coincidently, these morphological attributes are also shared by another genus of doubtful affiliation, *Perucamptus*, which was established to accommodate a single species, *Hemimesochra rapiens*, from the Peru–Chile (Atacama) Trench (Becker 1979, Huys and Thistle 1989). All three genera could potentially be synonymous with *Pyrocletodes* taking priority over the other two. However, both *Pyrocletodes* and *Perucamptus* are known from females only and the sexual dimorphism expressed in the swimming legs is of primary importance in elucidating the relationships within the Canthocamptidae in general and the Hemimesochrinae in particular. For example, Huys and Kihara (2010) assigned *Metahuntemannia* Smirnov, 1946 and *Dahmsopottekina* Özdikmen, 2009 [note that Huys and Kihara (2010) cite the name *Pottekia* Huys, 2009, a new generic name intended to replace *Talpina* Dahms and Pottek, 1992 in Huys (2009) but which was subsequently withdrawn at the proof stage of that publication in favour of *Dahmsopottekina*] to the Hemimesochrinae based on the sexual dimorphism expressed on the P4 endopod (distal inner seta of the female modified into a serrate curved spine in the male; cf. *Pottekia pectinata* (Dahms & Pottek, 1992): Dahms and Pottek, 1992: Fig. 35), a character indicating affinity with genera such as *Bathycamptus*, *Micropsammis* Mielke, 1975 and *Isthmiocaris*. In addition to the lack of information on the male, the difficulties in confirming the validity of *Perucamptus* are exacerbated by the fact that the type and only species, *P. rapiens* (Becker, 1979), may be based on a juvenile. Becker's (1979) dorsal habitus drawing of the holotype suggests that he was dealing with a copepodid V stage, presumably a CV♀, since the purported genital double-somite is remarkably short for an adult female.

Acknowledgements

The present work was carried out under a Royal Society Royal Fellowship awarded to F.-h. Mu and also funded jointly by the National Science Foundation of China (41576153; 41106122; 40906063) and National Science Foundation of Shandong Province (ZR2010CM013). Dr Kate Shalaeva (AKT Solutions Ltd, Rayleigh, U.K.) is gratefully acknowledged for her help in translating Kornev and Chertoprud's (2008) Russian text. The authors would like to thank the three reviewers for their helpful and constructive comments.

References

Baguley JG (2004) Meiofauna community structure and function in the northern Gulf of Mexico deep Sea. PhD Thesis, The University of Texas at Austin, Austin.

Becker K-H (1972) Eidonomie und Taxonomie abyssaler Harpacticoidea. PhD Thesis, Christian Albrechts Universität, Kiel.

Becker K-H (1979) Eidonomie und Taxonomie abyssaler Harpacticoida (Crustacea, Copepoda). Teil II. Paramesochridae, Cylindropsyllidae und Cletodidae. Meteor Forschungs-Ergebnisse (D)31: 1–37.

Bodin P (1997) Catalogue of the new marine harpacticoid copepods (1997 edition). Documents de Travail, Institut royal des Sciences naturelles de Belgique 89: 1–304.

Bodin P, Le Guellec C (1992) Meiobenthos of the Bay of Saint-Brieuc (North Brittany, France). II: Harpacticoid copepod diversity and species assemblages. Oceanologica Acta 15: 673–686.

Brooks JM, Fisher C, Roberts H, Bernard B, McDonald I, Carney R, Joye S, Cordes E, Wolff G, Goehring E (2009) Investigations of chemosynthetic communities on the lower continental slope of the Gulf of Mexico: Interim Report 2. U.S. Dept. of the Interior, Minerals Management Service, Gulf of Mexico OCS Region, New Orleans, LA. OCS Study MMS 2009-046, 360 pp.

Bruch K, Glatzel T, Veit-Köhler G (2011) *Isthmiocaris laurae* sp. nov. (Crustacea, Copepoda, Harpacticoida) from the Angola Basin – First deep-sea species of the genus with remarks on its copepodid development. Meiofauna marina 19: 173–193.

Coull BC (1973a) Meiobenthic Harpacticoida (Crustacea, Copepoda) from the deep sea off North Carolina. I. The genera *Hemimesochra* Sars, *Paranannopus* Lang, and *Cylindronannopus* n. g. Transactions of the American microscopical Society 92: 185–198. https://doi.org/10.2307/3224915

Coull BC (1973b) Meiobenthic Harpacticoida (Crustacea, Copepoda) from the deep sea off North Carolina. IV. The families Cletodidae T. Scott and Ancorabolidae Sars. Transactions of the American microscopical Society 92: 604–629. https://doi.org/10.2307/3225271

Dahms H-U, Pottek M (1992) *Metahuntemannia* Smirnov, 1946 and *Talpina* gen. nov. (Copepoda, Harpacticoida) from the deep-sea of the high Antarctic Weddell Sea with a description of eight new species. Microfauna marina 7: 7–78.

Dinet A (1976) Sur une nouvelle forme du genre *Pyrocletodes* Coull, 1973 (Copepoda, Harpacticoida) à position systématique incertaine. Bulletin de la Société zoologique de France 100: 437–442.

Fiers F (1995) New Tetragonicipitidae (Copepoda, Harpacticoida) from the Yucatecan continental shelf (Mexico), including a revision of the genus *Diagoniceps* Willey. Bulletin de l'Institut royal des Sciences naturelles de Belgique, Biologie 65: 151–236.

Garlitska LA, Azovsky AI (2016) Benthic harpacticoid copepods of the Yenisei Gulf and the adjacent shallow waters of the Kara Sea. Journal of natural History 50: 2941–2959. https://doi.org/10.1080/00222933.2016.1219410

George KH (1999) Gemeinschaftsanalytische Untersuchungen der Harpacticoidenfauna der Magellanregion, sowie erste similaritätsanalytische Vergleiche mit Assoziationen aus der Antarktis [Community analysis of the harpacticoid fauna of the Magellan Region, as well as first comparisons with Antarctic associations, basing on similarity analyses.]. Berichte zur Polarforschung 327: 1–187. https://doi.org/10.1163/20021975-99990321

George KH (2005) Sublittoral and bathyal Harpacticoida (Crustacea: Copepoda) of the Magellan region. Composition, distribution and species diversity of selected major taxa. In: Arntz WE, Lovrich GA, Thatje S (Eds) The Magellan-Antarctic connection: links and frontiers at high southern latitudes. Scientia marina 69(Suppl. 2), 147–158.

George KH (2013) Faunistic research on metazoan meiofauna from seamounts – a review. Meiofauna marina 20: 1–32.

George KH, Schminke HK (2003) *Isthmiocaris longitelson* gen. et sp. nov., a strongly derived harpacticoid (Copepoda) from the Magellan region, and its systematic affinities to certain "canthocamptid" taxa. Journal of crustacean Biology 23: 119–130.

Gheerardyn H, De Troch M, Vincx M, Vanreusel A (2009) Harpacticoida (Crustacea: Copepoda) associated with cold-water coral substrates in the Porcupine Seabight (NE Atlantic): species composition, diversity and reflections on the origin of the fauna. Scientia marina 73: 747–760. https://doi.org/10.3989/scimar.2009.73n4747

Grego M, Riedel B, Stachowitsch M, De Troch M (2014) Meiofauna winners and losers of coastal hypoxia: case study harpacticoid copepods. Biogeosciences 11: 281–192. https://doi.org/10.5194/bg-11-281-2014

Huys R (1995) Some remarks on the taxonomic status of *Paraschizopera* Wells, 1981 (Copepoda: Harpacticoida). Hydrobiologia 308: 23–28. https://doi.org/10.1007/BF00037783

Huys R (2009) Unresolved cases of type fixation, synonymy and homonymy in harpacticoid copepod nomenclature (Crustacea: Copepoda). Zootaxa 2183: 1–99.

Huys R, Boxshall GA, 1991. Copepod Evolution. The Ray Society, London, 468 pp.

Huys R, Gee JM, Moore CG, Hamond R (1996) Marine and brackish water harpacticoid copepods. Part 1. Synopses of the British Fauna (New Series), 51. Field Studies Council, Shrewsbury, 352 pp.

Huys R, Kihara TC (2010) Systematics and phylogeny of Cristacoxidae (Copepoda, Harpacticoida): a review. Zootaxa 2568: 1–38.

Huys R, Thistle D (1989) *Bathycamptus eckmani* gen. et spec. nov. (Copepoda, Harpacticoida) with a review of the taxonomic status of certain other deepwater harpacticoids. Hydrobiologia 185: 101–126. https://doi.org/10.1007/BF00010809

Janssen A, Chevaldonné P, Martínez Arbizu P (2013) Meiobenthic copepod fauna of a marine cave (NW Mediterranean) closely resembles that of deep-sea communities. Marine Ecology Progress Series 479: 99–113. https://doi.org/10.3354/meps10207

Karaytuğ S, Huys R (2004) Taxonomic position of and generic distinction between *Parepactophanes* Kunz, 1935 and *Taurocletodes* Kunz, 1975 (Copepoda, Canthocamptidae *incertae sedis*), with description of a new species from the Black Sea. Zoological Journal of the Linnean Society 140: 469–486. https://doi.org/10.1111/j.1096-3642.2003.00101.x

Kim K, Lee W, Huys R (2011) A new species of *Sentiropsis* (Copepoda: Harpacticoida: Pseudotachidiidae) from the upper sublittoral zone off Hyeopjae beach, Jeju Island, Korea, and a key to genera of the subfamily Danielsseniinae. Proceedings of the biological Society of Washington 124: 179–197. https:/doi.org/10.2988/11-08.1

Kitahashi T, Kawamura K, Kojima S, Shimanaga M (2013) Assemblages gradually change from bathyal to hadal depth: A case study on harpacticoid copepods around the Kuril Trench (north west Pacific Ocean). Deep Sea Research Part I: Oceanographic Research Papers 74: 39–47. https://doi.org/10.1016/j.dsr.2012.12.010

Kornev PN, Chertoprud ES (2008) Veslonogie rakoobraznye otryada Harpacticoida Belogo Morya: morfologiya, sistematika, ecologiya. [Copepod crustaceans of the order Harpacti-

coida of the White Sea: morphology, systematics, ecology]. Tovarischchestvo Nauchnikh Izdanii KMK, Moscow, 379 pp. [in Russian]

Kotwicki L (2002) Benthic Harpacticoida (Crustacea, Copepoda) from the Svalbard archipelago. Polish polar Research 23: 185–191.

Kunz H (1994) Eine neue unterart von *Laophontella horrida* (Por) (Copepoda, Harpacticoida) von der Küste Namibias. Mitteilungen aus dem hamburgischen zoologischen Museum und Institut 91: 53–60.

Lang K (1936) Die Familie der Cletodidae Sars, 1909. Zoologische Jahrbücher für Systematik 68: 445–480.

Lang K (1944) Monographie der Harpacticiden (Vorläufige Mitteilung). Almqvist & Wiksells Boktryckeri Ab, Uppsala, 39 pp.

Lang K (1948) Monographie der Harpacticiden. Håkan Ohlsson, Lund, 1682 pp.

Lang K (1965) Copepoda Harpacticoidea from the Californian Pacific coast. Kungliga Svenska Vetenskapsakademiens Handlingar (4)10(2): 1–566.

Marinov T, Apostolov AM (1981) Contribution à l'étude des Copépodes Harpacticoïdes de la mer Adriatique (Côte yougoslave). 2. Sur le méiobenthos du Cap Piran. Acta zoologica bulgarica 18: 23–30.

Mielke W (1975) Systematik der Copepoda eines Sandstrandes der Nordseeinsel Sylt. Mikrofauna des Meeresbodens 52: 1–134.

Mielke W (1997) Interstitial Fauna of Galapagos. XL. Copepoda, Part 8. Microfauna marina 11: 153–192.

Monard A (1927) Synopsis universalis generum harpacticoidarum. Zoologische Jahrbücher für Systematik 54: 139–176.

Mu F-h, Zhang Z-n, Guo Y-q (2001) The study on the community structure of benthic copepods in the Bohai Sea. Acta oceanologica sinica 23: 120–127. [In Chinese with English summary]

Plum C, Gollner S, Martínez-Arbizu P, Bright M (2015) Diversity and composition of the copepod communities associated with megafauna around a cold seep in the Gulf of Mexico with remarks on species biogeography. Marine Biodiversity 45: 419–432. https://doi.org/10.1007/s12526-014-0310-8

Por FD (1960) *Mesopsyllus atargatis*, n. g., n. sp., ein neuer Harpacticoid (Copepoda Crustacea) aus dem Schwarzen Meer. Travaux du Muséum d'Histoire naturelle "Gr. Antipa" 2: 177–181.

Por FD (1964a) A study of the Levantine and Pontic Harpacticoida (Copepoda Crustacea). Zoologische Verhandelingen, Leiden 64: 1–128.

Por FD (1964b) Les Harpacticoïdes (Crustacea, Copepoda) des fonds meubles du Skagerak. Cahiers de Biologie marine 5: 233–270.

Por FD (1986) A re-evaluation of the Cletodidae Sars, Lang (Copepoda, Harpacticoida). In: Schriever G, Schminke HK, Shih C-t (Eds) Proceedings of the Second International Conference on Copepoda, Ottawa, Canada, 13–17 August, 1984. Syllogeus 58: 420–425.

Sars GO (1920) Copepoda Supplement. Parts V & VI. Harpacticoida (continued). An Account of the Crustacea of Norway, with short Descriptions and Figures of all the Species 7: 53–72. [plates XXXIII–XLVIII]

Seifried S (2003) Phylogeny of Harpacticoida (Copepoda): Revision of "Maxillipedasphalea" and Exanechentera. Cuvillier Verlag, Göttingen, 259 pp.

Seifried S, Schminke HK (2003) Phylogenetic relationships at the base of Oligoarthra (Copepoda, Harpacticoida) with a new species as the cornerstone. Organisms, Diversity and Evolution 3: 13–37. https://doi.org/10.1078/1439-6092-00056

Soyer J (1971) Bionomie benthique du plateau continental de la côte catalane française. III. Les peuplements de Copépodes Harpacticoïdes (Crustacea). Vie et Milieu (B)21: 337–511. [+ annexe]

Villiers L, Bodiou J-Y (1996) Community structure of harpacticoid copepods in a tropical reef lagoon (Frangataufa Atoll – French Polynesia). Oceanologica Acta 19: 155–162.

Wells JBJ (1965) Copepoda (Crustacea) from the meiobenthos of some Scottish marine sublittoral muds. Proceedings of the Royal Society of Edinburgh, Section B (Biology) 69(I-1): 1–33. https://doi.org/10.1017/S0080455X00010110

Wells JBJ (2007) An annotated checklist and keys to the species of Copepoda Harpacticoida (Crustacea). Zootaxa 1568: 1–872.

Willen E (2000) Phylogeny of the Thalestridimorpha Lang, 1944 (Crustacea, Copepoda). Cuvilier Verlag, Göttingen, 233 pp.

ZooKeys 718: 35–64 (2017)
doi: 10.3897/zookeys.718.19959
http://zookeys.pensoft.net

RESEARCH ARTICLE

A peer-reviewed open-access journal
ZooKeys
Launched to accelerate biodiversity research

Two new species of the genus *Emertonia* Wilson, 1932 from Korean waters (Copepoda, Harpacticoida, Paramesochridae)

Jinwook Back[1], Wonchoel Lee[2]

1 *Department of Taxonomy and Systematics, National Marine Biodiversity Institute of Korea, Seocheon 33662, Korea* **2** *Department of Life Science, College of Natural Sciences, Hanyang University, Seoul 04763, Korea*

Corresponding author: *Wonchoel Lee* (wlee@hanyang.ac.kr)

Academic editor: *K.H. George* | Received 1 August 2016 | Accepted 23 October 2017 | Published 4 December 2017

http://zoobank.org/2EFE0195-2167-4FCA-8DAC-44E14CB9BBD0

Citation: Back J, Lee W (2017) Two new species of the genus *Emertonia* Wilson, 1932 from Korean waters (Copepoda, Harpacticoida, Paramesochridae). ZooKeys 718: 35–64. https://doi.org/10.3897/zookeys.718.19959

Abstract

Two new species of the genus *Emertonia* were found from the west coast of Korea. The first new species, *E. koreana* **sp. n.**, is closely related to *E. acutifurcata*. However, the new species is clearly distinguished by the presence of two modified pinnate setae on the P5 baseoendopodal lobe. All body somites of the new species except for the last two urosomites have strongly developed hyaline frills forming quadrilateral lappets. The second new species, *E. simplex* **sp. n.**, superficially resembles *E. mielkei* in the structure of antennary exopod (with five setae), and the shape of P5. However, this new species differs from its congener mainly by having a caudal ramus 3.5 times as long as width, and P1 enp-2 with two claw-like setae. In addition, a key to the worldwide species of *Emertonia* is provided.

Keywords

Crustacea, Jeju Island, *Kliopsyllus*, Taxonomy, Yellow Sea

Introduction

The family Paramesochridae consists of 13 genera and more than 150 species distributed worldwide. Within the family, the genus *Emertonia* Wilson, 1932 is seen to be the most species-rich genus. Despite the rich diversity, there are still many unidentified species to be regarded as new species within the genus (Plum and George 2009; Back and Lee 2014). According to Plum and George (2009), most of the species of

Emertonia are discovered in the interstitial and coastal zone with an exception to four species found from the deep sea, *E. andeep* (Veit-Köhler, 2004), *E. diva* (Veit-Köhler, 2005), *E. minor* (Vasconcelos, Veit-Köhler, Drewes & Parreira dos Santos, 2009), and *E. schminkei* (Veit-Köhler & Drewes, 2009).

Kunz (1962) divided the family Paramesochridae into nine genera based on the segmentation, and setae formula of swimming legs. Although Kunz (1962) proposed the name *Kliopsyllus* with the generic diagnosis based on four species (*Leptopsyllus coelebs* Monard, 1928; *Paramesochra holsatica* Klie, 1929; *L. constrictus* Nicholls, 1935, and *P. major* Nicholls, 1939) and two sub-species (*P. holsatica varians* Kunz, 1951, and *P. constricata orotavae* Noodt, 1958), he failed to fix the type species for the genus. Huys (2009) claimed that *Emertonia* Wilson, 1932 is the replacement name for *Kliopsyllus*. To date, 48 species including six sub-species have been reported in *Emertonia*, and most species are found from sandy sediments.

In Korea, taxonomic studies on coastal benthic copepods are underway. Song et al. (2012) summarized the marine and brackish-water harpacticoids found in Korea. They reported a list including 88 marine and brackish-water harpacticoids belonging to 23 families (Song et al. 2012). Especially in the case of the family Paramesochridae, 11 species are found in the coastal sandy sediments (Back and Lee 2014; Back and Lee 2017). As a part of ongoing taxonomical study on the harpacticoid copepods, we aim to describe two new species of *Emertonia* sampled from sandy beaches in Korean Waters.

Materials and methods

The sediment samples for *Emertonia koreana* sp. n. were collected from the Chulripo Beach in the west coast of the Korean peninsula. The sediment samples for *E. simplex* sp. n. were collected from a subtidal zone of Jeju Island. Samples were fixed with 5% buffered formalin and dissected specimens were mounted on several slides separately using lactophenol as mounting medium. Slides were sealed with transparent nail varnish. Observations of the specimens were carried out using an LEICA DM 6000 equipped with a drawing tube. Specimens were deposited in the Marine Biodiversity Institute of Korea (MABIK).

To prepare specimens for scanning electron microscope analysis (SU3500; Hitachi, in National Marine Biodiversity Institute of Korea), specimens were transferred to 100 % ethanol, dehydrated by t-BuOH freeze dryer (VFD-21S; Vacuum Device), mounted on stubs using double-sided tape, coated with gold-palladium, and then photographed.

The descriptive terminology was adopted from Huys et al. (1996). Abbreviations used in the text are:

A1 antennule;
A2 antenna;
ae aesthetasc;
exp exopod;
enp endopod;
exp (enp)-1 **(2, 3)** to denote the proximal (middle, distal) segment;
P1–P6 first to sixth thoracopod;
benp baseoendopod.

Systematics

Order Harpacticoida Dana, 1846
Family Paramesochridae Lang, 1944
Genus *Emertonia* Wilson, 1932

***Emertonia koreana* sp. n.**
http://zoobank.org/FE323D1F-32E2-412B-93DF-38AFF9B6A2BF
Figs 1–5

Type locality. The Chulripo Beach, intertidal zone in the west coast of Korea, Yellow Sea (36°48'11.46"N, 126°08'58"E) by sand rinsing collected by J. Back on 14 May 2010 (Back and Lee 2014, as *Emertonia* sp. 3)

Material examined. Holotype 1♀ dissected on 4 slides (MABIK CR00241565). Paratypes: 1♂ on 3 slides (MABIK CR00241566), and 5 ♀♀ (MABIK CR00241570 – 00241574), 3 ♂♂ (MABIK CR00241567 – CR00241569) in 70 % ethanol. 1♀ and 1♂ dried, mounted on stub, and coated with gold-palladium for SEM.

Diagnosis. Female P5 deeply divided into two parts in the center of both P5 baseoendopods. Two setae of baseoendopod swollen near the base. Innermost seta of P5 exopods somewhat swollen at base, similar to setae of baseoendopod. Urosomites armed with rectangular frills, except for the last two segments.

Description of female. Body. Length 330 μm (n = 6, mean = 325 μm); largest width measured at cephalic shield; 55 μm; cylindrical, slightly depressed dorsoventrally; whole body very hyaline; sensilla and pores on dorsal surface as figured (Fig. 1A, B).

Prosome (Fig. 1A, B). Comprising cephalothorax, and three free pedigerous somites; cephalothorax bell-shaped, with sensilla and pores as figured; pleural areas weakly developed and posterolateral angles rounded; posterior margin smooth; somites bearing P2–P4 with strongly developed hyaline frills forming quadrilateral lappets (Fig. 1A–C).

Urosome (Fig. 1A–C) Genital somite and first abdominal somite completely fused forming genital double-somite; genital field located mid-ventrally at approximately half length of genital double-somite; copulatory pore presumably covered by P6; P6 (Figs 1C, 5C) represented by one plate with one uni-pinnate seta each side; penultimate somite with bilobed, smooth pseudoperculum; anal somite small, with two pores dorsally.

Caudal ramus (Figs 1D, E, 5A). Juxtaposed, approximately 2.8 times as long as greatest width, conical, distal margin acutely pointed; each ramus armed with seven setae; seta I small, bare, arising ventrally; seta II bare; setae III stout, ornamented with spinule-like elements; seta IV bare; seta V pinnate, longest; seta VI shortest, bare; setae IV–VII displaced onto dorsal surface of ramus; seta VII bi-articulate at base and arising from inner dorsal surface.

Rostrum (Fig. 1A). Triangular, ventrally directed, fused with cephalic shield, without sensilla.

Antennule (Fig. 2A). Eight-segmented; proximal segment longest and ornamented with a few long spinules along lateral margin; fourth segment (Fig. $2A_1$) forming sub-

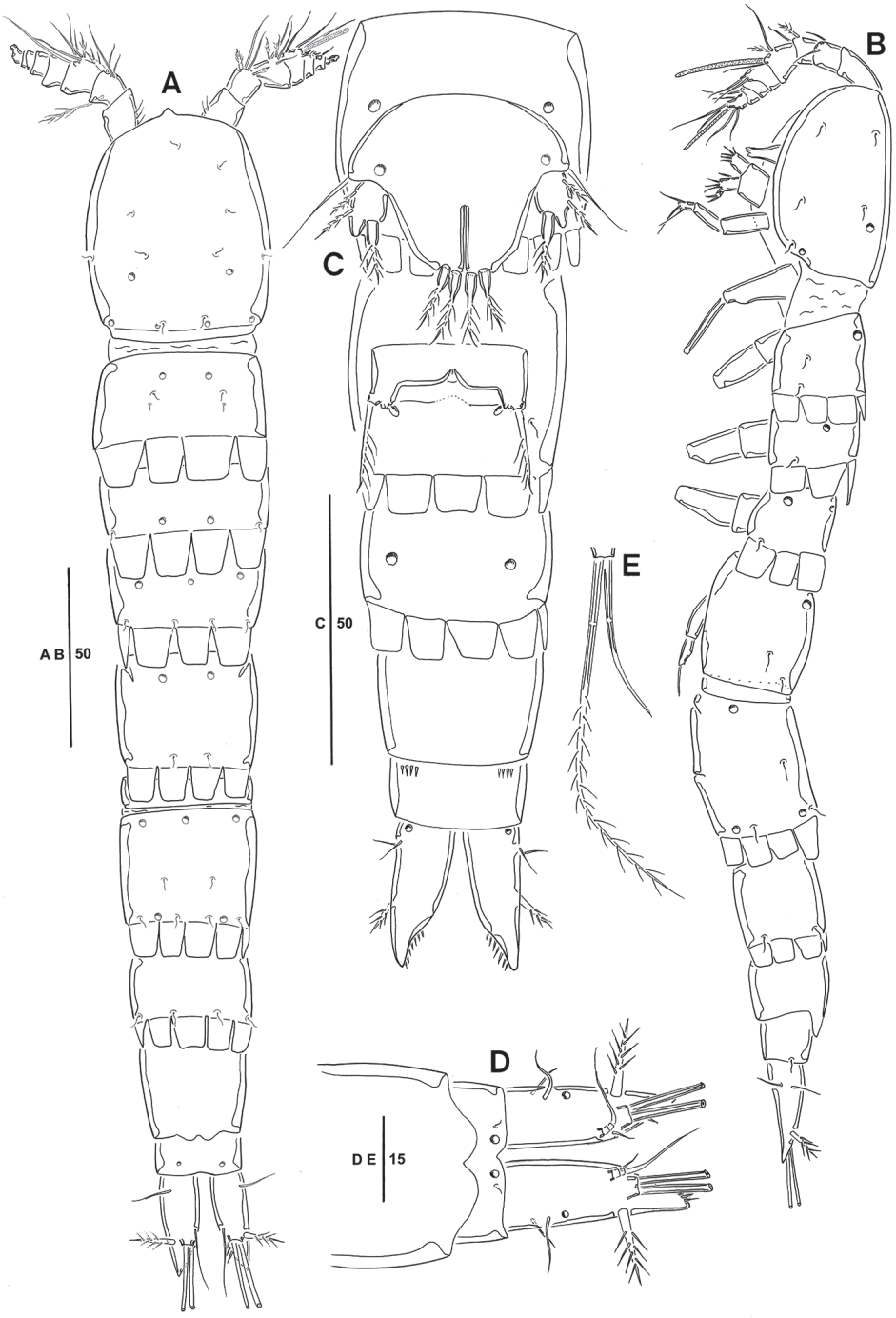

Figure 1. *Emertonia koreana* sp. n., holotype (♀). **A** habitus, dorsal **B** habitus lateral **C** urosome, ventral **D** caudal rami, dorsal **E** caudal seta IV and V. Scale bars are in μm.

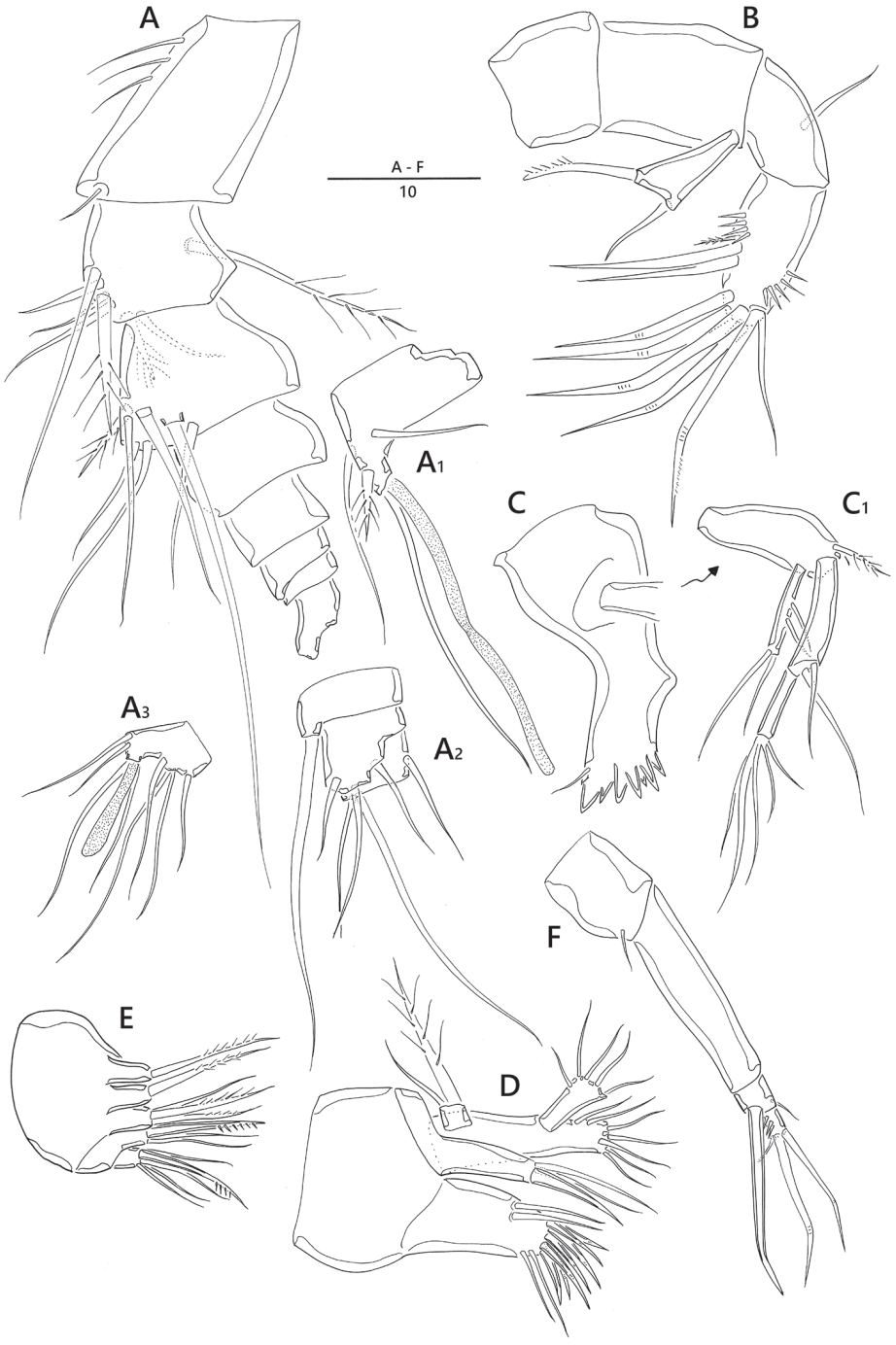

Figure 2. *Emertonia koreana* sp. n., holotype (♀). **A** antennule (**A**$_1$ fourth segment **A**$_2$ fifth, sixth, and seventh segments **A**$_3$ last segment) **B** antenna **C** mandible (**C**$_1$ plap) **D** maxillule **E** maxilla **F** maxilliped. Scale bar is in μm

cylindrical process armed with one long slender seta fused basally to aesthetasc; sixth segment (Fig. $2A_2$) armed with one slender bare seta arising from ventral sub-cylindrical process; armature formula: 1 – [1 bare], 2 – [5 bare + 3 pinnate], 3 – [6 bare + 1 pinnate], 4 – [2 bare + 1 pinnate + (1 + ae)], 5 – [1 bare], 6 – [3 bare], 7 – [3 bare], 8 – [6 bare + acrothek]; apical acrothek (Fig. $2A_3$) consisting of short aesthetasc fused basally to two naked setae.

Antenna (Fig. 2B). Four-segmented, comprising coxa, basis, one-segmented exp, and two-segmented enp; coxa small and bare; basis without any surface ornamentation; exp unequal Y-shape with one bare and one uni-pinnate setae; enp-1 with one bare abexopodal seta; enp-2 armed with one pinnate spine, two spine-like setae laterally, four geniculate setae around distal margin, and one longest geniculate seta fused at base with one bare seta.

Mandible (Fig. 2C). Coxa with gnathobase bearing one bare seta at dorsal corner and seven teeth; palp (Fig. $2C_1$) biramous, comprising basis, one-segmented exp and two-segmented enp; basis widening distally, with one pinnate seta; exp with two lateral and two distal setae; enp-1 with two bare setae; enp-2 with five basally fused setae at apex.

Maxillule (Fig. 2D). Praecoxal arthrite well developed, with seven spines, two bare setae around distal margin, and two juxtaposed slender setae on anterior surface near outer margin; coxa fused with cylindrical endite, armed with two bare setae and one stout spine; basis fused with endite, armed with seven bare setae; exp one-segmented, small, with one bare and one pinnate setae; enp one-segmented, with five bare setae.

Maxilla (Fig. 2E). Syncoxa with three endites; proximal and second endites with one pinnate seta; third endite with one bare and two uni-pinnate setae; allobasis with one strong pinnate claw and two bare setae; enp one-segmented, with one stout spine and four bare setae.

Maxilliped (Fig. 2F) four-segmented, comprising syncoxa, basis and two-segmented enp; syncoxa with one bare seta distally; basis bare; enp-1 with one geniculate and one small setae; enp-2 small, with two geniculate and one bare setae around distal margin.

P1 (Fig. 3A). Coxa ornamented with rows of spinules; basis with one pinnate inner seta and one bare outer seta, and ornamented with one pore near base of outer seta; enp 1.9 times as long as exp; exp two-segmented; exp-1 with one pinnate outer seta; exp-2 short, sub-quadrilateral, with three pinnate and one uni-pinnate setae; enp two-segmented; enp-1 long, bare; enp-2 small, with two short geniculate setae.

P2, P3 (Fig. 3B, C). Coxa ornamented with rows of spinules; basis with one bare outer seta, one pore near base of exp, and rows of spinules as figured; exp three-segmented; exp-1 with one outer spine and ornamented with row of long spinules along inner margin; exp-2 with one outer spine, inner distal corner forming spinous projection; exp-3 with two outer spines and two pinnate setae; enp one-segmented, with one plumose apical seta.

P4 (Fig. 3D). Coxa ornamented with two rows of spinules on anterior surface; basis with one bare outer seta and one pore; exp three-segmented; exp-1 and exp-2 with one outer spine; exp-3 with one outer spines and one pinnate apical seta; enp one-segmented with one apical seta.

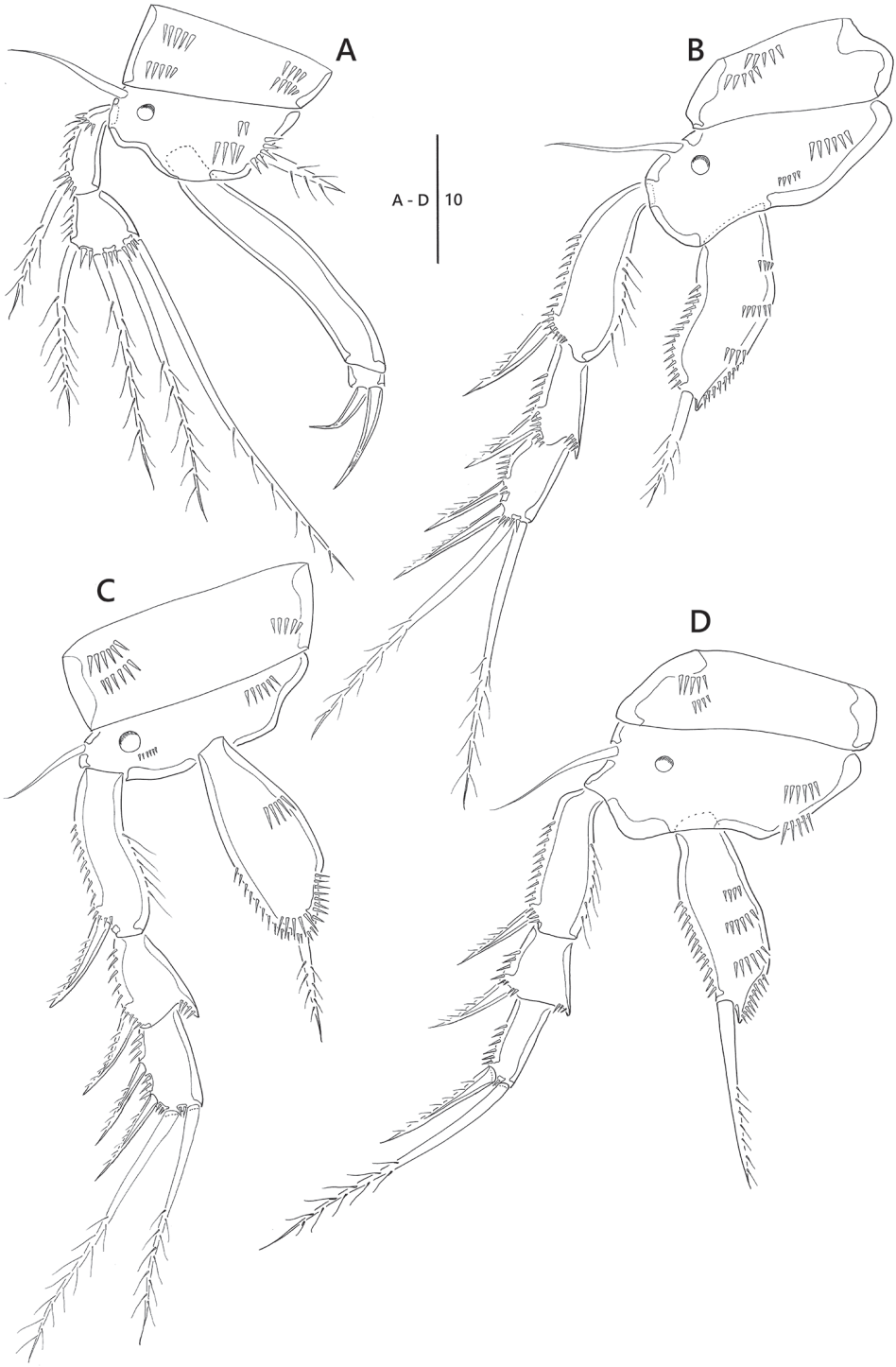

Figure 3. *Emertonia koreana* sp. n., holotype (♀). **A** P1 **B** P2 **C** P3 **D** P4. Scale bar is in μm.

Armature formula as follows:

	Exopod	Endopod
P1	0.121	0.011
P2	0.0.112	010
P3	0.0.112	010
P4	0.0.011	010

P5 (Figs 1C, 5B). Comprising medially fused benps and discrete exps; benp with one basal seta and ornamented with one pore; endopodal lobes elongated and separated by median cleft; each with two pinnate modified setae; exopod with two pinnate and one modified setae, and outer corner forming projection.

Description of male. Body (Fig. 4A) length 320 μm (n = 4, mean = 315 μm); largest width measured at posterior margin of cephalic shield: 45 μm; general body shape and ornamentation as in female; except for last two urosomites, urosome somites present strongly developed hyaline frills from dorsal to venteral (Fig. 5D); additional sexual dimorphism in A1, P5, and P6.

Antennule (Fig. 4B). Seven-segmented, short, robust, subchirocer; fifth-segment (Fig. $4B_1$) swollen, largest, forming sub-cylindrical process with one long slender seta fused basally to aesthetasc. Armature formula: 1 – [1 bare], 2 – [7 bare + 1 pinnate], 3 – [2 bare + 1 pinnate], 4 – [2 bare], 5 – [3 bare + 2 pinnate + (1 + ae)], 6 – [2 bare], 7 – [5 bare + acrothek], acrothek (Fig. $4B_2$) consisting of aesthetasc and two bare setae.

Swimming legs P1–P4 shape and setae formulae as in female (Fig. 5E, F)

P5 (Figs 4C, 5G). Comprising medially fused benp and discrete exp; benp with one basal seta; endopodal lobes weakly developed, without any element; exopod small, with two pinnate outer and one modified inner setae.

P6 (Figs 4D, 5H). Asymmetrical; each P6 with one outer and two inner setae, ornamented with one pore.

Etymology. The species name refers the type locality of new species, Republic of Korea.

Remarks. The new species *Emertonia koreana* sp. n. is closely related with *E. acutifurcata* (Mielke, 1985). They share similar shape of caudal ramus. *E. koreana* sp. n. and *E. acutifurcata* only have sub-triangular caudal ramus. Within the genus *Paramesochra*, similar morphology of caudal ramus is observed in *P. acutata acutata* Klie, 1935, *P. acutata hawaiiensis* Kunz, 1981, and *P. taeana* Back & Lee, 2010. They also have same setal formula of P1–P5. *E. koreana* sp. n. can be easily distinguished from those species based on the following unique characteristics: 1) female P5 is deeply divided into two parts in the center of both P5 baseoendopods. 2) Two setae at the end of baseoendopod are swollen near the base. In addition, the base of the innermost seta of P5 exopods is swollen, similar to setae of baseoendopod. 3) There are rectangular frills, except for the last two segments of urosomite. This structure is similar to that of *P. taeana*, but has not been reported in the genus *Emertonia* yet.

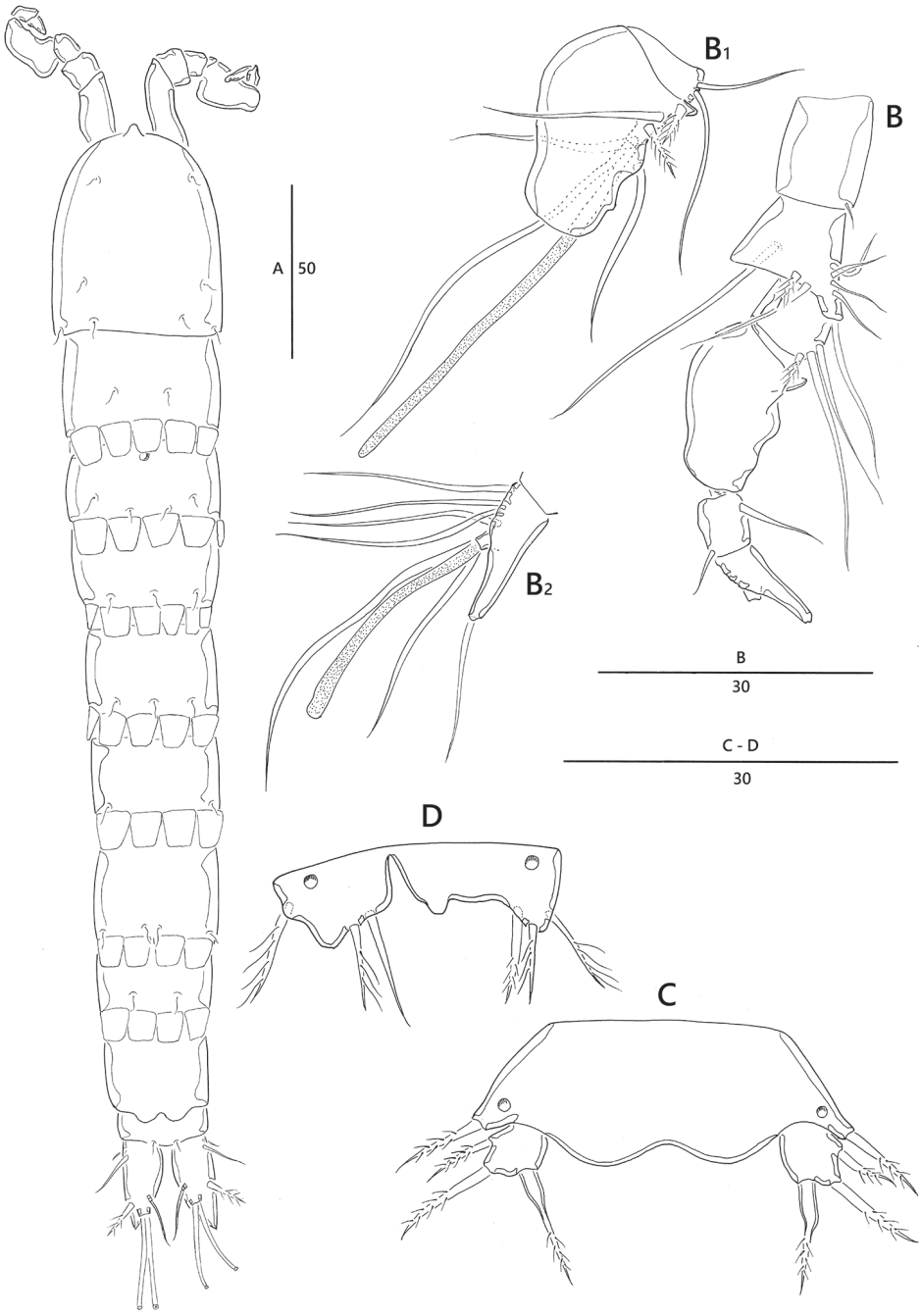

Figure 4. *Emertonia koreana* sp. n., (♂). **A** habitus, dorsal **B** antennule (**B**$_1$ fifth segment **B**$_2$ last segment) **C** P5 **D** P6. Scale bars are in μm.

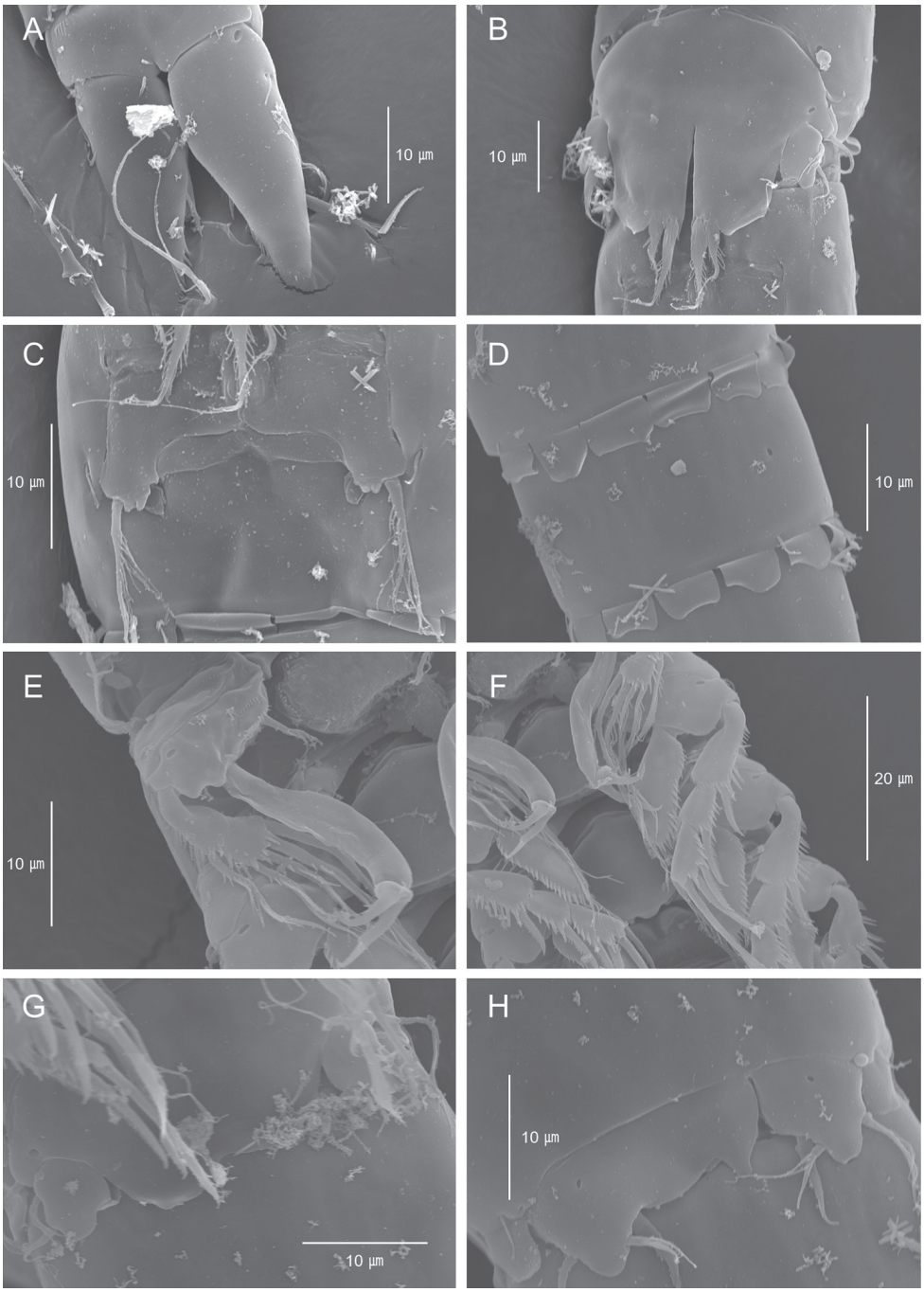

Figure 5. *Emertonia koreana* sp. n., SEM photographs. **A** caudal rami, ventral (♀) **B** P5 (♀) **C** P6 (♀) **D** sixth and seventh somites, ventral (♂) **E** P1 (♂) **F** P2 and P3 (♂) **G** P5 (♂) **H** P6 (♂).

***Emertonia simplex* sp. n.**
http://zoobank.org/2E7AB618-93AA-4942-AC8C-B3DB5183CFF9
Figs 6–11

Type locality. A subtidal zone near the Seogwipo Port in Jeju Island, Korea (33°13'33"N, 126°34'39"E), and sampled by using a grab (surface area: 0.1 m^2) on a fishing boat (Back and Lee 2014, as *Emertonia* sp. 2), depth 15–20 m, sand.

Material examined. Holotype 1♀ dissected on 7 slides (MABIK CR00241575), and paratypes: 1♂ on 5 slides (MABIK CR00241576). Additional paratypes represented by 3 ♀♀ (MABIK CR00241577 ~ CR00241579) and 2 ♂♂ (MABIK CR00241580, CR00241581) in 70 % ethanol. 2♀♀ dried, mounted on stub, and coated with gold-palladium for SEM. All samples were collected from the type locality by J. Back on 4 June 2010.

Diagnosis. *Emertonia simplex* sp. n. with four setae at P5 exopod in male, and one short Inner seta at P5 baseoendopod in female. Caudal rami rectangular, approximately 3.8 times as long as its width. Body armed with long dorsal sensilla.

Description of female. Body cylindrical, slightly depressed dorsoventrally (Figs 6A–B, 11A), with long sensilla (Fig. 11B); total body length, 390 μm (n = 7, mean = 376 μm); largest width (85 μm) measured at posterior margin of cephalic shield; body somites without hyaline frills forming quadrilateral lappets.

Prosome (Fig. 6A, B). Comprising cephalothorax, and three free pedigerous somites; Cephalothorax bell-shaped, with several sensilla; pleural areas weakly developed, posterolateral angles rounded.

Urosomites (Fig. 6A, B). Gradually tapering posteriorly; genital somite and third urosomite completely fused forming genital double-somite (Figs 9C, 11E); genital field located in proximal half of genital double-somite, with copulatory pore positioned medially, and two pores; P6 (Figs 9C, 11E) represented by narrow transverse plate, each side armed with one pinnate seta; anal somite (Fig. 9A) without anal operculum, but with rounded pseudoperculum arising from penultimate somite.

Caudal rami (Figs 9A, 11F). Rectangular, approximately 3.2 times as long as wide; with seven setae; setae III–VI located around distal margin of ramus; seta I small, bare, arising laterally; seta II bare; seta III cylindrical, bare; seta IV well developed, bare, seta V longest, pinnate in middle; seta VI bare; dorsal seta VII bi-articulate at base, bipinnate in middle.

Rostrum (Fig. 6A) small, with rounded tip, fused with cephalothorax; without sensilla.

Antennule (Fig. 6C) slender, eight-segmented; proximal segment with row of long spinules along anterior margin and blunt process on lateral margin; fourth segment with sub-cylindrical process bearing one bare seta fused basally to aesthetasc; fifth segment with sub-cylindrical process with one bare seta (Fig. $6C_1$); armature formula: 1 – [1], 2 – [7 bare + 1 spinulose], 3 – [6 bare], 4 – [2 bare + (1 + ae)], 5 – [1 bare], 6 – [2 bare], 7 – [4 bare], 8 – [5 bare + (2 + ae)]; apical acrothek consisting of one apical aesthetasc and two basally fused bare setae (Fig. $6C_2$).

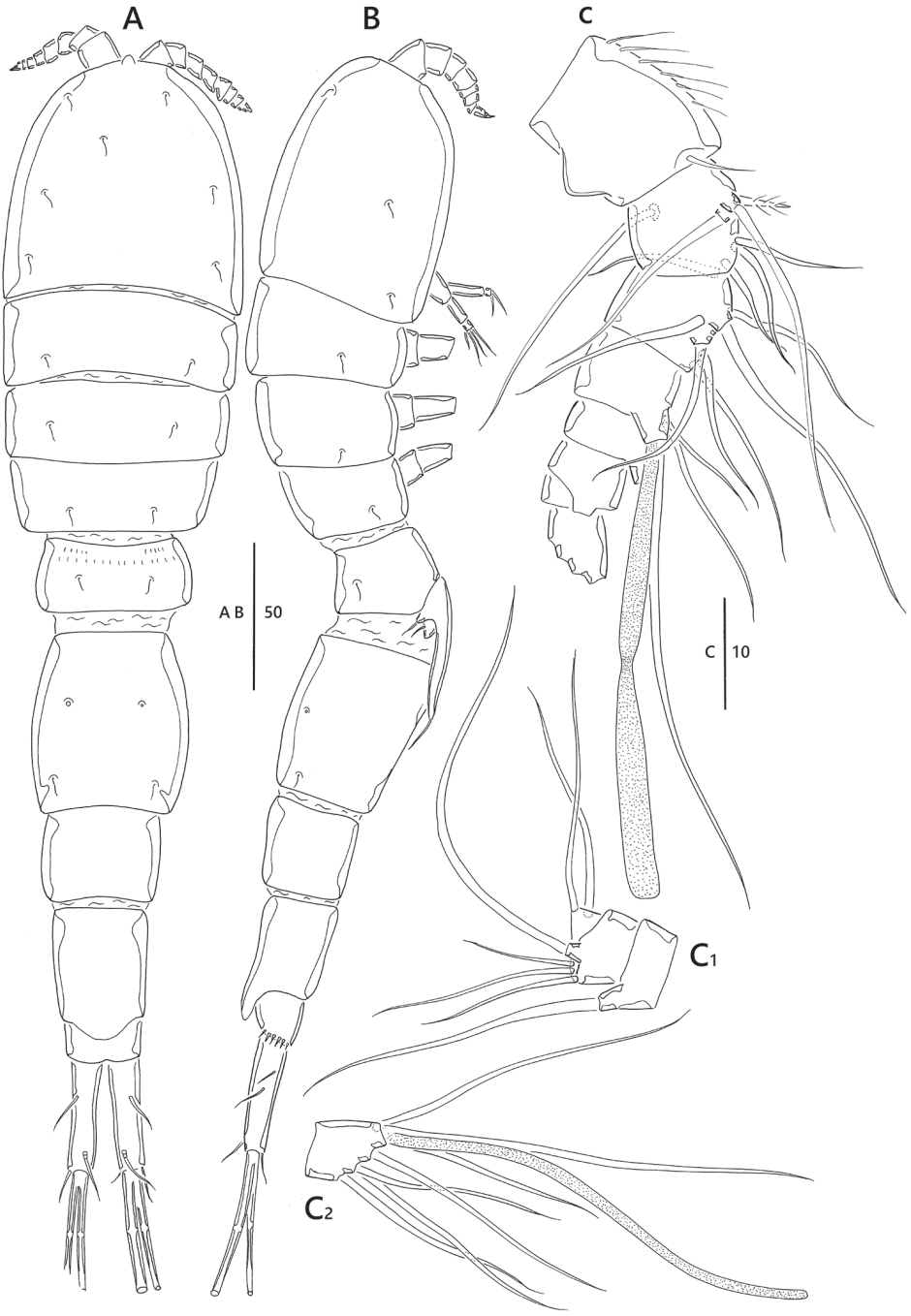

Figure 6. *Emertonia simplex* sp. n., (♀) **A** habitus, dorsal **B** habitus, lateral **C** antennule (**C**$_1$ fifth, sixth, and seventh segments **C**$_2$ last segment). Scale bars are in μm.

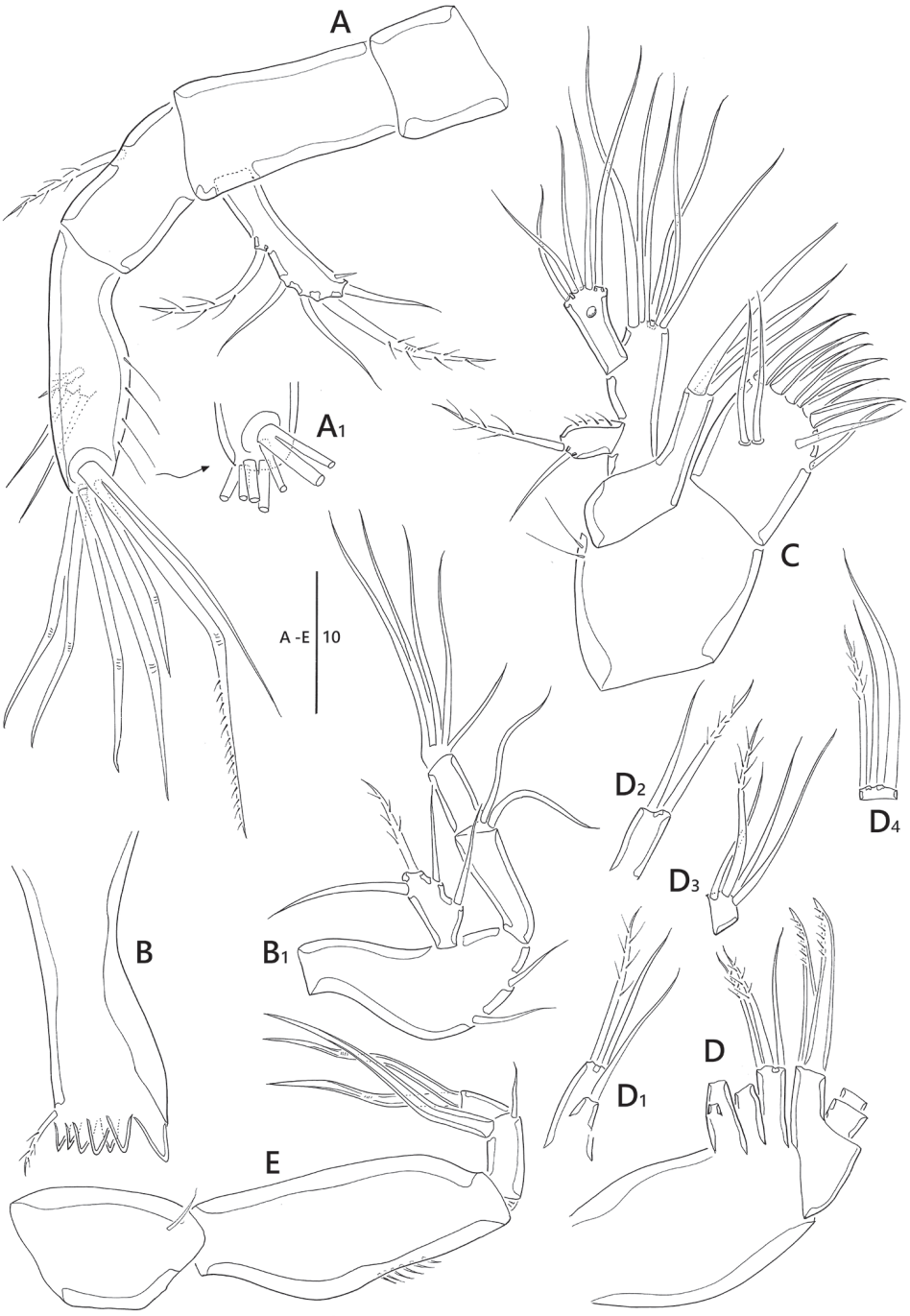

Figure 7. *Emertonia simplex* sp. n., (♀). **A** antenna (**A**$_1$ end of second segment in antenna endopod) **B** mandible (**B**$_1$ palp) **C** maxillule **D** maxilla (**D**$_1$ first endite **D**$_2$ second endite **D**$_3$ first segment of endopod **D**$_4$ second segment of endopod) **E** maxilliped. Scale bar is in μm.

Antenna (Fig. 7A). Coxa and basis without surface ornamentation; exp one-segmented, with two pinnate and three bare setae, and one spinule near outer distal corner; enp two-segmented; enp-1 with one pinnate seta, without surface ornamentation; lateral armature of enp-2 consisting of two bare setae, one pinnate seta, and long spinules along outer margin; distal armature of enp-2 (Fig. $7A_1$) consisting of six geniculate and one bare setae (one long bare seta fused at base to largest geniculate seta).

Mandible (Fig. 7B). Coxa well developed; gnathobase with seven blunt teeth and one small pinnate seta at dorsal corner; palp biramous (Fig $7B_1$), basis elongate, with two bare setae; exp one-segmented, with one pinnate and three bare setae; enp two-segmented, enp-1 1.7 times as long as enp-2, enp-1 with two bare setae; enp-2 with five setae fused at base.

Maxillule (Fig. 7C). Praecoxa subquadrate, with two long spinules; arthrite well developed, with six strong spines and two bare lateral setae, and two juxtaposed setae on surface; coxa with fused endite and three bare setae; basis fused with endites, with six setae; exp one-segmented, with one pinnate and one bare setae, and ornamented with row of spinules along inner margin; enp one-segmented, longer than exopod, with five bare setae around distal margin and one pore sub-distally.

Maxilla (Fig. 7D). Syncoxa armed with three endites; first endite (Fig. $7D_1$) bilobed, with one pinnate and two bare setae; second endite (Fig. $7D_2$) with one pinnate seta and one bare setae; distal endite with two pinnate and one bare setae; allobasis with two uni-pinnate stout setae on distal margin; enp two-segmented; enp-1 rectangular, with one pinnate seta near base, two bare and one pinnate setae; enp-2 with one pinnate and two bare setae along distal margin.

Maxilliped (Figs 7E, 11C) four-segmented; syncoxa with one bare seta; basis and ornamented with row of spinules along outer margin; enp two-segmented; enp-1 with one small bare seta laterally and one stout claw on distal margin; enp-2 with two geniculate setae.

P1 (Fig. 8A). Coxa and basis with spinules as figured; the latter with one bare outer and one bare inner setae; exp two-segmented; exp-1 longer than exp-2, the former with row of spinules along outer margin and one uni-pinnate outer spine; exp-2 with two uni-pinnate and two bare setae; enp approximately 1.8 times as long as exp; enp-1 elongate, bare, approximately five times as long as enp-2; enp-2 small, slightly longer than wide, with two claw-like setae.

P2, P3 (Figs 8B, C, 11D). Coxa with row of spinules on outer distal corner; basis with one bare outer seta, one pore near base of outer seta; exp three-segmented; exp-1 and exp-2 with one uni-pinnate spine; exp-3 with two uni-pinnate outer spines, one stout apical seta, and one pinnate seta; enp one-segmented with one pinnate apical seta.

P4 (Fig. 8D). Coxa ornamented with one row of spinules on outer distal corner; basis with one bare outer seta, one pore near base of outer seta; exp three-segmented; exp-1 and exp-2 with one uni-pinnate outer spine; exp-3 with one uni-pinnate outer spine and one apical seta; enp one-segmented, with one modified seta.

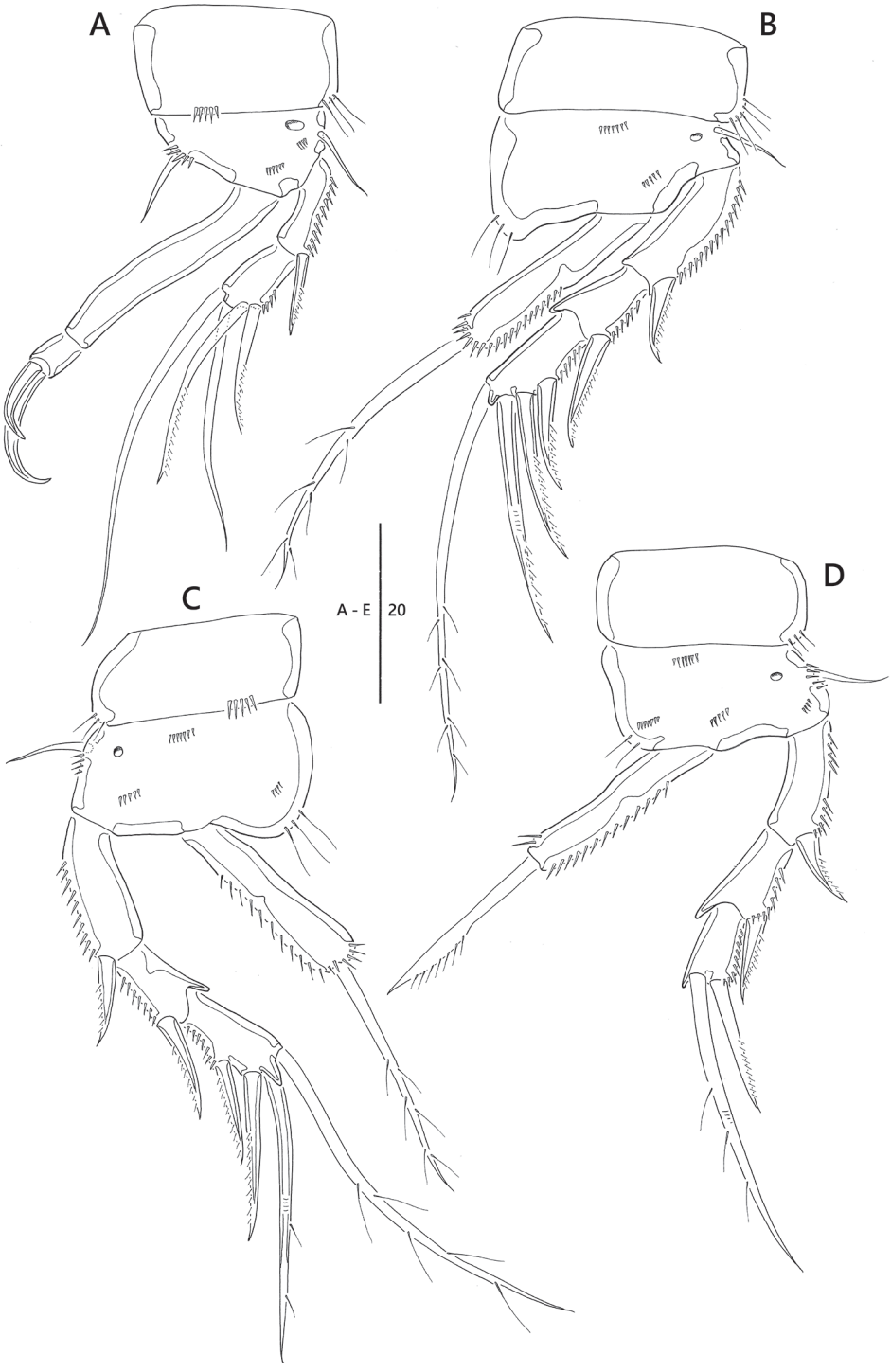

Figure 8. *Emertonia simplex* sp. n., (♀). **A** P1 **B** P2 **C** P3 **D** P4. Scale bar is in μm.

Armature formula as follows:

	Exopod	Endopod
P1	0.121	0.011
P2	0.0.112	010
P3	0.0.112	010
P4	0.0.011	010

P5 (Figs 9B, 11E) with medially fused benps and discrete exps; benp with one pinnate outer basal seta; endopodal lobes well-developed, rounded, median cleft reaching at distal margin of exp, with one shorter inner and one longer outer setae; exp well developed, with one pinnate outer seta and two bare inner setae, and ornamented with a row of long spinules along inner margin.

Description of male. Smaller than female, body length 345 μm (n = 3, mean = 344 μm) (Fig. 10A); largest width (80 μm) measured at posterior margin of cephalic shield; general body shape and ornamentation as in female except for separation of genital somite; additional sexual dimorphism in antennule, A1, P5, and P6.

Antennule (Fig. 10B). Seven-segmented, subchirocer; fifth segment (Fig. $10B_2$) swollen, largest; aesthetascs on fifth and seventh segments (Fig. $10B_1$); armature formula: 1 – [1 bare], 2 – [8 bare], 3 [5 –bare], 4 – [2 bare], 5 – [6 bare + 2 spinulose + (1 +ae)], 6 – [2 bare], 7 – [7 bare + (2 + ae)]; apical acrothek consisting of apical aesthetasc and two basally fused bare setae.

P5 (Fig. 10C). Benp confluent, forming large transverse plate, with one bare outer basal seta and one pore on either side; exp ovate bearing setules on inner margin, with two pinnate and two bare setae, innermost longest.

P6 (Fig. 10D). Clearly distinct medially, each P6 with one outer pinnate and two bare inner setae.

Etymology. The species name refers to the simple somites without hyaline frills forming quadrilateral lappets.

Remarks. The second new species, *Emertonia simplex* sp. n., shares the general characteristics of other species like *E. holsatica holsatica* (Klie, 1929) and *E. major* (Nicholls, 1939), including segmentation and setal formula of swimming legs, rectangular caudal rami, and a well-developed P5 baseoendopod and separated exopod. However, *E. simplex* sp. n. has a combination of all the following characteristics: 1) exopod of antenna has five setae. This characteristic is found in eleven species of *Emertonia*, for instance *E. regulexstans* (Mielke, 1984b), and *E. diva* (Veit-Köhler, 2005), and 2) Two claw-like setae are present on the second segment of P1, which can be found in *E. brevicaudata* (Kornev and Chertoprud, 2008), *E. californica* (Kunz, 1981), *E. insularis* (Kunz, 1981), *E. holsatica* s. str., *E. longifurcata* (Scheibel, 1975), and *E. unguiseta* (Mielke, 1984). Of these, *E. unguiseta* is the species closest to *E. simplex* sp. n. since they share all of the characteristics mentioned above. However, differences between *E. simplex* sp. n. and *E. unguiseta* are as follows: 1) *E. simplex* sp. n. has four setae at P5 exopod in male, whereas *E. unguiseta* bears only three setae, 2) the new species has a shorter inner seta at P5 baseoendopod in female, whereas

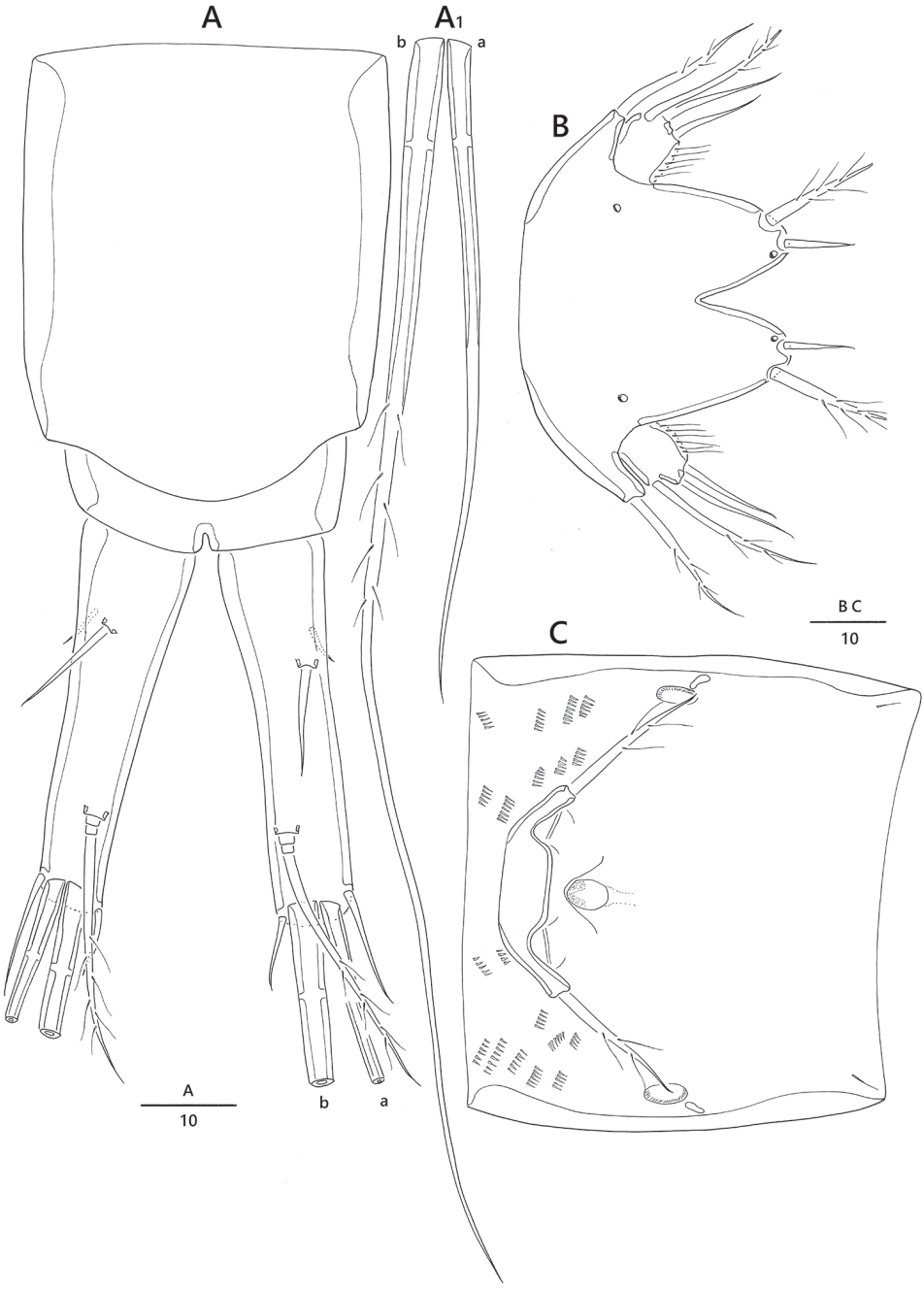

Figure 9. *Emertonia simplex* sp. n., (♀). **A** last two segments of urosomite and caudal rami **B** P5 **C** P6 and genital field. Scale bars are in μm.

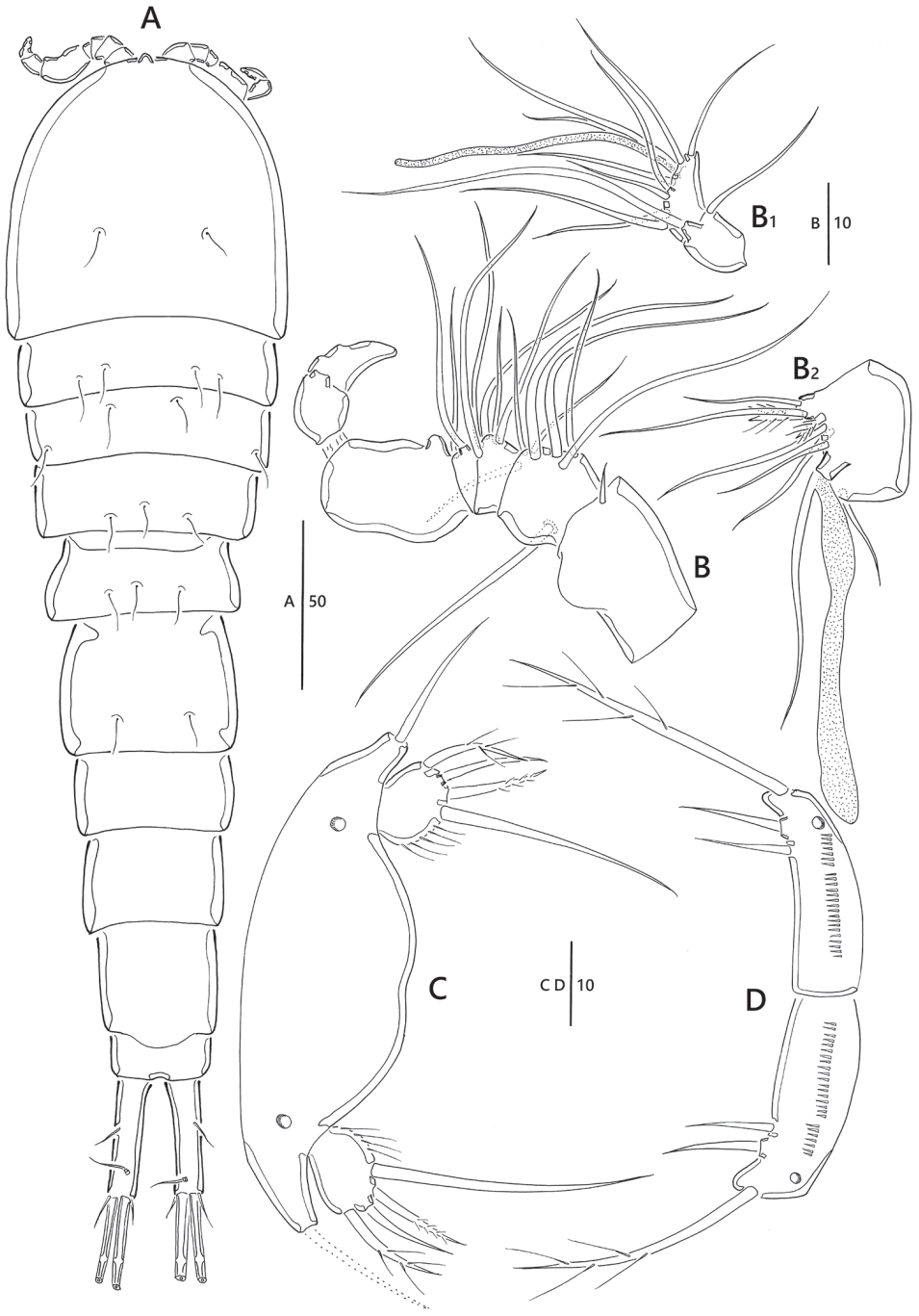

Figure 10. *Emertonia simplex* sp. n., (♂). **A** habitus, dorsal **B** antennule (**B**$_1$ last two segments **B**$_2$ fifth segment) **C** P5 **D** P6. Scale bars are in μm.

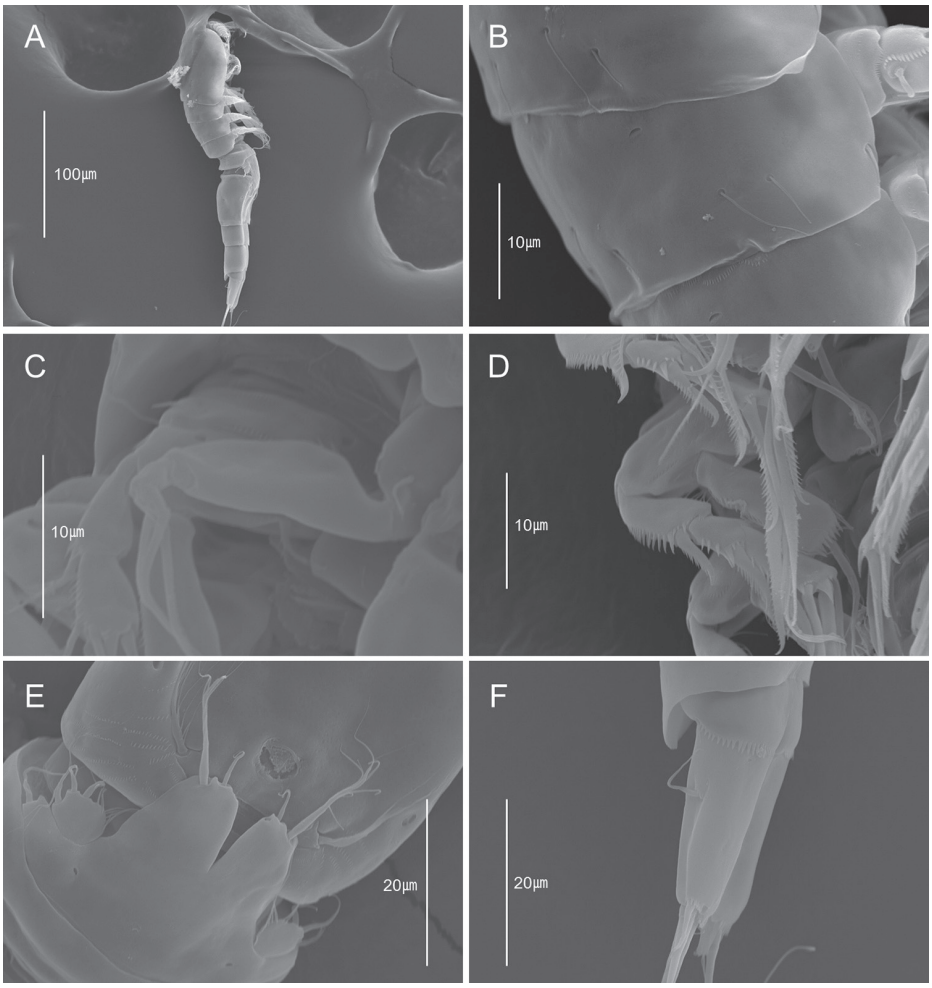

Figure 11. *Emertonia simplex* sp. n. (♀), SEM photographs. **A** habitus, lateral **B** first and second segment, lateral **C** P1 **D** P3 **C** P3 **E** P5 **F** caudal rami, lateral.

E. unguiseta bears two subequal setae, 3) the length of caudal rami is approximately 3.8 times as long as its width, whereas that of *E. unguiseta* is 3.2 times of the width. In addition, the new species has long dorsal sensilla. The major morphological characteristics of the genus *Emertonia*, including the two new species were summarized in Table 1.

Discussion. The family Parameseochridae is divided into nine genera based on segmentation, and setal formula of swimming legs. Two new species clearly belongs to the genus *Emertonia*, because of: 1) one-segmented endopods of P2–P4 with one seta each, 2) three-segmented exopods of P2–P4, and 3) the one-segmented exopod of antenna. Kunz (1981) compared the width:length ratio of the caudal rami, the characteristics of caudal setae, and the number of setae on antenna, P4, and P5. Wells (2007) also considered the characteristics of caudal seta III, and the setae on P5, and the number and position of setae in antenna for identifying species of *Emertonia*.

Table 1. Species list and morphological comparison of the species in genus *Emertonia* Wilson, 1932 based on female.

Species	A1	A2	P1			P2		P3			P4				P5		Caudal rami
	number of seg.	exp setae	exp-1	exp-2	enp-2	exp-2	exp-3	exp-2	exp-3	enp-1	exp-2	exp-3	enp-1	enp-2	exp setae	benp setae	shape width:lenth
gracilis-group																	
E. gracilis Wilson, 1932	8	3	023	·	011	0	011	0	011	010	0	011	010		3	2	square 1:2
E. pseudogracilis Krishnaswamy, 1957	7	2	122	·	011	0	012	0	012	010	0	011	010		3	1	square 1:2.5
laurentica-group																	
E. laurentica (Nicholls, 1939)	7	?	0	121	011	221	·	221	·	010	112	·	010		3	2	square 1:2
andeep-group																	
E. andeep (Veit-Köhler, 2004)	8	5	0	121	011	0	112	0	112	110	0	011	1	011	3	2	square 1:4
E. minor (Vasconcelos, Veit-Köhler, Drewes & Parreira dos Santos, 2009)	7	4	0	121	011	0	112	0	112	010	0	011	0	010	?	?	square 1:5
coelebs-group																	
E. coelebs (Monard, 1935)	7	4	0	121	011	0	112	0	112	010	1	011	110	·	3	?[1]	square 1:5
E. psammophila (Noodt, 1964)	8	3	0	121	011	0	112	0	112	010	1	011	010	·	3	2	square 1:2.5
E. furcavaricata Kunz, 1974	8	?	0	121	011	1	112	1	112	010	1	011	010	·	3	2	square 1:2.5
E. atlantica (Kunz, 1983)	7	3	0	121	011	0	112	0	112	010	1	011	110	·	3	1	square 1:3
holsatica-group																	
E. holsatica holsatica (Klie, 1929)	7	4(5)[2]	0	121	011	0	112	0	112	010	0	011	010	·	3	2	square 1:2
E. holsatica varians (Kunz, 1951)	7	5	0	121	011	0	112	0	112	010	0	011	110	·	3	2	square 1:3.5

Species	A1	A2	P1			P2		P3			P4				P5		Caudal rami
	number of seg.	exp setae	exp-1	exp-2	enp-2	exp-2	exp-3	exp-2	exp-3	enp-1	exp-2	exp-3	enp-1	enp-2	exp setae	benp setae	shape width:lenth
E. holsatica longicaudata (Galhano, 1970)	7	2(3)[3]	0	121	011	0	112	0	112	010	0	011	010	·	3	2	square 1:3.5
E. constricta constricta (Nicholls, 1935)	7	2(1)[4]	0	121	011	0	012	0	012	010	0	012 (011)[4]	010	·	3	?	square 1:3
E. constricta orotavae (Noodt, 1958)	7	2(3)[5]	0	121	011	0	012	0	012	010	0	011	010	·	3	2	square 1:2
E. constricta pacifica (Mielke, 1984a)	8	4	0	121	011	0	012	0	012	010	0	011	010	·	3	2	square 1:3
E. constricta egyptica (Mittwally & Montagna, 2001)	8	4	0	121	011	0	012	0	012	010	0	011	010	·	3	2	square 1:4
E. major (Nicholls, 1939)	9	3	0	121	011	0	112	0	012	010	0	011	010	·	3	2	square 1:3
E. pygmaea (Nicholls, 1939)	7	3	0	121	011	0	112	0	112	010	0	011	010	·	5	2	square 1:2
E. longisetosa (Krishnaswamy, 1951)	7	2	0	121	011	0	112	0	112	010	0	011	010	·	3	2	square 1:3
E. arenicola (Krishnaswamy, 1957)	7	2	0	121	011	0	112	0	112	010	0	011	010	·	3	2	square 1:3
E. capensis Krishnaswamy, 1957	7	1	0	121	011	0	012	0	012	010	0	011	010	·	3	0	square 1:2
E. minuta Krishnaswamy, 1957	7	3	0	122	011	0	012	0	012	010	0	011	010	·	3	0	square 1:2
E. enalia (Krishnaswamy, 1957)	8	1	0	022	011	0	112	0	112	010	0	011	010	·	3	2	square 1:4(?)[6]
E. wilsoni (Krishnaswamy, 1957)	7	3	0	121	011	0	112	0	112	010	0	011	010	·	3	2	square 1:3
E. pontica (Serban, 1959)	9	3	?	?	?	?	?	?	?	?	?	?	?	·	3	2	square 1:3.5
E. perharidiensis (Wells, 1963)	7	4	0	121	011	0	112	0	012	010	0	011	110	·	3	2	square 1:5

Species	A1	A2	P1			P2		P3			P4				P5		Caudal rami
	number of seg.	exp setae	exp-1	exp-2	enp-2	exp-2	exp-3	exp-2	exp-3	enp-1	exp-2	exp-3	enp-1	enp-2	exp setae	benp setae	shape width:lenth
E. psammobionta (Noodt, 1964)	7	3	0	121	011	0	112	0	112	010	0	011	010	·	3(2)	?	square 1:2
E. idiotes (Wells, 1967)	6	3	0	121	011	0	112	0	112	010	0	111	010	·	3	2	square 1:2.5
E. paraholsatica (Mielke, 1975)	7	4	0	121	011	0	112	0	112	010	0	011	010	·	3	2	square 1:3
E. longifurcata (Scheibel, 1975)	7	4	0	121	011	0	112	0	112	010	0	011	010	·	3	2	square 1:2.5
E. spiniger spiniger (Wells, Kunz & Rao, 1975)	7	5	0	022	020	0	112	0	112	010	0	011	110	·	3	2	square 1:6.5
E. spiniger ornata (Kunz, 1981)	7	5	0	022	020	0	112	0	112	010	0	011	110	·	3	2	square 1:9
E. masryi (Bodin, 1979)[7]	8	2	0	121	011	0	012	0	012	010	0	011	010	·	3	3	square 1:2
E. californica (Kunz, 1981)	7	3	0	121	011	0	112	0	112	010	0	020	010	·	3	2	square 1:3
E. debilis (Kunz, 1981)	8	3	0	121	011	0	112	0	112	010	0	011	010	·	3	2	square 1:2
E. insularis (Kunz, 1981)	8	4	0	121	011	0	112	0	112	010	0	011	010	·	3	2	square 1:3
E. miguelensis (Kunz,1983)	?	3	0	121	011	0	112	0	112	010	0	011	010	·	?	?	square 1:3.5
E. panamensis (Mielke, 1984a)	8	2	0	121	011	0	112	0	112	010	0	111	010	·	3	1	square 1:2
E. regulexstans (Mielke, 1984b)	8	5	0	121	011	0	112	0	112	010	0	011	010	·	3	2	square 1:2.3
E. similis (Mielke, 1984b)	8	5	0	121	011	0	112	0	112	010	0	011	010	·	3	2	square 1:3
E. unguiseta (Mielke, 1984b)	8	5	0	121	011	0	112	0	112	010	0	011	010	·	3	2	square 1:3.2

Species	A1	A2	P1			P2		P3			P4				P5		Caudal rami
	number of seg.	exp setae	exp-1	exp-2	enp-2	exp-2	exp-3	exp-2	exp-3	enp-1	exp-2	exp-3	enp-1	enp-2	exp setae	benp setae	shape width:lenth
E. acutifurcata (Mielke, 1985)	?	4	0	121	011	0	112	0	112	010	0	011	010	·	3	2	subtriangular 1:4
E. chilensis (Mielke, 1985)	8	4	0	121	011	0	112	0	112	010	0	011	010	·	3	2	square 1:2
E. diva (Veit-Köhler, 2005)	8	5	0	121	011	0	112	0	112	010	0	011	011	·	3	2	square 1:5.5
E. brevicaudata (Kornev & Chertoprud, 2008)	7	4	0	121	011	0	112	0	112	010	0	011	010	·	3	2	square 1:1.6
E. schminkei (Veit-Köhler & Drewes 2009).	8	5	0	121	011	0	112	0	112	010	0	011	010	·	3	2	square 1:9
E. clausi Pointner & Veit-Köhler, 2013	7	5(6)[8]	0	121	010	0	112	0	112	010	0	011	010	·	3	2	square 1:5.5
E. ingridae Pointner & Veit-Köhler, 2013	8	5	0	121	010	0	112	0	112	010	0	011	010	·	3	2	square 1:4.5
E. koreana sp. n. (This study)	8	2	0	121	011	0	112	0	112	010	0	011	010	·	3	2	subtriangular 1:3
E. simplex sp. n. (This study)	8	5	0	121	011	0	112	0	112	010	0	011	010	·	3	2	square 1:3.8

[1]Chappuis (1954) described P5 benp with two setae, however we doubt he described a different species instead of *E. constricta constricta*. In contrast to description of Nicholls (1935) and Marinov (1971), Chappuis (1954) described that the innermost seta of P5 exp is the longest among three setae.

[2]Mielke(1975) illustrated A2 exp with five setae.

[3]Galhano (1970) described exp of A2 with two setae in the manuscript but with three in the figure.

[4]Marinov (1971) illustrated A2 exp with one seta and P4 exp-3 with two elements.

[5]Though Masry (1970) supported the redescription of *E. constricta orotavae*, Masry's material had these differences as follow: A2 exopod with three setae (Noodt's species has two setae), baseoendopodal lobe with two bare equal length setae (Noodt's species has one longer inner and one shorter inner pinnate setae, caudal seta III ornamented with strong spinules (Noodt's species has a pinnate seta), and the innermost seta of P1 enp-2 bare (Noodt's species has a uni-pinnate seta).

[6]Krishnaswamy (1957) illustrated the habitus with very small caudal ramus. It is very difficult to calculate the ratio of width:length.

[7]The characters of *E. masryi* (Bodin, 1979) were based on *Kliopsyllus minutus* in Masry (1970).

[8]Pointner et al. (2013) described exp of A2 with six setae in the manuscript but with five in the figure.

Kunz (1981) and Huys (1987) proposed the phylogenetic position of the genera within the Paramesochridae. Kunz (1981) mentioned the diagnosis of *Kliopsyllus* based on the segmentation, and the seta formula of appendages. However, some species do not fit to the diagnosis by Kunz (1981). According to Huys' (1987) cladogram of Paramesochridae, three genera in the *Paramesochra*-group are divided by six apomorphies: 1) four setae on distal segment of P1 exopod, 2) one-segemented endopod of P2–P4, 3) three setae on the distal segment of P4 exopod, 4) one-segmented exopod of P1, 5) P1 endopod without element, and 6) two setae on distal segment of P4 exopod and one seta on P4 endopod. However, some species of *Emertonia* do not fit to Huys' cladogram as well. For example, *E. andeep* (Veit-Köhler, 2004) and *E. minor* (Vasconcelos, Veit-Köhler, Drewes & Parreira dos Santos, 2009) have two-segmented endopod of P4, *E. idiotes* (Wells, 1967) has three setae on P4 exp-3, and *E. gracilis* Wilson, 1932 and *E. pseudogracilis* Krishnaswamy, 1957 have one-segmented exopod of P1 (Table 1). Therefore the diagnosis of *Emertonia* needs to be amended as follows:

Amended diagnosis. Paramesochridae. Body cylindrical, broad anteriorly, rather flattened; with distinct separation between prosome and urosome; rostrum small, fused at base. Operculum not developed. Caudal ramus with 6 or 7 setae, seta I small or obscure. Antennule 7- or 8-segmented in female. Antennary exopod 1-segmented with 1–5 setae. Mandible biramous; exopod 1-segmented with 2–4 setae; distal segment of endopod with several basally fused setae at apex. Maxilla with 3 endites on syncoxa, first endite bilobed; endopod 1- or 2-segmented. Maxilliped with elongate basis. P1 biramous, with 2-segmented endopod and 1-or 2-segmented exopod. P2–P3 biramous, with 2- or 3-segmented exopods and 1-segmented endopods; P4 biramous, with 1- or 2-segmented endopod and 2- or 3-segmented exopod.

Five distinctive groups within genus *Emertonia* can be recognized based on segmentation and setal formula in swimming legs: 1) *gracilis*-group, 1-segmented exopod of P1; 2) *laurentica*-group, 2-segmented exopod of P2–P4; 3) *andeep*-group, 2-segmented endopod of P4; 4) *coelebs*-group, P4 exp-2 with one inner seta; 5) *holsatica*-group, 2-segmented exopod of P1, 3-segmented exopod of P2–P4, 1-segmented endopod of P2–P4, and P2–P4 exp-2 without inner seta. However, more studies including the mouthparts, and the numbers and shapes of elements on the appendages will be necessary to confirm the phylogenetic relationships among the species of *Emertonia*.

A taxonomic key for the worldwide species of *Emertonia* is constructed as follows. Unfortunately, *E. pontica* (Serban, 1959) is excluded from the key due to incomplete original description (Serban, 1959; Wells, 2007)

1	P1 exopod 1-segmented…(*gracilis*-group)	**2**
–	P1–P4 exopod 2-segmented…(*laurentica*-group)	***E. laurentica***
–	P1 exopod 2-segmented , P4 endopod 2-segmented…(*andeep*-group)	**3**
–	P1 exopod 2-segmented, P4 exopod 3-segmented; P4 exp-2 with 1 inner seta (*coelebs*- group)	**4**
–	Theses character not combined…(*holsatica*-group)	**7**

2	P2–P3 exp-3 with 2 setae/spines ..... ***E. gracilis***
–	P2–P3 exp-3 with 3 setae/spines ..... ***E. pseudogracilis***
3	P4 enp-2 with 2 setae..... ***E. andeep***
–	P4 enp-2 with 1 seta ..... ***E. minor***
4	P2–P3 exp-2 with 1 inner seta ..... ***E. furcavaricata***
–	P2–P3 exp-2 without inner seta..... **5**
5	Length of caudal rami 5 times as long as wide; P4 enp-1 with 2 setae... ***E. coelebs***
–	These characters not combined **6**
6	P4 enp-1 with 1 seta; P4 baseoendopodal lobe with 2 setae .... ***E. psammophila***
–	P4 enp-1 with 2 setae; P4 baseoendopodal lobe with 1 seta ..... ***E. atlantica***
7	P2 exp-3 with 3 setae/spines **8**
–	P2 exp-3 with 4 setae/spines **14**
8	P1 exp-2 with 5 setae/spines ..... ***E. minuta***
–	P1 exp-2 with 4 setae/spines **9**
9	A2 exopod with 1 seta at most ..... ***E. capensis***
–	A2 exopod with 2 setae at least **10**
10	A2 exopod with 2 setae and P5 baseoendopodal lobe with 3 setae .... ***E. masryi***
–	These characters not combined…(*E. constrictus* s. str.) **11**
11	A1 7-segmented and A2 exp with 3 setae at most..... **12**
–	A1 8-segmented and A2 exp with 4 setae **13**
12	P1 enp-1 length 1.6 times longer than P1 exp, length of caudal rami 3 times as long as wide ..... ***E. constricta constricta***
–	P1 enp-1 length 1.2 times longer than P1 exp, length of caudal rami 2 times as long as wide ..... ***E. constricta orotavae***
13	V-shaped baseoendopod of male P5 without setules..... ***E. constricta pacifica***
–	Each side baseoendopodal lobe almost fused ornamented with row of setules ..... ***E. constricta egyptica***
14	P4 exp-3 with 3 setae **15**
–	P4 exp-3 with 2 setae **16**
15	A2 exp with 2 elements and P5 baseoendopod with 1 seta..... ***E. panamensis***
–	A2 exp with 3 elements and P5 baseoendopod with 2 setae ..... ***E. idiotes***
16	P4 enp-1 with 2 setae..... **17**
–	P4 enp-1 with 1 setae..... **21**
17	P3 exp-3 with 3 setae ..... ***E. perharidiensis***
–	P3 exp-3 with 4 setae **18**
18–	Length of caudal rami more than 3.5 times as long as wide; penultimate somite normal..... ***E. holsatica varians***
–	Length of caudal rami more than 5 times as long as wide..... **19**
19	Penultimate somite normal; endopod of P4 with 2 pinnate setae ..... ***E. diva***
–	Penultimate somite elongated and ornamented 2 dorsal processes/spines; endopod of P4 with 1 bare and 1 brushlike setae..... **20**
20	Length of caudal rami over 6–7 times as long as wide ..... ***E. spiniger spiniger***
–	Length of caudal rami over 9 times as long as wide ..... ***E. spiniger ornata***

21	P5 exopod with 5 setae	***E. pygmaea***
–	P5 exopod with 3 setae	**22**
22	Shape of caudal rami conical, sub-triangular	**23**
–	Shape of caudal rami square	**24**
23	A2 exopod with 4 setae; median depression between baseoendopodal lobes shallow	***E. acutifurcata***
–	A2 exopod with 2 setae; median depression between baseoendopodal lobes deeply	***E. koreana* sp. n.**
24	A2 exopod with 1 seta	***E. enalia***
–	A2 exopod with at least 2 setae	**25**
25	A2 exopod with 2 setae	**26**
–	A2 exopod with 3 setae	**28**
–	A2 exopod with 4 setae	**33**
–	A2 exopod with 5 setae	**38**
26	Caudal rami with inwardly pointed spine and long seta V	***E. longisetosa***
–	These characters not combined	**27**
27	End of P2–P3 enp globular; A2 exopod with 2 or 3 setae	***E. holsatica longicaudata***
–	Shape of P2–P3 endopods normal; A2 exopod with 2 setae	***E. arenicola***
28	Distal segment of P3 exopod with 3 setae	***E. major***
–	Distal segment of P3 exopod with 4 setae	**29**
29	Seta V of caudal rami consisted of two type elements, proximal half stout and distal half slender seta	***E. miguelensis***
–	Seta V of caudal rami normal	**30**
30	A1 8-segmented; P1 endopod 1.3 times longer than exopod; length of caudal rami twice as long as wide	***E. debilis***
–	These characters not combined	**31**
31	A1 7-segmented; P2 and P3 endopod with a single tiny spinule-like seta each; length of caudal rami 3 times as long as wide	***E. wilsoni***
–	These characters not combined	**32**
32	Baseoendopod of P5 with two apical setae; male exp of P5 with 3 setae	***E. californica***
–	Baseoendopod of P5 with one apical and one outer setae; male exp of P5 with four setae	***E. psammobionta***
33	Baseoendopodal lobes fused forming large plate; A1 8-segmented; male exp of P5 with four setae	***E. insularis***
–	These characters not combined	**34**
34	A1 8-segmented; P1 enp-1 ornamented with long setules; length of P1 enp-1 1.6 times as long as P1 enp-2; male P5 exp with three setae	***E. chilensis***
–	These characters not combined	**35**
35	Seta III of caudal rami blunt spine; apical seta of A2 exp stout comparison with other three setae; Caudal rami length approx. 2.5 times as long as wide	***E. longifurcata***
–	These characters not combined	**36**

36 Maxilliped enp 2-segmented; Caudal rami length approx. 1.6 times as long as wide ..... ***E. brevicaudata***
– These characters not combined **37**
37 Caudal rami length approx. 2 times as long as wide; length of P1 enp-1 7 times as long as P1 enp-2 ..... ***E. holsatica holsatica***
– Caudal rami length approx. 3 times as long as wide; length of P1 enp-1 approx. 2.7 times as long as P1 enp-2 ..... ***E. paraholsatica***
38 Baseoendopodal lobes fused forming large plate; P1 enp-1 and P1 exp equal in length ..... ***E. regulexstans***
– These character not combined **39**
39 Caudal rami length more than 5 times as long as wide **40**
– Caudal rami length under 5 times as long as wide **41**
40 Caudal rami length 9 times as long as wide; P5 exp with 1 pinnate and 2 bare setae, outermost longest ..... ***E. schminkei***
– Caudal rami length 5.5 times as long as wide; P5 exp with 3 bare setae, innermost longest ..... ***E. clausi***
41 P2–P3 enp apical seta length longer than enp **42**
– P2–P3 enp apical seta length shorter than enp **43**
42 P1 enp-2 with 1 seta ..... ***E. ingridae***
– P1 enp-2 with 2 setae/spine ..... ***E. simplex* sp. n.**
43 Length of P1 enp-1 2.5 times as long as P1 exp; male P5 exp with 3 setae .... ***E. unguiseta***
– P1 enp-1 and P1 exp same length; male P5 exp with 4 setae ..... ***E. similis***

Acknowledgements

This research was supported by Evaluation of Marine Invertebrate Bioresources (MABIK 2017M00600) sponsored by the National Marine Biodiversity Institute of Korea. Authors express a hearty thanks to Raehyuk Jung (Hanyang University) for his help in English correction of the early version of manuscript. We are also very grateful to subject editor, Dr. Kai Horst George and the two reviewers, Dr. Elena Chertoprud, and Dr. Sung Joon Song, for their help in greatly improving this manuscript.

References

Back J, Lee W (2014) Two new species of the genus *Wellsopsyllus* (Copepoda; Harpacticoida; Paramesochridae) from the Yellow Sea. Zootaxa 3895: 246–366. https://doi.org/10.11646/zootaxa.3895.3.2

Back J, Lee W (2017) Two new species of *Leptopsyllus* from Korea (Copepoda, Harpacticoida, Paramesochridae). Zookeys 665: 37–57. https://doi.org/10.3897/zookeys.665.6150

Chappuis PA (1954) Harpacticides psammiques récoltés par Cl. Delamare Deboutteville en Mediterranée. Vie et Milieu 4: 259–276.

Galhano MH (1970) Contribuição para o conhecimento da fauna intersticial em Portugal. Publições do Instituto de Zoologia "Dr. Augusto Nobre" 110: 8–206.

Huys R (2009) Unresolved cases of type fixation, synonymy and homonymy in harpacticoid copepod nomenclature (Crustacea: Copepoda). Zootaxa 2183: 1–99.

Huys R, Gee JM, Moore CG, Hamond R (1996) Synopses of the British Fauna (New Series) No. 51. Marine and Brackish Water Harpacticoids, Part 1. Field Studies Council, Shrewsbury, 352 pp.

Klie W (1929) Die Copepoda Harpacticoida der südlichen und westlichen Ostsee mit besonderer Berücksichtigung der Sandfauna der Kieler Bucht. Zoologische Jahrbücher, Systematik 57: 329–386.

Kornev PN, Chertoprud ES (2008) Harpacticoid Copepods of the White Sea: Morphology, Systematics, Ecology. KMK Scientific Press Ltd, Moscow, 379 pp. [In Russian]

Krishnaswamy S (1951) Three new species of sand-dwelling copepods from the Madras coast. Annals and Magazine of natural History 12: 273–280. https://doi.org/10.1080/00222935108654151

Krishnaswamy S (1957) Studies on the Copepoda of Madras. University of Madras, 168 pp.

Kunz H (1951) Marine Harpacticoiden aus dem Küstensand von Südwestafrika. Kieler Meeresforschungen 8: 76–81.

Kunz H (1962) Revision der Paramesochridae (Crust. Copepoda). Kieler Meeresforschungen 18: 245–257.

Kunz H (1974) Zwei neue afrikanische Paramesochridae (Copepoda Harpacticoidea) mit Darstellung eines Bewegungsmechanismus für die Furkaläste. Mikrofauna des Meeresbodens 36: 1–20.

Kunz H (1981) Beitrag zur Systematik der Paramesochridae (Copepoda, Harpacticoida) mit Beschreibung einiger neuer Arten. Mitteilungen aus dem Zoologischen Museum der Universität Kiel 1: 1–33.

Kunz H (1983) Harpacticoiden (Crustacea: Copepoda) aus dem Litoral der Azoren. Arquipélago: revista da Universidade dos Açores. Série ciências da natureza 4: 117–208.

Masry D (1970) Ecological study of some sandy beaches along the Israeli mediterranean coast, with a description of the interstitial harpacticoids (Crustacea, Copepoda). Cahiers de Biologie Marine 11: 229–258.

Marinov T (1971) Harpacticoids of the Bulgarian Black Sea coast. Proceedings of the Institute of Oceanography and Fisheries, Varna 11: 43–87. [In Bulgarian]

Mielke W (1975) Systematik der Copepoda eines Sandstrandes der Nordseeinsel Sylt. Mikrofauna des Meeresbodens 52: 1–134.

Mielke W (1984a) Einige Paramesochridae (Copepoda) von Panamá. Spixiana 7: 217–243.

Mielke W (1984b) Interstitielle Fauna von Galapagos. XXXI. Paramesochridae (Harpacticoida). Microfauna Marina 1: 63–147.

Mielke W (1985) Zwei neue *Klliopsyllus*-Arten (Copepoda) aus Chile. Studies on Neotropical Fauna and Environment 20: 97–105. https://doi.org/10.1080/01650528509360677

Mitwally H, Montagna PA (2001) Egyptian interstitial Copepoda Harpacticoida with the description of two new species and one new subspecies. Crustaceana 64: 513–544. https://doi.org/10.1163/156854001300228825

Monard A (1935) Étude sur la faune des Harpacticoïdes marins de Roscoff. Travaux de la Station biologique de Roscoff 13: 5–88.

Nicholls AG (1935) Copepods from the interstitial fauna of a sandy beach. Journal of the marine biological Association of the United Kingdom, new series 20: 379–405. https://doi.org/10.1017/S0025315400045306

Nicholls AG (1939) Some new sand-dwelling copepods. Journal of the marine biological Association of the United Kingdom, new series 23: 327–341. https://doi.org/10.1017/S0025315400013928

Noodt W (1958) Die Copepoda des Brandungsstrandes von Teneriffa (Kanarische Inseln). Abhandlungen der mathematisch-naturwissenschaftlichen Klasse, Akademie de Wissenchaften und der Literatur in Mainz 1958: 51–116.

Noodt W (1964) Copepoda Harpacticoidea aus dem Litoral des Roten Meeres. Kieler Meeresforschungen 20: 128–154.

Plum C, George KH (2009) The paramesochrid fauna of the Great Meteor Seamount (Northeast Atlantic) including the description of a new species of *Scottopsyllus* (*Intermedopsyllus*) Kunz (Copepoda: Harpacticoida: Paramesochridae). Marine Biodiversity 39: 265–289. https://doi.org/10.1007/s12526-009-0022-7

Pointner K, Kihara TC, Glatzel T, Veit-Köhler G (2013) Two new closely related deep-sea species of Paramesochridae (Copepoda, Harpacticoida) with extremely differing geographical range sizes. Marine Biodiversity 43: 293–319. https://doi.org/10.1007/s12526-013-0158-3

Scheibel W (1975) *Kliopsyllus longifurcatus* n. sp., ein sandbewohnender Harpacticoide (Copepoda) der Kieler Bucht. Crustaceana 29: 235–240. https://doi.org/10.1163/156854075X00270

Serban M (1959) Les Copépodes de la mer Noire. Note préliminaire sur les Harpacticides de la côte Roumaine. Lucrările ale Statiei Zoologice Maritime "Regele Ferdinand I" dela Agigea vol. festival 1956: 259–302.

Song SJ, Park J, Kwon B-O, Ryu J, Khim JS (2012) Ecological Checklist of the Marine and Brackish-Water Harpacticoid Copepod Fauna in Korean Waters. Zoological Studies 51: 1397–1410.

Vasconcelos DM, Veit-Köhler G, Drewes J, Santos PJP (2009) First record of the genus *Kliopsyllus* Kunz, 1962 (Copepoda Harpacticoida, Paramesochridae) from Northeastern Brazil with description of the deep-sea species *Kliopsyllus minor* sp.n. Zootaxa 2096: 327–337.

Veit-Köhler G (2004) *Kliopsyllus andeep* sp. n. (Copepoda: Harpacticoida) from the Antarctic deep sea – a copepod closely related to certain shallow-water species. Deep-Sea Research II 51: 1629–1641. https://doi.org/10.1016/j.dsr2.2004.06.027

Veit-Köhler G (2005) Results of the DIVA-1 expedition of RV "Meteor" (Cruise M48/1). First deep-sea record of the genus *Kliopsyllus* Kunz, 1962 (Copepoda: Harpacticoida) with the description of *Kliopsyllus diva* sp. n. – the most abundant member of Paramesochridae at two different sites of the Angola Basin. Organisms, Diversity and Evolution 5: 29–41. https://doi.org/10.1016/j.ode.2004.10.003

Veit-Köhler G, Drewes J (2009) *Kliopsyllus schminkei* sp. n. (Copepoda, Harpacticoida, Paramesochridae) – new copepod from the southeast Atlantic deep sea (Angola Basin). Zootaxa 2096: 313–326.

Wells JBJ (1963) Copepoda from the littoral region of the estuary of the River Exe (Devon, England). Crustaceana 5: 10–26. https://doi.org/10.1163/156854063X00020

Wells JBJ (1967) The littoral Copepoda (Crustacea) of Inhaca Island, Mozambique. Transactions of the Royal Society of Edinburgh 67: 189–358. https://doi.org/10.1017/S0080456800024017

Wells JBJ (2007) An annotated checklist and keys to the species of Copepoda Harpacticoida (Crustacea). Zootaxa 1568: 1–872.

Wells JBJ, Kunz H, Rao GC (1975) A review of the mechanisms for movement of the caudal furca in the family Paramesochridae (Copepoda Harpacticoida), with a description of a new species of *Kliopsyllus* Kunz. Mikrofauna des Meeresbodens 53: 1–16.

Wilson CB (1932) The copepods of the Woods Hole region, Massachusetts. Bulletin of the United States National Museum 158: 1–635. https://doi.org/10.5479/si.03629236.158.i

ZooKeys 718: 65–94 (2017)
doi: 10.3897/zookeys.718.21151
http://zookeys.pensoft.net

RESEARCH ARTICLE

A peer-reviewed open-access journal
ZooKeys
Launched to accelerate biodiversity research

A revision of the tribe Planitorini van Achterberg (Hymenoptera, Braconidae, Euphorinae), with description of a new genus from Australia

Cornelis van Achterberg[1], Donald L.J. Quicke[2], C. Andrew Boring[3]

1 *Department of Terrestrial Zoology, Naturalis Biodiversity Center, Postbus 9517, 2300 RA Leiden, The Netherlands* **2** *Integrative Ecology Laboratory, Department of Biology, Faculty of Science, Chulalongkorn University, Phayathai Road, Pathumwan, BKK 10330, Thailand* **3** *Florida Department of Agriculture and Food Services, Division of Plant Industry, 1911 SW 34th St, Gainesville FL 32608, U.S.A.*

Corresponding author: *Cornelis van Achterberg* (c.vanachterberg@xs4all.nl)

Academic editor: *J. Fernandez-Triana* | Received 22 September 2017 | Accepted 3 November 2017 | Published 4 December 2017

http://zoobank.org/71BE800F-8994-4130-B627-B1A62CFE2830

Citation: van Achterberg C, Quicke DLJ, Boring CA (2017) A revision of the tribe Planitorini van Achterberg (Hymenoptera, Braconidae, Euphorinae), with description of a new genus from Australia. ZooKeys 718: 65–94. https://doi.org/10.3897/zookeys.718.21151

Abstract

The tribe Planitorini van Achterberg (Hymenoptera: Braconidae: Euphorinae) is revised. One new genus *Paramannokeraia* **gen. n.** (type species: *P. gibsoni* **sp. n.**) and five new species from Australia are described and illustrated: *Mannokeraia albipalpis* van Achterberg, **sp. n.**, *M. nigrita* van Achterberg, **sp. n.**, *M. punctata* van Achterberg, **sp. n.**, *Paramannokeraia gibsoni* van Achterberg & Quicke, **sp. n.** and *P. juliae* van Achterberg, **sp. n.** The tribe Mannokeraiini van Achterberg, 1995, is synonymized with the tribe Planitorini (**syn. n.**).

Keywords

Braconidae, Euphorinae, Planitorini, Mannokeraiini, *Paramannokeraia*, *Mannokeraia*, *Planitorus*, key, new genus, new species, distribution, Australia

Introduction

The subfamily Euphorinae Foerster, 1863 (Hymenoptera, Braconidae) is morphologically a very diverse group (Stigenberg et al. 2015), including many genera containing parasitoids of adult insects (Shaw and Huddleston 1991). The entirely Australian tribes Mannokeraiini van Achterberg, 1995, and Planitorini van Achterberg, 1995, are two aberrant groups, each containing only a single genus: *Mannokeraia* van Achterberg, 1995, with wingless females and *Planitorus* van Achterberg, 1995, with normally winged females (van Achterberg 1995). Accidently (partly because of their very derived morphology), the senior author referred the genera to the subfamilies Masoninae van Achterberg, 1995, and Betylobraconinae Tobias, 1979, respectively, but according to DNA analysis (Stigenberg et al. 2015) and some details of their morphology (e.g. the petiolate first metasomal tergite with its submedially situated spiracles) they belong to the subfamily Euphorinae. Earlier DNA analysis by Belshaw and Quicke (2002) and Sharanowski et al. (2011) corroborated already the inclusion of this group in the Euphorinae. In this paper the tribes Planitorini and Mannokeraiini are formally synonymised, and a new genus (*Paramannokeraia* gen. n.) and four new species are described and illustrated.

For the identification of the subfamily Euphorinae, see van Achterberg (1993), for more references see Yu et al. (2016) and for the terminology used in this paper, see van Achterberg (1979, 1988, 1993).

Material and methods

The studied material concerns all the Planitorini and Mannokeraiini specimens used for DNA analysis and some additional specimens collected by Dr L. Masner (Ottawa). So far, the specimens have been provisionally identified up to genus level (Belshaw and Quicke 2002, Sharanowski et al. 2011, and Stigenberg et al. 2015). Observations and descriptions were made with an Olympus SZX11 stereomicroscope and fluorescent lamps. Photographic images were made with the Keyence VHX-5000 digital microscope and processed with Adobe Photoshop CS5, mostly to adjust the size and background.

Measurements are performed as indicated in van Achterberg (1988). The length of the first metasomal tergite is measured medially from apex of adductor muscle to apex of tergite. Additional non-exclusive characters in the key are between square brackets. The following abbreviations are used for the depositories: ANIC = Australian National Insect Collection, Canberra, Australia; CNC = Canadian National Collection of Insects, Ottawa, Canada; HIC = Hymenoptera Institute Collection, University of Kentucky, Lexington, USA; NHRS = Naturhistoriska Riksmuseet, Stockholm, Sweden.

Taxonomy

Planitorini van Achterberg, 1995
Figs 1–96

Planitorini van Achterberg, 1995: 46.
Mannokeraiini van Achterberg, 1995: 95. **Syn. n**.

Diagnosis. Antenna of ♀ with 16–20 segments, and segments of apical half moniliform (Figs 11, 19, 38, 87), of ♂ with 28–32 segments and segments much longer than wide (Figs 13, 44, 51), pedicellus of ♀ narrower than scapus (Figs 19, 35, 58, 75; but much less so in *Planitorus*: Fig. 95); maxillary palp with 6 segments and labial palp with 4 segments; antennal sockets on facial protuberance, sockets remain separated from each other by distance from socket to eye (Figs 23, 35, 57) or touching each other (Fig. 85); mesosoma depressed (Figs 19, 87) or normal (Figs 3, 28, 58); scutellar sulcus wide and more or less curved (Figs 41, 62, 69) or narrow and curved (Figs 90); ♀ wingless (Fig. 18) or macropterous (Figs 2, 56, 84) as males; veins 3-M and 2-1A of fore wing largely unsclerotized (Figs 67, 84); vein m-cu of fore wing postfurcal (Figs 2, 56, 84); vein CU1b of fore wing absent (Figs 2, 29, 56, 84); vein 2-M of fore wing distinctly longer than vein 3-SR (Figs 2, 56, 84); vein M+CU of hind wing 2.0–2.5 times as long as vein 1-M and vein 1-M 1.3–2.0 times as long as vein 1r-m (Figs 2, 29, 56, 84); fore leg of ♀ robust (Figs 7, 21, 37, 63, 76, 89); first metasomal tergite narrow basally, more or less petiolate and its spiracle submedially situated (Figs 22, 32, 49, 59, 93), basal quarter or half of first metasomal tergite tube-shaped, first sternite more or less free from tergite in males of *Mannokeraia* and in other Planitorini, but ventrally closed in females of *Mannokeraia*.

Notes. The DNA analysis by Stigenberg et al. (2015) clearly shows that despite the different general morphology of the adults both tribes belong together. The more or less developed facial prominence, the largely unsclerotized vein 3-M of fore wing, the basally narrow first tergite and the apical moniliform antennal segments of females are shared by all three genera.

Key to genera of the Planitorini van Achterberg

1 Antennal sockets touching each other (Fig. 85); epistomal suture absent and clypeus not differentiated from face dorsally (Fig. 86); scutellar sulcus narrow and finely crenulate (Fig. 90); head elongate ventrally, malar space about 0.7 times height of eye in anterior view (Fig. 86); posterior half of mesopleuron depressed and divided into two parts by linear episternal scrobe (Fig. 87); fore tarsal segments of both sexes strongly widened (Fig. 94); face strongly convex medio-dorsally (Fig. 86); mesosternal sulcus absent and area smooth; postpectal carina absent medio-ventrally; pedicellus slightly narrower than scapus (Fig. 87).....***Planitorus* van Achterberg, 1995**

– Antennal sockets remaining separate from each other (Figs 8, 35, 57); epistomal suture distinctly impressed and clypeus differentiated from face

dorsally (Figs 8, 34, 52, 57); scutellar sulcus wide and coarsely crenulate (Figs 4, 62; less in wingless specimens: Fig. 18); head normal ventrally, malar space 0.15–0.30 times height of eye in anterior view (Figs 8, 23, 34, 57); posterior half of mesopleuron convex and undivided, only with elliptical episternal scrobe (Figs 30, 58); fore tarsal segments of ♂ slender and of ♀ moderately wide (Figs 37, 64); face moderately convex medio-dorsally (Figs 34, 57); mesosternal sulcus distinctly impressed and crenulate; postpectal carina variable, often present medio-ventrally; pedicellus much narrower than scapus (Figs 35, 58) **2**

2 Dorsope of first tergite large and deep and tergite about 1.5 times longer than its apical width (Figs 59, 70, 78); ovipositor nearly cylindrical (Fig. 58); clypeus elliptical, medially high and ventrally flattened, without space between closed mandibles and clypeus (Figs 57, 73, 82); hind coxa at most basally finely rugose and remainder largely smooth (Figs 65, 66, 68); fore tibia of ♀ with at most some spiny bristles (Fig. 63, 76); both sexes macropterous ..... ***Paramannokeraia*** **van Achterberg & Quicke, gen. n.**

– Dorsope of first tergite absent or (rarely) shallowly impressed and tergite 2.2–2.9 times longer than its apical width (Figs 5, 22, 32, 49); ovipositor strongly compressed (Figs 1, 19, 20, 28); clypeus strongly transverse, medially low and with steep ventral face, and often with space between closed mandibles and clypeus (Figs 8, 23, 34); hind coxa completely rugose or punctate (Figs 27, 47); fore tibia of ♀ with distinct spines (Figs 7, 21, 37); ♀ wingless (Fig. 19) or both sexes macropterous ..... ***Mannokeraia*** **van Achterberg, 1995**

Mannokeraia van Achterberg, 1995

Figs 1–55

Mannokeraia van Achterberg, 1995: 96–97.

Type species. *Mannokeraia aptera* van Achterberg, 1995 (examined).

Diagnosis. Antenna of ♀ with 16–20 segments, and segments of apical half moniliform (Figs 11, 19, 38), of ♂ with 31–32 segments and segments much longer than wide (Figs 12, 44); clypeus strongly transverse and with steep ventral face, usually with transverse space between clypeus and closed mandibles (Figs 34, 52); absent in *M. aptera*: Fig. 23); head transverse and enlarged behind eyes (Figs 9, 17, 35, 43, 53); pronotal collar reaching level of mesoscutum in wingless females (Fig. 19), but much lower in macropterous specimens (Figs 3, 47); notauli reduced or united posteriorly (Figs 31, 41, 48); mesosternal sulcus distinct and crenulate; postpectal carina distinct medio-ventrally (but not visible in *M. aptera*); fore tibia of ♀ with distinct spines; hind coxa completely rugose; hind tibia densely striated; tarsal claws with a rounded lobe; dorsope of first tergite absent (at most weakly developed in *M. albipalpis*), 2.2–2.9 times longer than its apical width and tergite weakly widened posteriorly (Figs 5, 22,

32, 49); ovipositor strongly compressed (Figs 1, 19, 20, 28); ♀ wingless (Fig. 19) or both sexes macropterous (Figs 1, 28).

Distribution. Australia: four species.

Biology. Unknown.

Key to species of *Mannokeraia* van Achterberg

1 Setose part of ovipositor sheath about 0.2 times as long as hind tibia (Fig. 19); propodeum smooth medially (Fig. 18); mesoscutum of ♀ at upper level of pronotum (Fig. 19); without space between clypeus and closed mandibles (Fig. 23); ♀ apterous (only with short wing pads: Fig. 18; ♂ unknown) ....***M. aptera*** van Achterberg, 1995

– Setose part of ovipositor sheath 0.5–0.6 times as long as hind tibia (Figs 1, 28); propodeum rugose or densely punctate medially (Figs 4, 31, 41, 49); mesosternum of both sexes far above upper level of pronotum (Figs 3, 30, 47); with transverse space between clypeus and closed mandibles (Figs 34, 52); both sexes macropterous.....**2**

2 Propodeum densely and coarsely punctate (Figs 48, 49); pronotum and mesoscutum yellowish brown; [♀ unknown] .....***M. punctata*** **sp. n.**

– Propodeum only densely rugose (Figs 4, 31, 41); pronotum and mesoscutum dark brown or black.....**3**

3 Basal 7 antennal segments of both sexes dark brown or blackish (Fig. 35); legs black; length of malar space equal to basal width of mandible (Fig. 34); palpi grey..... ***M. nigrita*** **sp. n.**

– Basal 7 antennal segments of ♀ brownish yellow (Fig. 11), of ♂ scapus and pedicellus yellow and following 5 segments brown or dark brown; legs (except hind coxa) largely brownish yellow or yellowish brown; length of malar space 0.3 times basal width of mandible (Fig. 8); palpi white...***M. albipalpis*** **sp. n.**

Mannokeraia albipalpis **van Achterberg, sp. n.**
http://zoobank.org/54781D90-B529-41EE-9B8A-EE9CFAA9C787
Figs 1–16

Mannokeraia sp. 4 Stigenberg et al., 2015: 575.

Type material. Holotype, ♀ (CNC), "**Austr[alia]**, Qld., Mt. Glorious N.P., 630 m, 28.ii.1984, L. Masner s.s.", "Wet rain forest". Paratypes: 1 ♀ + 1 ♂ (HIC), "Australia: Qld., Main Range National Park, Nunningham's Gap, Box Forest Track, elev. 700 m, yellow/blue/red pan traps (4:1:1) in creek bed, 400 m, S of parking area, 28°3.243'S 152°22.764'E, 10–11.xii.2005, A.R. Deans & M.L. Buffington", "H4038" (only ♀), "DNA primary voucher AB 086 (♀) or AB 087 (♂), Hymenoptera Institute, University of Kentucky".

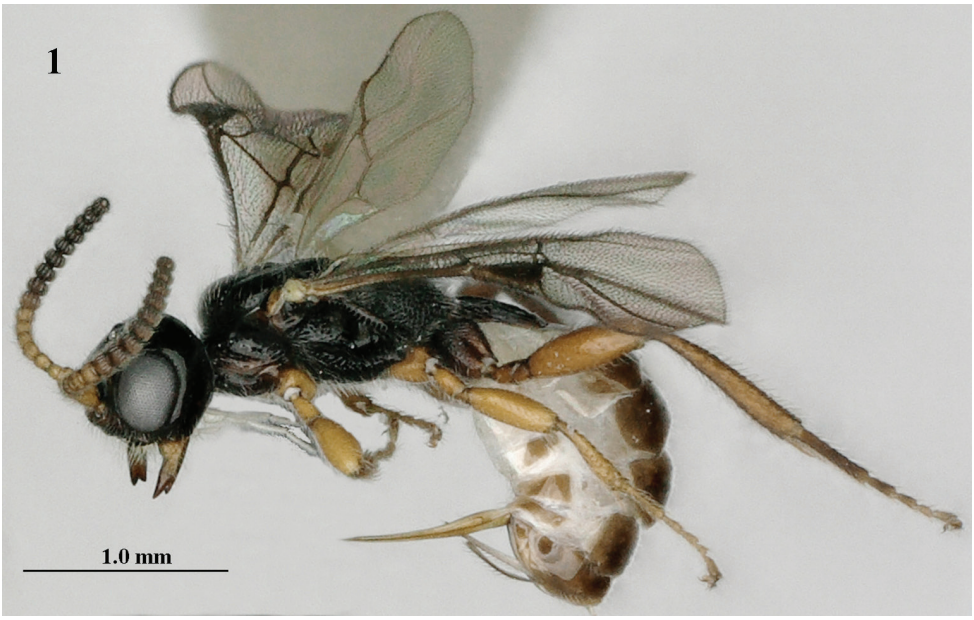

Figure 1. *Mannokeraia albipalpis* sp. n., ♀, holotype, habitus, lateral aspect.

Diagnosis. Antenna of ♀ with 20 segments and medially slightly widened (Fig. 11), and basal 7 segments brownish yellow and apical 12 segments strongly moniliform, of ♂ scapus and pedicellus yellow and following 5 segments brown or dark brown; palpi white; with transverse space between clypeus and closed mandibles; head moderately enlarged behind eyes in dorsal view (Fig. 9); length of malar space 0.3 times basal width of mandible (Fig. 8); mesosoma of ♀ normal, with mesoscutum far above upper level of pronotum (Fig. 3); pronotum and mesoscutum black; propodeum rugose medially (Fig. 4); legs (except hind coxa) largely brownish yellow or yellowish brown; setose part of ovipositor sheath 0.5–0.6 times as long as hind tibia; both sexes macropterous.

Description. Holotype, ♀, length of fore wing 2.9 mm, and of body 3.7 mm.

Head. Antenna with 16+ segments (apical segments missing, ♀ paratype has 20 antennal segments), length of third segment 1.1 times fourth segment, third and fourth segments 1.1 and 1.0 times as long as wide, respectively (Fig. 11) and with apical 9+ segments pedunculate, medially antenna wider than as apically; length of maxillary palp equal to height of head; occipital carina complete, comparatively low dorsally (Fig. 10), joining hypostomal carina below mandible and occipital flange elongate; eye 1.3 times as long as temple in dorsal view; temples subparallel-sided behind eyes; OOL:diameter of posterior ocellus:POL = 13:5:11; vertex and frons smooth and strongly shiny, with some long setae, convex, without median groove, and anteriorly flattened; face sparsely coarsely punctate and with some superficial rugae (Fig. 8); clypeus depressed and smooth ventrally, with ventral rim slightly upcurved, dorsally weakly convex and with some coarse punctures; length of malar space 0.3 times basal width of mandible; man-

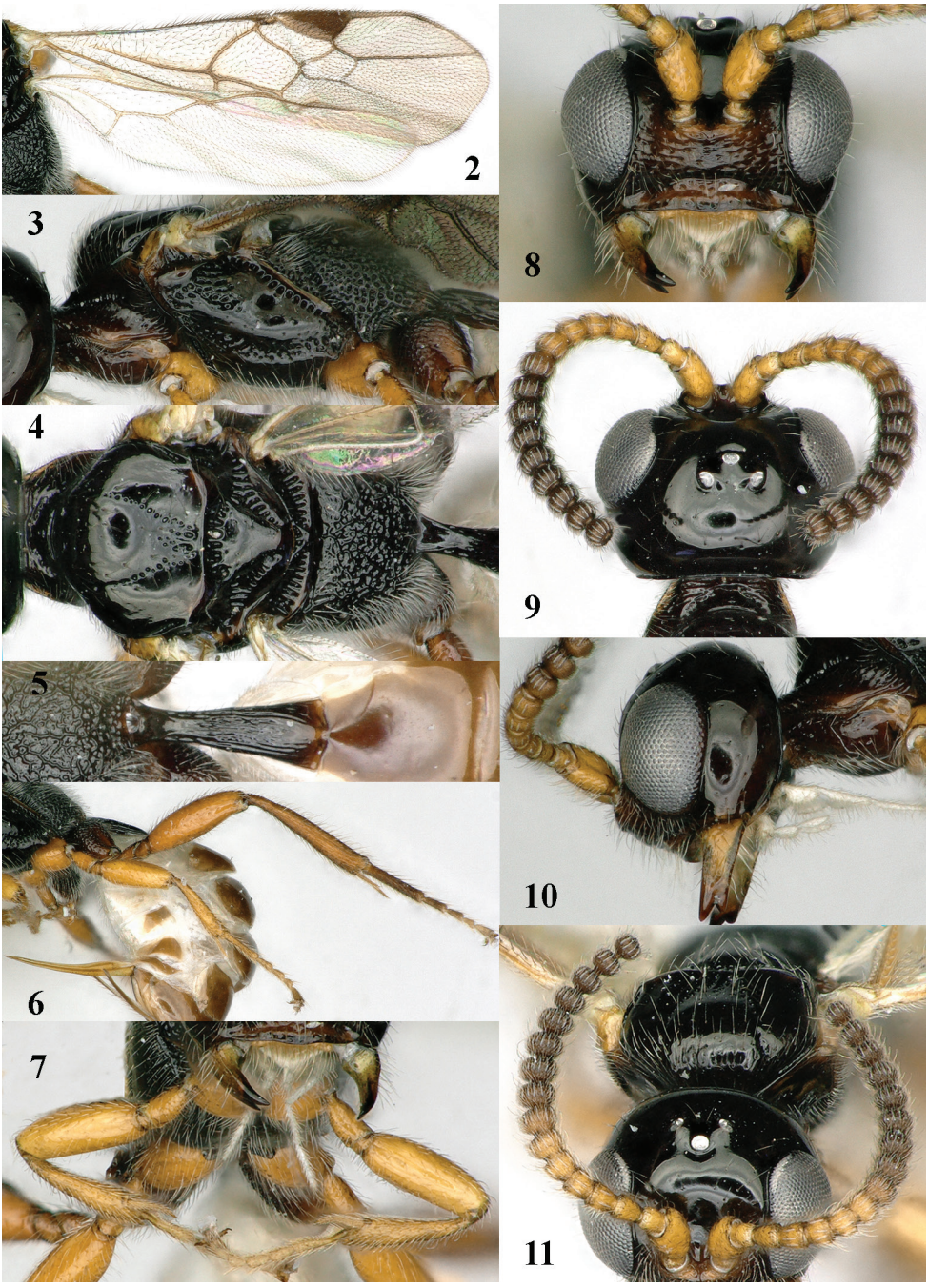

Figures 2–11. *Mannokeraia albipalpis* sp. n., ♀, holotype. **2** wings **3** mesosoma, lateral aspect **4** mesosoma, dorsal aspect **5** propodeum, first–third metasomal tergites, dorsal aspect **6** hind leg, lateral aspect **7** fore legs, inner aspect **8** head, anterior aspect **9** head, dorsal aspect **10** head, lateral aspect **11** antennae, ventral aspect.

dible flattened medially and with some striae, apically with large upper and medium-sized lower tooth (Fig. 10).

Mesosoma. Length of mesosoma 1.9 times its height; dorsal pronope and antescutal depression absent; side of pronotum narrowly crenulate antero-medially, widely crenulate postero-ventrally and remainder largely smooth; mesopleuron coarsely punctate dorsally; precoxal sulcus complete, rather widely crenulate-punctate (Fig. 3); remainder of mesopleuron smooth except for a few punctures; mesosternal suture rather deep and distinctly crenulate; postpectal carina distinct medio-ventrally; notauli complete and formed by narrow row of punctures; mesoscutum slightly convex, strongly shiny, and largely smooth, except for some coarse punctures medio-posteriorly (Fig. 4), glabrous laterally and with few long setae medially; scutellar sulcus with six costae; scutellum flat, smooth (except for some setiferous punctures) and shiny; metapleuron entirely coarsely punctate; propodeum entirely moderately reticulate-rugose (Figs 4, 5), its median carina absent, its posterior face rather differentiated and without tubercle postero-laterally (Fig. 4).

Wings. Fore wing: 1-M weakly curved; 1-SR short (Fig. 2); marginal cell closed anteriorly; 1-R1 1.7 times longer than pterostigma (Fig. 2); vein r emitted distinctly after middle of pterostigma; r:3-SR:SR1 = 4:16:87; vein SR1 straight; 2-SR:3-SR:r-m = 26:16:17; 2-M much longer than 3-SR; m-cu slightly postfurcal; 1-CU1 oblique and narrow, about as long as cu-a; 1-CU1:2-CU1 = 5:29; basal and subbasal cells of fore wing setose as other cells. Hind wing: marginal cell parallel-sided apically (Fig. 2); M+CU:1-M:1r-m = 28:14:10; basal and subbasal cells sparsely setose.

Legs. Hind coxa densely rugose-punctate, its outer side mainly punctate (Fig. 3); tarsal claws with wide truncate lamelliform lobe (Figs 6, 7); length of femur, tibia and basitarsus of hind leg 3.3, 6.4 and 6.2 times as long as their maximum width; fore femur inflated, 2.4 times longer than wide and apically rounded (Fig. 7); fore and middle tarsi slender (Figs 6, 7).

Metasoma. First tergite 2.5 times longer than its apical width, petiolate basally and gradually widened apically (Fig. 5), striate, dorsal carinae unite to form a median carina (Fig. 5), basal half of tergite closed ventrally and sternite differentiated; laterope absent; second tergite smooth; ovipositor sheath somewhat widened basally and obtuse apically (Fig. 1), its setose part 0.17 times as long as fore wing and 0.55 times hind tibia; ovipositor with minute subapical notch, compressed and basally widened (Fig. 6).

Colour. Black; palpi and basal half metasoma ventrally white; tegulae pale yellowish; seven basal segments of antenna, fore and middle legs brownish yellow; hind leg (except dark brown coxa) yellowish brown, but tibia and tarsus slightly darkened; face, clypeus, remainder of antenna and of metasoma (except black first tergite), pterostigma and most veins of fore wing dark brown; wing membrane weakly infuscate.

Male. Similar to female paratype except for the shape of the antennal segments (22+, apical segments missing; Fig. 12), slender fore femur and the different colour of base of antenna, legs and clypeus. Length of fore wing 3.3 mm, and of body 4.1 mm; antenna dark brown except for yellow scapus and pedicellus; clypeus brown ventrally;

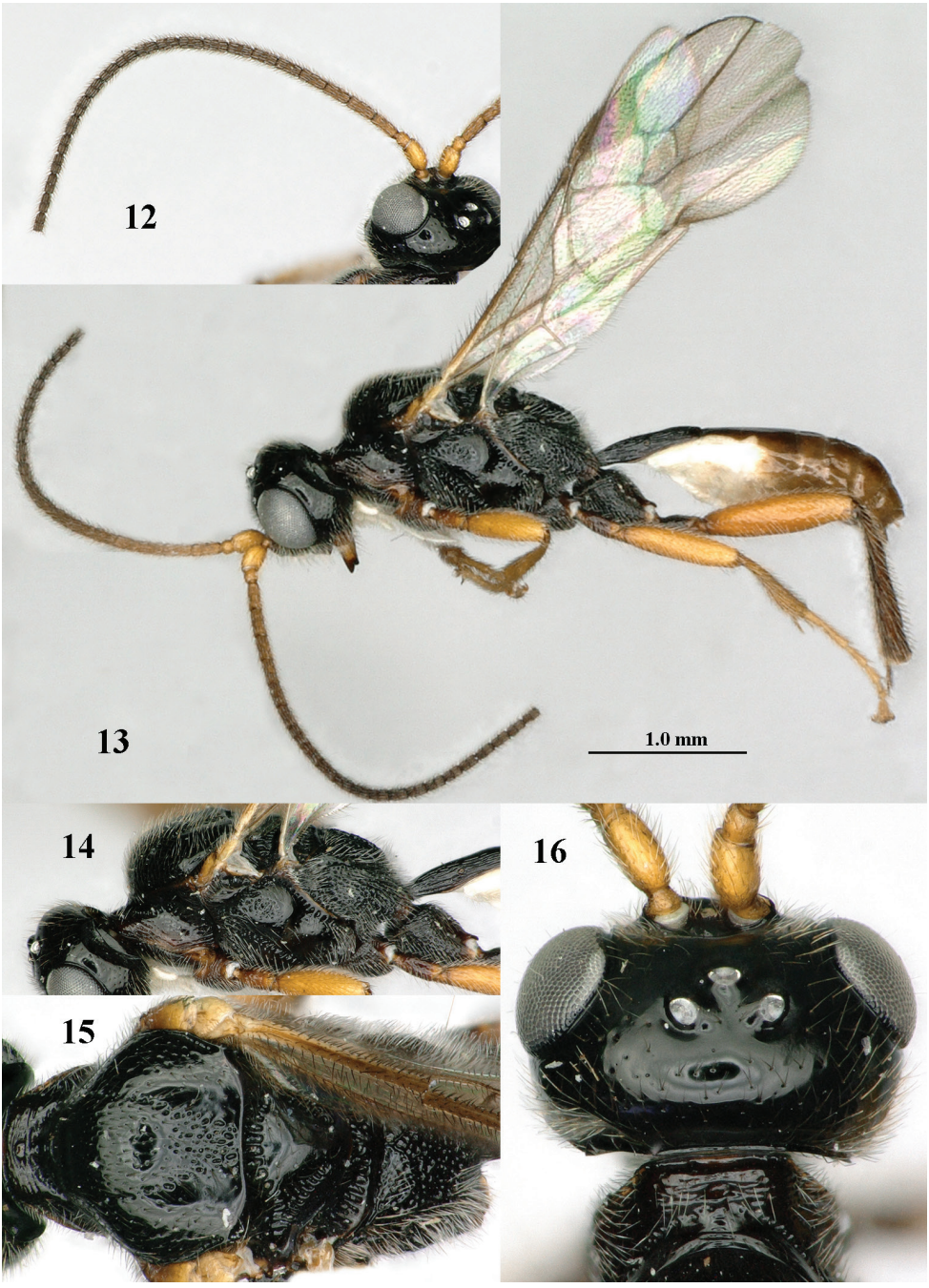

Figures 12–16. *Mannokeraia albipalpis* sp. n., ♂, paratype. **12** antenna, dorso-lateral aspect **13** habitus, lateral aspect **14** mesosoma, lateral aspect **15** mesosoma, dorsal aspect **16** head, dorsal aspect.

medio-posterior punctate area of mesoscutum rather large; coxae, trochanters, trochantelli, and hind tibia blackish or dark brown (hind tarsus missing); first tergite 2.9 times longer than wide apically, with dorsope shallowly impressed and distinctly longitudinally striate.

Variation. Female paratype is very similar to holotype. Length of fore wing 2.9 mm, of body 3.0 mm; antenna with 20 segments, its penultimate segment as long as wide (without pedunculus 0.8 times); both teeth of mandible large; first metasomal tergite 2.3 times longer than its apical width and with slightly indicated dorsope; setose part of ovipositor sheath 0.18 times as long as fore wing and 0.54 times hind tibia.

Etymology. Named after its white palpi ("albus" is white in Latin).

Distribution. Australia (Queensland). Collected in December and February.

Mannokeraia aptera van Achterberg, 1995

Figs 17–27

Mannokeraia apterus van Achterberg, 1995: 96-97, 153 (examined).

Diagnosis. Antenna of ♀ with 16 segments and medially widened (Fig. 19), basal 7 segments brownish yellow and apical 8 segments strongly moniliform; without space between clypeus and closed mandibles (Fig. 23); palpi pale yellowish; head strongly enlarged behind eyes in dorsal view (Fig. 17); length of malar space 0.8 times basal width of mandible; mesosoma of ♀ strongly depressed, with mesoscutum at upper level of pronotum (Fig. 19); pronotum and mesoscutum brown; propodeum smooth medially (Fig. 18); legs brownish yellow, except dark brown hind coxa and basitarsus; setose part of ovipositor sheath about 0.2 times as long as hind tibia; ♀ apterous (Figs 18, 19; ♂ unknown).

Distribution. Australia (New South Wales, A.C.T.).

Mannokeraia nigrita van Achterberg, sp. n.

http://zoobank.org/8ABDB811-A37A-4E6A-A333-2BF7768FAD70

Figs 28–44

Mannokeraia sp. 1–3 Saranowski et al., 2011: 555, 559.

Type material. Holotype, ♀ (ANIC), "**Australia:** Victoria, Bendae-Bonan, SE: Bonang Hwy, 56 km NNE Orbos, MT. in tree ferns in gully, 11.i.–12.ii.2005, 135 m, bulk no. 2619, 34°15'42"S 148°43'49"E, C. Lambkin, N. Starick, ANIC", "DNA Voucher # BJS104, Hymenoptera Institute, University of Kentucky". Paratypes: 3 ♂ (ANIC), same label data, but voucher numbers # BJS100, BJS100S and BJS105.

Diagnosis. Antenna of ♀ with 19+ segments and medially rather widened (Fig. 38), and basal 7 segments dark brown and apical 12 segments strongly moniliform, of

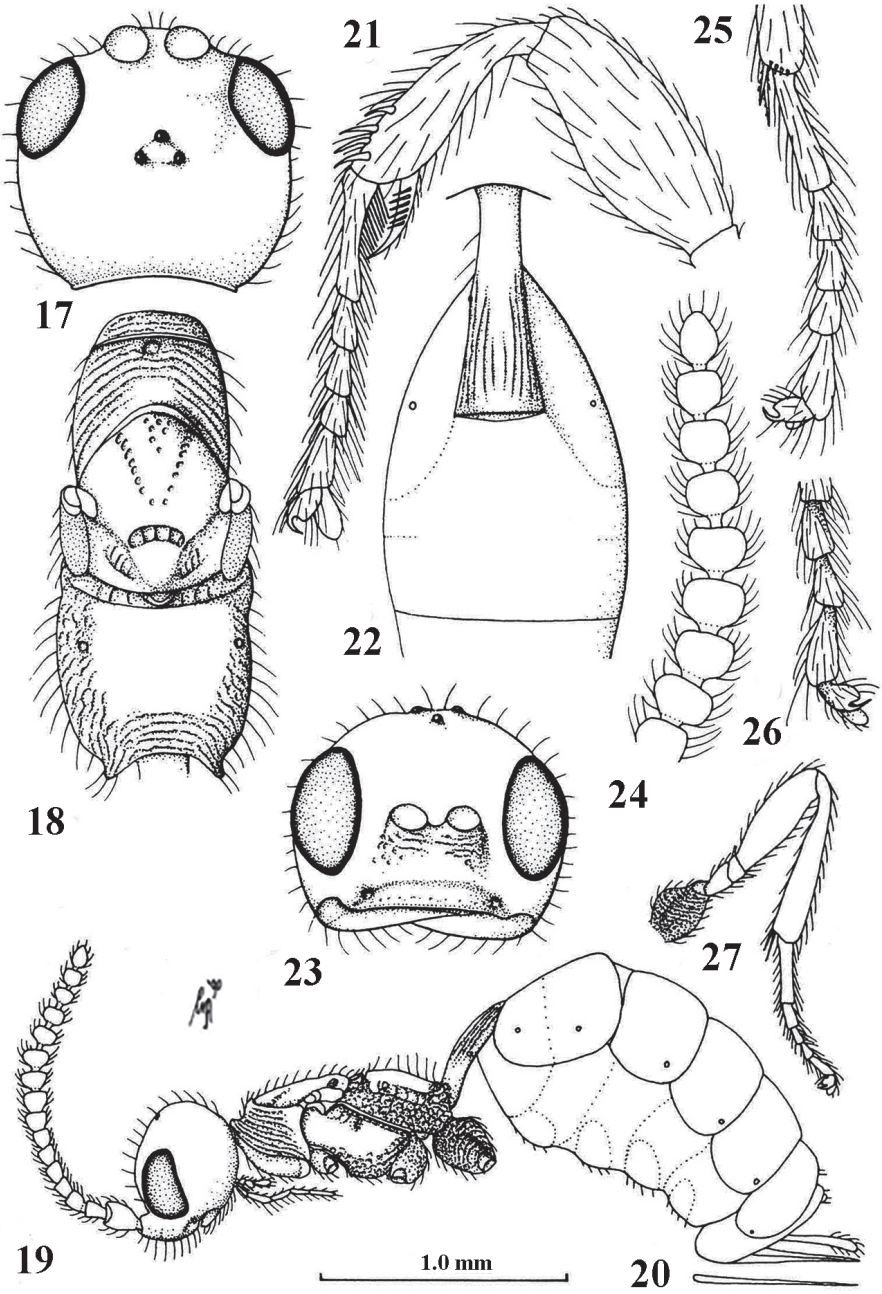

Figures 17–27. *Mannokeraia aptera* van Achterberg, ♀, holotype. **17** head, dorsal aspect **18** mesosoma, dorsal aspect **19** habitus, lateral aspect **20** ovipositor, ventral aspect **21**, fore tarsus, lateral aspect **22** first-third metasomal tergites, dorsal aspect **23** head, anterior aspect **24** apex of antenna, lateral aspect **25** middle tarsus, lateral aspect **26** outer hind claw, lateral aspect **27** hind leg, lateral aspect. 17, 18, 22, 23: 2.2× scale-line; 19, 20, 27: 1.0×; 21, 24, 25: 3.3×; 26: 2.5×. From: van Achterberg (1995).

Figure 28. *Mannokeraia nigrita* sp. n., ♀, holotype, habitus, lateral aspect.

♂ blackish (Fig. 44); palpi grey; with transverse space between clypeus and closed mandibles; head moderately enlarged behind eyes in dorsal view (Figs 35, 43); length of malar space equal to basal width of mandible (Fig. 34); mesosoma of ♀ normal, with mesoscutum far above upper level of pronotum (Fig. 30); pronotum and mesoscutum black; propodeum rugose medially (Fig. 31); legs blackish or dark brown; setose part of ovipositor sheath 0.7 times as long as hind tibia; both sexes macropterous.

Description. Holotype, ♀, length of fore wing 3.6 mm, and of body 5.1 mm.

Head. Antenna with 19+ segments (apical segment(s) missing), pedicellus short (Figs 35, 38), length of third segment 1.3 times fourth segment, third and fourth segments 1.3 and 1.0 times as long as wide, respectively (Fig. 38) and with apical 9+ segments pedunculate, medially antenna slightly wider than subbasally and apically distinctly narrowed (Fig. 38); length of maxillary palp 0.9 times height of head; occipital carina complete, comparatively low dorsally (Fig. 36), strongly curved ventrally and joining hypostomal carina below mandible and occipital flange curved and elongate; eye 1.1 times as long as temple in dorsal view; temples subparallel-sided behind eyes; OOL:diameter of posterior ocellus:POL = 14:5:15; vertex and frons smooth (but vertex with some punctures) and moderately shiny, with some long setae, convex, without median groove, and anteriorly flattened; face sparsely coarsely punctate and with some

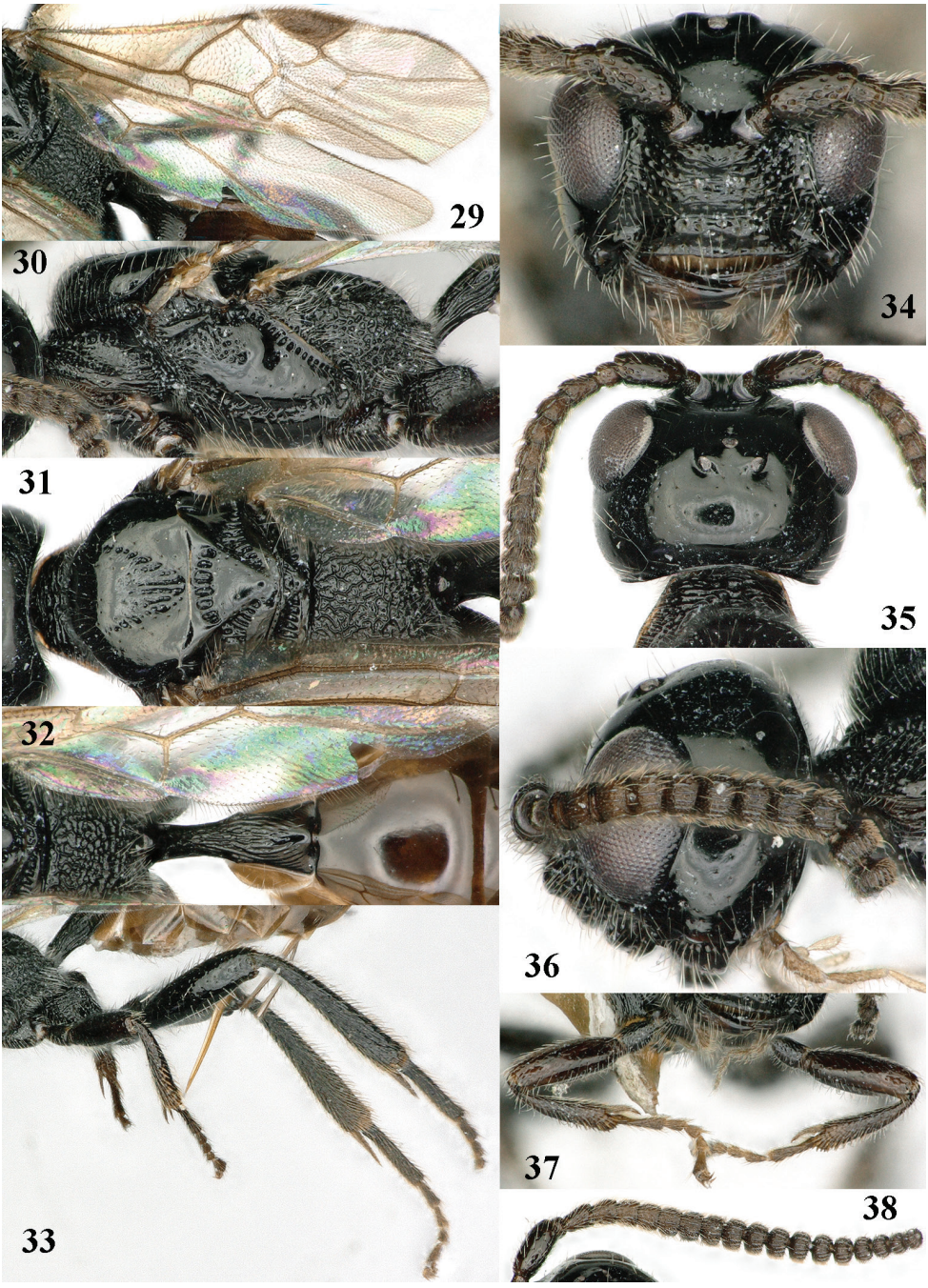

Figures 29–38. *Mannokeraia nigrita* sp. n., ♀, holotype. **29** wings **30** mesosoma, lateral aspect **31** mesosoma, dorsal aspect **32** propodeum, first–third metasomal tergites, dorsal aspect **33** hind leg, lateral aspect **34** head, anterior aspect **35** head, dorsal aspect **36** head, lateral aspect **37** fore legs, inner aspect **38** antenna, lateral aspect.

superficial rugae (Fig. 34); clypeus truncate (resulting in steep ventral face) and smooth ventrally, without ventral rim, dorsally weakly convex and with some coarse punctures; with wide transverse space between closed mandibles and clypeus; length of malar space equal to basal width of mandible; mandible flattened medially and coarsely striate, both apical teeth large.

Mesosoma. Length of mesosoma 1.9 times its height; dorsal pronope and antescutal depression absent; side of pronotum rugose, but medially and dorsally largely smooth; mesopleuron coarsely punctate dorsally; precoxal sulcus complete, rather narrow crenulate-punctate (Fig. 30); remainder of mesopleuron smooth except for a few punctures; mesosternal suture rather deep and coarsely crenulate; postpectal carina distinct medio-ventrally, straight; notauli complete, anteriorly a narrow row of punctures and posteriorly widely crenulate (Fig. 31); remainder of mesoscutum slightly convex, strongly shiny, and largely smooth, except for some coarse striae and punctures medio-posteriorly (Fig. 31), mesoscutum glabrous laterally and with few medium-sized setae medially; scutellar sulcus with five costae; scutellum flat, smooth (except for some setiferous punctures) and shiny; metapleuron entirely coarsely vermiculate-rugose; propodeum entirely moderately reticulate-rugose (Fig. 31), its median carina absent, its posterior face medially rather differentiated and without tubercle postero-laterally (Fig. 31).

Wings. Fore wing: pterostigma wide (Fig. 29); 1-M nearly straight; 1-SR short (Fig. 29); marginal cell closed anteriorly; 1-R1 1.5 times longer than pterostigma and direct after pterostigma hardly pigmented (as apex of pterostigma: Fig. 29); vein r emitted far after middle of pterostigma; r:3-SR:SR1 = 5:18:83; vein SR1 straight; 2-SR:3-SR:r-m = 28:18:19; 2-M much longer than 3-SR; m-cu slightly postfurcal; 1-CU1 oblique and narrow, about as long as cu-a; 1-CU1:2-CU1 = 5:31; basal and subbasal cells of fore wing similarly setose as other cells. Hind wing: marginal cell parallel-sided apically (Fig. 29); M+CU:1-M:1r-m = 32:15:10; basal and subbasal cells less densely setose than other cells.

Legs. Hind coxa largely rugose, dorso-basally transversely rugose; tarsal claws with wide truncate lamelliform lobe (Fig. 37); length of femur, tibia and basitarsus of hind leg 3.4, 5.5 and 5.2 times as long as their maximum width; fore femur inflated and ventrally flattened, 3.0 times longer than wide and apically rounded (Fig. 37); fore and middle tarsi rather flattened (Figs 33, 37); hind tibia distinctly striate.

Metasoma. First tergite 2.2 times longer than its apical width, petiolate basally and gradually widened apically (Fig. 32), coarsely striate but smooth posteriorly, dorsal carinae unite to form a median carina (Fig. 32), basal half of tergite closed ventrally and sternite differentiated; laterope absent; second tergite smooth; ovipositor sheath subparallel-sided and apically obtuse (Figs 28, 33), its setose part 0.26 times as long as fore wing and 0.73 times hind tibia; ovipositor with minute subapical notch, compressed and basally widened (Fig. 28).

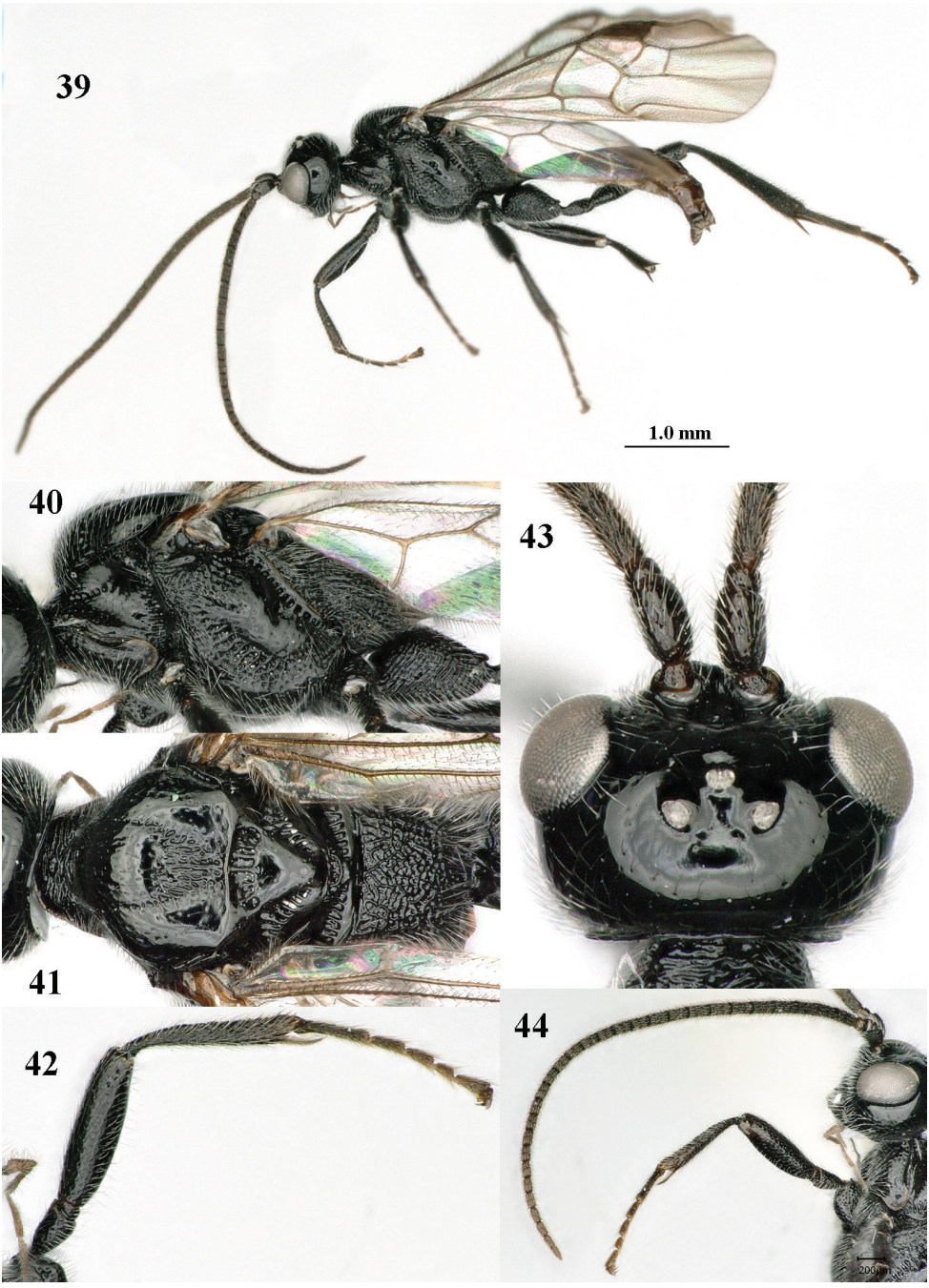

Figures 39–44. *Mannokeraia nigrita* sp. n., ♂, paratype. **39** habitus, lateral aspect **40** mesosoma, lateral aspect **41** mesosoma, dorsal aspect **42** fore leg, lateral aspect **43** head, dorsal aspect **44** antenna, lateral aspect.

Colour. Black; antenna and legs blackish or dark brown; palpi pale brown; tegulae, pterostigma (but apex pale), most veins of fore wing and metasoma (except black first tergite) dark brown; wing membrane weakly infuscate.

Male. Rather different (Fig. 39) from female holotype: clypeus more or less protruding medio-ventrally and with a weak rim ventrally, precoxal sulcus moderately to widely rugose (Fig. 40), distinctly curved postpectal carina, slender tarsi (Figs 39, 42, 44) and more pronounced sculpture of body. Length of fore wing 4.0–4.3 mm, and of body 4.3–4.6 mm; antenna with 31(2) or 32(1) segments; fore and middle tarsal segments slender; first tergite 2.2–2.3 times longer than wide apically and dorsope absent or slightly indicated.

Etymology. Named after its blackish antenna ("niger" is black in Latin).

Distribution. Australia (Victoria). Collected in January–February.

***Mannokeraia punctata* van Achterberg, sp. n.**
http://zoobank.org/2C86782D-16FA-469A-9E4E-A3DE62FDCDEC
Figs 45–55

Type material. Holotype, ♂ (CNC), "**Aust[ralia]:** Qld., Mt. Glorious N.P., 630 m, 28.ii.1984, L. Masner s.s.".

Diagnosis. Antenna of ♀ unknown, of ♂ with 30 segments, cylindrical and slender, dark brown but scapus and pedicellus brownish yellow ventrally; palpi pale yellowish; with transverse space between clypeus and closed mandibles (Fig. 52); head moderately enlarged behind eyes in dorsal view (Fig. 53); length of malar space 0.9 times basal width of mandible (Fig. 52); mesosoma of ♀ normal, with mesoscutum far above upper level of pronotum (Fig. 47); pronotum and mesoscutum yellowish brown; propodeum mainly punctate medially (Fig. 49); fore and middle legs (but tibiae and tarsi darkened) brownish yellow, and hind leg dark brown; length of setose part of ovipositor sheath unknown.

Description. Holotype, ♂, length of fore wing 2.8 mm, and of body 3.5 mm.

Head. Antenna with 30 segments, pedicellus short (Figs 51, 54), length of third segment 1.2 times fourth segment, third, fourth and penultimate segments 2.9, 2.4 and 2.7 times as long as wide, respectively (Fig. 51) and with apical segments sessile, medially parallel-sided and apically slightly narrowed (Fig. 51); length of maxillary palp 1.1 times height of head; occipital carina complete, comparatively low dorsally (Fig. 54), strongly curved ventrally and joining hypostomal carina far below mandible and occipital flange curved and elongate; eye 1.1 times as long as temple in dorsal view; temples slightly narrowed behind eyes; OOL:diameter of posterior ocellus:POL = 6:5:8; vertex and frons smooth (but vertex with some punctures) and moderately shiny, with some long setae, convex, frons without median groove, and anteriorly flattened; face sparsely coarsely punctate and with some superficial rugae (Fig. 52); clypeus flattened and smooth ventrally, with medially weakly protruding thick ventral rim (resulting in steep ventral area), dorsally weakly convex and with few coarse punctures;

Figure 45. *Mannokeraia punctata* sp. n., ♂, holotype, habitus, lateral aspect.

with medium-sized transverse space between closed mandibles and clypeus; length of malar space 0.9 times basal width of mandible; mandible slightly convex medially and with few punctures, both apical teeth large.

Mesosoma. Length of mesosoma 1.7 times its height; dorsal pronope and antescutal depression absent; side of pronotum antero-medially and posteriorly coarsely crenulate, rugose, antero-ventrally rugose and remainder largely smooth; mesopleuron coarsely punctate dorsally; precoxal sulcus complete, wide medially and coarsely punctate (Fig. 47); remainder of mesopleuron smooth; mesosternal suture rather narrow and finely crenulate; postpectal carina complete medio-ventrally, curved; notauli complete, anteriorly moderately crenulate and posteriorly ending in wide rugose area (Fig. 48); remainder of mesoscutum slightly convex, strongly shiny, and largely smooth, except for some fine punctures (Fig. 48), mesoscutum sparsely setose laterally and moderately setose medially; scutellar sulcus with six costae; scutellum slightly convex, smooth (except for some setiferous punctures) and shiny; metapleuron entirely coarsely punctate; propodeum coarsely punctate, only anteriorly partly sparsely punctate (Figs 48, 49), its median carina absent, its posterior face medially rather differentiated and without tubercle postero-laterally (Fig. 47).

Wings. Fore wing: pterostigma wide (Fig. 46); 1-M slightly curved; 1-SR short (Fig. 46); marginal cell closed anteriorly; 1-R1 1.3 times longer than pterostigma and direct after pterostigma weakly pigmented (as apex of pterostigma: Fig. 46); vein r emitted far after middle of pterostigma; r:3-SR:SR1 = 5:6:53; vein SR1 straight; 2-SR:3-SR:r-m = 19:6:11; 2-M much longer than 3-SR; m-cu interstitial; 1-CU1 oblique and narrow,

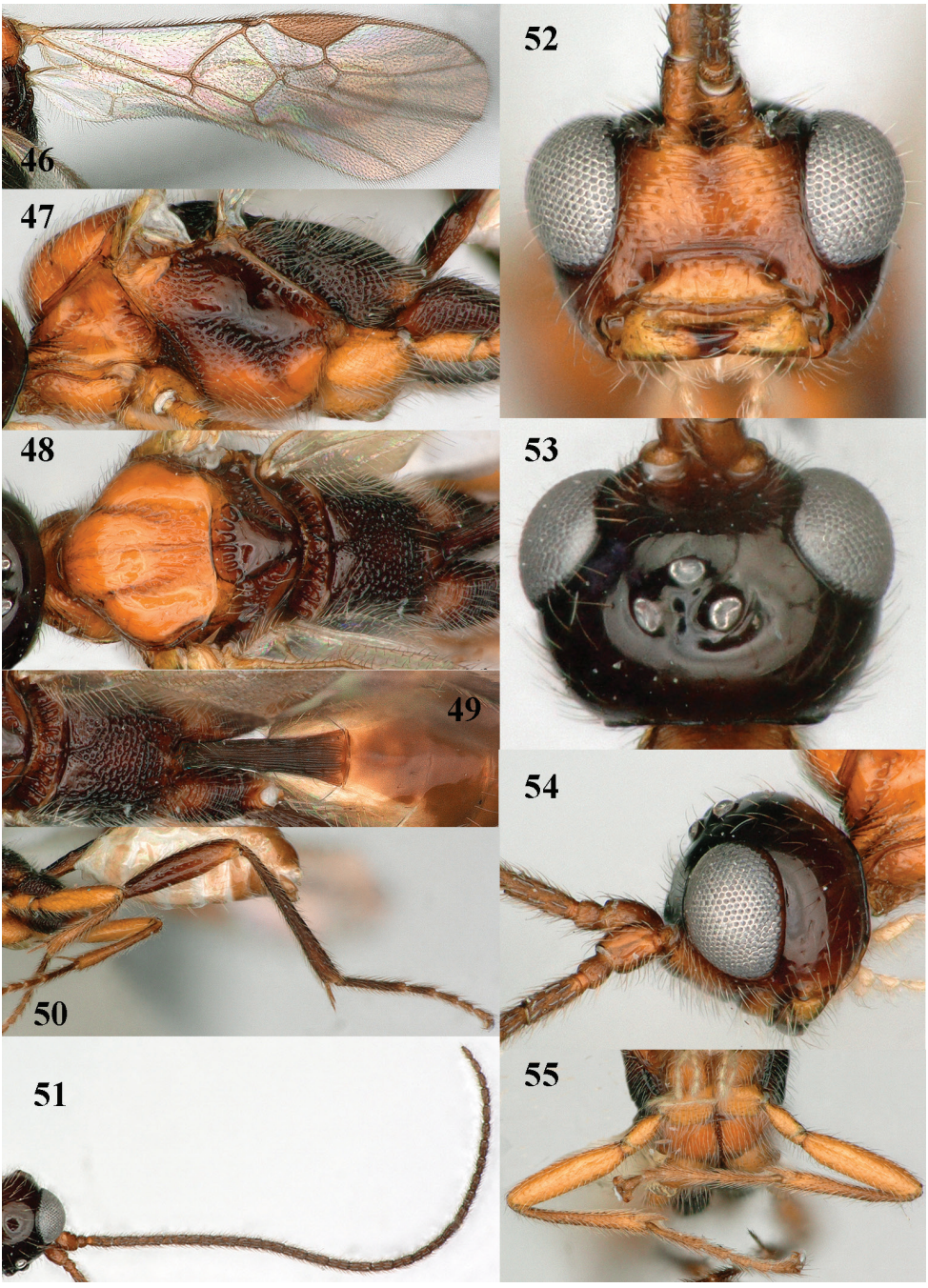

Figures 46–55. *Mannokeraia punctata* sp. n., ♂, holotype. **46** wings **47** mesosoma, lateral aspect **48** mesosoma, dorsal aspect **49** propodeum, first–third metasomal tergites, dorsal aspect **50** hind leg, lateral aspect **51** antenna, lateral aspect **52** head, anterior aspect **53** head, dorsal aspect **54** head, lateral aspect **55** fore legs, inner aspect.

about as long as cu-a; 1-CU1:2-CU1 = 1:8; basal and subbasal cells of fore wing similarly setose as other cells. Hind wing: marginal cell parallel-sided apically, but hardly visible; M+CU:1-M:1r-m = 27:13:10; basal and subbasal cells less densely setose than other cells.

Legs. Hind coxa largely transversely striate but basally punctate (Figs 49, 50); tarsal claws with wide truncate lamelliform lobe (Fig. 55); length of femur, tibia and basitarsus of hind leg 4.3, 8.4 and 6.8 times as long as their maximum width; fore femur moderately widened and ventrally convex, 4.0 times longer than wide and apically rounded (Fig. 55); fore and middle tarsi slender and subcylindrical (Figs 45, 55); hind tibia distinctly striate.

Metasoma. First tergite 2.8 times longer than its apical width, petiolate basally and gradually widened apically (Fig. 49), coarsely striate, dorsal carinae unite to form a median carina (Fig. 49), basal half of tergite closed ventrally and sternite distinctly differentiated; laterope absent; second tergite smooth.

Colour. Black; scapus and pedicellus ventrally, clypeus, mandible, fore and middle legs (but tibiae and tarsi darkened) brownish yellow; palpi and tegulae pale yellow; face, pronotum, mesoscutum, mesosternum and mesopleuron antero-dorsally and ventrally yellowish brown; remainder of antenna and of mesosoma, first metasomal tergite, hind leg, pterostigma (but apex pale), most veins of fore wing dark brown; remainder of metasoma brown, but ventrally membranes whitish; wing membrane subhyaline.

Etymology. Named after its punctate propodeum ("punctus" is puncture in Latin).

Distribution. Australia (Queensland). Collected in February.

Paramannokeraia van Achterberg & Quicke, gen. n.

http://zoobank.org/FC549892-3C5F-49AB-A922-319F9948553E

Figs 56–83

Type species. *Paramannokeraia gibsoni* van Achterberg & Quicke, sp. n. Gender: feminine.

Etymology. From "para" (= Greek for "near") and the generic name *Mannokeraia* van Achterberg, 1995, because the new genus is related to it.

Diagnosis. Antenna of ♀ with 19 segments, pedicellus much narrower than scapus and most segments moniliform (Fig. 58), of ♂ with about 28 segments and segments much longer than wide; scapus much longer and wider than pedicellus (Fig. 58); face convex medio-dorsally (Fig. 58); maxillary palp with 6 segments and labial palp with 4 segments; eyes distinctly setose; clypeus rather large and elliptical (Fig. 57), dorsally differentiated from face and ventrally flattened; face moderately convex medio-dorsally (Fig. 57); pronotal collar long (Figs 58, 62) and distinctly below level of mesoscutum; notauli nearly complete (Fig. 64); scutellum without medio-posterior depression; mesosternal sulcus distinct and crenulate; postpectal carina variable (distinct in *P. gibsoni*, and absent, with at most the area between middle coxae rugose in *P. juliae*); vein M+CU1 of fore wing sclerotised; vein cu-a of hind wing present and comparatively close to vein 1r-m (Fig. 56); fore femur robust and flattened ventrally (Fig. 63); fore

tibia without distinct spines and apically with wide tooth-like protuberance (Fig. 63); fore tibial spur medium-sized; base of fore basitarsus angulate (Fig. 64); telotarsi hardly widened (Figs 64, 65); hind tibia largely smooth between pimply protrusions; tarsal claws angularly bent and with truncate lobe (Fig. 60); propodeum without large posterior areola and median carina absent (Fig. 62), medio-posteriorly gradually lowered (Fig. 62); first tergite gradually widened posteriorly and with its spiracles submedially situated (Fig. 59) and tergite inserted near condyli of hind coxa; dorsope present (Fig. 59); laterope absent; ovipositor nearly cylindrical.

Distribution. Australia (two species).

Notes. Because of its venation, shape of the telotarsi, submedial position of the spiracle of the first tergite and shape of the first tergite, the genus belongs to the subfamily Euphorinae within which it belongs to the tribe Planitorini. It resembles *Mannokeraia*, because of the small pedicellus (much narrower than the scapus; Fig. 58), apical antennal segments of the female strongly moniliform and pedunculate, the face moderately convex medio-dorsally, the lack of the medio-posterior depression of the scutellum, the robust fore femur, the setose eyes and the long pronotal collar. According to the DNA analysis by Stigenberg et al. (2015) *Paramannokeraia* is sister to *Planitorus* (sharing the presence of dorsope on the first tergite, and the ventrally flattened and narrower clypeus); the two genera forming a sister group to *Mannokeraia* which has the first tergite lacking dorsope, and the clypeus transverse and with a steep ventral face.

Key to species of *Paramannokeraia* gen. n.

1 Face rugose dorsally and densely punctate ventrally (Fig. 57); base of hind coxa finely rugose dorsally (Fig. 65); hind femur rather slender (Fig. 65); setose part of ovipositor sheath 0.2 times as long as hind tibia (Fig. 58); basal half of antenna and legs dark yellowish brown; apically fore tibia with tooth-like protuberance (Fig. 63); notauli on mesoscutal disk narrow (Fig. 62); fore and middle tarsi of ♀ slender (Fig. 64) ..... ***P. gibsoni* sp. n.**

– Face mainly sparsely punctate (Fig. 73); base of hind coxa smooth dorsally (Fig. 68); hind femur rather swollen (Fig. 71); setose part of ovipositor sheath 0.4 times as long as hind tibia (Fig. 66); basal half of antenna of both sexes and legs dark brown; fore tibia rounded apically, without tooth-like protuberance apically (Fig. 76); notauli on mesoscutal disk widened (Fig. 69); fore and middle tarsi of ♀ widened (Figs 66, 76) ..... ***P. juliae* sp. n.**

***Paramannokeraia gibsoni* van Achterberg & Quicke, sp. n.**
http://zoobank.org/232633BF-B8BA-4AEF-81BF-C3E2FA06C0F1
Figs 56–65

Mannokeraia gibsoni; Belshaw and Quicke 2002: 474 (MS name for "Australia AJ416968"). Nomen nudum.

Type material. Holotype, ♀ (CNC), "**Australia**: N.S.W., Mt. Keira via Wollongong, iv.2005", "BF000332, RJF 004 D8", "gen. n. aff. *Planitorus*, det. Belokobylskij, [20]08".

Diagnosis. Antenna of ♀ with 15+ robust segments, apical segments pedunculate (Fig 58), of ♂ unknown; head transverse, not enlarged behind eyes in dorsal view (Fig. 61); face rugose dorsally and densely punctate ventrally (Fig. 57); mesosoma of ♀ normal, with mesoscutum above upper level of pronotum (Fig. 58); notauli on mesoscutal disk narrow (Fig. 62); propodeum rugose medially (Fig. 62); base of hind coxa finely rugose dorsally (Fig. 65); hind femur rather slender (Fig. 65); apically fore tibia with tooth-like protuberance (Fig. 62); fore and middle tarsi of ♀ slender (Fig. 64); basal half of antenna and legs rather dark yellowish brown; setose part of ovipositor sheath about 0.2 times as long as hind tibia; ♀ macropterous.

Description. Holotype, ♀, length of fore wing 2.1 mm, and of body 2.2 mm.

Head. Antenna with 15+ segments, length of third segment 1.1 times fourth segment, third and fourth segments 1.7 and 1.6 times as long as wide, respectively (Fig. 58), apical segments pedunculate (Fig. 58); length of maxillary palp 1.1 times height of head; occipital carina complete, low dorsally (Fig. 58); eye 1.8 times as long as temple in dorsal view; temples gradually narrowed behind eyes (Fig. 61); OOL:diameter of posterior ocellus:POL = 6:3:9; frons smooth, with long setae and without median groove or carina, slightly depressed; face rather coarsely rugose dorsally and punctate ventrally (Fig. 57); clypeus depressed and smooth ventrally, dorsally weakly convex and with some punctures (Fig. 57); length of malar space 0.8 times basal width of mandible; occipital carina about joining hypostomal carina and occipital flange subcircular (Fig. 58); mandible flat and shiny basally.

Mesosoma. Length of mesosoma 1.8 times its height; dorsal pronope small, round (Fig. 62); antescutal depression absent; side of pronotum largely reticulate-punctate anteriorly, medially largely smooth and posteriorly punctate-costate (Fig. 58); epicnemial area coarsely punctate dorsally; precoxal sulcus complete, coarsely punctate (Fig. 58) and remainder of mesopleuron smooth; mesosternal suture rather deep and moderately crenulate; postpectal carina present medio-ventrally; mesoscutum flat, smooth (except five grooves medio-posteriorly: Fig. 62), glabrous laterally and with long setae medially; notauli nearly complete, largely smooth and narrow (Fig. 62); scutellar sulcus with five costae; scutellum flat, smooth (also medio-posteriorly: Fig. 62); metapleuron coarsely and densely rugose-punctate; propodeum coarsely and densely rugose but less so posteriorly, its median carina absent except posteriorly (Fig. 62), its posterior face weakly differentiated and with an obtuse tubercle postero-laterally, just above level of socket of first tergite (Fig. 58).

Wings. Fore wing: 1-M distinctly curved; 1-SR very short (Fig. 56); marginal cell closed anteriorly; vein r emitted distinctly after middle of pterostigma; r:3-SR:SR1 = 3:10:54; vein 1-R1 somewhat longer than pterostigma; vein SR1 straight; 2-SR:3-SR:r-m = 10:5:6; 2-M distinctly longer than 3-SR; m-cu postfurcal; 1-CU1 oblique and narrow; 1-CU1:2-CU1 = 7:20; basal and subbasal cells of fore wing setose as other cells. Hind wing: marginal cell subparallel medially and absent apically (Fig. 56); M+CU:1-M:1r-m = 38:15:12.

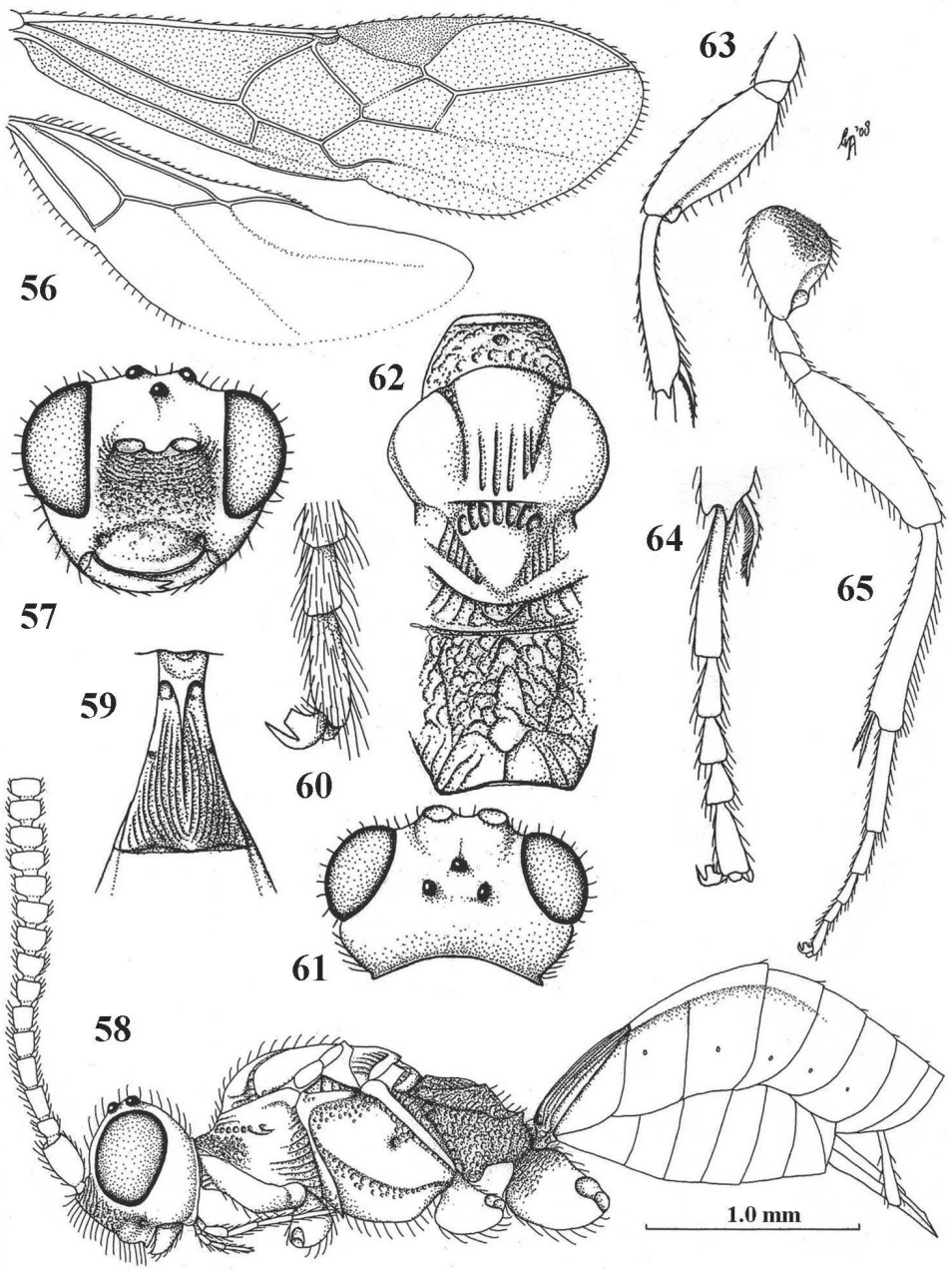

Figures 56–65. *Paramannokeraia gibsoni* gen. n. & sp. n., ♀, holotype. **56** wings **57** head, anterior aspect **58** habitus, lateral aspect **59** first metasomal tergite, dorsal aspect **60** outer hind claw, lateral aspect **61** head, dorsal aspect **62** mesosoma, dorsal aspect **63** fore femur and tibia, lateral aspect **64** fore tarsus, dorsal aspect **65** hind leg, lateral aspect. 56, 58, 65: scale-line (= 1×); 57, 59, 61, 62, 64: 2.0×; 63: 2.2×; 60: 3.2×.

Legs. Hind coxa basally finely rugose and remainder largely smooth (Fig. 58); tarsal claws with wide truncate lamelliform lobe (Fig. 60); length of femur, tibia and basitarsus of hind leg 3.2, 6.2 and 6.0 times as long as their maximum width; fore femur rather inflated, 2.7 times longer than wide, with apical tooth and with some spiny bristles (Fig. 63).

Metasoma. First tergite 1.5 times longer than its apical width, distinctly petiolate (Fig. 59), with coarse curved striae, dorsal carinae unite to form a median carina and dorsope deep and large (Fig. 59), only basal quarter closed ventrally; laterope absent, tergite widened latero-basally (Fig. 58); second tergite smooth; ovipositor sheath somewhat widened and obtuse apically (Fig. 58), its setose part 0.10 times as long as fore wing and 0.23 times hind tibia; ovipositor with minute subapical nodus and wide basally (Fig. 58).

Colour. Black; basal half of antenna, pronotum narrowly antero-ventrally and legs rather dark yellowish brown; tegulae and palpi pale yellowish; metasoma (except black first tergite), pterostigma (but narrowly paler basally) and apical half of antenna dark brown; veins brown; wing membrane weakly infuscate.

Etymology. Named after Dr Gary A.P. Gibson (Ottawa), for his extensive contribution to our knowledge of Chalcidoidea (especially of the families Eupelmidae and Pteromalidae), and of Mymarommatidae.

Distribution. Australia (New South Wales). Collected in April.

***Paramannokeraia juliae* van Achterberg, sp. n.**
http://zoobank.org/964AFC04-F505-4C18-ADC3-2F72062294D6
Figs 66–83

Mannokeraia sp.; Stigenberg et al. 2015: 575.

Type material. Holotype, ♀ (NHRS), "**Australia**, **Tasmania**, Cradle Mtn NP, creek from Crater Lake to Ronny Creek, 100 m upstr. boardwalk, 867 mao, S41°38.667' E145°56.755', 23.ii–4.iii.2006, Malaise trap, loc. 14, N. Jönsson, T. Malm & D. Williams", "DNA voucher DNA JS10_00282", "NHRS-HEVA 000004017". Paratype: 1 ♂ (CNC), "Australia, Tas[mania], Mt. Field NP, 7.i.1984, L. Masner, s. s.".

Diagnosis. Antenna of ♀ with 19 robust segments, apical segments pedunculate (Fig 72), of ♂ cylindrical and elongate (Fig. 81); head transverse, not enlarged behind eyes in dorsal view (Fig. 74); face mainly sparsely punctate (Fig. 73); mesosoma of ♀ normal, with mesoscutum distinctly above upper level of pronotum (Fig. 68); notauli on mesoscutal disk widened (Fig. 69); propodeum rather sparsely rugulose but sublaterally largely smooth (Fig. 69); base of hind coxa smooth dorsally (Fig. 68); hind femur rather swollen (Fig. 71); fore tibia rounded apically, without tooth-like protuberance apically (Fig. 76); fore and middle tarsi of ♀ widened (Figs 66, 76); basal half of antenna of both sexes and legs dark brown; setose part of ovipositor sheath about 0.4 times as long as hind tibia (Fig. 66); both sexes macropterous.

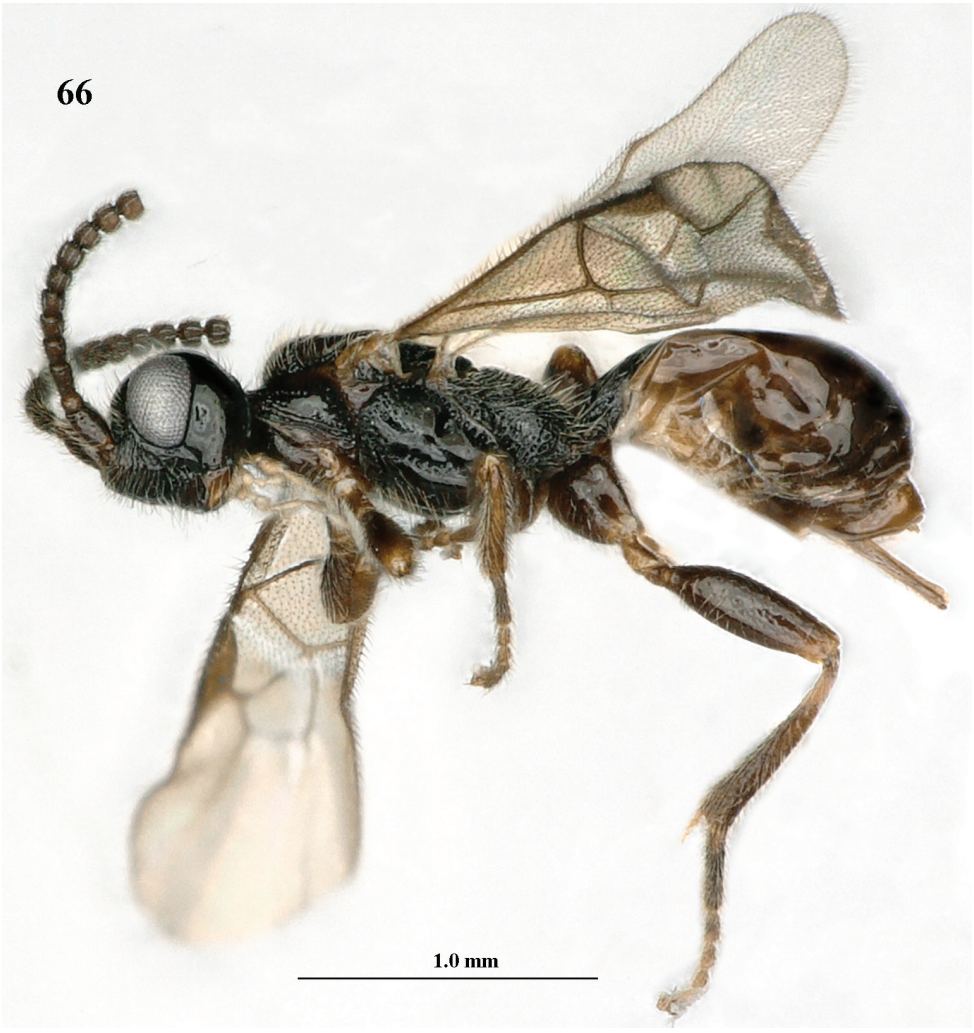

Figure 66. *Paramannokeraia juliae* gen. n. & sp. n., ♀, holotype, habitus, lateral aspect.

Description. Holotype, ♀, length of fore wing 2.5 mm, and of body 2.7 mm.

Head. Antenna with 19 segments, length of third segment 1.1 times fourth segment, third, fourth and penultimate segments 1.6, 1.4 and 0.9 (without pedunculus 0.8) times as long as wide, respectively (Fig. 72) and with apical 12 segments pedunculate, medially antenna as wide as apically; length of maxillary palp 0.8 times height of head; occipital carina complete, low dorsally (Fig. 75); eye 1.5 times as long as temple in dorsal view; temples subparallel-sided behind eyes; OOL:diameter of posterior ocellus:POL = 9:5:11; frons smooth and shiny, with some long setae, convex, with shallow median groove, and anteriorly flattened; face with some rugae dorsally below antennal sockets and remainder sparsely coarsely punctate (Fig. 73); clypeus depressed

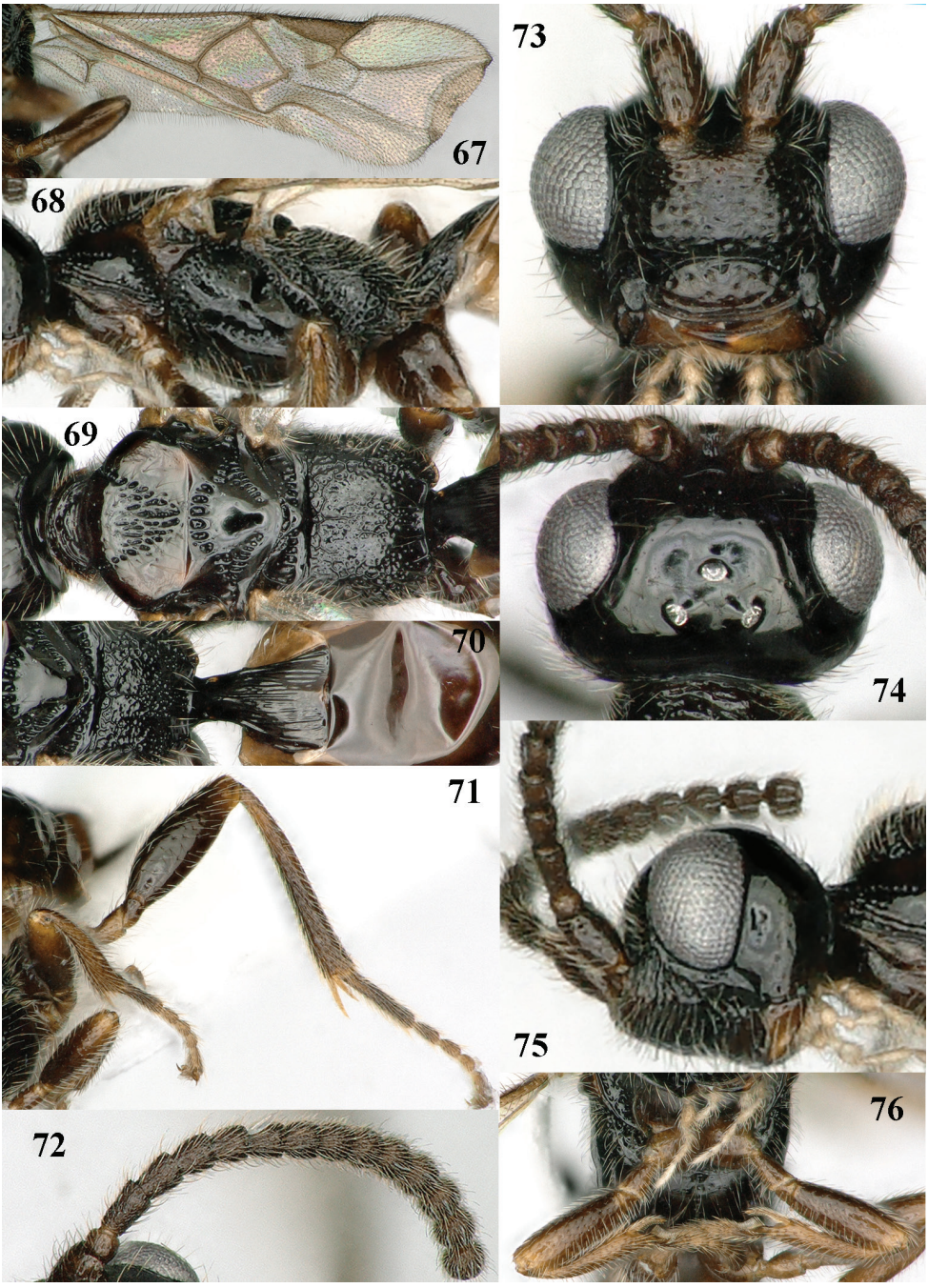

Figures 67–76. *Paramannokeraia juliae* gen. n. & sp. n., ♀, holotype. **67** wings **68** mesosoma, lateral aspect **69** mesosoma, dorsal aspect **70** propodeum, first–third metasomal tergites, dorsal aspect **71** hind leg, lateral aspect **72** antenna **73** head, anterior aspect **74** head, dorsal aspect **75** head, lateral aspect **76** fore legs, inner aspect.

and smooth ventrally, with ventral rim slightly upcurved, dorsally weakly convex and with some coarse punctures (Fig. 73); length of malar space 1.1 times basal width of mandible; occipital carina joining hypostomal carina and occipital flange subcircular; mandible depressed medially and shiny, apically with large upper and small lower tooth.

Mesosoma. Length of mesosoma 1.9 times its height; dorsal pronope and antescutal depression absent; side of pronotum largely punctate-rugose ventrally, largely smooth medially, with narrow crenulate groove antero-dorsally and punctate-costate posteriorly; epicnemial area punctate dorsally; precoxal sulcus complete, narrowly crenulate-punctate (Fig. 68); remainder of mesopleuron smooth; mesosternal suture deep and coarsely crenulate; postpectal carina absent; notauli complete, coarsely punctate and rather wide, ending in wide punctate area (Fig. 69); scutellar sulcus with five costae; scutellum flat, smooth and shiny; metapleuron punctate medially and coarsely reticulate-punctate ventrally; postpectal carina absent and area between middle coxae with few punctures; propodeum rather sparsely rugulose but sublaterally largely smooth (Fig. 69), posterior face weakly differentiated and without an obtuse tubercle posterolaterally (Fig. 68).

Wings. Fore wing: 1-M weakly curved; 1-SR short (Fig. 67); marginal cell open anteriorly because of most of 1-R1 absent and sclerotized part of 1-R1 about 0.2 times as long as pterostigma (Fig. 67); vein r emitted distinctly after middle of pterostigma; r:3-SR:SR1 = 2:11:62; vein SR1 straight; 2-SR:3-SR:r-m = 27:11:15; 2-M much longer than 3-SR; m-cu slightly postfurcal; 1-CU1 oblique and narrow, about as long as cu-a; 1-CU1:2-CU1 = 5:27; basal and subbasal cells of fore wing setose as other cells. Hind wing: marginal cell subparallel-sided medially and obsolescent apically; M+CU:1-M:1r-m = 41:18:10.

Legs. Hind coxa basally smooth; tarsal claws with wide truncate lamelliform lobe (Fig. 71); length of femur, tibia and basitarsus of hind leg 3.0, 7.3 and 6.0 times as long as their maximum width; fore femur rather inflated, 2.9 times longer than wide and apically rounded (Fig. 76); fore and middle tarsi widened (Figs 66, 76).

Metasoma. First tergite 1.5 times longer than its apical width, distinctly petiolate (Fig. 70), with incomplete straight striae, dorsal carinae unite to form a median carina and dorsope deep and large (Fig. 70), only basal quarter closed ventrally; laterope absent, tergite widened latero-basally; second tergite smooth; ovipositor sheath somewhat widened and obtuse apically (Fig. 66), its setose part 0.14 times as long as fore wing and 0.40 times hind tibia; ovipositor with minute subapical nodus and widened basally.

Colour. Black; antenna, metasoma except black first tergite and legs dark brown, but hind trochanter and tibial spurs brown; tegulae and palpi pale yellowish; pterostigma and veins brown; wing membrane weakly infuscate.

Male. Similar to female holotype except for the shape of the antennal segments, slender fore and middle tarsi (Figs 77, 80, the rugose area between middle coxae and the different sculpture of the propodeum and face (Figs. 78, 82). Antenna with 28 segments, length of fore wing 3.6 mm, and of body 3.6 mm; face and clypeus rather finely

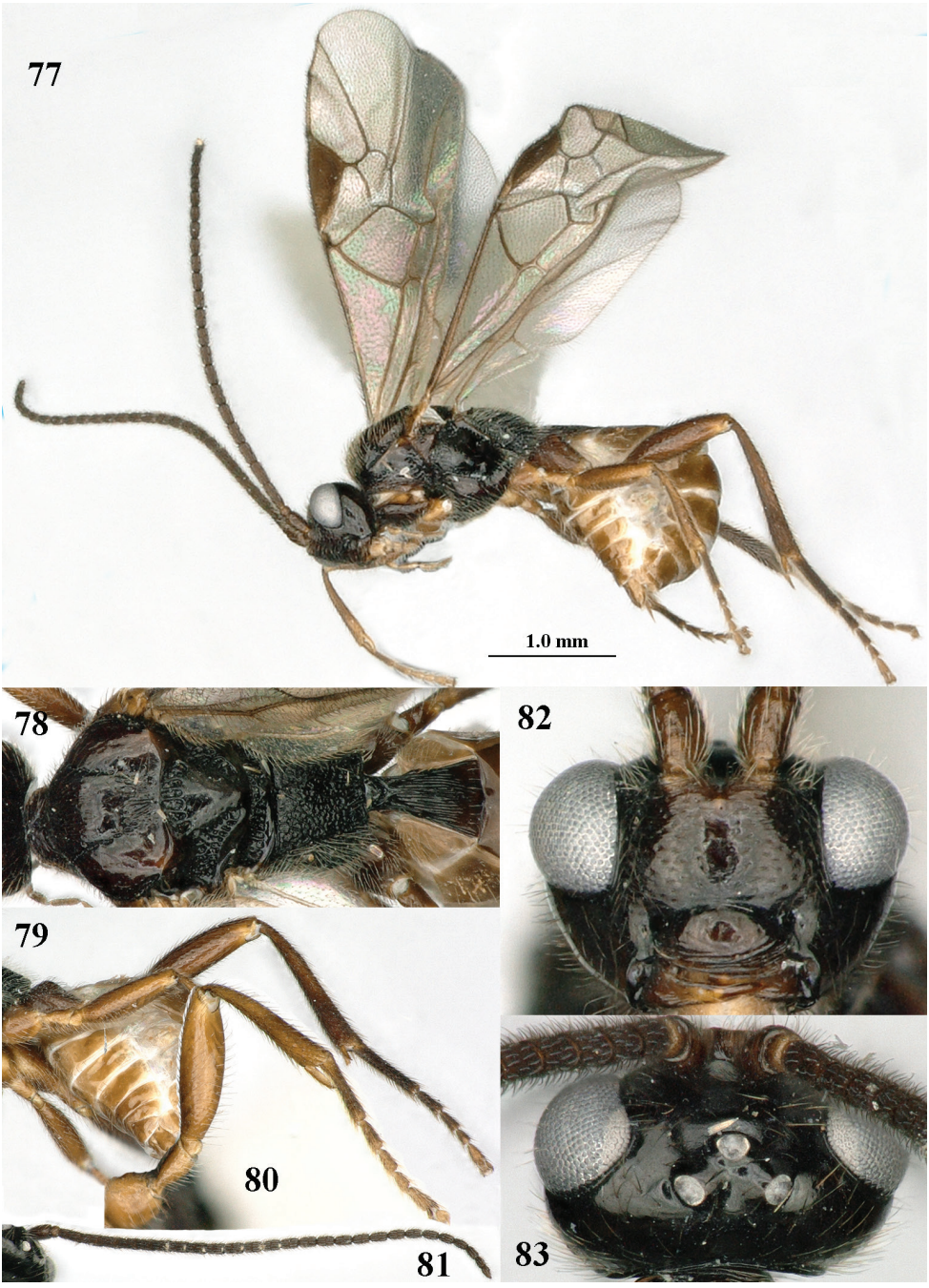

Figures 77–83. *Paramannokeraia juliae* gen. n. & sp. n., ♂, paratype. **77** habitus, lateral aspect **78** mesosoma, dorsal aspect **79** hind leg, lateral aspect **80** fore leg, lateral aspect **81** antenna **82** head, anterior aspect **83** head, dorsal aspect.

punctate; metasoma (except most of first tergite) brown; mesoscutum less flattened; medio-posterior punctate area of mesoscutum small; propodeum largely finely rugulose; first tergite 1.5 times longer than wide apically and distinctly longitudinally striate.

Etymology. Named after Dr Julia Stigenberg (Stockholm), who generously made the holotype available for this study.

Distribution. Australia (Tasmania). Collected in January–March.

Planitorus van Achterberg, 1995

Figs 84–96

Planitorus van Achterberg, 1995: 46–47.

Type species. *Planitorus breviflagellaris* van Achterberg, 1995 (examined).

Diagnosis. Antenna of ♀ with 17 segments, and segments of apical half moniliform (Figs 87, 91), of ♂ unknown; antennal sockets touching each other (Fig. 85); clypeus not differentiated from face (Fig. 86); head elongated below eyes (Fig. 86); pronotal collar below level of mesoscutum (Fig. 87), but mesoscutum low anteriorly; notauli largely reduced, united posteriorly (Fig. 90); scutellar sulcus narrow and curved (Fig. 90); mesosternal sulcus absent and area smooth; vein M+CU1 of fore wing of type species largely unsclerotized (Fig. 84); fore tibia with spiny setae (Fig. 94); hind coxa only basally rugose (Fig. 87); fore and middle tarsal claws with a lamelliform lobe (Fig. 94) and hind claws simple (Fig. 92); dorsope of first tergite distinct and tergite distinctly widened posteriorly (Fig. 93); ovipositor strongly compressed (Figs 87, 88); ♀ macropterous.

Distribution. Australia: one species.

Biology. Unknown.

Planitorus breviflagellaris van Achterberg, 1995

Figs 84–96

Planitorus breviflagellaris van Achterberg, 1995: 47-48, 192.

Diagnosis. See generic diagnosis.

Distribution. Australia (Queensland, A.C.T.). Collected in December–March.

Notes. A headless and also otherwise severely damaged male from near Mount Barker (HIC: Western Australia, 25.iv.2000, DNA voucher BJS101 (as "*Planitorus* sp." in Sharanowski et al. (2011)), and incorrectly labelled as "Mount Baker") may belong to an undescribed second species. It has the notauli entirely absent, vein M+CU1 of fore wing largely sclerotized and the precoxal sulcus present medially.

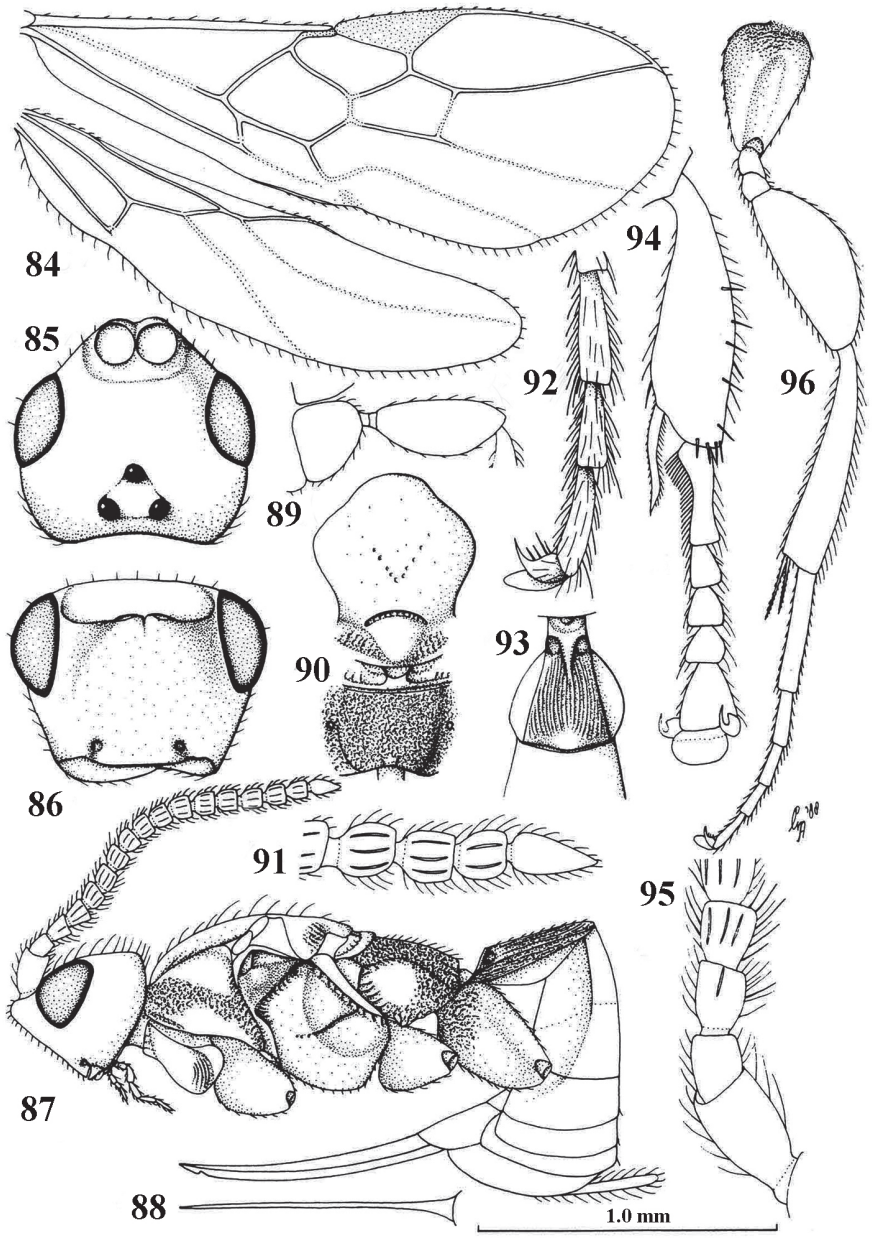

Figures 84–96. *Planitorus breviflagellaris* van Achterberg, ♀, holotype. **84** wings **85** head, dorsal aspect **86** head, frontal aspect **87** habitus, lateral aspect **88** ovipositor, ventral aspect **89** fore femur, lateral aspect **90** mesosoma, dorsal aspect **91** apex of antenna **92** outer hind claw, lateral aspect **93** first metasomal tergite, dorsal aspect **94** fore tibia and tarsus, mainly lateral aspect **95** base of antenna, lateral aspect **96** hind leg, lateral aspect. 84, 87–90, 93, 95: 1.0× scale-line; 85, 86: 1.6×; 91, 92, 94, 96: 2.5×. From: van Achterberg (1995).

Acknowledgements

We are grateful to Julia Stigenberg and Hege Vårdal (NHRS, Stockholm) for the loan of the female of *Paramannokeraia juliae*. DLJQ was supported by the award of a Senior Postdoctoral Fellowship from the Rachadaphiseksomphot Fund, Graduate School, Chulalongkorn University.

References

Belshaw R, Quicke DLJ (2002) Robustness of ancestral state estimates: evolution of life history strategy in ichneumonoid parasitoids. Systematic Biology 51(3): 450-477. https://doi.org/10.1080/10635150290069896

Sharanowski BJ, Dowling APG, Sharkey MJ (2011) Molecular phylogenetics of Braconidae (Hymenoptera: Ichneumonoidea), based on multiple nuclear genes, and implications for classification. Systematic Entomology 36: 549–572. https://doi.org/10.1111/j.1365-3113.2011.00580.x

Shaw MR, Huddleston T (1991) Classification and biology of braconid wasps (Hymenoptera: Braconidae). Handbooks for the Identification of British Insects 7(11): 1–126.

Stigenberg J, Boring CA, Ronquist F (2015) Phylogeny of the parasitic wasp subfamily Euphorinae (Braconidae) and evolution of its host preferences. Systematic Entomology 40: 570–591. https://doi.org/10.1111/syen.12122

van Achterberg C (1979) A revision of the subfamily Zelinae auct. (Hymenoptera, Braconidae). Tijdschrift voor Entomologie 122: 241–479.

van Achterberg C (1988) Revision of the subfamily Blacinae Foerster (Hymenoptera, Braconidae). Zoologische Verhandelingen, Leiden 249: 1–324.

van Achterberg C (1993) Illustrated key to the subfamilies of the Braconidae (Hymenoptera: Ichneumonoidea). Zoologische Verhandelingen, Leiden 283: 1–189.

van Achterberg C (1995) Generic revision of the subfamily Betylobraconinae (Hymenoptera: Braconidae) and other groups with modified fore tarsus. Zoologische Verhandelingen, Leiden 298: 1–242.

Yu DS, van Achterberg C, Horstmann K (2016) Taxapad 2016, Ichneumonoidea 2015. Database on flash-drive. www.taxapad.com, Nepean, Ontario, Canada.

ZooKeys 718: 95–114 (2017)
doi: 10.3897/zookeys.718.20726
http://zookeys.pensoft.net

RESEARCH ARTICLE

A peer-reviewed open-access journal
ZooKeys
Launched to accelerate biodiversity research

Larval description and chaetotaxic analysis of *Dineutus sinuosipennis* Laporte, 1840, with a key for the identification of larvae of the tribe Dineutini (Coleoptera, Gyrinidae)

Mariano C. Michat[1,2], Grey T. Gustafson[3], Johannes Bergsten[4]

1 *University of Buenos Aires, Faculty of Exact and Natural Sciences, Department of Biodiversity and Experimental Biology, Laboratory of Entomology, Buenos Aires, Argentina* **2** *CONICET–University of Buenos Aires, Institute of Biodiversity and Experimental and Applied Biology, Buenos Aires, Argentina* **3** *Department of Ecology and Evolutionary Biology, University of Kansas, Lawrence, KS 66045, USA* **4** *Department of Zoology, Swedish Museum of Natural History, Stockholm, Sweden*

Corresponding author: *Mariano C. Michat* (marianoide@gmail.com)

Academic editor: *K. Miller* | Received 31 August 2017 | Accepted 21 November 2017 | Published 4 December 2017

http://zoobank.org/A46B0826-1459-4337-8C43-2CFC93DCD15A

Citation: Michat MC, Gustafson GT, Bergsten J (2017) Larval description and chaetotaxic analysis of *Dineutus sinuosipennis* Laporte, 1840, with a key for the identification of larvae of the tribe Dineutini (Coleoptera, Gyrinidae). ZooKeys 718: 95–114. https://doi.org/10.3897/zookeys.718.20726

Abstract

The larvae of the Malagasy whirligig beetle *Dineutus sinuosipennis* Laporte, 1840, identified using DNA sequence data, are described and illustrated for the first time, including detailed morphometric and chaetotaxic analyses of selected structures and a description of larval habitat. Larvae of the genus *Dineutus* Macleay, 1825 are diagnosed, and a key to identify the genera of the tribe Dineutini is presented. Larvae of *Dineutus* exhibit the characters traditionally recognized as autapomorphies of the Gyrinidae: body less sclerotized, egg bursters located on the parietal, one additional sensorial plate on the third antennomere, cardo and lacinia well developed, prementum completely divided, abdominal tracheal gills, and four terminal hooks on the pygopod. They also share with larvae of the other Dineutini genera these putative synapomorphies: numerous minute pore-like additional structures on the ultimate maxillary and labial palpomeres, coxal primary seta CO12 inserted submedially, and trochanteral primary seta TR2 absent. Larvae of *Dineutus* can be distinguished from those of other known genera of Dineutini by the posterior margin of the lacinia not dentate, tracheal gills plumose, parietal seta PA5 inserted relatively far from setae PA7–9, mandibular pores MNb and MNc inserted relatively far from each other, and tarsal seta TA1 inserted submedially.

Keywords
Adephaga, whirligig beetles, larva, sensilla, DNA-based association

Introduction

The genus *Dineutus* Macleay, 1825 comprises 92 relatively large-sized species and has a near global distribution, being absent from Europe and, notably, from South America (Gustafson and Miller 2017). The species are common in both lotic and lentic aquatic environments including ponds, lakes, rivers, and streams, although most individuals are found in slower parts of streams and rivers (Gustafson and Miller 2015). It is included in the tribe Dineutini together with the extant genera *Enhydrus* Laporte, 1835, *Macrogyrus* Régimbart, 1882 and *Porrorhynchus* Laporte, 1835, and one extinct genus (Gustafson and Miller 2017). Numerous subgenera were erected within *Dineutus*, although presently only three are recognized: *Dineutus* s.str., *Rhomborhynchus* Ochs, 1926, and *Cyclous* Dejean, 1833, the largest subgenus, to which the species described here belongs (Gustafson and Miller 2017). *Dineutus sinuosipennis* Laporte, 1840 is endemic to Madagascar and the Comoro Islands (Brinck 1955). On Madagascar, it is a common and widespread species in slow-flowing, running waters. It can tolerate substantial anthropogenic disturbance, for instance it is often found in man-made water canals along rice paddy fields.

Larval morphology of *Dineutus* is poorly known. Larvae of a vast majority of species are unknown, and the few described ones are insufficiently documented. Nowrojee (1912) shortly described the mature larva of *D. unidentatus* Aubé, 1838, including a habitus drawing. Wilson (1923) studied the three larval instars of *D. assimilis* Kirby, 1937, focusing on the third instar for the description and illustrations, which to date remains the most detailed morphological treatment of a larva of the genus. Hatch (1927) provided an unillustrated key to separate the first instars of four species. Brief descriptions and comments, including some drawings, of a few *Dineutus* larvae were provided by Bertrand (summarized in Bertrand 1963). An unidentified species was partially examined for chaetotaxy by Archangelsky and Michat (2007), although lacking illustrations and a formal description of the chaetotaxy pattern. Images of the larvae of three species were provided by Istock (1967), without information as to which instar they belong, although their size suggests third instar. Other descriptions or treatments of *Dineutus* larvae are lacking in the literature, with the exception of some drawings of the head of *D. discolor* Aubé, 1838 in the context of phylogenetic studies (Beutel 1993, Beutel and Roughley 1994). A detailed morphological description, including chaetotaxic analysis, of all larval instars of this genus is lacking.

In recent years, several descriptions of gyrinid larvae were published, emphasizing not only general morphology but also including chaetotaxic analyses in the following genera and subgenera: *Macrogyrus* (*Andogyrus*) Ochs, 1924 (Archangelsky and Michat 2007), *Gyrinus* Müller, 1764 (Michat et al. 2010), *Macrogyrus* (*Macrogyrus*) (Michat

and Gustafson 2016), and *Enhydrus* (Michat et al. 2016). A system of nomenclature for the primary sensilla of larvae of the family Gyrinidae has not been fully developed so far, mainly because larvae of several genera are still unknown. However, although likely subject to improvement based on the discovery of more gyrinid larvae, these studies provide a descriptive template to which larvae of additional genera can be incorporated.

In the present paper, a detailed description of all larval instars of the genus *Dineutus* is provided, including, for the first time, morphometric and chaetotaxic analyses of the cephalic capsule, head appendages and legs of *D. sinuosipennis*. Comparisons with other gyrinid genera for which the larvae have been described in detail are also provided, and an identification key to separate all instars of the known genera of the tribe Dineutini is presented. Despite adults being collected readily by the hundreds, larvae of many gyrinid species remain frustratingly elusive. For this reason, we also provide a description of the precise habitat where larvae of *D. sinuosipennis* were collected to aid future collection.

Material and methods

The descriptions provided in this paper are based on two specimens of instar I, three of instar II and three of instar III collected in Madagascar, at the locality described below.

Identification of larvae and molecular procedures

There are three species of *Dineutus* known from Madagascar: *D. proximus* Aubé, 1838, *D. sinuosipennis* and *D. subspinosus* (Klug, 1834). Only adults of *D. sinuosipennis* were found at the locality where the larvae were collected, but for unambiguous association we extracted DNA from four larvae of instar III and sequenced mitochondrial cytochrome c oxidase subunit I (COI) using the primers 'Jerry' (Simon et al. 1994) and 'Pat Dyt' (Isambert et al. 2011). The legs of one side were removed for lysis and DNA extraction using Qiagen Blood and Tissue kit following standard protocol; remaining body was retained as vouchers (Catalogue numbers: NHRS-JLKB000001600 – NHRS-JLKB000001603).

PCRs were set up in 25 ul reactions using Illustra Hot start mix RTG (GE Healthcare, Little Chalfont, Buckinghamshire, UK), 1 ul each of the Primers (10 uM), 2ul of DNA template and 21 ul water. Thermal cycling profile included the following steps: 95 °C for 5 min followed by 40 cycles of 95 °C for 30 s, 50 °C for 30 s and 72 °C for 60 s, and finally 72 °C for 8 min. Products were cleaned with the ExoFast method, using a combination of Exonuclease 1 and FastAP (ThermoFisher Scientific, Waltham, MA, USA). Cleaned products were sequenced using Big Dye version 3.1 on an ABI 3130XL Genetic Analyzer. The molecular lab work was carried out by the Centre for Genetic Identification (CGI), Swedish Museum of Natural History, Stockholm, Sweden.

Forward and reverse reads were combined into contigs in Sequencher (version 4) and primer regions were removed. The sequences were trimmed to the 740bp length fragment used by Isambert et al. (2011). All full-length fragments of the three known Madagascan species of *Dineutus* were downloaded from Genbank and combined with the new data. New sequences were submitted to Genbank under accession codes MG489880–MG489883. For the 80 terminal taxa, 740 bp alignment contained no gaps and matrix completeness was 100%. For a tree-based association of larvae with adults we used Beast, with the input xml-file set up in Beauti (both v. 1.8.4). We used a strict clock model to root the tree and a HKY+G substitution model, with codon positions partitioned to allow them separate overall rates but with tree, clock and substitution models linked. We used a constant-size coalescent tree prior as most branching events in the tree are within species coalescence events. Other prior settings were left as default. Two separate runs, each with 10M generations (sampling frequency 2000) were run, 25% burn-in removed from each run before combined in LogCombiner and a maximum clade credibility tree calculated with TreeAnnotator. Convergence between runs and ESS values (all >200) were evaluated in Tracer v. 1.6. We used the Generalized Mixed Yule Coalescent (GMYC) method (Fujisawa and Barraclough 2013) to test for conspecificity between larvae and identified adults. The GMYC analysis using the ultrametric tree from Beast applied the single threshold method and was run in R with the Splits package.

Methods for the study of larvae

The larvae were cleared in lactic acid, dissected, and mounted on glass slides in polyvinyl-lacto-glycerol. Microscopic examination at magnifications up to 1,000× and drawings were made using an Olympus CX31 (Olympus Corporation, Tokyo, Japan) compound microscope equipped with a camera lucida. Drawings were scanned and digitally inked using a Genius PenSketch tablet (KYE Corporation, Taipei, Taiwan). The material is held in the collection of the senior author (Laboratory of Entomology, Buenos Aires University, Argentina).

Morphometric analysis

We employed the terms used in previous papers dealing with the larval morphology of Gyrinidae (Archangelsky and Michat 2007; Michat et al. 2010, 2016; Michat and Gustafson 2016). The following measurements were taken (with abbreviations shown in parentheses). Total length (excluding terminal tracheal gills) (TL); maximum width (excluding tracheal gills) (MW); head length (HL) (total head length including the frontoclypeus, measured medially along the epicranial stem); maximum head width (HW); length of frontoclypeus (from anterior margin to the joint of frontal and coronal sutures) (FRL); occipital foramen width (maximum width measured along dorsal margin of occipital foramen) (OCW); coronal suture length (COL); length of mandible (MNL)

(measured from laterobasal angle to apex); width of mandible (MNW) (maximum width measured at base); length of maxillary palpifer (PPF); length of galea (GA). Length of antenna (A), maxillary (MP) and labial (LP) palpi were derived by adding the lengths of the individual segments; each segment is denoted by the corresponding letter(s) followed by a number (e.g., A1, first antennomere). The maxillary palpus was considered as being composed of three segments united to the stipes through a palpifer (Archangelsky and Michat 2007). Length of leg, including the longest claw (CL), was derived by adding the lengths of the individual segments; each leg is denoted by the letter L followed by a number (e.g., L1, prothoracic leg); the length of trochanter includes only the proximal portion, considered from the base to the beginning of the femur; the leg was considered as being composed of six segments (Lawrence 1991). Length of terminal hooks of abdominal segment X, separated in medial hook (MH) and lateral hook (LH). These measurements were used to calculate several ratios that characterize body shape.

Chaetotaxic analysis

Primary setae and pores were distinguished in the cephalic capsule, head appendages and legs. Sensilla were coded by two capital letters, in most cases corresponding to the first two letters of the name of the structure on which they are located, and a number (setae) or a lower case letter (pores). The following abbreviations were used: AN, antenna; CO, coxa; FE, femur; FR, frontoclypeus; LA, labium; MN, mandible; MX, maxilla; PA, parietal; PT, pretarsus; TA, tarsus; TI, tibia; TR, trochanter. Setae and pores present in the first-instar larva of *D. sinuosipennis* were labeled by comparison with previous papers dealing with the primary chaetotaxy of members of the family Gyrinidae (Archangelsky and Michat 2007, Michat et al. 2010, 2016; Michat and Gustafson 2016). Homologies were recognized using the criterion of similarity of position (Wiley 1981). Setae located at the apices of the maxillary and labial palpi were extremely difficult to distinguish due to their position and small size. Accordingly, they are not well represented in the drawings.

Results

Molecular results

The 740 bp COI fragment matching the dataset of Isambert et al. (2011) was successfully amplified for all four larvae. The ultrametric gene tree from Beast recovered the four larvae in a cluster together with adults identified as *D. sinuosipennis* (Fig. 1). The maximum genetic distance, calculated as uncorrected p-distances, between a larva and its closest match among *D. sinuosipennis* was 0.41%. The intraspecific genetic variation within *D. sinuosipennis* was 0.59% on average (min-max: 0–1.49%). Likewise, the intraspecific variation for *D. subspinosus* was small (0–0.81%, mean 0.37%). However, *D. subspinosus* is

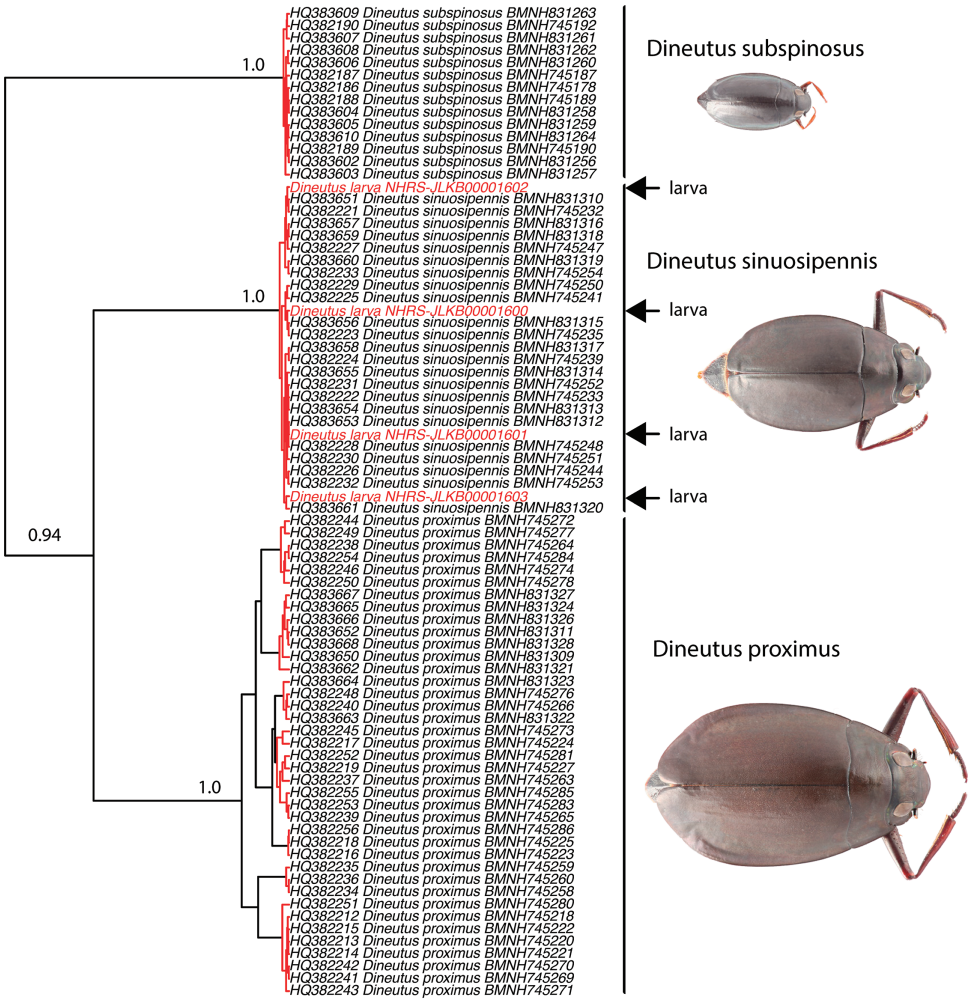

Figure 1. Ultrametric COI gene tree from Beast used to test larvae conspecificity with identified adults using GMYC. Red branches are intraspecific coalecence events, black branches represent divergence between separately evolving lineages. Numbers at nodes are posterior probability values from Beast (only given for species nodes). Sequences from the four larvae are conspecific with adults of *Dineutus sinuosipennis* but heterospecific to adults of *D. proximus* and *D. subspinosus*, according to the GMYC results.

the only Madagascan gyrinid that also occurs on mainland Africa, and a larger geographic sampling would likely yield a larger intraspecific distance (Bergsten et al. 2012). Intraspecific variation in *D. proximus*, by contrast, was larger (0–5.27%, mean 3.19%). Interspecific genetic distances between all three species were much larger (9.5–13.1%), including those between the larvae and any of the other two species. The GMYC analysis recovered the four larvae as conspecific with the adults identified as *D. sinuosipennis* in the maximum likelihood solution (Fig. 1). As has been reported before (Isambert et al. 2011), *D. proximus* represented multiple separately evolving lineages in the maximum likelihood solution from the GMYC analysis, a genetic structure that also has a geographic correlation.

Diagnosis of larvae of *Dineutus* Macleay, 1825

Cephalic capsule constricted at level of occipital region (Figs 2–3, 16); occipital suture absent in instar I (Fig. 2), absent or weakly delimited in instars II and III (Fig. 16); coronal suture relatively long (Fig. 2); medial lobe of frontoclypeus well produced forward, clearly asymmetrical in instar I (sometimes also in instars II and III), with four relatively well defined teeth (Figs 2, 16), medial teeth sometimes not well differentiated from each other (Fig. 26); cardo subrectangular in instar I (Figs 7–8); lacinia not serrate on posterior margin, indented apically (Figs 7–8); claws lacking basoventral spinulae (Figs 11–12); tracheal gills bearing long spinulae; terminal hooks subequal in length (Figs 13–15); seta PA5 inserted relatively far from setae PA7–9 (Fig. 2); pores MNb and MNc inserted relatively far from each other (Fig. 6); mandible with additional setae (instar I) (Fig. 6); cardo with a single additional seta (instar I) (Fig. 8); pore MXg proximal (Fig. 8); maxillary palpomeres 1 and 2 and labial palpomere 1 lacking minute pore-like additional structures (Figs 7–10); prementum with one additional pore (Fig. 10); seta CO12 inserted submedially (Fig. 12); coxa lacking additional setae (Figs 11–12); seta TR2 absent (Fig. 11); seta TA1 inserted submedially (Fig. 12); coxa with secondary setae (instars II–III); abdominal segment X lacking ventral spinulae (Fig. 13).

Description of larvae of *Dineutus sinuosipennis* Laporte, 1840

Instar I (Figs 2–15)

Color. Cephalic capsule and mandibles light brown, antennae, maxillae and labium testaceous; thoracic sclerites light brown, rest of thorax and legs testaceous; abdomen testaceous except terminal hooks light brown.

Body. Elongate, parallel sided, head and pronotum strongly sclerotized, rest of thorax and abdomen soft. Measurements and ratios that characterize the body shape are shown in Table 1.

Head. *Cephalic capsule* (Figs 2–3). Subrectangular (excluding neck), longer than broad, parallel-sided with distinct narrow neck; occipital foramen emarginate both dorsally and ventrally; occipital suture absent; coronal suture relatively long; frontal sutures U-shaped, extending to antennal bases; anterior tentorial pits elongate, visible dorsally near antennal bases; posterior tentorial pits elongate, visible ventromedially; neck area rugose; FR relatively short, roughly subtriangular, anterior margin with three lobes; medial lobe well produced anteriorly, clearly asymmetrical, with four teeth, right tooth smaller and somewhat detached, the other three well developed; lateral lobes well developed, truncate, not projected beyond medial lobe; PA with egg bursters formed by a single small cuticular spine on each posterolateral surface, and six stemmata at each side, four dorsal and two ventral. *Antenna* (Figs 4–5). Moderately long, slender, slightly longer than HW, composed of four antennomeres; A1 shortest, A3 and A4 longest, subequal in length; A3 with two minute structures (probably spinulae or

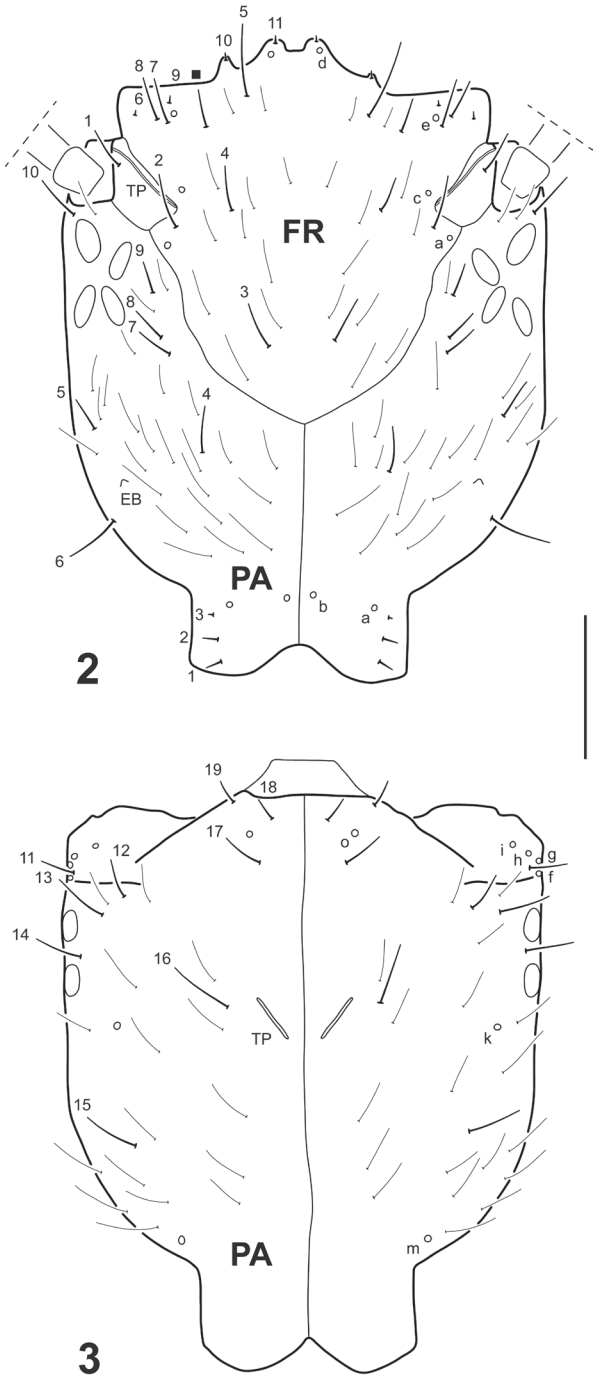

Figures 2–3. *Dineutus sinuosipennis* Laporte, 1840, instar I. **2** Cephalic capsule, dorsal view **3** Cephalic capsule, ventral view. Numbers and lowercase letters indicate primary setae and pores, respectively. Conspicuous additional seta on frontoclypeus indicated by a solid square. Inconspicuous additional setae not labeled. EB: egg burster; FR: frontoclypeus; PA: parietal; TP: tentorial pit. Scale bar: 0.20 mm.

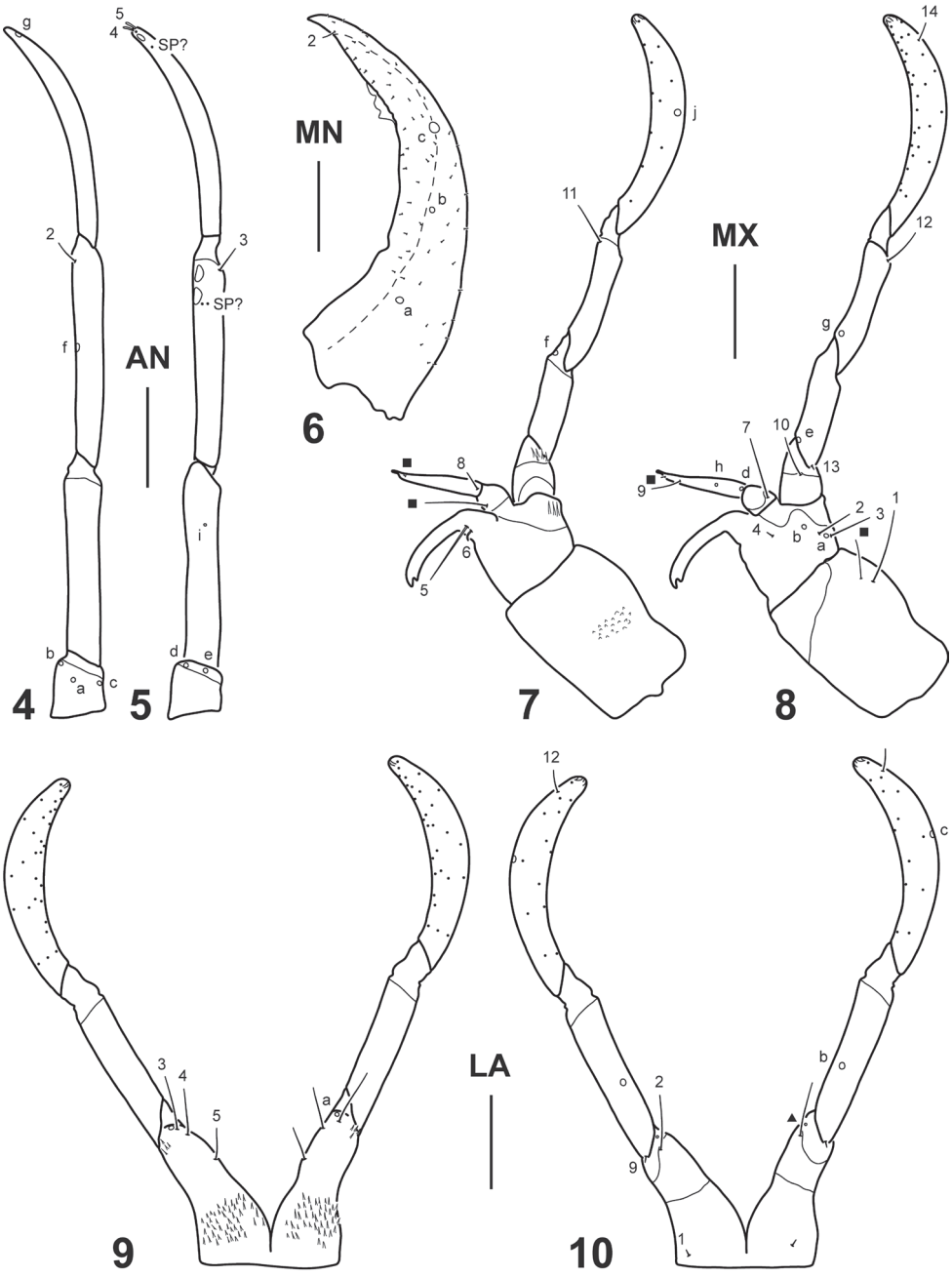

Figures 4–10. *Dineutus sinuosipennis* Laporte, 1840, instar I. **4** Right antenna, dorsal view **5** Left antenna, ventral view **6** Right mandible, dorsal view **7** Right maxilla, dorsal view **8** Left maxilla, ventral view **9** Labium, dorsal view **10** Labium, ventral view. Numbers and lowercase letters indicate primary setae and pores, respectively. Additional setae indicated by solid squares (except for minute additional setae on the mandible which are not labeled). Additional pore on prementum indicated by a solid triangle. AN: antenna; LA: labium; MN: mandible; MX: maxilla; SP: spinulae. Scale bars: 0.10 mm.

Table 1. Measurements and ratios for the larvae of *Dineutus sinuosipennis* Laporte, 1840.

Measure	Instar I (n = 2)	Instar II (n = 3)	Instar III (n = 3)
TL (mm)	5.50	14.80	20.10–28.30
MW (mm)	0.70	2.20	2.40–3.30
HL (mm)	0.87–0.91	1.38–1.42	2.02–2.05
HW (mm)	0.65–0.66	0.99–1.01	1.42–1.51
FRL (mm)	0.51–0.55	0.78–0.81	1.14–1.19
OCW (mm)	0.28–0.30	0.55–0.60	0.94–0.99
COL (mm)	0.36	0.59–0.60	0.84–0.88
HL/HW	1.34–1.37	1.37–1.43	1.34–1.43
HW/OCW	2.20–2.30	1.64–1.79	1.49–1.53
COL/HL	0.39–0.41	0.43	0.41–0.44
FRL/HL	0.59–0.61	0.57	0.56–0.59
A/HW	1.07	0.97–1.01	0.83–0.90
A1/A3	0.24–0.25	0.24–0.29	0.28–0.30
A2/A3	0.71–0.83	1.07–1.15	1.28–1.43
A4/A3	0.96–1.04	0.80–0.88	0.73–0.74
MNL/MNW	2.94–3.21	3.05–3.12	2.85–2.93
MNL/HL	0.49–0.53	0.45–0.47	0.43
A/MP	1.34–1.36	1.22–1.40	1.25–1.28
GA/MP1	1.00–1.04	0.77–0.84	0.65–0.72
PPF/MP1	0.50–0.55	0.48–0.50	0.31–0.36
MP1/MP2	0.65–0.75	0.88–0.96	1.19–1.30
MP3/MP2	1.38–1.59	1.15–1.26	1.06–1.12
MP/LP	1.22–1.29	1.23–1.28	1.28–1.31
LP2/LP1	1.16–1.20	0.84–0.89	0.70–0.73
L3 (mm)	1.74–1.85	2.86–2.88	4.72–4.75
L3/L1	1.13–1.15	1.21	1.26–1.27
L3/L2	1.06–1.07	1.08–1.10	1.11–1.12
L3/HW	2.68–2.78	2.86–2.91	3.12–3.35
L3 (CO/FE)	1.00–1.05	1.03–1.07	1.08–1.09
L3 (TI/FE)	0.61–0.67	0.56–0.57	0.54–0.58
L3 (TA/FE)	0.90–0.92	0.78–0.84	0.66–0.70
L3 (CL/TA)	0.48–0.49	0.36–0.41	0.35
MH/LH	1.02–1.05	1.04–1.06	1.07–1.17

pores) on ventrodistal surface, and two subapical flat plates on inner margin, distal one interpreted as the sensorium (A3') which does not protrude; A4 with a subapical flat sensorial plate on inner margin, accompanied by two minute structures (probably spinulae or pores). *Mandible* (Fig. 6). Relatively elongate, curved, broad basally, distal half projected inward, apex sharp; inner margin more or less toothed on distal third; retinaculum absent, although one of the teeth may be interpreted as that structure; mandibular channel present. *Maxilla* (Figs 7–8). Well developed, prominent; cardo strongly developed, subrectangular, bearing a group of minute spinulae on dorsal surface; stipes short, broad, subtrapezoidal, bearing a lacinia and GA on distal inner

margin and a PPF on distal outer margin; lacinia well developed, slender, indented apically; GA elongate, two-segmented, basal segment shorter, distal segment longer, narrowing to apex; PPF short, palpomere-like, projected apicointernally in a subtriangular process; MP long, composed of three palpomeres separated by oblique joints; MP1 shortest, MP3 longest. *Labium* (Figs 9–10). Well developed, prominent; prementum divided longitudinally into two subcylindrical halves fused basally, each half bearing minute spinulae on dorsal surface and projected apicointernally in a subtriangular process; LP long, composed of two palpomeres separated by oblique joints; LP1 slightly shorter than LP2.

Thorax. Long, narrow, subcylindrical; pronotum somewhat larger that subequal meso- and metanotum; protergite well developed, covering whole segment dorsally, anterior margin truncate, lateral and posterior margins rounded; membrane between pro- and mesonotum with a single narrow transverse sclerite; both sclerites with sagittal line, lacking anterior transverse carina; meso- and metaterga lacking sclerites; ventral surface membranous except for a large subrectangular sclerite (divided in two halves by broad sagittal line) on anterior third of prothorax, and small sclerites on the regions of articulation of coxae; spiracles absent. *Legs* (Figs 11–12). Long, slender, composed of six segments; L3 longest, L1 shortest; CO elongate, robust, TR short, lacking annulus, FE, TI and TA slender, subcylindrical, PT with two long, slender, slightly curved claws, posterior claw shorter than anterior claw on L1 and L2, claws subequal in length on L3; spinulae absent.

Abdomen. Ten-segmented, long, narrow, subcylindrical, entirely membranous; segments I–VIII similar in shape, progressively smaller to apex, bearing a tracheal gill on posterolateral angle; segment IX smaller than segment VIII, bearing two tracheal gills on posterolateral angle; tracheal gills slender, plumose, those of segment IX longer than the others; all tracheal gills bearing an anterior and a posterior row of long setiform spinulae, those of segment I and, to a lesser extent of segment II with less spinulae; segment X (Fig. 13) narrowest, pygopod-like, arising on posteroventral surface of segment IX, lacking gills and ventral spinulae, bearing four strongly sclerotized terminal hooks, medial hook slightly longer than lateral hook (Figs 14–15).

Chaetotaxy. *Frontoclypeus* (Fig. 2). Medial lobe of anterior margin with two spine-like setae (FR10, FR11), one short hair-like seta (FR5), and one pore (FRd); lateral lobe of anterior margin with two minute spine-like setae (FR6, FR9), two short hair-like setae (FR7, FR8), and one pore (FRe); lateral margin with two short hair-like setae (FR1, FR2) and two pores (FRa, FRc) on distal half and one short hair-like seta (FR3) on basal half; central portion with one short hair-like seta (FR4); surface with numerous short hair-like additional setae. *Parietal* (Figs 2–3). Dorsal surface with one short hair-like seta (PA10) posterior to antennal base, a longitudinal row of three short hair-like setae (PA7, PA8, PA9) close to frontoclypeal margin, three short hair-like setae (PA4, PA5, PA6) on basal third, close to egg bursters, and three short spine-like setae (PA1, PA2, PA3) and two pores (PAa, PAb) on neck region; ventral surface with three short hair-like setae (PA17, PA18, PA19) and one pore (PAo) on anteromedial region, four short hair-like setae (PA11, PA12, PA13, PA14) and four

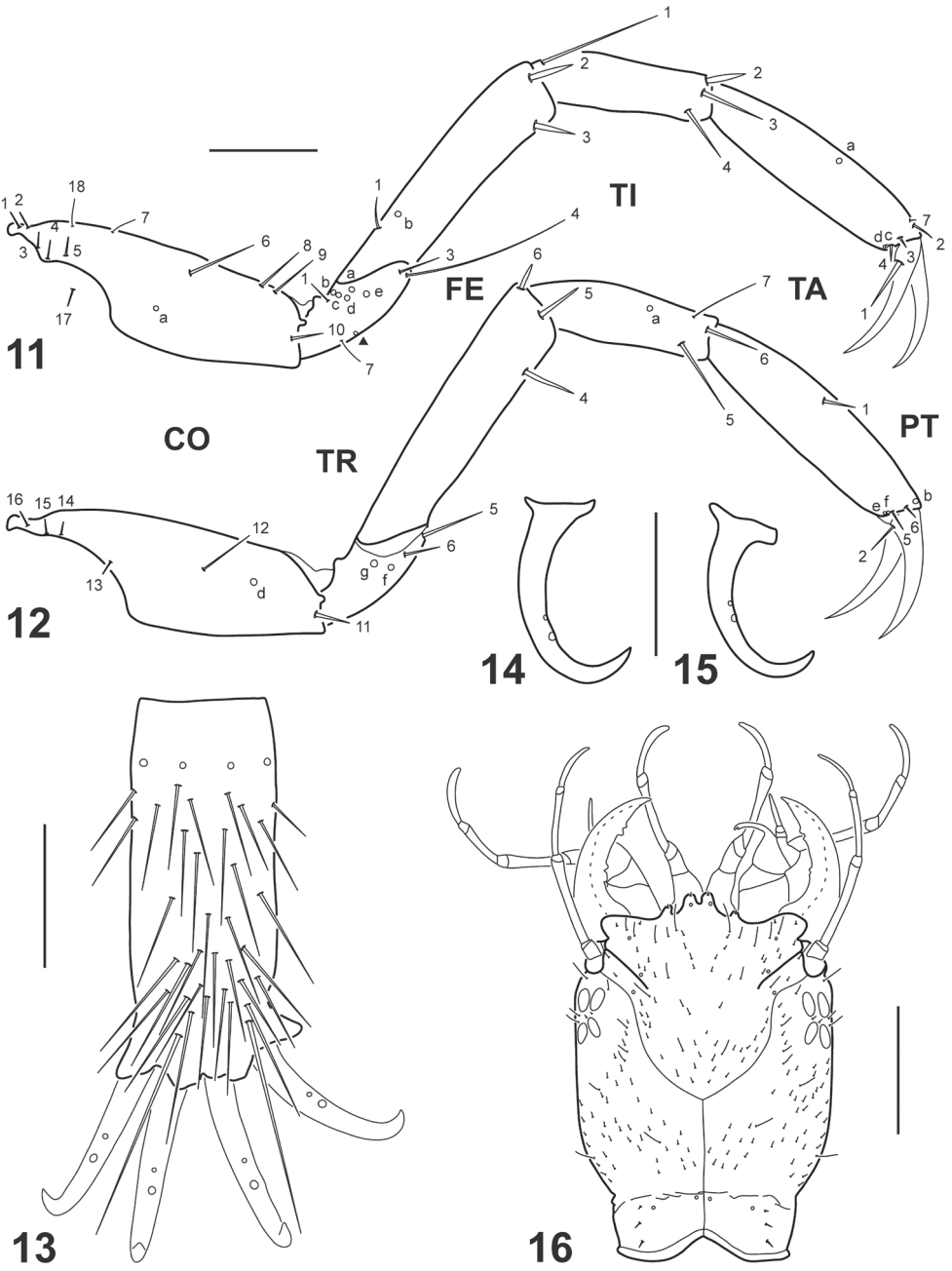

Figures 11–16. *Dineutus sinuosipennis* Laporte, 1840. **11–15** Instar I **16** Instar III **11** Left metathoracic leg, anterior view **12** Right metathoracic leg, posterior view **13** Abdominal segment X, ventral view **14** Medial hook, lateral view **15** Lateral hook, lateral view **16** Head, dorsal view. Numbers and lowercase letters indicate primary setae and pores, respectively. Additional pore on trochanter indicated by solid triangle. Sensilla on abdominal segment X not labeled. CO: coxa; FE: femur; PT: pretarsus; TA: tarsus; TI: tibia; TR: trochanter. Scale bars: 0.15 mm (**11–15**); 0.70 mm (**16**).

pores (PAf, PAg, PAh, PAi) on anterolateral angle, one short hair-like seta (PA16) and one pore (PAk) at mid length, and one long hair-like seta (PA15) and one pore (PAm) on basal third; dorsal and ventral surface with numerous short hair-like additional setae (except on neck region). *Antenna* (Figs 4–5). A1 with three pores (ANa, ANb, ANc) on dorsal surface and two pores (ANd, ANe) on ventral surface; A2 with one minute pore (ANi) on ventral surface; A3 with one pore (ANf) on lateromedial region, one short hair-like seta (AN2) on dorsodistal portion and one short hair-like seta (AN3) on ventrodistal portion; A4 with one pore (ANg) on dorsodistal portion and two minute spine-like setae (AN4, AN5) at apex. *Mandible* (Fig. 6). Dorsal surface with one pore (MNa) on basal fourth, two pores (MNb, MNc) at about mid length, and one short hair-like setae (MN2) near tip; dorsal and lateral surfaces with numerous minute additional setae; we were unable to identify seta MN1, although it is most likely present and obscured by the additional setae. *Maxilla* (Figs 7–8). Cardo with one short hair-like seta (MX1) and one short additional seta on ventral surface; stipes with two short hair-like setae (MX2, MX3) and two pores (MXa, MXb) on ventroexternal margin, one very short seta (MX4) ventrally near base of lacinia, and one short straight hair-like seta (MX5) and one very short curved spine-like seta (MX6) dorsally at base of lacinia; proximal segment of GA with one short hair-like seta (MX7) on ventral surface and one short hair-like additional seta on dorsal surface; distal segment of GA with one short hair-like seta (MX8) on dorsoproximal surface, two pores (MXd, MXh) on ventroproximal surface, and one short hair-like seta (MX9) and two minute additional setae near apex; PPF with one short hair-like seta (MX10) on ventral margin; MP1 with one pore (MXe) and one minute seta (MX13) on ventroproximal portion, and one pore (MXf) on dorsodistal portion; MP2 with one pore (MXg) on ventroproximal portion and two short hair-like setae (MX11, MX12) on dorsodistal and ventrodistal portions respectively; MP3 with one pore (MXj) dorsally at about mid length, one short hair-like seta (MX14) ventrally near apex, and several minute pore-like additional structures both on dorsal and ventral surface. *Labium* (Figs 9–10). Prementum with three short hair-like setae (LA3, LA4, LA5) and one pore (LAa) on dorsodistal surface, one short hair-like seta (LA2) and one minute additional pore on ventrodistal surface, and one minute seta (LA1) on ventroproximal surface; LP1 with one minute seta (LA9) on ventroproximal portion and one pore (LAb) on ventrointernal margin at about mid length; LP2 with one pore (LAc) on external margin at about mid length, one short hair-like seta (LA12) ventrally near apex, and several minute pore-like additional structures both on dorsal and ventral surface. *Thorax*. Surface of thoracic terga with numerous hair-like setae. *Legs* (Figs 11–12). Anterior surface of CO with six very short spine-like setae (CO1, CO2, CO3, CO4, CO5, CO17) and two short hair-like setae (CO7, CO18) on proximal portion, one long hair-like seta (CO6) and one pore (COa) on medial portion, and three short hair-like setae (CO8, CO9, CO10) on distal portion; posterior surface of CO with four very short spine-like setae (CO13, CO14, CO15, CO16) on proximal portion, one short hair-like seta (CO12) on medial portion, and one short spine-like seta (CO11) and one pore (COd) on distal portion; anterior surface

of TR with one short hair-like seta (TR1) on dorsal margin, one long (TR4) and one short (TR3) hair-like setae on ventrodistal margin, five pores (TRa, TRb, TRc, TRd, TRe) on central portion, and one short hair-like seta (TR7) and one additional pore on ventral margin; posterior surface of TR with two short hair-like setae (TR5, TR6) and two pores (TRf, TRg) on distal margin; anterior surface of FE with one short spine-like seta (FE1) and one pore (FEb) on proximal portion and two short spine-like setae (FE2, FE3) on distal portion; posterior surface of FE with three short spine-like setae (FE4, FE5, FE6) on distal portion; anterior surface of TI with one long hair-like seta (TI1) on proximal portion and three short spine-like setae (TI2, TI3, TI4) on distal portion; posterior surface of TI with one pore (TIa) on central portion, and two short spine-like setae (TI5, TI6) and one short hair-like seta (TI7) on distal portion; anterior surface of TA with one pore (TAa) at about mid length, and three short spine-like setae (TA2, TA3, TA4), one minute seta (TA7), and two pores (TAc, TAd) on distal portion; posterior surface of TA with one short spine-like seta (TA1) at mid length, and two short spine-like setae (TA5, TA6) and three pores (TAb, TAe, TAf) on distal portion; anterior surface of PT with one short spine-like seta (PT1) on basoventral portion; posterior surface of PT with one short spine-like seta (PT2) on basoventral portion. *Abdomen*. Segments I–IX with several mostly hair-like setae on dorsal and ventral surfaces; tracheal gills with one long hair-like seta at tip and one relatively shorter hair-like seta near tip, other setae (if present) obscured by spinulae; segment X (Fig. 13) with numerous spine-like setae and four pores on ventral surface; terminal hooks (Figs 13–15) with two pores on ventral margin at about mid length.

Instar II

As instar I except for the following features:

Color. Frontoclypeus, region of parietals posterior to frontoclypeus, and neck region brown, rest of cephalic capsule testaceous to light brown; mandible brown, rest of head appendages testaceous to light brown; protergite with a large subtriangular brown macula on anteromedial region.

Body. Measurements and ratios that characterize the body shape are shown in Table 1.

Head. *Cephalic capsule*. Occipital suture weakly delimited; rugosity on neck restricted to area of occipital suture; egg bursters absent. *Antenna*. About as long as HW; A2 the longest, A3 slightly shorter than A2, A4 slightly shorter than A3. *Maxilla*. MP1 and MP2 subequal in length, somewhat shorter than MP3. *Labium*. LP1 somewhat longer than LP2.

Thorax. Ventral sclerite of prothorax lacking sagittal line. *Legs*. Posterior claw shorter than anterior claw on all legs.

Abdomen. Tracheal gills of segment I almost devoid of spinulae, those of segment II with few spinulae.

Chaetotaxy. Cardo with 7–10 short hair-like secondary setae; secondary leg setation detailed in Table 2.

Table 2. Number and position of secondary setae on the legs of larvae of *Dineutus sinuosipennis* Laporte, 1840. Numbers between slash marks refer to pro-, meso-, and metathoracic legs, respectively. A: anterior; D: dorsal; P: posterior; V: ventral.

Segment	Position	Instar II (n = 3)	Instar III (n = 3)
Coxa	A+AD	13–16 / 14–15 / 11–18	20–26 / 19–25 / 22–27
	PD	5–9 / 6–7 / 6–8	7–9 / 6–11 / 7–9
Femur	AV	4–7 / 6–7 / 6–8	4–5 / 6–8 / 8–9
Tibia	AV	2–3 / 3–4 / 4–5	3–4 / 4–5 / 4–5
Tarsus	PV	5–6 / 5–6 / 6–7	5–6 / 6–7 / 7

Instar III (Fig. 16)

As instar II except for the following features:

Color. Same pattern but darker and more obvious in general.

Body. Measurements and ratios that characterize the body shape are shown in Table 1.

Head (Fig. 16). *Antenna*. Somewhat shorter than HW. *Maxilla*. MP1 longest, MP2 shortest, MP3 slightly longer than MP2. *Labium*. LP1 considerably longer than LP2.

Abdomen. Spiracles present on dorsolateral margin of segments I–III.

Chaetotaxy. Cardo with 8–10 short hair-like secondary setae; secondary leg setation detailed in Table 2.

Larval habitat

Specimens of *D. sinuosipennis* were collected on November 28th 2014 in the Betsabora River at crossing of Route National 2, Madagascar (Figs 17–18). The locality is situated near Antsampanana Village, 6 km W of Moramanga (18.9247S, 48.1828E). This is part of the eastern Escarpment and lies at an altitude of 900 m. The main body of the river was relatively slow moving with brown, murky water, and a stone and mud bottom (Fig. 17). Marginal vegetation consisted of reeds in some areas, with most margins having only grass and sparse vegetation. Adults of *D. sinuosipennis* were found in the main river-body near the margins. The river also had a small rivulet that left the main river-body, flowing swiftly over reeds before rejoining it a short distance later (Fig. 18). Larvae of *D. sinuosipennis* were discovered amongst the submerged reeds within this more swiftly flowing rivulet. One dip of the aquatic net within the reeds produced several larvae, while attempts to collect at the margins of the rivulet and the main river-body did not. Nearly 80 larvae of all three instars were collected from this habitat (Fig. 18).

Very few other aquatic beetle adults (notably no adult *D. sinuosipennis*) but many juvenile aquatic insects (such as odonates) were found in this habitat, and it was the only place where larval *D. sinuosipennis* were collected in abundance during the 2014 Madagascar expedition. Given the lack of adult *D. sinuosipennis*, the abundance of its larval form, and lack of similar numbers of larval specimens encountered elsewhere, such fast-flowing, reedy habitats may represent a preferred larval habitat. This type of habitat is

Figures 17–18. Betsabora River, Madagascar, where *D. sinuosipennis* was collected. **17** General habitat, arrow indicates location of rivulet **18** Specific habitat where larvae were collected within the rivulet.

easily over-looked, and may explain why ample larval specimens of one of Madagascar's most common *Dineutus* species have not been previously collected or described.

Key to larvae of the tribes of Gyrininae and genera of *Dineutini*

The key was constructed for all instars. Although larvae of *Enhydrus* were examined only as instar I, the selected character likely applies also to later instars. Larvae of *Porrorhynchus* are unknown and could not be included. It is likely that larvae of this genus key to the closely related genus *Dineutus*. Known distribution of *Porrorhynchus* comprises southeast Asia from southern China to the greater Sunda Islands and west to Myanmar; also in Sri Lanka (Gustafson and Miller 2017).

1 Anterior margin of frontoclypeus lacking teeth (Fig. 21)..... **Orectochilini**
– Anterior margin of frontoclypeus with more or less well developed teeth (Figs 22–26)..... **2**
2 Stipes with a series of small hook-like setae on internal margin (Fig. 27)..... **Gyrinini**
– Stipes lacking a series of small hook-like setae on internal margin (Figs 28–29) (Dineutini)..... **3**
3 Lacinia with posterior margin dentate and apex not deeply indented (Fig. 28) (*Macrogyrus*) **4**
– Lacinia with posterior margin not dentate and apex deeply indented (Fig. 29)... **5**
4 Neck constriction present (Fig. 19)..... **Subgenus *Andogyrus***
– Neck constriction absent (Fig. 20) ..... **Subgenus *Macrogyrus***
5 Tracheal gills devoid of spinulae (Fig. 30)..... ***Enhydrus***
– Tracheal gills bearing two rows of long spinulae (Fig. 31)..... ***Dineutus***

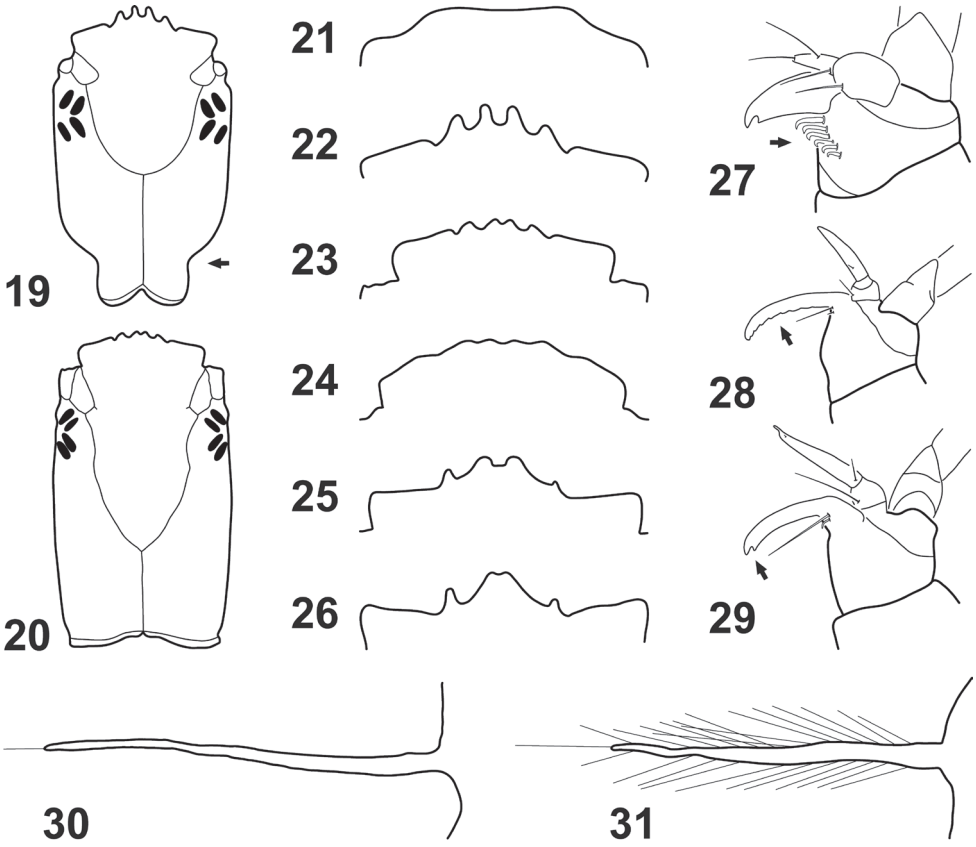

Figures 19–31. Larval structures (instar I). **19–20** Cephalic capsule, dorsal view **21–26** Anterior margin of frontoclypeus, dorsal view **27–29** Stipes, lacinia and galea, dorsal view **30–31** Tracheal gills, dorsal view **19** *Macrogyrus* (*Andogyrus*) *seriatopunctatus* (Régimbart, 1883) **20** *Macrogyrus* (*Macrogyrus*) *oblongus* (Boisduval, 1835) **21** *Gyretes* sp. **22** *M.* (*A.*) *seriatopunctatus* **23** *M.* (*M.*) *oblongus* **24** *Enhydrus sulcatus* (Wiedemann, 1821) **25** *Dineutus sinuosipennis* Laporte, 1840 **26** *Dineutus* sp. (specimen from Bayfield County, Wisconsin, USA) **27** *Gyrinus monrosi* Mouchamps, 1957 **28** *M.* (*M.*) *oblongus* **29** *D. sinuosipennis* **30** *E. sulcatus* **31** *D. sinuosipennis*.

Discussion

The description provided here adds *Dineutus* to the group of gyrinid genera for which the ground plan of primary chaetotaxy has been described. Considering this description, within the tribe Dineutini only the larvae of the genus *Porrorhynchus* remain unknown.

Dineutus larvae bear the characters considered as putative autapomorphies of Gyrinidae by previous authors (Beutel and Roughley 1994, 2005, Archangelsky and Michat 2007, Michat and Gustafson 2016, Michat et al. 2016): a less sclerotized body, egg bursters located on the parietal, one additional sensorial plate on the third antennomere, a well-developed cardo and lacinia, a completely divided prementum, lateral abdominal tracheal gills, and four terminal hooks on the pygopod. They also share with larvae of the other known Dineutini genera these putative synapomor-

phies: presence of numerous minute pore-like additional structures on the ultimate maxillary and labial palpomeres, submedial position of the primary seta CO12 on the coxa, and absence of the primary seta TR2 on the trochanter.

Compared to those of the other known Dineutini genera, larvae of *Dineutus* can be distinguished by the lacinia not dentate on posterior margin (= *Enhydrus*, dentate in *Macrogyrus*); tracheal gills plumose (= *Macrogyrus*, not plumose in *Enhydrus*); parietal seta PA5 inserted relatively far from setae PA7–9 (closer to PA7–9 in *Enhydrus* and *Macrogyrus*); mandibular pores MNb and MNc inserted relatively far from each other (closer to each other in *Enhydrus* and *Macrogyrus*); and tarsal seta TA1 inserted submedially (inserted distally in *Enhydrus* and *Macrogyrus*). Information regarding these characters in other Dineutini species is scarce, since the larvae of most species are unknown. Therefore, their phylogenetic significance remains to be tested when larvae of more species are studied.

Acknowledgements

We thank Helena Shaverdo and Cesar Benetti for their valuable comments to the manuscript. MCM was supported by Agencia Nacional de Promoción Científica y Tecnológica under Grant PICT–2014–0853 and by Universidad de Buenos Aires under Grant UBACyT–20020150100170BA. GTG was supported by a NIH IRACDA postdoctoral fellowship (5K12GM064651). Part of this project was funded by NSF #DEB–1402446. We thank Niclas Gyllenstrand at the Centre for Genetic Identification (CGI), Swedish Museum of Natural History, Stockholm, Sweden for the molecular lab work.

References

Archangelsky M, Michat MC (2007) Morphology and chaetotaxy of the larval stages of *Andogyrus seriatopunctatus* Régimbart (Coleoptera: Adephaga: Gyrinidae). Zootaxa 1645: 19–33.

Aubé C (1838) Hydrocanthares et gyriniens. In: Dejean PFMA (Ed.) Species général des coléoptères de la collection de M. le Comte Dejean. Méquignon Père et Fils, Paris, 804 pp.

Bergsten J, Bilton DT, Fujisawa T, Elliott M, Monaghan MT, Balke M, Hendrich L, Geijer J, Herrmann J, Foster GN, Ribera I, Nilsson AN, Barraclough TG, Vogler AP (2012) The effect of geographical scale of sampling on DNA barcoding. Systematic Biology 61: 851–869. https://doi.org/10.1093/sysbio/sys037

Bertrand H (1963) Contribution à l'étude des premiers états des Coléoptères aquatiques de la région éthiopienne (5º note). Families: Haliplidae, Dytiscidae, Gyrinidae (Hydrocanthares). Bulletin de l'I.F.A.N. 25(Ser. A, 2): 389–466.

Beutel RG (1993) Phylogenetic analysis of Adephaga (Coleoptera) based on characters of the larval head. Systematic Entomology 18: 127–147. https://doi.org/10.1111/j.1365-3113.1993.tb00658.x

Beutel RG, Roughley RE (1994) Phylogenetic analysis of Gyrinidae based on characters of the larval head (Coleoptera: Adephaga). Entomologica Scandinavica 24: 459–468. https://doi.org/10.1163/187631293X00217

Beutel RG, Roughley RE (2005) Gyrinidae Latreille, 1810. In: Beutel RG, Leschen RAB (Eds) Handbook of Zoology (Vol. IV) Arthropoda: Insecta, Part 38, Coleoptera (Vol. 1), Morphology and Systematics (Archostemata, Adephaga, Myxophaga, Polyphaga (partim)). Walter De Gruyter, Berlin, New York, 55–64.

Boisduval JBA (1835) Faune Entomologique de l'Océan Pacifique, avec l'illustration des insectes nouveaux recueillis pendant le voyage; par le docteur Boisduval. Deuxième Partie. Coléoptères et autres orders. J. Tastu, Paris, 716 pp.

Brinck P (1955) Gyrinidae. A monograph of the whirligig beetles of Southern Africa. South African Animal Life 2: 329–518.

Dejean PFMA (1833) Catalogue des coléoptères de la collection de M. le comte Dejean. Chez Méquignon-Marvis Père et fils, Paris, 443 pp.

Fujisawa T, Barraclough TG (2013) Delimiting species using single-locus data and the Generalized Mixed Yule Coalescent approach: a revised method and evaluation on simulated data sets. Systematic Biology 62: 707–724. https://doi.org/10.1093/sysbio/syt033

Gustafson GT, Miller KB (2015) The New World whirligig beetles of the genus *Dineutus* Macleay, 1825 (Coleoptera, Gyrinidae, Gyrininae, Dineutini). ZooKeys 476: 1–135. https://doi.org/10.3897/zookeys.476.8630

Gustafson GT, Miller KB (2017) Systematics and evolution of the whirligig beetle tribe Dineutini (Coleoptera: Gyrinidae: Gyrininae). Zoological Journal of the Linnean Society 181: 118–150. https://doi.org/10.1093/zoolinnean/zlw014

Hatch MH (1927) Notes on the biology of *Dineutus* (Gyrinidae). Bulletin of the Brooklyn Entomological Society 22: 27–28.

Isambert B, Bergsten J, Monaghan MT, Andriamizehy H, Ranarilalatiana T, Ratsimbazafy M, Andriniainimanana JR, Vogler AP (2011) Endemism and evolutionary history in conflict over Madagascar's freshwater conservation priorities. Biological Conservation 144: 1902–1909. https://doi.org/10.1016/j.biocon.2011.04.016

Istock CA (1967) Transient competitive displacement in natural populations of whirligig beetles. Ecology 48: 929–937. https://doi.org/10.2307/1934536

Kirby W (1837) Fauna boreali-americana, or, the zoology of the northern parts of British America: containing descriptions of the objects of natural history collected on the late northern land expeditions, under command of Captain Sir John Franklin, R.N./by John Richardson, surgeon and naturalist to the expeditions; assisted by William Swainson and the Reverend William Kirby. John Murray, London, 380 pp.

Laporte FL (1835) *Études entomologiques, ou description* d'insectes nouveaux et observations sur leur synonymie. Par F. L. de Laporte Comte de Castelnau. Coléoptères. Première partie. Carnassiers. Méquignon-Marvis Père et Fils, Paris, 95–159.

Laporte FL (1840) Histoire naturelle des animaux articulés, Annélides, Crustacés, Arachnides, Myriapodes et Insectes. Histoire naturelle des Insectes Coléoptères. Tome 2. Duménil, Paris, 563 pp.

Lawrence JF (1991) Order Coleoptera. In: Stehr FW (Ed.) Immature Insects, Volume 2. Kendall/Hunt Publishing Company, Iowa, 144–658.

Macleay WS (1825) Annulosa javanica, or an attempt to illustrate the natural affinities and analogies of the insects collected in Java by Thomas Horsfield and deposited by him in the Museum of the Honourable East-India Company. Kingsbury, Parbury and Allen, London, 150 pp.

Michat MC, Archangelsky M, Fernández LA (2010) Larval description and chaetotaxic analysis of *Gyrinus monrosi* Mouchamps, 1957 (Coleoptera: Gyrinidae). Koleopterologische Rundschau 80: 1–14.

Michat MC, Gustafson GT (2016) Larval morphology and chaetotaxy of *Macrogyrus oblongus* (Boisduval, 1835) (Coleoptera: Gyrinidae). Aquatic Insects 37: 87–98. https://doi.org/10.1080/01650424.2016.1186280

Michat MC, Marinho Alvarenga T, Souza Silva M, Alarie Y (2016) First larval description and chaetotaxic analysis of the neotropical whirligig beetle genus *Enhydrus* Laporte, 1834 (Coleoptera: Gyrinidae). Revista Brasileira de Entomologia 60: 231–237. https://doi.org/10.1016/j.rbe.2016.05.005

Mouchamps R (1957) Sur quelques *Gyrinus* de l´Amérique du Sud (Coleoptera, Gyrinidae) (10ª note). Revue française d'Entomologie 24: 244–252.

Müller OF (1764) Fauna insectorum Fridrichsdalina sive Methodica, descriptio Insectorum Agri Fridrichsdalensis, cum characteribus genericis et specificis, nominibus trivialibus, locis natalibus, iconibus allegatis, novisque pluribus speciebus additis. I. F. Gleditschii, Hafniae et Lipsiae, 96 pp.

Nowrojee BA (1912) Life-histories of indian insects. II. Some aquatic Rhynchota and Coleoptera. Memoirs of the Department of Agriculture in India 2: 164–191.

Ochs G (1924) Über neue und interessante Gyriniden aus dem British Museum in London. Entomologische Blätter 20: 228–244.

Ochs G (1926) Die Dineutini. 2. Tribus der Unterfamilien Enhydrinae Fam. Gyrinidae (Col). A. Allgemeiner Teil. Entomologische Zeitschrift 40: 61–74; 65: 112–126; 116: 129–140; 118: 190–197.

Régimbart M (1882a–1883) Essai monographique de la famille des Gyrinidae. 1e partie. Annales de la Société Entomologique de France 6: 379–458. [379–400 in 1882, 401–458 in 1883]

Régimbart M (1883) Essai monographique de la famille des Gyrinidae. Annales de la Société entomologique de France 6(2): 121–190; 6(3): 381–482.

Simon C, Frati F, Beckenbach A, Crespi B, Liu H, Flook P (1994) Evolution, weighting, and phylogenetic utility of mitochondrial gene sequences and a compilation of conserved polymerase chain reaction primers. Annals of the Entomological Society of America 87: 651–701. https://doi.org/10.1093/aesa/87.6.651

Wiedemann CRW (1821) Neue exotische käfer. Magazin der Entomologie Herausgegeben von E. F. Germar 4: 107–183.

Wiley EO (1981) Phylogenetics. The theory and practice of phylogenetic systematics. John Wiley and Sons, New York, 439 pp.

Wilson CB (1923) Water beetles in relation to pondfish culture, with life histories of those found in fishponds at Fairport, Iowa. Bulletin of the Bureau of Fisheries 39: 232–345.

ZooKeys 718: 115–131 (2017)
doi: 10.3897/zookeys.718.13574
http://zookeys.pensoft.net

RESEARCH ARTICLE

A peer-reviewed open-access journal
ZooKeys
Launched to accelerate biodiversity research

Evolution of the connection patterns of the cephalic lateral line canal system and its use to diagnose opsariichthyin cyprinid fishes (Teleostei, Cyprinidae)

Taiki Ito[1], Toyoaki Fukuda[2], Toshihiko Morimune[3], Kazumi Hosoya[3]

1 *Wetlands International Japan, 2F Jono Building II 17-1, Odenma-cho, Nihonbashi, Chuo-ku, Tokyo, 103-0011, Japan* **2** *Tezukayama Junior & Senior High School, Gakuen-minami 3-1-3, Nara 631-0034, Japan* **3** *Department of Environmental Management, Faculty of Agriculture, Kindai University, Nakamachi 3327-204, Nara 631-8505, Japan*

Corresponding author: *Taiki Ito* (qqx36bd@gmail.com)

Academic editor: *S. Kullander* | Received 7 May 2017 | Accepted 28 October 2017 | Published 4 December 2017

http://zoobank.org/DFD89691-39A8-43F5-AE62-999206687317

Citation: Ito T, Fukuda T, Morimune T, Hosoya K (2017) Evolution of the connection patterns of the cephalic lateral line canal system and its use to diagnose opsariichthyin cyprinid fishes (Teleostei, Cyprinidae). ZooKeys 718: 115–131. https://doi.org/10.3897/zookeys.718.13574

Abstract

The cephalic lateral line canal systems were compared among 12 species of the cyprinid tribe Opsariichthyini. All species were characterized by the separation of the supraorbital canal from both the infraorbital and the temporal canals, and the left side of the supratemporal canal from the right side of the canal. In species of *Candidia*, *Opsariichthys*, *Parazacco*, and *Zacco*, and *Nipponocypris sieboldii* the temporal canal was separated from the preoperculomandibular canal. In *Nipponocypris temminckii* and *N. koreanus*, the temporal canal was connected to the preoperculomandibular canal. Separation of the left and right sides of the supratemporal canal is a possible synapomorphy of the opsariichthyin cyprinids. *Opsariichthys uncirostris* and *O. bidens* are unique among the opsariichthyins in that the connection between the infraorbital and temporal canals is retarded. The variation in arrangement of the cephalic lateral line canal system can be used as diagnostic characters for the opsariichthyin species.

Keywords

Candidia, heterochrony, morphology, *Parazacco*, sensory organs, *Zacco*

Introduction

The cyprinid tribe Opsariichthyini, of the subfamily Xenocypridinae (Liao et al. 2011; Kottelat 2013), comprises the East Asian genera *Opsariichthys* Bleeker, 1863, *Zacco* Jordan & Evermann, 1902, *Candidia* Jordan & Richardson, 1909, *Parazacco* Chen, 1982, and *Nipponocypris* Chen, Wu & Hsu, 2008 (Wang et al. 2007, Chen et al. 2008, Kottelat 2013). The opsariichthyins comprise approximately 19 species (Kim et al. 2005, Huynh and Chen 2013, Ito and Hosoya 2016). The opsariichthyin fishes are distributed in eastern Asia from Russia, Japan, through the Korean Peninsula to China, Taiwan, and northern Vietnam (Kottelat 2001, Kim and Park 2002, Chen and Chang 2005, Serov et al. 2006). They are loosely defined as a monophyletic group on the basis of a single character, namely, a long anal fin (Chen 1982), and recent molecular phylogenetic analyses support the monophyly of the group (e.g., Wang et al. 2007, Tang et al. 2013). However, morphological characters relevant for taxonomy have not been examined in detail for this group.

Variations in the connection pattern of the cephalic lateral line canals, and the number and the distribution of canal pores on the head have often been used in the study of interrelationships within the family Cyprinidae (Lekander 1949, Gosline 1975, Howes 1980, Chen et al. 1984, Hosoya 1986, Cavender and Coburn 1992, Arai and Kato 2003, Fujita and Hosoya 2005). Characteristics of the cephalic lateral line canal system have also been useful as diagnostic characters within the Cyprinidae (e.g., Illick 1956, Reno 1969, Gosline 1974, Kurawaka 1977). In particular, the connection pattern of the cephalic lateral line canal systems is species diagnostic in some cyprinid subfamilies such as the Acheilognathinae, Gobioninae, and Leuciscinae (Illick 1956, Kurawaka 1977, Arai and Kato 2003, Fujita and Hosoya 2005, Kawase and Hosoya 2015). However, the opsariichthyin cyprinids have not been thoroughly studied in terms of their cephalic lateral line canal system.

The objectives of the present study are to: (a) describe the connecting patterns of the cephalic lateral line canal system in the opsariichthyins, (b) provide diagnostic characters for the opsariichthyin species, (c) discuss the evolution of the connecting patterns observed.

Materials and methods

The genus level classification of the Opsariichthyini follows Chen et al. (2008), although that classification still needs to be confirmed (Yin et al. 2015, cf. Hosoya 2013). The cephalic lateral line canal system was observed in 12 species of opsariichthyins; data on the canal system in the out-group were compiled from previous studies (Tables 1–2).

Methods used for observation of the cephalic lateral line canal systems followed those of Fujita and Hosoya (2005). The canals were stained using Cyanine suminol 5R. The canal terminology follows that of Arai and Kato (2003), with additional reference

Table 1. Fish species used in the present molecular phylogenetic analysis.

Classification	Species	Source	Accession no.
Xenocypridinae			
opsariichthyin			
	Candidia barbata	Wang et al. (2007)	AY958200
	Candidia pingtungensis[*1]	Wang et al. (2007)	AY958201
	Nipponocypris koreanus	Chen et al. (2016b)	NC025286
	Nipponocypris sieboldii	Wang et al. (2007)	AY958198
	Nipponocypris temminckii	Wang et al. (2007)	AY958199
	Opsariichthys bidens	Wang et al. (2007)	AY958197
	Opsariichthys evolans[*2]	Wang et al. (2007)	AY968191
	Opsariichthys kaopingensis[*3]	Wang et al. (2007)	AY958189
	Opsariichthys pachycephalus	Wang et al. (2007)	AY958190
	Opsariichthys uncirostris	Wang et al. (2007)	AY958193
	Parazacco spilurus	Chang et al. (2016a)	NC023786
	Zacco platypus	Wang et al. (2007)	AY958194
others			
	Culter alburnus	unpublished	GU190362
	Ctenopharyngodon idella	Wang et al. (2008)	EU391390
	Hemigrammocypris rasborella	Tang et al. (2010)	AP011422
	Hypophthalmichthys nobilis	unpublished	EU343733
	Ischikauia steenackeri	He et al. (2004)	AF375862
	Macrochirichthys macrochirus	Tang et al. (2010)	AP011234
	Metzia lineata	Tang et al. (2010)	HM224305
	Ochetobius elongatus	He et al. (2004)	AF309506
	Parachela siamensis	Tang et al. (2010)	HM224300
	Paralaubuca typus	Saitoh et al. (2011)	AP011211
	Squaliobarbus curriculus	Tang et al. (2010)	HM224308
	Xenocypris macrolepis[*4]	Tang et al. (2010)	HM224310
Acheilognathinae			
	Acheilognathus typus	Saitoh et al. (2006)	AB239602
	Rhodeus ocellatus	Saitoh et al. (2006)	AB070205
	Tanakia limbata	Tang et al. (2010)	HM224309
Gobioninae			
	Hemibarbus barbus	Saitoh et al. (2006)	AB070241
	Pseudorasbora parva	Tang et al. (2010)	HM224302
Leuciscinae			
	Scardinius erythrophthalmus	unpublished	NC031561
	Tribolodon hakonensis	Imoto et al. (2013)	NC018820

[*1] treated as *Candidia barbatus* (S); [*2] *Zacco* sp. E; [*3] *Z. pachycephalus* (S); [*4] *Xenocypris argentea* by the authors.

to that of Fujita and Hosoya (2005). These are as follows: infraorbital canal (**IO**), preoperculomandibular canal (**POM**), supraorbital canal (**SO**), supratemporal canal (**ST**), and temporal canal (**TC**) (Fig. 1).

Table 2. The connection states of the cephalic lateral line canal system in the opsariichthyins and out-group.

Classification	Species	SO-IO	IO-TC	TC-POM	ST-ST	Source
Xenocypridinae						
opsariichthyin						
	Candidia barbata[*1]	–	+	–	–	This study
	Candidia pingtungensis	–	+	–	–	This study
	Nipponocypris koreanus	–	+	+	–	This study
	Nipponocypris sieboldii	–	+	–	–	This study
	Nipponocypris temminckii	–	+	+	–	This study
	Opsariichthys bidens	–	±	–	–	This study
	Opsariichthys evolans	–	+	–	–	This study
	Opsariichthys kaopingensis	–	+	–	–	This study
	Opsariichthys pachycephalus	–	+	–	–	This study
	Opsariichthys uncirostris	–	±	–	–	This study
	Parazacco spilurus[*2]	–	+	–	–	This study
	Zacco platypus	–	+	–	–	This study
others						
	Culter alburnus	+	+	+	+	Takeuchi (2012)
	Ctenopharyngodon idella	+	+	+	+	Takeuchi (2012)
	Hemigrammocypris rasborella	–	+	–	+	Takeuchi et al. (2011)
	Hypophthalmichthys nobilis	–	+	+	+	Takeuchi (2012)
	Ischikauia steenackeri	+	+	+	+	Takeuchi (2012)
	Macrochirichthys macrochirus	+	+	+	†	Takeuchi (2012)
	Metzia lineata	–	+	+	+	Takeuchi (2012)
	Ochetobius elongatus	+	+	+	+	Takeuchi (2012)
	Parachela siamensis	+	+	+	†	Takeuchi (2012)
	Paralaubuca typus	+	+	+	+	Takeuchi (2012)
	Squaliobarbus curriculus	+	+	+	+	Takeuchi (2012)
	Xenocypris macrolepis	+	+	+	+	Takeuchi (2012)
Acheilognathinae						
	Acheilognathus typus	–	+	–	–	Arai and Kato (2003)
	Rhodeus ocellatus	–	+	–	–	Arai and Kato (2003)
	Tanakia limbata	–	+	–	–	Arai and Kato (2003)
Gobioninae						
	Hemibarbus barbus	+	+	+	+	Hosoya (1986)
	Pseudorasbora parva	–	+	–	+	Kawase and Hosoya (2015)
Leuciscinae						
	Scardinius erythrophthalmus	+	+	+	+	Takeuchi (2012)
	Tribolodon hakonensis	–	+	–	+	Kurawaka (1977)

IO, infraorbital canal; POM, preoperculomandibular canal; SO, supraorbital canal; ST, supratemporal canal; TC, temporal canal. SO-IO, continuity between the SO and IO; TC-IO, continuity between the TC and IO; TC-POM, continuity between the TC and POM; ST-ST, continuity between the left and right sides of the ST. Continuity (+), discontinuity (–), delay (±), and both sides of the ST connected and extending anteriorly (†). *[1]Three specimens had connected left and right sides of the ST. *[2]One specimen had a connected SO and IO.

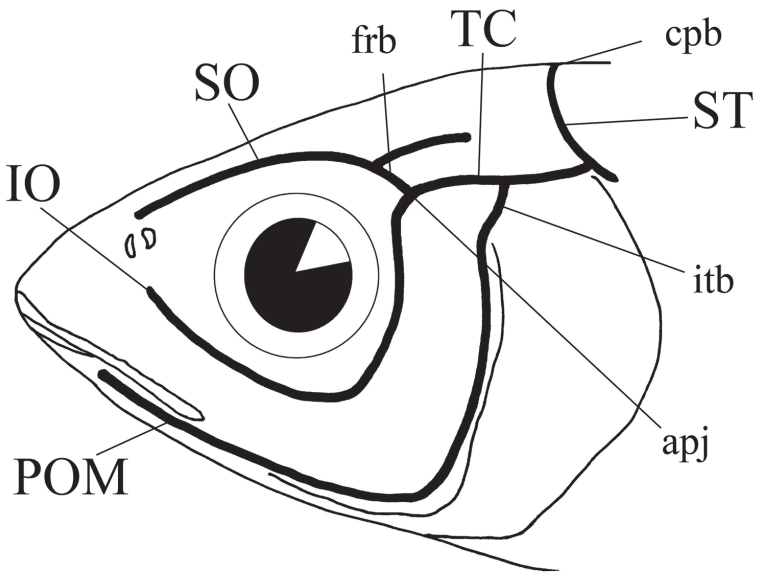

Figure 1. Terminology used for cephalic lateral line canal systems: **SO** supraorbital canal **IO** infraorbital canal **TC** temporal canal **POM** preoperculomandibular canal **ST** supratemporal canal **frb** frontal bridge **cpb** centroparietal bridge **itb** infratemporal bridge **apj** anteropteroitic joint.

Furthermore, the canaliculi branching from each canal are defined as "bridges," whereas the junctions connecting canals were termed "joints." The three bridges and one joint were as follows: "frontal bridge" between SO and IO; "centroparietal bridge" recognizing that ST meets the opposite side ST; "infratemporal bridge" between POM and TC; and "anteropterotic joint" between IO and TC (Fig. 1).

In some species in cyprinid subfamilies such as Gobioninae and Leuciscinae, development of the cephalic lateral line canal system is generally completed when the fish is approximately 60 mm in total length (= TL) (Lekander 1949, Disler 1971, Hosoya 1986). Therefore, in the present study, specimens larger than 60 mm in TL were selected for examination. The pores on each canal were counted from end to end. Statistical tests were used to assess differences in the number of pores among the species. Tests for homogeneity of variance were carried out on the number of pores on each canal using Bartlett's test in R 3.3.1 (R Core Team 2016). When the variances were homogeneous, the Tukey-Kramer test was used, whereas when variances were heterogeneous, the Steel-Dwass test in R 3. 3.1 was used.

To obtain a hypothesis about the branching pattern of the opsariichthyin species, we analyzed mitochondrial cytochrome *b* (cyt *b*) gene sequences downloaded from GenBank. This is because molecular data for the cyt *b* gene sequence of all the species examined in the present study have been accumulated by previous studies (Table 1). Cyt *b* sequence alignment of 1137 bp long sequences was performed using MEGA 7 (Kumar et al. 2016) and checked manually for accuracy. Maximum likelihood (ML) analysis for

phylogenetic reconstruction was applied using PAUP* v. 4.0b10 (Swofford 2002). Models of molecular evolution were selected using the program MODELTEST v.3.7 (Posada and Crandall 1998), with the best fitting model being determined by the Akaike information criteria (AIC) (= GTR+G+I model, in the present analysis). Three species of the subfamily Acheilognathinae, two species of the subfamily Gobioninae, two species of the subfamily Leuciscinae, and 12 species of the Xenocypridinae were chosen as out-groups (Table 1). Polarity in the character evolutions of the connecting pattern of the cephalic lateral line canals was determined by character state reconstruction using Mesquite v.2.75 (Maddison and Maddison 2010) with maximum parsimony methodology. Maximum parsimony character state reconstruction was performed on the ML tree.

Specimens studied are deposited in the following institutions: Chonbuk National University, Jeollabuk-do, Korea (**CNUC**); Department of Fisheries, Faculty of Agriculture, Kyoto University, Kyoto, Japan (**FAKU**); Fisheries Research Laboratory, Mie University, Mie, Japan (**FRLM**); Lake Biwa Museum, Shiga, Japan (**LBM**); the National Museum of Nature and Science, Tsukuba, Japan (**NSMT**); Swedish Museum of Natural History, Stockholm, Sweden (**NRM**); Smithsonian Institution National Museum of Natural History, Washington DC, United States (**USNM**). The institutional code of the Faculty of Agriculture, Kindai University, was changed from **FKUN** (Department of Fisheries, Kindai University, Nara) to **KUN-P** (Kindai University, Nara, Pisces) with faculty reorganization in 2005.

Material examined

Candidia barbata (Regan, 1908): FKUN 34180, 1, 94.8 mm standard length (= SL), Tamsui River, Taipei, Taiwan; FKUN 35264–35272, 9 , 49.3–94.8 mm SL, Shueili River, Nantou, Taiwan; KUN-P 44430–44433, 4 , 94.7–103.0 mm SL, Houlong River, Miaoli, Taiwan.

Candidia pingtungensis Chen Wu & Hsu, 2008: FKUN 35214–35215, KUN-P 44492, 44515–44516, 5, 53.3–112.9 mm SL, Kaoping River, Pingtung, Taiwan.

Nipponocypris koreanus (Kim, Oh & Hosoya, 2005): KUN-P 40584–40591, 8, 69.3–111.9 mm SL, Nakdong River, Yeongwol, Korea; KUN-P 44463, 44475–44476, 3, 111.3–137.2 mm SL, Nakdong River, Gyongnam, Korea.

Nipponocypris sieboldii (Temminck & Schlegel, 1846): KUN-P 40564–40573, 10, 81.3–105.0 mm SL, Yamato River Nara Pref., Japan; KUN-P 44764–44767, 4, 63.7–85.8 mm SL, Kizu River, Kyoto Pref., Japan.

Nipponocypris temminckii (Temminck & Schlegel, 1846): KUN-P 40574–40581, 40583, 9, 85.2–100.9 mm SL, Kizu River, Kyoto Pref., Japan; KUN-P 45003, 45005–45006, 3, 79.1–145.3 mm SL, Shiomi River, Saga Pref., Japan; KUN-P 45104–45105, 45109, 3, 110.8–130.9 mm SL, Kawatana River, Nagasaki Pref., Japan.

Opsariichthys bidens Günther, 1873: LBM 8852, 47588, FRLM 28191–28192 (captive bred individuals), USNM 86307, 5, 66.7–108.1 mm SL, ChangJiang River, Sichuan, China; NSMT 12464, 10, 61.7–80.5 mm SL, Cheng-te, Hebei, China.

Opsariichthys evolans (Jordan & Evermann, 1902): FKUN 35196–35199, 35255, 35256, 6, 50.9–81.1 mm SL, Fengshan River, Hsinchu, Taiwan; KUN-P 44427–44429, 3, 69.5–80.6 mm SL, Houlong River, Miaoli, Taiwan.

Opsariichthys kaopingensis Chen, Wu & Huang, 2009: KUN-P 40545–40547, 44402, 44404–44405, 44407, 7, 69.2–83.0 mm SL, Kaoping River, Pingtung, Taiwan.

Opsariichthys pachycephalus (Günther,1868): FKUN 35179–35183, 35194, 35195, 7, 69.4–95.4 mm SL, Fengshan River, Hsinchu, Taiwan; FKUN 35245, 35250, 35252, 3, 56.0–70.3 mm SL, Keelung River, Taipei, Taiwan.

Opsariichthys uncirostris (Temminck & Schlegel, 1846): FKUN 16487–16488, 16492, 16495, 4, 211.5–228.0 mm SL, Ishida River, Shiga Pref., Japan; FKUN 16561, 16569, 16574, 3, 83.9–139.6 mm SL, Lake Biwa, Shiga Pref., Japan; KUN-P 40548–40554, 40592, 44528, 44529, 10, 145.1–231.8 mm SL, Mano River, Shiga Pref., Japan; FKUN 31878–31880, 3, 65.8–80.7 mm SL, Bukhan River, Korea; KUN-P 40636, 1, 206.5 mm SL, Gupo fish market, Korea; CNUC 37632, 1, 213.1 mm SL, Mangyeong River, Korea.

Parazacco spilurus (Günther, 1868): NRM 59489, 2, 56.6–82.8 mm SL, Pearl River, Guangxi Province, China; KUN-P 44899, 45852, 2, 57.5–105.6 mm SL, Pearl River, Hongkong, China.

Zacco platypus (Temminck & Schlegel, 1846): KUN-P 40555–40563, 9, 79.1–93.0 mm SL, Yamato River, Nara Pref., Japan; KUN-P 44379, 44381, 44383, 44386–44388, 6, 114.5–123.4 mm SL, Mono River, Shiga Pref., Japan.

Results

The cephalic lateral line canal system is comprised of five canals, three bridges, and one joint in all opsariichthyin specimens examined (Fig. 2A–L). No intraspecific variation was found in the connection patterns of the cephalic lateral line canals when conspecific specimens of similar size were compared.

The canals were usually well ossified, although part of the POM (see below), the frontal bridge, the infratemporal bridge, and the anteropterotic joint were cutaneous tubes. The SO was housed in the nasal and frontal bones. This canal was separated from the IO and TC in all the opsariichthyin fishes (with the exception of one specimen of *P. spilurus* in which the SO and IO were connected: NRM 59489, 82.8 mm SL).The IO runs along a series of five infraorbital bones. This canal was connected with the TC in all species; however, the canal was separated from the TC in individuals less than ca. 180 mm SL in *O. uncirostris* and ca. 100 mm SL in *O. bidens*. The POM was found in the anguloarticular, dentary, and preopercular bones. In the anguloarticular, the canal was cutaneous. The TC runs in the pterotic. No connection between the TC and POM was observed, except in *N. temminckii* and *N. koreanus*, in which the TC was connected with the POM by the infratemporal bridge. The ST passes through the parietal bone. In all the opsariichthyin species, the left and right sides of the ST were typically separated (except for three specimens of *C. barbata* in which left and right

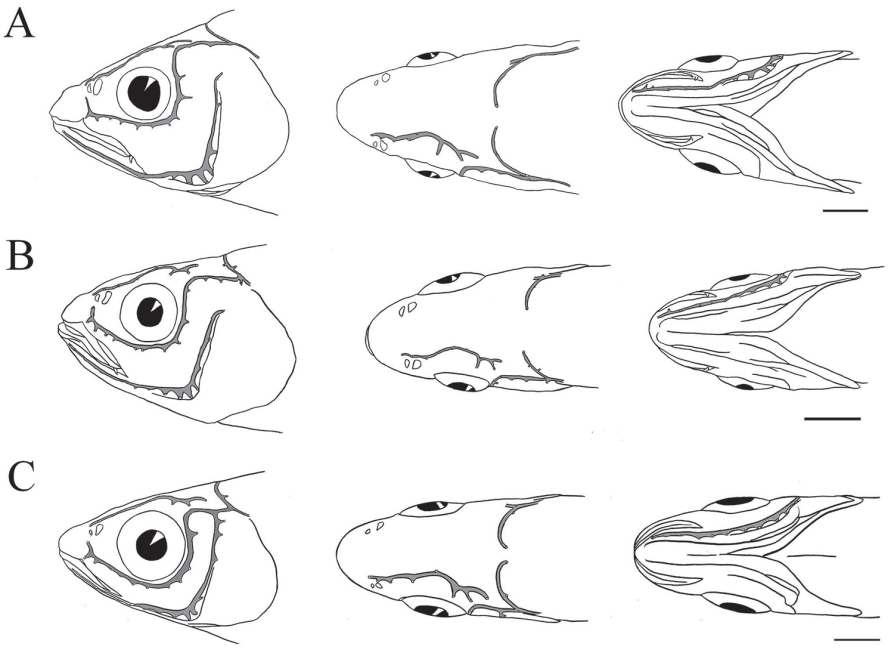

Figure 2. Diagram of the cephalic lateral line canal systems in the opsariichthyin fishes. **A** *Candidia barbata*, FKUN 34180, 94.8 mm SL **B** *C. pingtungensis*, FKUN 35215, 72.9 mm SL **C** *Nipponocypris koreanus*, FKUN 40587, 94.1 mm SL. Scale bar 5 mm.

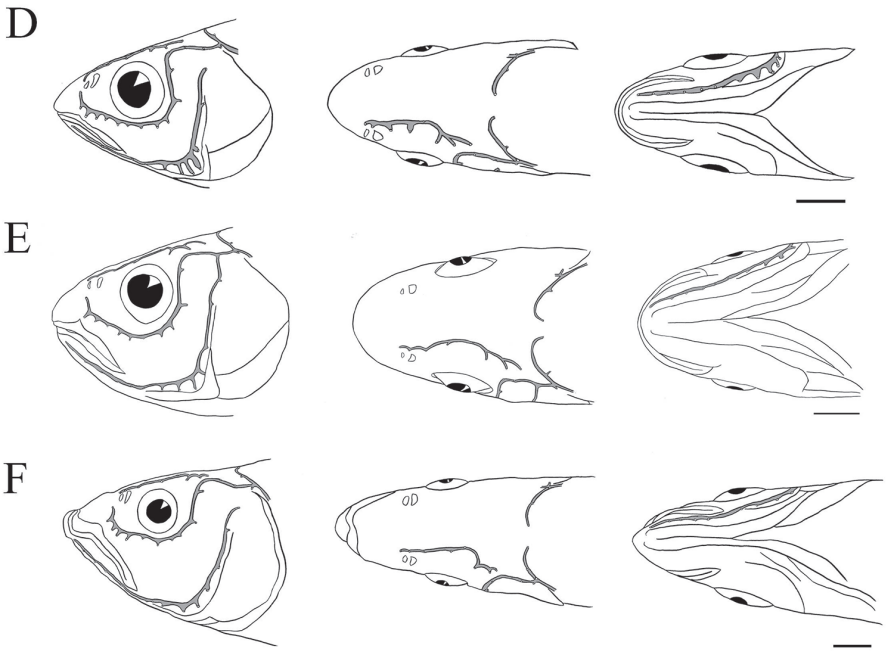

Figure 2. Continued. **D** *N. sieboldii*, FKUN 40571, 90.5 mm SL **E** *N. temminckii*, FKUN 40575, 94.5 mm SL **F** *Opsariichthys bidens*, LBM 8852, 94.8 mm SL. Scale bar 5 mm.

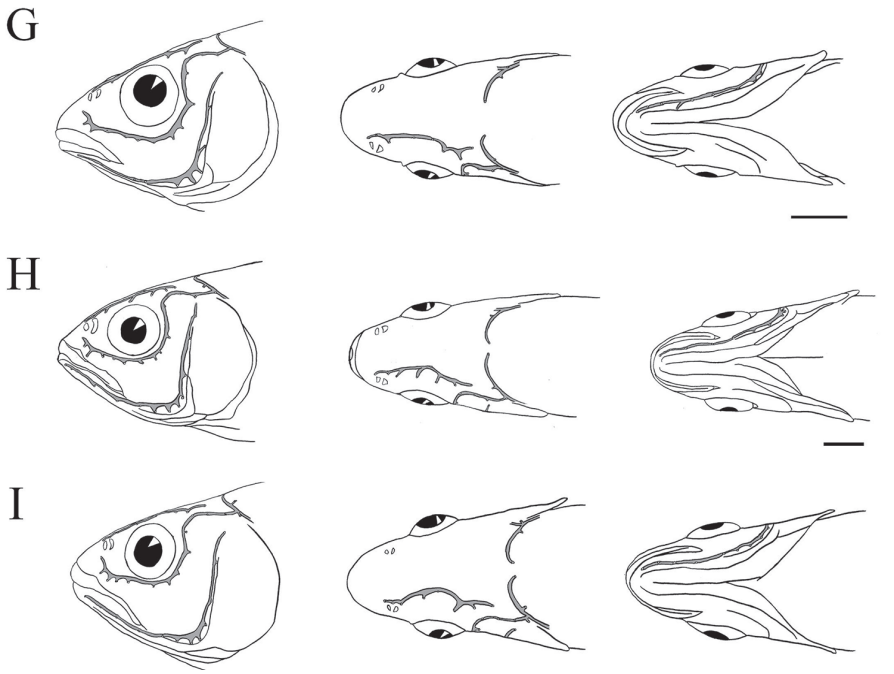

Figure 2. Continued. **G** *O. evolans*, FKUN 35199, 81.1 mm SL **H** *O. kaopingensis*, KUN-P40545, 80.0 mm SL **I** *O. pachycephalus*, FKUN 35181, 69.4 mm SL. Scale bar 5 mm.

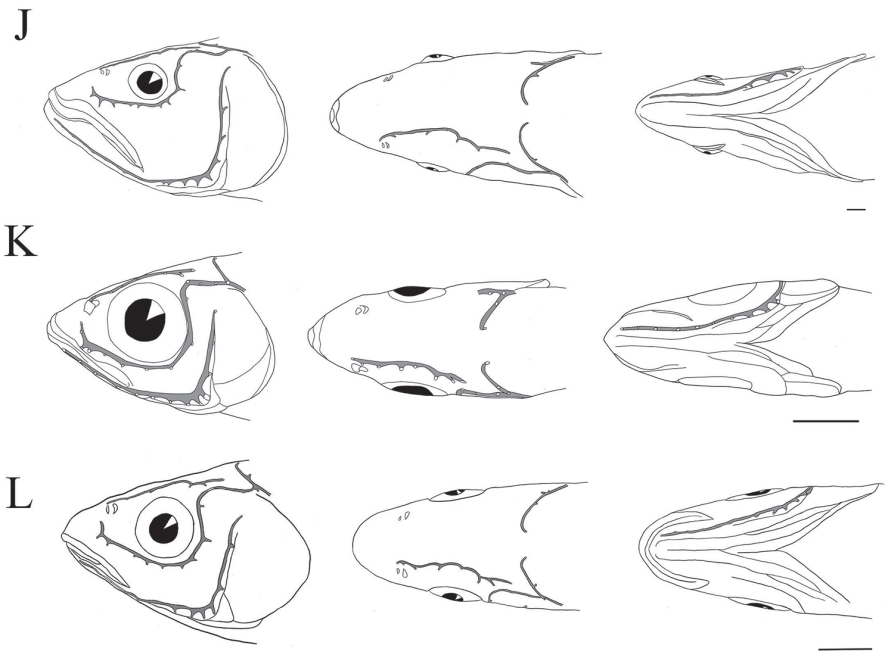

Figure 2. Continued. **J** *O. uncirostris*, FKUN 16487, 219.0 mm SL **K** *Parazacco spilurus*, KUN-P45852, 57.5 mm SL **L** *Zacco platypus*, FKUN 40558, 93.0 mm SL. Scale bar 5 mm.

sides of the ST connected: FKUN 35270–35272, 49.3–54.7 mm SL). The ST was connected with the TC and the trunk canal in all the opsariichthyin species.

Connecting patterns of the cephalic lateral line canal system of the out-groups are shown in Table 2.

The number of pores on each canal are shown in Table 3. The opsariichthyins had 8–9 pores on the SO; 10–14 pores on the IO, 3–5 pores on the TC; 12–17 pores on the POM; 2–3 pores on the ST. The number of pores on the POM differs significantly between *O. uncirostris* and *O. pachycephalus*, *O. evolans*, *Z. platypus* ($P < 0.01$), *O. kaopingensis* and *N. sieboldii* ($P < 0.05$); between *O. bidens* and *O. evolans* ($P < 0.05$) and *Z. platypus* ($P < 0.01$); between *N. koreanus* and *O. pachycephalus*, *O. evolans,* and *Z. platypus* ($P < 0.01$); between *N. temminckii* and *O. evolans*, *Z. platypus* ($P < 0.01$) and *O. pachycephalus* ($P < 0.05$); and between *C. barbata* and *Z. platypus* ($P < 0.05$). No significant difference was found in the number of pores on the IO, SO, TC, and ST among the opsariichthyin fishes.

The topology of the ML tree is shown Figure 3. The ancestor at the root of the opsariichthyins on the ML tree was reconstructed as having canal separation between the SO and IO (Fig. 3A). The canal connection between the SO and IO was estimated to have occurred in at least four independent lineages in the out-group (see Fig. 3A). The ancestor at the root of the opsariichthyins was reconstructed as having canal separation between the TC and POM. In the opsariichthyins, the canal connection between the TC and POM emerged in the ancestor of *N. temminckii* and *N. koreanus* (Fig. 3B). The canal connection between the TC and POM emerged at least five lineages in the out-groups (Fig. 3B). The canal separation between the left and right sides of the ST independently emerged twice in the ancestors of the Acheilognathinae and the opsariichthyin (Fig. 3C). The canal connection and anterior extension between the right and left of the ST occurred at least twice in the out-groups (see Fig. 3C).

Discussion

The cephalic lateral line canal systems as a diagnostic character

Significant differences were found in the number of pores on the POM among some opsariichthyin species. However, the number of pores on these canals was found to vary within each species, and there was an overlap of ranges among all observed species (Table 3). Therefore, the number of pores on the cephalic lateral line canals does not provide reliable diagnostic character states for the opsariichthyin species.

In contrast, the connecting pattern of the cephalic lateral line canals provides useful diagnostic character states for some species of the opsariichthyins. *Nipponocypris temminckii* and *N. koreanus* are clearly distinguished from the very similar species *N. sieboldii* by the connection between the POM and TC through the infratemporal bridge. Similarly, *O. uncirostris* can be distinguished from *O. bidens* on the basis that the two species have different sizes at which the connection between the IO and TC

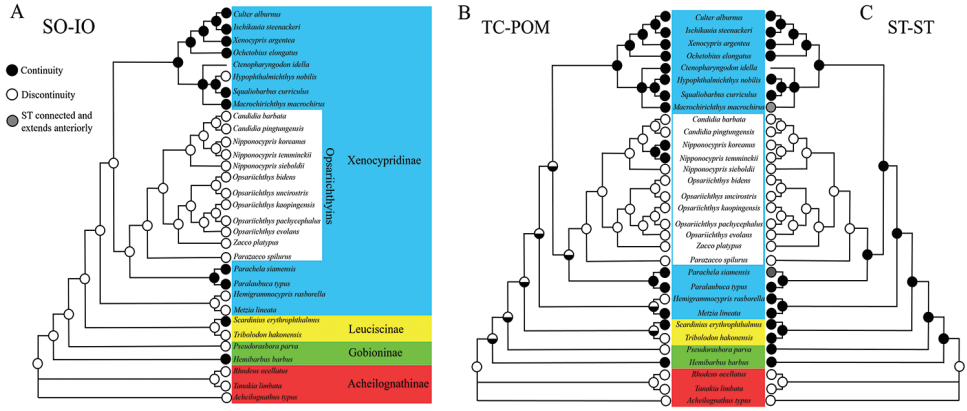

Figure 3. Parsimonious ancestral state reconstruction of the connecting states of the cephalic lateral line canal systems of the opsariichthyin fishes and their out-groups from the maximum likelihood tree inferred from cytochrome *b* sequences (InL = 12054.39). **A** The connecting states between the supraorbital (**SO**) and infraorbital (**IO**) canals **B** the connecting states between the temporal (**TC**) and preoperculomandibular (**POM**) canals **C** the connecting states between the left and right sides of the supratemporal canals (**ST**). The color of each node indicates the connecting states of the cephalic lateral line canal system: black, continuity; white, discontinuity; gray, both sides of the **ST** connected and extending anteriorly.

Table 3. Mode, average ± standard deviation, and range of the number of pores in each part of the cephalic lateral line canal in the opsariichthyin cyprinids.

Species	SO	IO	TC	POM	ST
Candidia barbata	8, 8.00 ± 0, 8	12, 11.91 ± 0.30, 11–12	4, 4.00 ± 0, 4	14, 14.27 ± 1.27, 12–16	3, 3.00 ± 0, 3
Candidia pingtungensis	8, 8.20 ± 0.45, 8–9	12, 12.60 ± 0.89, 12–14	4, 4.00 ± 0, 4	15, 14.20 ± 0.84, 13–15	3, 2.80 ± 0.45, 2–3
Nipponocypris koreanus	8, 8.00 ± 0, 8	12, 11.82 ± 0.60, 11–13	4, 3.91 ± 0.30, 3–4	15, 14.91 ± 0.83, 13–16	3, 3.00 ± 0, 3
Nipponocypris sieboldii	8, 8.00 ± 0, 8	12, 11.93 ± 0.83, 10–13	4, 4.11 ± 0.31, 4–5	14, 13.79 ± 0.97, 12–15	3, 3.00 ± 0, 3
Nipponocypris temminckii	8, 8.00 ± 0, 8	12, 11.67 ± 0.49, 11–12	4, 4.07 ± 0.26, 4–5	15, 14.53 ± 0.99, 13–17	3, 3.00 ± 0, 3
Opsariichthys bidens	8, 8.00 ± 0, 8	12, 12 ± 0.37, 11-13	4, 4 ± 0.37, 3-5	14, 14.33 ± 0.70, 13–16	3, 3.00 ± 0, 3
Opsariichthys evolans	8, 8.00 ± 0, 8	12, 11.56 ± 0.73, 10–12	4, 4.00 ± 0, 4	12, 13.00 ± 0.87, 12–14	3, 3.00 ± 0, 3
Opsariichthys kaopingensis	8, 8.00 ± 0, 8	12, 11.57 ± 0.53, 11–12	4, 4.00 ± 0, 4	13, 13.43 ± 0.79, 13–15	3, 3.00 ± 0, 3
Opsariichthys pachycephalus	8, 8.00 ± 0, 8	12, 12.22 ± 0.67, 11–13	4, 4.11 ± 0.33, 4–5	14, 13.22 ± 0.83, 12–14	3, 3.00 ± 0, 3
Opsariichthys uncirostris	8, 8.05 ± 0.22, 8–9	12, 11.95 ± 0.51, 11–13	4, 4.05 ± 0.22, 4–5	14, 14.95 ± 1.10, 14–17	3, 3.00 ± 0, 3
Parazacco spilurus	8, 8.00 ± 0, 8	11, 11.25 ± 0.50, 11–12	4, 4.00 ± 0.82, 3–5	14, 13.50 ± 1.00, 12–14	3, 3.00 ± 0, 3
Zacco platypus	8, 8.07 ± 0.27, 8–9	12, 11.79 ± 0.43, 11–12	4, 4.00 ± 0, 4	13, 13.00 ± 0.55, 12–14	3, 3.00 ± 0, 3

IO, infraorbital canal; POM, preoperculomandibular canal; SO, supraorbital canal; ST, supratemporal canal; TC, temporal canal. When both sides of the ST canal were connected to form a single pore on the parietal, the numbers shown include this pore.

attains completion (ca. 180 mm SL vs. ca. 100 mm SL, respectively), although many investigators have indicated that these two species can only be distinguished by the number of scales in the lateral series (e.g., Bănărescu 1968, Chen 1982).

Character evolution

All opsariichthyin species share the canal separation between the left and right sides of the ST. Although, this character state also occurs at the root of the Acheilognathinae, this characteristic strongly supports the monophyly of the opsariichthyins, because the characteristic was derived only once from the common ancestor of the opsariichthyins in the Xenocypridinae. The opsariichthyins have been defined in terms of a single shared character state, viz. a long anal fin (Chen 1982). Based on our analysis, the canal separation between the left and right sides of the ST is suggested as a possible synapomorphy of the opsariichthyin by the character state reconstruction. In addition, in the opsariichthyins, the canal connection between the POM and TC emerged in the ancestor of *N. temminckii* and *N. koreanus* (Fig. 3). The canal connection between the POM and TC is a possible synapomorphy of *N. temminckii* and *N. koreanus*. In the present study, there was no synapomorphy to link *N. temminckii* and *N. koreanus*, and *N. sieboldii*, and the current recognized genus *Nipponocypris* is not monophyletic. Our analyses suggested that *Nipponocypris* is paraphyletic, but further taxonomic study is required.

Evolution of the cephalic lateral line canal system ontogeny in *Opsariichthys uncirostris* and *O. bidens*

Opsariichthys uncirostris and *O. bidens* have a unique ontogeny of the cephalic lateral line canal system. In the Cyprinidae, the cephalic lateral line canal systems are generally completed at 40–60 mm in TL (Lekander 1949, Disler 1971, Hosoya 1986). In the opsariichthyins (with the exception of *O. uncirostris* and *O. bidens*), they are completed by approximately 60 mm SL. In *O. uncirostris* and *O. bidens*, canalization of the IO and TC through the anteropterotic joint is delayed until the individual reaches a mature size. Retardation of cephalic lateral line formation in both species can be explained in as a form of "isomorphosis", a term proposed by Reilly et al. (1997) for cases in which heterochrony does not affect the offset shape. This is exemplified by a character state that is identical in the ancestor and descendant, although the descendant arrives at the same shape via a different ontogenetic trajectory. The delayed offset of cephalic lateral line formation seen in *O. uncirostris* and *O. bidens* is identical to "hypermorphosis" (sensu Reilly et al. 1997; cf. Hanken 2015), and the retardation of its developmental rate is identical to "deceleration" (sensu Reilly et al. 1997; cf. Hanken 2015). Both species are unique among opsariichthyin fishes in that they grow to between 250 (*O. bidens*) and 300 (*O. uncirostris*) mm TL (other opsariichthyin species are typically

< 200 mm TL), and thus require more time to reach their mature size than other opsariichthyin species (Nakamura 1969, Tanaka 1970, Xing et al. 2007, Sui et al. 2012). Therefore, the retardation of cephalic lateral line formation in both species may be attributable to prolongation of the immature stage.

Acknowledgments

This study was funded in part by a Grant-in-Aid for Scientific Exploratory Research (20657019). We are grateful to I. S. Chen, his students at the National Taiwan Ocean University, M. K. Oh, H. T. Lai (National Chia-Yi University: NCU), C. H. Tung (NCU), C. C. Han (National Museum of Marine Biology & Aquarium), M. Nitta (Hiroshima University) and S. Kunimatsu (Osaka University) for their cooperation in collecting materials. We are greatly indebted to C. H. Kim (National Fisheries Research and Development Institute), J. Y. Park (CNUC), S. Kimura (FRLM), Y. Kai (FAKU), T. Nakajima (LBM), S. Kullander (NRM), G. Shinohara (NSMT) and M. Nakae (NSMT) for providing materials, and to T. Fujita (Civil Engineering & Eco-Technology Consultants), Y. Kubo and T. Kitagawa (KUN) for their technical advice and helpful comments.

References

Arai R, Kato K (2003) Gross morphology and evolution of the cephalic lateral line system and infraorbital bone in bitterlings (Cyprinidae, Acheilognathinae), with an overview of the cephalic lateral line system in the family Cyprinidae. Bulletin of the National Science Museum 40: 1–42.

Bănărescu PM (1968) Revision of the genera *Zacco* and *Opsariichthys* (Pisces, Cyprinidae). Věstník Československé Společnosti Zoologické 32: 305–311.

Bleeker P (1863) Systema cyprinoideorum revisum. Nederlandsch Tijdschrift voor de Dierkunde 1: 203.

Cavender TM, Coburn MM (1992) Phylogenetic relationships of North American Cyprinidae. In: Mayden RL (Ed.) Systematics, historical ecology and North American freshwater fishes. Stanford University Press, Stanford, 293–327.

Chang HY, Yuan LY, Hu TL, Chien CL, Lin YC, Tsenq SF, Chang TW, Wang WK (2016a) Complete mitochondrial DNA genome of *Parazacco spilurus* (Cypriniformes: Cyprinidae). Mitochondrial DNA. Part A, DNA Mapping, Sequencing and Analysis 27: 165–166. https://doi.org/10.3109/19401736.2013.878926

Chen IS, Chang YC (2005) The Photographic Guide of Inland Water Fishes, Vol. I, Cypriniformes. Sheichuan Press, Keelung, Taiwan, 284 pp.

Chen IS, Liu YW, Huang SP, Shen CN (2016b) The complete mitochondrial genome of the Korean minnow *Nipponocypris koreanus* (Cypriniformes, Cyprinidae). Mitochondrial

DNA. Part A, DNA Mapping, Sequencing and Analysis 27: 708–710. https://doi.org/10.3109/19401736.2014.913153

Chen IS, Wu JH, Hsu CH (2008) The taxonomy and phylogeny of *Candidia* (Teleostei: Cyprinidae) from Taiwan, with description of a new species and comments on a new genus. Raffles Bulletin of Zoology 19: 203–214.

Chen XL, Yue PQ, Lin RD (1984) Major groups within the family Cyprinidae and their phylogenetic relationships. Acta Zootaxonomica Sinica 9: 424–440.

Chen IS, Wu JH, Huang SP (2009) The taxonomy and phylogeny of the cyprinid genus *Opsariichthys* Bleeker (Teleostei: Cyprinidae) from Taiwan, with description of a new species. Environmental Biology of Fishes 86: 165–183. https://doi.org/10.10007/s10641-009-9499-y

Chen YY (1982) A revision of opsariichthine cyprinid fishes. Oceanologia et Limnologia Sinica 13: 293–299.

Disler NN (1971) Lateral line sense organs and their importance in fish behavior (Translated from Russian). Israel Program for Scientific Translations, Jerusalem, 328 pp.

Fujita T, Hosoya K (2005) Cephalic lateral line systems in the Far Eastern species of the genus *Phoxinus* (Cyprinidae). Ichthyological Research 52: 336–342. https://doi.org/10.1007/s10228-005-0290-6

Gosline WA (1974) Certain lateral-line canals of the head in cyprinid fishes, with particular reference to the derivation of North American forms. Japanese Journal of Ichthyology 21: 9–15.

Gosline WA (1975) The cyprinid dermosphenotic and the subfamily Rasborinae. Occasional Papers of the Museum of Zoology University of Michigan 673: 1–13.

Günther A (1868) Catalogue of the Fishes in the British Museum. Catalogue of the Physostomi, Containing the Families Heteropygii, Cyprinidae, Gonorhynchidae, Hyodontidae, Osteoglossidae, Clupeidae, Hirocentridae, Alepocephalidae, Notopteridae, Halosauridae, in the Collection of the British Museum. Volume Seventh. The Trustees, London, 512 pp.

Günther A (1873) Report on a collection of fishes from China. Annals and Magazine of Natural History (Series 4) 12: 239–250. https://doi.org/10.1080/00222937308680749

Hanken J (2015) Is heterochrony still an effective paradigm for contemporary studies of Evo-devo? In: Love AC (Ed.) Conceptual Change in Biology: Scientific and Philosophical Perspectives on Evolution and Development. Boston Studies in the Philosophy and History of Science, Volume 307. Springer, New York, 97–110. https://doi.org/10.1007/978-94-017-9412-1_4

He S, Liu H, Kuwahara M, Nakajima T, Zhong Y (2004) Molecular phylogenetic relationships of Eastern Asian Cyprinidae (Pisces: Cypriniformes) inferred from cytochrome b sequences. Science China Life Sciences 47: 130–138. https://doi.org/10.1360/03yc0034

Hosoya K (1986) Interrelationships of the Gobioninae (Cyprinidae). In: Uyeno T, Arai R, Taniuchi T, Matsuura K (Eds) Indo-Pacific Fish Biology. Japanese Ichthyology Society, Tokyo, 484–501.

Hosoya K (2013) Danioninae. In: Nakabo T (Ed.) Fishes of Japan with Pictorial Keys to the Species (Third Edition). Tokai University Press, Tokyo, 317–319, 1815.

Howes GJ (1980) The anatomy, phylogeny and classification of bariliine cyprinid fishes. Bulletin of the British Museum (Natural History) 37: 129–198.

Huynh TQ, Chen I (2013) A new species of cyprinid fish of genus *Opsariichthys* from Ky Cung-Bang Giang river basin, northern Vietnam with notes on the taxonomic status of

the genus from northern Vietnam and southern China. Journal of Marine Science and Technology 21: 135–145.

Illick HJ (1956) A comparative study of the cephalic lateral-line system of North American Cyprinidae. American Midland Naturalist 56: 204–223. https://doi.org/10.2307/2422456

Imoto JM, Saitoh K, Sasaki T, Yonezawa T, Adachi J, Kartavtsev YP, Miya M, Nishida M, Hanzawa N (2013) Phylogeny and biogeography of highly diverged freshwater fish species (Leuciscinae, Cyprinidae, Teleostei) inferred from mitochondrial genome analysis. Gene 514: 112–124. https://doi.org/10.1016/j.gene.2012.10.019

Ito T, Hosoya K (2016) Re-examination of the type series of *Parazacco spilurus* (Teleostei: Cyprinidae). FishTaxa 1: 89–93. https://doi.org/10.7508/fishtaxa.2016.02.004

Jordan DS, Evermann BW (1902) Notes on a collection of fishes from the island of Formosa. Proceedings of the United States National Museum 25: 315–368.

Jordan DS, Richardson RE (1909) A catalog of fishes of the Island of Formosa, or Taiwan: based the collections of Dr. Hans Sauter. Memoirs of Carnegie Museum 4: 159–204.

Kawase S, Hosoya K (2015) *Pseudorasbora pugnax*, a new species of minnow from Japan, and redescription of *P. pumila* (Teleostei: Cyprinidae). Ichthyological Exploration of Freshwaters 25: 289–298.

Kim IS, Park JY (2002) Freshwater Fishes of Korea. Kyo-Hak Publishing, Seoul, 465 pp.

Kim IS, Oh MK, Hosoya K (2005) A new species of cyprinid fish, *Zacco koreanus* with redescription of *Z. temminckii* (Cyprinidae) from Korea. Korean Journal of Ichthyology 17: 1–7.

Kottelat M (2001) Fishes of Laos. Wildlife Heritage Trust Publications, Colombo, 198 pp.

Kottelat M (2013) The fishes of the inland waters of Southeast Asia: a catalogue and core bibliography of the fishes known to occur in freshwaters, mangroves and estuaries. The Raffles Bulletin of Zoology 27: 1–663.

Kumar S, Stecher G, Tamura K (2016) MEGA7: Molecular evolutionary genetics analysis Version 7.0 for bigger datasets. Molecular Biology and Evolution 33: 1870–1874. https://doi.org/10.1093/molbev/msw054

Kurawaka K (1977) Cephalic lateral-line systems and geographical distribution in the genus *Tribolodon* (Cyprinidae). Japanese Journal of Ichthyology 24: 167–175.

Lekander B (1949) The sensory line system and the canal bones in the head of some Ostariophysi. Acta Zoologica 30: 1–131. https://doi.org/10.1111/j.1463-6395.1949.tb00503.x

Liao TY, Kullander SO, Fang F (2011) Phylogenetic position of rasborin cyprinids and monophyly of major lineages among the Danioninae, based on morphological characters (Cypriniformes: Cyprinidae). Journal of Systematics and Evolutionary Research 49: 224–232. https://doi.org/10.1111/j.1439-0469.2011.00621.x

Maddison WP, Maddison DR (2010) Mesquite: a modular system for evolutionary analysis. http://www.mesquiteproject.org

Nakamura M (1969) Cyprinid Fishes of Japan. Research Institute for Natural Resources, Tokyo, 455 pp.

Posada D, Crandall KA (1998) MODELTEST: testing the model of DNA substitution. Bioinformatics 14: 817–818. https://doi.org/10.1093/bioinformatics/14.9.817

R Core Team (2016) R: a language and environment for statistical computing. R Foundation for Statistical Computing, Vienna.

Regan CT (1908) Description of new fishes from Lake Candidius, Formosa, collected by Dr. A. Moltrecht. Annals and Magazine of Natural History 2: 358–360. https://doi.org/10.1080/00222930808692494

Reilly SM, Wiley EO, Meinhardt DJ (1997) An integrative approach to heterochrony: the distinction between interspecific and intraspecific phenomena. Biological Journal of the Linnean Society 60: 119–143. https://doi.org/10.1111/j.1095-8312.1997.tb01487.x

Reno HW (1969) Cephalic lateral-line systems of the cyprinid genus *Hybopsis*. Copeia 1969: 736–773. https://doi.org/10.2307/1441800

Saitoh K, Sado T, Doosey MH, Bart HL Jr., Inoue JG, Nishida M, Mayden RL, Miya M (2011) Evidence from mitochondrial genomics supports the lower Mesozoic of South Asia as the time and place of basal divergence of cypriniform fishes (Actinopterygii: Ostariophysi). Zoological Journal of the Linnean Society 161: 633–662. https://doi.org/10.1111/j.1096-3642.2010.00651.x

Saitoh K, Sado T, Mayden RL, Hanzawa N, Nakamura K, Nishida M, Miya M (2006) Mitogenomic evolution and interrelationships of the Cypriniformes (Actinopterygii: Ostariophysi): the first evidence toward resolution of higher-level relationships of the world's largest freshwater fish clade based on 59 whole mitogenome sequences. Journal of Molecular Evolution 63: 826–841. https://doi.org/10.1007/s00239-005-0293-y

Serov DV, Nezdoliy VK, Pavlov DS (2006) The Freshwater Fishes of Central Vietnam. Scientific Press, Moscow, 363 pp.

Sui XY, Yan YZ, Chen YF (2012) Age growth, and reproduction of *Opsariichthys bidens* (Cyprinidae) from the Qingyi river at Huangshan Mountain, China. Zoological Studies 51: 476–483.

Swofford DL (2002) PAUP* Phylogenetic Analysis Using Parsimony (*and other methods), v. 4.0 beta 10. Sinauer Associates, Sunderland, Massachusetts.

Takeuchi H (2012) Phylogeny of the cyprinid subfamily Cultrinae and related taxa (Teleostei: Cypriniformes). PhD thesis, Nara, Japan: Kindai University.

Takeuchi H, Tokuda K, Kanagawa N, Hosoya K (2011) Cephalic lateral line canal system of the golden venus chub, *Hemigrammocypris rasborella* (Teleostei: Cypriniformes). Ichthyological Research 58: 175–179. https://doi.org/10.1007/s10228-010-0203-1

Tanaka S (1970) Studies on the growth of "Hasu," *Opsariichthys uncirostris*, in Lake Biwa I. On the body length at each age and the growth curve estimated from the spawning populations. Japanese Journal of Ecology 20: 13–25.

Tang KL, Agnew MK, Hirt MV, Lumbantobing DN, Raley ME, Sado T, Teoh V-H, Yang L, Bart HL, Harris PH, He S, Miya M, Saitoh K, Simons AM, Wood RM, Mayden RL (2013) Limits and phylogenetic relationships of East Asian fishes in the subfamily Oxygastrinae (Teleostei: Cypriniformes: Cyprinidae). Zootaxa 3681: 101–135. https://doi.org/10.11646/zootaxa.3681.2.1

Tang KL, Agnew MK, Hirt MV, Sado T, Schneider LM, Freyhof J, Sulaiman Z, Swartz E, Vidthayanon C, Miya M, Saitoh K, Simons AM, Wood RM, Mayden RL (2010) Systematics of the subfamily Danioninae (Teleostei: Cypriniformes: Cyprinidae). Molecular Phylogenetics and Evolution 57: 189–214. https://doi.org/10.1016/j.ympev.2010.05.021

Temminck CJ, Schlegel H (1846) Pisces. In: Siebold PF (Ed.) Fauna Japonica. Lugduni Batavorum 314 pp.

Xing YC, Zhao YH, Zhang J, Wang YF, Zhao XR, Zhang CG, Wang BL, Chang BQ, Zhang LJ, Hu YJ (2007) Growth and diets of *Zacco platypus* distributed in Beijing. Acta Zoologica Sinica 53: 982–993.

Wang C, Chen Q, Lu G, Xu J, Yang Q, Li S (2008) Complete mitochondrial genome of the grass carp (*Ctenopharyngodon idella*, Teleostei): insight into its phylogenic position within Cyprinidae. Gene 424: 96–101. https://doi.org/10.1016/j.gene.2008.07.011

Wang HY, Wang CF, Du SY, Lee SC (2007) New insights on molecular systematics of opsariichthines based on cytochrome b sequencing. Journal of Fish Biology 71: 18–32. https://doi.org/10.1111/j.1095-8649.2007.01515.x

Yin W, Cao K, He H, Fu C (2015) Four complete mitochondrial genomes of the genera *Candidia*, *Opsariichthys*, and *Zacco* (Cypriniformes: Cyprinidae). Mitochondrial DNA. Part A, DNA Mapping, Sequencing and Analysis 27: 4613–4614. https://doi.org/10.3109/19401736.2015.1101582

ZooKeys 718: 133–137 (2017)
doi: 10.3897/zookeys.718.21361
http://zookeys.pensoft.net

RESEARCH ARTICLE

A peer-reviewed open-access journal
ZooKeys
Launched to accelerate biodiversity research

A remarkable new *Helophorus* species (Coleoptera, Helophoridae) from the Tibetan Plateau (China, Sichuan)

Robert B. Angus[1]

1 *Department of Life Sciences (Insects), The Natural History Museum, Cromwell Road, London SW7 5 BD, UK*

Corresponding author: *Robert B. Angus* (r.angus@rhul.ac.uk)

Academic editor: *M. Michat* | Received 1 October 2017 | Accepted 23 November 2017 | Published 4 December 2017

http://zoobank.org/6297092A-36A8-4011-A17E-A1477A5B0B77

Citation: Angus RB (2017) A remarkable new *Helophorus* species (Coleoptera, Helophoridae) from the Tibetan Plateau (China, Sichuan). ZooKeys 718: 133–137. https://doi.org/10.3897/zookeys.718.21361

Abstract

Helophorus dracomontanus **sp. n.** is described from the Tibetan Plateau near Kangding, Sichuan, China. It is a member of the subgenus *Helophorus* s. str. but the anterolateral part of the pronotum resembles subgenus *Gephelophorus* Sharp, 1915. The short metallic-black maxillary palpi with almost symmetrical apical segments are suggestive of subgenus *Kyphohelophorus* Kuwert, 1886, but the elytral flanks are narrower than the epipleurs, excluding the species from that subgenus. An adjusted key to *Helophorus* s. str. is given to identify the new species, as well as *H. jaechi* Angus, 1995 and *H. kozlovi* Zaitsev, 1908.

Keywords

Helophorus, Helophoridae, new species, *Helophorus* s. str., *Meghelophorus*, *H. dracomontanus* sp. n., *H. jaechi* Angus, *H. kozlovi* Zaitsev, Tibetan Plateau, China, Sichuan

Introduction

In the course of a beetle-collecting trip to the Kangding area of Sichuan in June-July 2016, two females of an unknown *Helophorus*, apparently a robust member of the *H. glacialis* Villa & Villa, 1833 species group, were taken. Despite further searching, no male was encountered. Study of the material back in the laboratory showed that the elytra had scutellary striae, and this, in conjunction with the fairly narrow elytral flanks, indicated that it was a member of the subgenus *Helophorus* s. str. It is described here as it is sufficiently distinctive to be easily recognised from females alone.

Taxonomy

***Helophorus* (*Helophorus* s. str.) *dracomontanus* sp. n.**
http://zoobank.org/87F18E76-D613-430B-A925-AA33A04EE4B6

Differential diagnosis. Placed in the subgenus *Helophorus* s. str. because of its scutellary striae on the elytra, and elytral flanks clearly narrower than the epipleurs opposite the metaventrite. Distinguished from all known species of *Helophorus* s. str. by the short metallic black maxillary palpi with their apical segments almost symmetrical. The other known species of *Helophorus* s. str. with dark maxillary palpi with almost symmetrical apical segments (*H.* (*H.* s. str.) *niger* J. Sahlberg, 1880 and *H.* (*H.* s. str.) *khnzoriani* Angus, 1970) have the palpi longer and their pronota totally devoid of granules.

Description. General appearance: Fig. 1a; Head and pronotum: Fig. 1b; Underside of lateral area of pronotum: Fig. 1c. Ventral view of elytra, metaventrite and abdomen: Fig. 1d; Basal part of elytra: Fig. 1e, f.

Length: 4.3–4.4 mm; breadth: 1.9 mm. Metallic black, elytra with dark brown undertone and legs dark brown.

Head: strongly granulate, slightly shining with dark green-bronze reflection. Stem of Y-groove narrow linear, 2× wider than arms. Maxillary palpi metallic black with dark brown undertone, short, apical segment almost symmetrical oval. Antennae 9-segmented, brownish black, clubs darker.

Pronotum: widest about a fifth of the way from the anterior margin, abruptly narrowed anteriorly with the sides sinuate just behind anterior angles, but almost straight behind widest point, convergent to hind angles. Moderately arched, middle portion of internal intervals somewhat bulging, outer part of middle intervals and inner part of external intervals somewhat depressed. Granulation somewhat reduced on middle part of internal intervals, stronger on middle intervals and coarse on externals. Grooves shallow, mid groove over most of its length as wide as the diameter of 3 punctures, tapered to a point anteriorly, slightly constricted but parallel-sided in basal quarter. Floor of groove shining with a few small sparse punctures. Submedian grooves about half width of mid groove, angled outwards medially, reflexed a quarter of the way from each end. Floors shining, rugulose. Submarginals about as wide as mid groove, their sides irregular, floors rugose, shining. Marginal grooves narrow, effaced in anterior quarter. Narrow raised margins finely crenulate. Underside of pronotum with shining suprapleural area narrow at front, widest in anterior quarter, then evenly narrowed to hind angles.

Elytra: widest just behind middle, then tapered to rounded apex. Striae weakly impressed – strial punctures strong but not connected by grooves. Interstices flat with one or two rows of fine punctures, but interstices 1–3 rugose over basal quarter. Scutellary striae of 3–4 punctures, partly concealed by the rugosity. Surface of elytra with a V-shaped depression over basal quarter. Interstice 11 strongly keeled, flanks opposite the metaventrite about three quarters the width of the epipleurs.

Abdomen: ventrites black with erect pubescence. Apical margin of sternite 7 not denticulate.

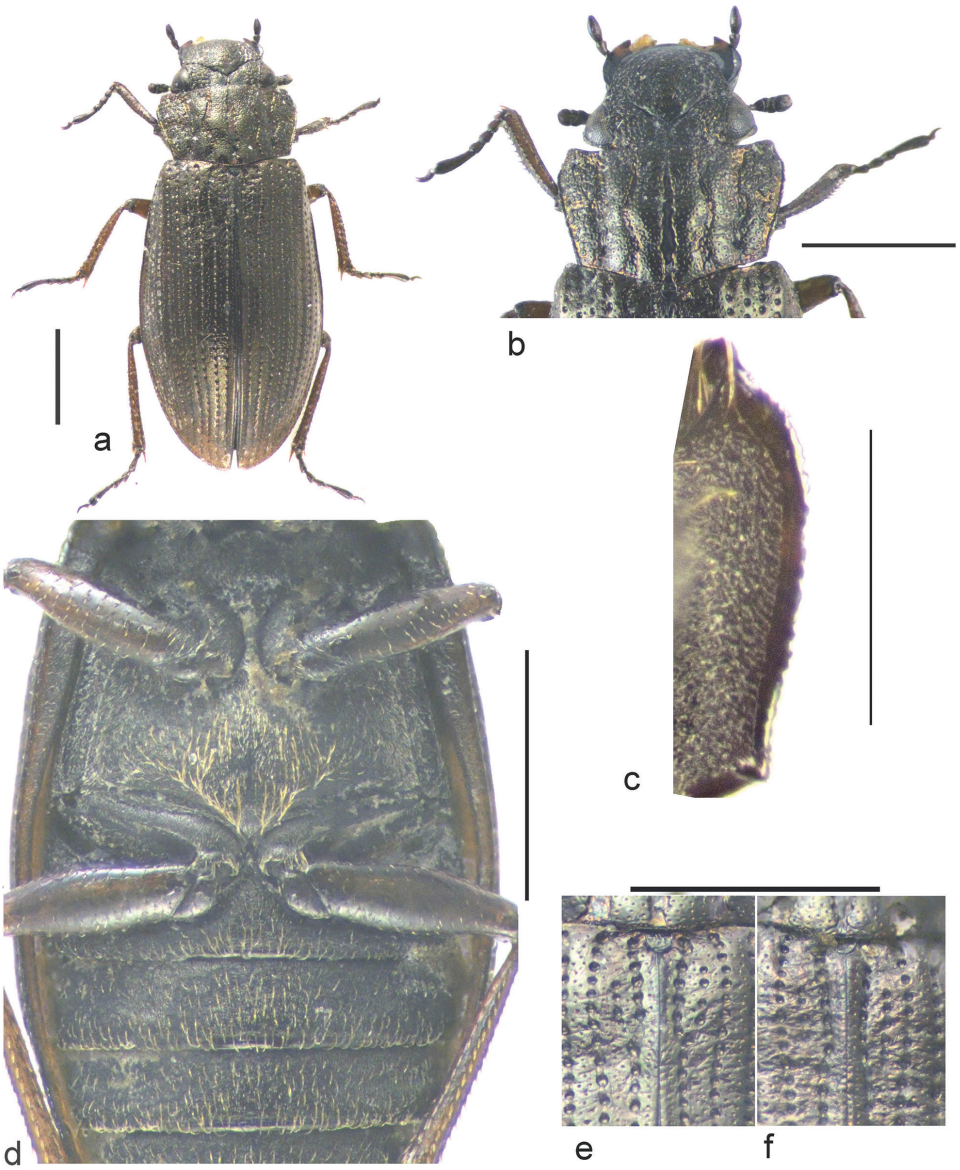

Figure 1. *Helophorus dracomontanus* sp. n. **a** holotype, dorsal **b** holotype head and pronotum, dorsal **c** paratype, lateral part of pronotum, ventral **d** paratype elytral epipleurs and flanks, metaventrite and abdomen, ventral **e, f** base of elytra and pronotum (dorsal) of holotype (**e**) and paratype (**f**) showing the scutellary striae. Scale bar: 1 mm (**a, b, d, e, f**); 0.5 mm (**c**).

Legs: dark brown, tarsi blackened apically. Rather short, tarsal hairs indistinct.

Holotype. ♀, CHINA, Sichuan. Kangding County. Yalashenshan 30°12'17.22"N 101°45'17.82"E. Small pools 4074 m a.s.l. (Fig. 2), R. B. Angus, F.-L. Jia & K. Chen. 27.vi.2016. In the Museum of Zoology, Sun Yat-sen University, Guangzhou, China (SYSU).

Figure 2. Habitat of *Helophorus dracomontanus* sp. n., Sichuan. Kangding County. Yalashenshan 30°12'17.22"N, 101°45'17.82"E. Small pools 4074 m above sea level. On the right is the driver and beside him Zhi-qiang Li. (For an account of this trip, see Angus 2017).

Paratype. ♀, data as holotype. In the Natural History Museum, London (BMNH).

Derivation of the name. *dracomontanus* – Latin, mountain dragon. The species is named after Dr Fenglong Jia. The first part of his name, Feng – phoenix, is a Chinese homophone of Feng – mountain peak. The second part, Long, is straightforward – dragon.

Discussion

Helophorus dracomontanus is placed in subgenus *Helophorus* s. str. because of its scutellary striae and elytral flanks not wider than the epipleurs. The suprapleural areas of the pronotum (pronotal epipleurs) are widest in basal quarter, distinctly narrower in front because of the sinuation of the lateral margins (Fig. 1c), and evenly narrowed to the hind angles. In this respect *H. dracomontanus* resembles the species of *Gephelophorus* Sharp, 1915. But in both of these (*H. sibiricus* Motschulsky, 1860 and *H. auriculatus* Sharp, 1884) the elytral flanks are at least as wide as the epipleurs. The metallic black maxillary palpi with almost symmetrical oval apical segments are shared by *H.* (*H.* s. str.) *niger* J. Sahlberg, 1880 and *H.* (*H.* s. str.) *khnzoriani* Angus, 1970, though the palpi are longer in these species, both of which have the pronota devoid of granulation. Neither of these

species has the lateral margins of the pronotum sinuate behind the anterior angles. Its general appearance resembles a non-tuberculate *H.* (*Kyphohelophorus*) *tuberculatus* Gyllenhal, 1808 but in *Kyphohelophorus* the elytral flanks are much wider than the epipleurs.

Shining, often metallic, black maxillary palpi are fairly unusual in *Helophorus*. *H. niger* is associated with very dark substratum (e.g. Sahlberg 1880) and *H. khnzoriani* is a high-altitude species (Angus 1970), occurring in areas which are frequently dark and unvegetated after snow-melt, and this is also true of the *H. glacialis* Villa & Villa, 1833 and other species of the *Helophorus glacialis* and *H. guttulus* Motschulsky, 1860 species groups of the former subgenus *Atractohelophorus* Kuwert, 1886 (Angus et al. 2017). Finally, *H. tuberculatus* is typically found in recently burned (and thus) black areas and is a superb charcoal-mimic (Angus 1992). It therefore seems that these dark metallic palpi are associated with adaptation to dark ground, generally at high altitude or latitude.

In the key to the world species of *Helophorus* s. str. (*Meghelophorus* Kuwert, 1886) (Angus 1970), and also in the key to the Western Palaearctic species (Angus 1992), *H. dracomontanus* would run to couplet 8 because abdominal sternite 7 lacks square-ended teeth and the head has distinct granules over most of its surface. *H. dracomontanus*, as well as *H. kozlovi* Zaitsev, 1908 (not available when the 1970 key was written) and *H. jaechi* Angus, 1995 can be accommodated by substitution of a new Couplet 8 followed by three additional ones, 8' – 8"', as follows:

8 Maxillary palpi short, metallic black, apical segment almost symmetrical oval ..... ***dracomontanus* sp. n.**

– Maxillary palpi longer, at least in part brownish or yellow, apical segment clearly asymmetrical ..... **8'**

8' Internal intervals of pronotum without granules. Elytra brown with extensive darker mottling as well as dark marks representing the sutural V-mark. Aedeagus either similar to that of *H. aequalis* (Angus, 1995, Fig. 14) or with the outer margins of the parameres more curved ..... ***kozlovi* Zaitsev, 1908**

– Internal intervals of the pronotum extensively granulate ..... **8"**

8" Conspicuously elongate beetles with relatively small pronota (Angus, 1995, figs 1, 5). Aedeagus with parameres narrow, slightly incurved apically (Angus, 1995, fig. 13) ..... ***jaechi* Angus, 1995**

– Less elongate beetles, pronotum relatively slightly larger (Angus, 1992, fig. 26 a, b) ..... **8"'** (*H. bergrothi* J. Sahlberg, 1880, *H. strandi* Angus, 1970, *H. hammondi* Angus, 1980), as from couplet 8 in the published keys

Acknowledgements

I thank Fenglong Jia for hosting my visit to China and for all his help, the Natural History Museum London and the Biology School of Sun Yat-sen University, Guangzhou for research facilities, Dandan Zhang for her help for booking hotel and flight tickets for the Kangding collection, Zhiqiang Li and Mr. Kai Chen for their help when we were working on field.

References

Angus RB (1970) A revision of the beetles of the genus *Helophorus* F. (Coleoptera: Hydrophilidae) subgenera *Orphelophorus* d'Orchymont, *Gephelophorus* Sharp and *Meghelophorus* Kuwert. Acta Zoologica Fennica 129: 1–56. [3 plates]

Angus RB (1992) Insecta Coleoptera Hydrophilidae Helophoridae. In: Schwoerbel J, Zwick P (Eds) Süßwasserfauna von Mitteleuropa Gustav Fischer Verlag, Heidelberg, Berlin, 144 pp.

Angus RB (1995) Helophoridae: The *Helophorus* species of China, with notes on the species from neighbouring areas (Coleoptera). In: Jäch MA, Ji L (Eds) Water Beetles of China 1. Wien, Zoologische-Botanische Gesellschaft in Österreich and Wiener Coleopterologenverein, 185–206.

Angus RB (2017) On and off the Plateau. Latissimus 39: 23–28.

Angus RB, Ryndevich SK, Zhang T (2017) A new species of *Helophorus* Fabricius, 1775 from the Chinese Altai, with notes on the former subgenus *Atractohelophorus* Kuwert, 1886 and selected species (Coleoptera: Helophoridae). Koleopterologische Rundschau 87: 239–252.

Kuwert AF (1886) General-Uebersicht der Helophorinen Europas und der angrenzenden Gebiete. Wiener Entomologische Zeitung 5: 221–228. https://doi.org/10.5962/bhl.part.20588

Sahlberg JR (1880) Bidrag till Nordvestra Sibiriens Insektfauna. Coleoptera. Insamlade under Expeditionerna till Obi och Jenessej 1876 och 1877. 1. Cicindellidae, Carabidae, Dytiscidae, Hydrophilidae, Gyrinidae, Dryopidae, Georyssidae, Limnichidae, Heteroceridae, Staphylinidae och Micropeplidae. Kongliga Svenska Vetenskaps-Akademiens Handlingar 17(4)[1879]: 1–115.

Sharp DS (1915) Studies in Helophorini 6. *Gephelophorus* and *Meghelophorus* Entomologist's Monthly Magazine 51: 198–204.

ZooKeys 718: 139–154 (2017)
doi: 10.3897/zookeys.718.21096
http://zookeys.pensoft.net

RESEARCH ARTICLE

A peer-reviewed open-access journal
ZooKeys
Launched to accelerate biodiversity research

New species of *Ancistrocerus* (Vespidae, Eumeninae) from the Neotropics with a checklist and key to all species south of the Rio Grande

Patrick K. Piekarski[1], James M. Carpenter[2], Barbara J. Sharanowski[1,3]

1 *Department of Biology, University of Central Florida, Orlando, FL 32816, USA* **2** *Division of Invertebrate Zoology, American Museum of Natural History, New York, NY 10024, USA* **3** *Department of Entomology, University of Manitoba, Winnipeg, MB R3T2N2, Canada*

Corresponding author: *Patrick K. Piekarski* (pkpiekarski@gmail.com)

Academic editor: *A. Köhler* | Received 20 September 2017 | Accepted 23 November 2017 | Published 4 December 2017

http://zoobank.org/738011DE-3320-47F1-8360-252F9BE7114B

Citation: Piekarski PK, Carpenter JM, Sharanowski BJ (2017) New species of *Ancistrocerus* (Vespidae, Eumeninae) from the Neotropics with a checklist and key to all species south of the Rio Grande. ZooKeys 718: 139–154. https://doi.org/10.3897/zookeys.718.21096

Abstract

A new species of potter wasp from South America, *Ancistrocerus sur* **sp. n.**, is described. A species key and checklist for all described *Ancistrocerus* that occur south of the Rio Grande are provided. New synonymy includes *Odynerus bolivianus* Brèthes = *Ancistrocerus pilosus* (de Saussure), while the subspecies *bustamente discopictus* Bequaert, *lineativentris kamloopsensis* Bequaert, *lineativentris sinopis* Bohart, *tuberculocephalus sutterianus* (de Saussure), and *pilosus ecuadorianus* Bertoni, are all sunk under their respective nominotypical taxa.

Keywords

Description, Eumeninae, morphology, taxonomy, Vespidae

Introduction

Ancistrocerus is a genus of potter wasps with a solitary lifestyle, and belongs to the subfamily Eumeninae (Vespidae). Unlike eusocial vespid wasps, mothers nest alone and rear daughters without the aid of other females, and do not provision offspring progressively throughout their larval development. Since all *Ancistrocerus* presumably mass provision their progeny, their sting is specialized to paralyze and preserve prey items (Cowan 1991). They prey upon Lepidopteran, Coleopteran and Hymenopteran larvae (Iwata 1971; Yamane 1990). *Ancistrocerus* are typically tube renters, utilizing pre-existing cavities such as borings in twigs, stems and wood, abandoned mud-dauber cells, and old burrows of ground-nesting bees and wasps to build their nest (Cowan 1991; Iwata 1971; Krombein 1979; Yamane 1990), but some species make aerial mud nests (e. g. *spilogaster* Cameron, 1905, *lutonidus* Bohart, 1974, *waldenii* Viereck, 1906; see Krombein 1979). *Ancistrocerus* occurs worldwide (except Australia), and currently 116 species (You et al. 2013), with seven occurring in the Neotropics and 22 in North America (Bequaert 1925; Carpenter and Garcete-Barrett 2003; Carpenter and Genaro 2011; Krombein 1979), have been described. Currently, 12 species have been described that can be found south of the Rio Grande.

Eumeninae phylogeny and taxonomy is not well resolved and ~65% of vespid species belong to the subfamily (Carpenter and Cumming 1985; Hermes et al. 2014; Pickett and Carpenter 2010; Vernier 1997). Recently, Eumeninae was limited to include only the tribes Eumenini and Odynerini, and is comprised of a total of 3407 described species (Bank et al. 2017; Piekarski 2017). *Ancistrocerus* belongs to the tribe Odynerini in the sense of Hermes et al. (2014), but that tribe was not supported by the large-scale phylogenomic analysis by Bank et al. (2017) and Piekarski (2017). Due to their close relationship to eusocial wasps, understanding the biology and relationships among solitary potter wasps has implications for the conception of how sociality emerged (Hunt 2007). Here we present a key and checklist for *Ancistrocerus* that occur south of the Rio Grande, and describe a new species.

Materials and methods

The specimens used in this study are deposited at the American Museum of Natural History (New York, USA). Specimens were examined under a stereomicroscope equipped with an ocular micrometer. Body length was measured from the frons to the apex of the abdomen. Photographs were taken using a Canon 7D Mark II with a Canon MP-E 65mm 1–5× Macro Photo lens. We utilized the Canon MT–24EX Macro Twin Lite for lighting, and used a custom-made diffuser to minimize hot spots. Each image is a montage of 50 layered photos that were taken using a StackShot. Photo layers were montaged using Zerene Stacker 1.04 (Zerene Systems LLC.).

Terminology follows Carpenter and Cumming (1985), and Carpenter and Garcete-Barrett (2002). Terga are referred to as T I, T II, etc.

Taxonomy

***Ancistrocerus sur* Piekarski & Carpenter, sp. n.**
http://zoobank.org/878A9495-0796-4CD6-9516-1EEDFDE34BFB

Material examined. Holotype. Female, ARGENT: Jujuy Posta Lozano 15–17 Dec 1967 C.C. Porter. Allotype. Male, BOLIVIA: Tarija, V-7 1969 C. Porter. Paratypes. 9 females, 12 males.

Diagnosis. This species can be distinguished from all other Neotropical *Ancistrocerus* using a combination of the following characters: sternum II lacking a longitudinal basomedian furrow; sternum II in lateral view strongly truncate posterior to transverse furrow (Fig. 2a); parategula broadly flattened (Fig. 3c); humeri with angular projection (Fig. 3c); T I with carina effaced dorsally (Fig. 3g); T II with punctation ending about one puncture diameter from apex (Fig. 4c); maculations reduced, on metasoma usually at most T II with a very narrow apical yellow band (Fig. 1a, b).

Description. ***Female.*** Body length 11.50–14.00 mm. **Color.** Almost entirely black; small traces of yellow may be present at apex of clypeus; small yellow dot in antennocular space, interantennal space, and upper gena; usually have thin, ferruginous band at apex of T II-VI and sterna II-VI (Fig. 1b). Tarsi ferruginous (Fig. 1a).

Head. Twelve antennal articles; 1st flagellomere ~1/3 the size of scape; pedicel ~1/2 size of 1st flagellomere; vertex with pubescence as long as distance between posterior ocelli; vertex with dense coarse punctures, much less dense than on clypeus; vertex without tubercle; clypeus about as long as wide, narrowed apically with slight concavity at tip; mandibles decussate, four teeth spaced along the edge; mandibular ridges present; antennal sockets less than 1/2 socket diameter away from clypeus; palpal formula 6:4; maxillary palpomere two about same length as palpomere three; a narrow interantennal distance, approximately the diameter of a antennal socket; ocello-occipital distance greater than the length of the ocellar triangle; cephalic foveae closely spaced, set in a slight medial depression which is delimited posteriorly by a carina; dorsal occipital carina simple and complete, without fork, running to mandible; gena most wide dorsally.

Mesosoma. Long thoracic hairs (Fig. 1a); puncture density similar throughout (except tegula and anterior pronotal face); anterior pronotal face largely impunctate, and without paired medial foveae; lateral pronotal foveae present; pronotal carina weaker on dorsum; humeral carina absent, but sharp angular projection at the humeri (Fig. 3c); pretegular carina present; epicnemial carina absent; no apparent notaulices and parapsidal furrows; tegula without large punctures, appearing smooth; tegula tapered posteriorly, reaching slightly beyond the parategula; parategula broadly flattened (Fig. 3c); axillary fossa oval, broader than long; metonotum rounded and sloped; metanotum without tubercles; propodeum without complete dorsal carinae (Fig. 3g); propodeum without shelf and sloping posteroventrally; propodeal valvula rounded, and not free posteriorly. **Wings.** Prestigma less than half length of pterostigma; marginal cell distally rounded with small appendix; both recurrent veins received by second submarginal cell; basal angle of second submarginal cell acute; second submarginal cell not petiolate. **Legs.** One midtibial spur; bifid tarsal claws.

Figure 1. *Ancistrocerus sur*, sp. n. **A** Lateral view of the holotype (female) **B** Dorsal view of the holotype.

Metasoma. Thin white or yellowish hairs on metasoma, longest on T I; T I carina effaced dorsally (Fig. 3g); width of T1 at least twice as long as wide; T1 without apical lamella; T II with very thin apical lamella; T II with punctation ending about one puncture diameter from apex (Fig. 4c); T I and T II punctation equally dense, but T II punctures slightly smaller; apices of terga not more punctate than rest of terga; bottom of basal sulcus with longitudinal ridges; sternum II in lateral view strongly truncate posterior to transverse furrow (Fig. 2a); sternum II without basomedian longitudinal sulcus; sterna with similar puncture size and density as corresponding terga.

Male. Body length 10.00–13.00 mm. **Color.** Almost entirely black; clypeus usually entirely yellow (Fig. 5b); scape may be yellow ventrally; mandible may have yellow traces; small yellow dot present on upper gena but typically absent in antennocular and interantennal space; usually have ferruginous band at apex of T II-VII and sterna II-VII (Fig. 5b). Tarsi ferruginous.

Figure 2. Lateral view of the metasoma of an **A** *Ancistrocerus sur* sp. n. male, with sternum II strongly truncate posterior to transverse furrow **B** *A. cingulatus* (Cresson) female, with sternum II convex posterior to transverse furrow **C** *A. santaanna* (de Saussure) male, with sternum II flat posterior to transverse furrow **D** Ventrolateral view of *A. tuberculocephalus* (de Saussure) female; sternum II with deep, longitudinal basomedian furrow. Frontal view of the clypeus for **E** *A. arista* (de Saussure) male with clypeus having a deep, semicircular emargination; and **F** *A. lineativentris* Cameron male with clypeus not having a deep, semicircular emargination. Dorsolateral view of vertex and pronotum of **G** *A. tuberculocephalus* (de Saussure) female, with pronotal carina present dorsolaterally and a polished tubercle posterior to ocelli; and **H** *A. lineativentris* Cameron male, with pronotal carina absent and vertex without tubercle. lbf = longitudinal basomedian furrow; tb = tubercle; dpc = dorsal pronotal carina.

Head. Identical to female, except for: 13 antennal articles; apex of antennae hooked; clypeus longer than wide, narrowed apically with slight concavity at tip; mandibles decussate, four (five on allotype) teeth spaced along the edge; cephalic foveae absent.

Mesosoma. Identical to female (Fig. 5a, b).

Metasoma. Identical to female, but 7 metasomal segments and male genitalia. T II apex in male not reflexed (cf. *A. arista* and *A. similis*).

Distribution. Argentina, Bolivia.

Etymology. The name is the Spanish word for "south," referring to its southerly distribution in the Neotropics. It is to be treated as a noun in apposition.

Figure 3. Dorsal view of mesosoma for **A** *Ancistrocerus bustamente* (de Saussure) female, with parategulae of mesonotum narrowed, and humeral angle obtuse and not projecting **B** *A. epicus* (Zavattari) female, with parategulae of mesonotum broadly flattened, and humeral angle approximately a right angle and projecting bluntly **C** *A. sur* sp. n. female, with parategulae broad and humeral angle acute and projecting sharply. Dorsoposterior view of propodeum and T I for **D** *A. bustamente* (de Saussure) female, with propodeal dorsal carina complete **E** *A. similis* (Smith) male, with propodeal dorsal carinae incomplete **F** *A. flavomarginatus* (Brèthes) female, without propodeal dorsal carina and T I with carina well developed dorsally; and **G** *A. sur* sp. n. female, without propodeal dorsal carina and tergum I with carina effaced dorsally. pt = paratregula; hum = pronotal humeri; pdc = propodeal dorsal carina; tc= T I carina.

Figure 4. Dorsal view of T II for **A** *Ancistrocerus epicus* (Zavattari) female, with punctures small and reduced apically, and ivory maculations **B** *A. similis* (Smith) male, with punctation dense apically; and **C** *A. sur* sp. n. female, with punctation less dense apically and ending about one puncture diameter from apex. Lateral view of metasoma for **D** *A. flavomarginatus* (Brèthes) female, with metasomal maculations abundant and orange-yellow; and **E** *A. pilosus* (de Saussure) female, with pale maculations and sparse after T II. Dorsal view of T I-III for **F** *A. durangoensis* Cameron female, with punctation coarse on T II and apices slightly thickened or reflexed, and pubescence consisting of long hairs **G** *A. cingulatus* (Cresson) female, with T I and II dull, with fine punctation, and T I carina sharp and thin; and (H) *A. isla* Carpenter female, with T I and II shiny with punctures superficial, and T I carina thick and blunt. tc = T I carina.

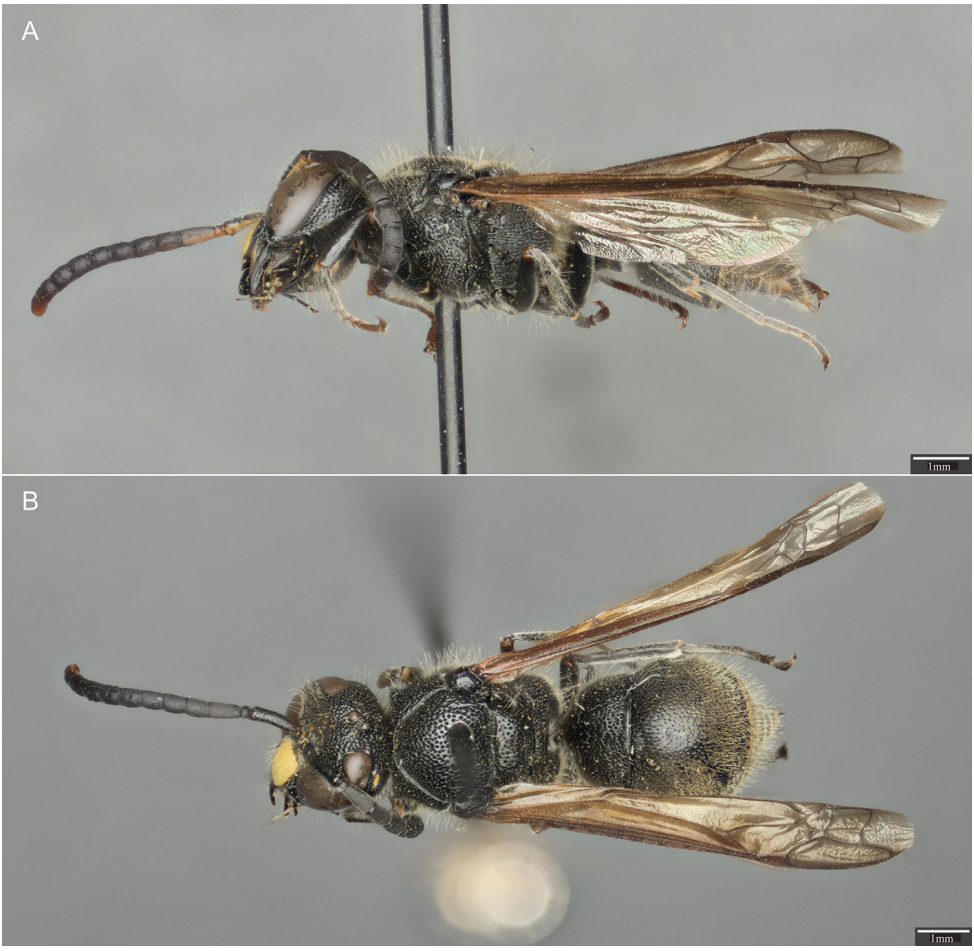

Figure 5. *Ancistrocerus sur*, sp. n. **A** Lateral view of the allotype (male) **B** Dorsal view of the allotype.

Key to the species of *Ancistrocerus* south of the Rio Grande

1 Sternum II with deep, longitudinal basomedian furrow at least one third the length of the sternum (Fig. 2d); T II usually coarsely punctate apically **2**

– Sternum II lacking longitudinal basomedian furrow, or if a shallow one is present it is less than one third the length of the sternum; T II coarsely punctate apically or not **4**

2 Pubescence on scutum fine, less than one ocellus diameter long; color gray with orange-yellow maculations; clypeus with deep, semicircular emargination (Fig. 2e) ..... ***arista*** **(de Saussure)**

– Pubescence on scutum longer than one ocellus diameter (Fig. 1a); color not gray; clypeus without deep, semicircular emargination (Fig. 2f) **3**

3 Pronotal carina present dorsolaterally (Fig. 2g); vertex with large, polished tubercle posterior to ocelli (Fig. 2g) which may be reduced in some females ..... ***berculocephalus* (de Saussure)**

– Pronotal carina absent; vertex without tubercle (Fig. 2h) ..... ***lineativentris* Cameron**

4 Sternum II in lateral view flat or slightly concave posterior to transverse furrow (Fig. 2c) ..... ***santaanna* (de Saussure)**

– Sternum II in lateral view evenly convex or strongly truncate posterior to transverse furrow..... **5**

5 Sternum II in lateral view strongly truncate posterior to transverse furrow (Fig. 2a) **6**

– Sternum II in lateral view evenly convex posterior to transverse furrow (Fig. 2b) **11**

6 Parategula narrow (Fig. 3a); propodeum with dorsal carinae (Fig. 3d); humeral angle obtuse and humeri not projecting (Fig. 3a); upper part of temple uniformly punctate; male clypeus emarginate apically, about as wide as long..... ***bustamente* (de Saussure)**

– Parategula broadly flattened (Fig. 3b, 3c); propodeum without dorsal carinae (Fig. 3e), or partially present but sublaterally incomplete; humeri with blunt (Fig. 3b) or sharp projections (Fig. 3c); upper part of gena with few large punctures beneath spot; male clypeus truncate apically, length greater than width 7

7 T II with punctation reduced apically, punctures small (Fig. 4a); humeri with blunt projections (Fig. 3b); maculations ivory-yellow..... ***epicus* (Zavattari)**

– T II with punctures as large or larger apically than rest of tergum, even if punctation is reduced; humeri with sharply angular projections (Fig. 3c); maculations pale to orange yellow..... **8**

8 T II with punctation dense apically (Fig. 4b), male with apex reflexed..... ***similis* (Smith)**

– T II with punctation less dense apically (Fig. 4c), often absent adjoining apex..... 9

9 T I with carina effaced dorsally (Fig. 3g); T II with punctation ending about one puncture diameter from apex (Fig. 4c); maculations reduced, on metasoma usually at most T II with a very narrow apical yellow band (Fig. 1b).... ***sur* Piekarski & Carpenter, sp. n.**

– T I with carina well developed dorsally (Fig. 3f); T II with punctation either extending to apex, or ending several puncture diameters before it; maculations rarely so reduced **10**

10 Maculations abundant, orange-yellow; all terga and sterna after II with bands (Fig. 4d) but no line on pronotum..... ***flavomarginatus* (Brèthes)**

– Maculations variable in extent, pale yellow (Fig. 4e) ..... ***pilosus* (de Saussure)**

11 Punctation coarse on mesosoma; T II and III with punctation dense, coarser near apices than on rest of surface, apices slightly thickened or reflexed (Fig. 4f); pubescence consisting of long hairs (Fig. 4f) (Rocky Mountains, New Mexico, Texas) ..... ***durangoensis*** **Cameron**

– Punctation fine on humeri and scutum, nearly absent on metasoma; pubescence reduced (Greater Antilles) **12**

12 T I and II dull, with fine punctation (Fig. 4g); T I carina sharp, thin (Fig. 4g) (Cuba) ..... ***cingulatus*** **(Cresson)**

– T I and II shiny (Fig. 4h), punctures superficial, appearing almost impunctate; T I with carina blunt, thick (Fig. 4h) (Puerto Rico) ..... ***isla*** **Carpenter**

Discussion

Color variability is usually a poor character to demarcate species due to large variability within and between closely related species, and because distantly related species occupying the same area share similar coloration patterns (Richards 1978). However, all described neotropical species, except *Ancistrocerus sur*, have distinct colored maculations on the mesosoma and/or metasoma. A darker gestalt is always in combination with the proposed diagnostic characters of *Ancistrocerus sur*, including sternum II strongly truncate posterior to transverse furrow, an effaced dorsal carina on tergum I and a projecting acute humeral angle. Although, the extent of coloration in the female clypeus varied, the lack of colored maculations on the mesosoma and metasoma is consistent across Bolivian and Argentine representatives. Thus, a lack of coloration on the metasoma and mesosoma is a reliable diagnostic character for *Ancistrocerus sur*.

There exists sexual dimorphism in clypeus color between males and females of *Ancistrocerus sur*, as well as presence/absence of yellow spots in the antennocular and interantennal space. Males lack a T2 with a reflexed apex, suggesting that the sexual dimorphism in this species may be less than in other *Ancistrocerus*. Typically, male vespids either have the same number of teeth as conspecific females, or fewer (Carpenter 1988b; c; Carpenter and Cumming 1985). Unusually, based on our examined material, it seems that females of *A. sur* have four mandibular teeth, while males tend to have five (some appearing to have four). Within *Ancistrocerus* there is variability as to what characters are sexually dimorphic across species. Thus, this genus may be an exceptional group for studying how traits diverge across sexes.

Checklist

Genus *Ancistrocerus* Wesmael

Ancistrocerus Wesmael, 1836, Bull. Acad. R. Belg. 3: 45, subgenus of *Odynerus* Latreille.

Type species: *Vespa parietum*, Linnaeus, 1758, by subsequent designation of Girard, 1879, Traité Élem. d'Entomol. II (2): 900.

Euancistrocerus Dalla Torre, 1904, Gen. Ins. 19: 36, name for division II of subgenus *Ancistrocerus* Wesmael of genus *Odynerus* Latreille in de Saussure, Ét. Fam. Vesp. 1: 127, 3: 209.

Type species: *Vespa parietum* Linnaeus, 1758, subsequent designation of van der Vecht and Carpenter, 1990, Zool. Verh. Leiden 260: 21.

Valid species: 116 spp.

Distr.: Ethiopian (22 spp.), Nearctic (22 spp.), Neotropical (7 spp.), Oriental (18 spp.) and Palearctic Region (57 spp.)

Diagnosis. Male antenna hooked apically; female cephalic foveae closely spaced, sometimes in slight depression, nearer occipital margin than posterior ocelli, but not in distinct area of differentiated cuticle; anterior face of pronotum without medial pits or foveae (cf. *Parancistrocerus*); pronotal carina weak or absent dorsally, but well developed laterally; pronotum without oblique humeral carina (cf. *Pachodynerus*); pretegular carina present; tegula tapered posteriorly, reaching slightly beyond the parategula; axillary fossa oval, broader than long; epicnemial carina absent; midtibia with one spur; metanotum somewhat flat, without tubercles; dorsal face of propodeum short or lacking, and sloped; propodeal concavity divided by well-developed median longitudinal carina; propodeal valvula not enlarged; metasoma sessile, not petiolate; T1 with width more than half that of T2 in dorsal view, and T1 less than twice as long as wide; T1 with single transverse carina near summit; T1 without broad longitudinal median groove posterior to carina (c.f. *Symmorphus*); sternum II with basal transverse furrow; prestigma length < one-third stigma; second recurrent vein received by second submarginal cell; second submarginal cell not petiolate.

arista (de Saussure)

Odynerus arista de Saussure, 1857, Rev. Mag. Zool. (2) 9: 274, sex not stated (in subgenus *Ancistrocerus*, division *Ancistrocerus*) – "Mexique: Cuernavaca" (Genève). Distr.: Mexico: Morelos.

bustamente (de Saussure)

Odynerus Bustamente de Saussure, 1857, Rev. Mag. Zool. (2) 9: 273, sex not stated (in subgenus *Ancistrocerus*, division *Ancistrocerus*) – "De Pérote, au Mexique" (lectotype female Genève).

Odynerus Bustamenti de Saussure, 1875, Smithson. Misc. Coll. 254: 157 (key), 172. Unjustified emendation.

Odynerus pictiventris Cameron, 1906, Trans. Am. Entomol. Soc. 39: 331, female – "New Mexico" (type depository unknown).

Ancistrocerus neocallosus Bequaert, 1944, Entomol. Amer. (N. S.) 23: 236, 239 (key), 264, fig. 3, female, male – "Arizona: Mt. Lemmon, Sa. Catalina Mts., Pima Co., 6,000 ft." (holotype female Cambridge); also from numerous other localities; and TX, KS, CO, UT, NV, CA.

Ancistrocerus neocallosus var. (or subsp.) *discopictus* Bequaert, 1944, Entomol. Amer. (N. S.) 23: 236, 268, female, male – "California: Round Valley, San Jacinto Mts., Riverside Co., 9,200 ft." (holotype female Cambridge); also from numerous other localities; and AZ. REVISED STATUS.
Distr.: U.S.A.: TX, KS, CO, UT, NV, CA, AZ, NM; Mexico: Veracruz.

Note: The subspecies *discopictus* is a minor color variant, like other cases in Eumeninae discussed by Carpenter (1988a, 2003) and Carpenter and van der Vecht (1991). In its description Bequaert (1944: 269) mentioned that both it and the nominotypical form occurred in the same locality, and were connected by transitional specimens. Bequaert stated that "It may, nevertheless, be useful to distinguish the variety by name, as it parallels similar color forms of other species of *Ancistrocerus* in the same area" but we disagree; formal nomina are a poor way to deal with continuous variation. We therefore synonymize it.

cingulatus (Cresson)

Odynerus cingulatus Cresson, 1865, Proc. Entomol. Soc. Philad. 4: 162, female – "Cuba" (coll. Gundlach, Habana).
Distr.: Cuba.

durangoensis Cameron

Ancistrocerus durangoensis Cameron, 1908, Trans. Am. Entomol. Soc. 34: 216, male – "Durango, Colorado" (Zürich).
Ancistrocerus fulvicarpus Cameron, 1908, Trans. Am. Entomol. Soc. 34: 222, female – "South-west Colorado" (Zürich).
"*Ancistrocerus behrensi* Cr." Tucker, 1909, Trans. Kans. Acad. Sci. 22: 286 – "Colorado, Buffalo." *Nomen nudum*.
Distr.: U. S. A.: OK, TX, NM, AZ, UT, CO, WY; Mexico: Chihuahua.

epicus (Zavattari)

Odynerus epicus Zavattari, 1912, Arch. Naturgesch. 78A (4): 174 (key), 191, female (in subgenus *Ancistrocerus*, division *Euancistrocerus*) – "Peru: San Paulo" (coll. Magretti, Milano; *recte*: Torino).
Distr.: Peru.

flavomarginatus (Brèthes)

Odynerus flavomarginatus Brèthes, 1906, An. Mus. Nac. Buenos Aires 13: 349, 371 (key), female (in subgenus *Ancistrocerus*) – "Brasil" (Buenos Aires, Montevideo).
Distr.: Brazil; Paraguay.

isla Carpenter

Ancistrocerus isla Carpenter, 2011, in Carpenter & Genaro, Insect. Mund. 0202: 1, 5 (key), 6, figs. 25-26, 41, female – "Puerto Rico: Mayaguez" (Washington); also from another locality.

Distr.: Puerto Rico.

lineativentris Cameron

Ancistrocerus lineativentris Cameron, 1906, Invert. Pacif. 1: 146, male – "Mountains near Claremont, California" (Pomona, no. 3949).

Ancistrocerus lineativentris var. (or subsp.) *kamloopsensis* Bequaert, 1944, Entomol. Amer. (N. S.) 23: 280, male, female – "British Columbia: Kamloops" (holotype female Cambridge); also from U. S. A.: OR, WY. REVISED STATUS.

Ancistrocerus lineativentris var. *fulvicarpus*; Bequaert, 1944, Entomol. Amer. (N. S.) 23: 236, 279 (key), 281. Misidentification.

Ancistrocerus lineativentris sinopis Bohart, 1974, in Bohart & Menke, J. Kans. Entomol. Soc. 47: 466, male, female – "Mt. Lemmon Lodge, Santa Catalina Mts., Arizona" (holotype male Davis); also from numerous other localities; and CO, TX, UT. REVISED STATUS.

Distr.: Canada: B. C.; Western U. S. A. east to SD, KS; Mexico: Chihuahua.

Note: The subspecies *kamloopsensis* and *sinopis* are both minor color variants, which are known to intergrade with the nominotypical form (Bequaert, 1944: 280), and we therefore synonymize them.

pilosus (de Saussure)

Odynerus pilosus de Saussure, 1855, Ét. Fam. Vesp. 3: 218, male (in subgenus *Ancistrocerus*) – "Le Perou" (Paris).

Ancistrocerus pilosus var. *ecuadorianus* Bertoni, 1918, An. Cient. Parag. (2) 3: 197, female – "Santa Inés, Ecuador" (San Lorenzo). REVISED STATUS.

Odynerus bolivianus Brèthes, 1920 (1919), Ann. Soc. Entomol. Fr. 88: 397, female (in subgenus *Euancistrocerus*) – "Bolivia: Beni" (Buenos Aires). NEW SYNONYMY.

Distr.: Venezuela; Colombia; Peru; Ecuador; Bolivia.

Note: One of us (JMC) has seen the types of both *pilosus* and *bolivianus*, and a specimen of *pilosus* var. *ecuadorianus* from the Bertoni collection in San Lorenzo that is probably a type. Female *pilosus* compare very well to the type female of *bolivianus* and are very similar in coloration, and we herewith synonymize these taxa. The variety *ecuadorianus* is a minor color variant, and is also synonymized.

santaanna (de Saussure)

Odynerus Santa-anna de Saussure, 1857, Rev. Mag. Zool. (2) 9: 273, female, male (in subgenus *Ancistrocerus*, division *Ancistrocerus*) – "Le Mexique" (Genève).
Odynerus Santa-annae de Saussure, 1875, Smithson. Misc. Coll. 254: 159 (key), 171. Unjustified emendation.
Distr.: Mexico: Veracruz, Jalapa, Michoacán.

similis (Smith)

Odynerus similis Smith, 1857 (April), Cat. Hym. Brit. Mus. 5: 80, female – "Mexico" (London).
Odynerus Parredes de Saussure, 1857 (June), Rev. Mag. Zool. (2) 9: 273, sex not stated (in subgenus *Ancistrocerus*, division *Ancistrocerus*) – "Le Mexique, Mextitlan" (Genève).
Odynerus Parredesi de Saussure, 1875, Smithson. Misc. Coll. 254: 158 (key), 180. Unjustified emendation.
Odynerus pilosellus Cameron, 1912, Timehri 2: 221, female – "Costa Rica" (London).
Distr.: U. S. A.; Mexico: Hidalgo, Nuevo León, Tamaulipas; Guatemala; Costa Rica; Panama.

tuberculocephalus (de Saussure)

Odynerus Tuberculocephalus de Saussure, 1852, Ét. Fam. Vesp. 1: 122 (key); 1853: 139, pl. XVI fig. 9, male, female (in subgenus *Ancistrocerus*) – "Le Mexique" (Genève?).
Odynerus tuberculiceps de Saussure, 1853, Ét. Fam. Vesp. 1: Errata and Explanation of pl. XVI fig. 9. Unjustified emendation.
Odynerus sutterianus de Saussure, 1875, Smithson. Misc. Coll. 254: 186, male, female (in subgenus *Ancistrocerus*) – "California" (Genève).
"*Odynerus nigrohirsutulus* Cameron" Bequaert, 1925, Trans. Am. Entomol. Soc. 51: 114 (label on possible type of *A.* (?) *nigro-hirsutus* Cameron; belongs in *Ancistrocerus*). *Nomen nudum*.
Ancistrocerus tuberculiceps var. *sutterianus* Bequaert, 1944, Entomol. Amer. (N. S.) 23: 236, 283 (key), 284. REVISED STATUS.
Distr.: Canada: B. C.; U. S. A.: CA, NV, UT, ID, OR, SD, WY, UT, CO, AZ, NM, TX; Mexico: Chihuahua, Hidalgo, Jalisco, Michocan, DF, Tamaulipas, Veracruz.

Note: The subspecies *sutterianus* is a minor color variant, which is known to intergrade and to co-occur with the nominotypical form (Bequaert 1944: 283), and we therefore synonymize it.

Acknowledgments

This research was supported by the University of Manitoba Graduate Fellowship to P.K.P, a NSERC CGS-M to P.K.P, and a NSERC discovery grant to B.J.S. Special thanks to Miles Zhang and Ryan Daley Ridenbaugh for training P.K.P on the imaging system.

References

Bank S, Sann M, Mayer C, Meusemann K, Donath A, Podsiadlowski L, Kozlov A, Petersen M, Krogmann L, Meier R, Rosa P, Schmitt T, Wurdack M, Liu S, Zhou X, Misof B, Peters RS, Niehuis O (2017) Transcriptome and target DNA enrichment sequence data provide new insights into the phylogeny of vespid wasps (Hymenoptera: Aculeata: Vespidae). Molecular Phylogenetics and Evolution 116: 213–226. https://doi.org/10.1016/j.ympev.2017.08.020

Bequaert J (1925) The genus *Ancistrocerus* (Hymenoptera: Vespidae) in North America, with a partial key to the species. Transactions of the American Entomological Society 51: 57–117.

Bequaert J (1944) The North American species of *Ancistrocerus*, proper (Hymenoptera, Vespidae). Entomologica Americana 23(4): 225–296.

Carpenter JM (1988a) A review of the subspecies concept in the eumenine genus *Zeta* (Hymenoptera: Vespidae). Psyche 94: 253–259. https://doi.org/10.1155/1987/82829

Carpenter JM (1988b) The phylogenetic system of the Gayellini (Hymenoptera: Vespidae; Masarinae). Psyche 95: 21–241. https://doi.org/10.1155/1988/45034

Carpenter JM (1988c) The phylogenetic system of the Stenogastrinae (Hymenoptera: Vespidae). Journal of the New York Entomological Society 96: 140–175.

Carpenter JM (2003) Return to the subspecies concept in the genus *Zeta* (Hymenoptera: Vespidae; Eumeninae). Boletín del Museo Nacional de Historia Natural del Paraguay 14(1-2): 19–24.

Carpenter JM, Cumming JM (1985) A character analysis of the North American potter wasps (Hymenoptera: Vespidae; Eumeninae). Journal of Natural History 19: 877–916. https://doi.org/10.1080/00222938500770551

Carpenter JM, Garcete–Barrett BR (2002) A key to the Neotropical genera of Eumeninae (Hymenoptera: Vespidae). Boletin del Museo Nacional de Historia Natural del Paraguay 14: 52–73.

Carpenter JM, Genaro JA (2011) Vespidae (Insecta: Hymenoptera) of Puerto Rico, West Indies. Insecta Mundi 0202: 1–35.

Carpenter JM, van der Vecht J (1991) A study of the Vespidae described by William J. Fox (Insecta: Hymenoptera), with assessment of taxonomic implications. Annals of the Carnegie Museum of Natural History 60(3): 211–241.

Cowan DP (1991) The solitary and presocial Vespidae. In: Ross KG, Matthews RW (Eds) The Social Biology of Wasps. Cornell University Press, London, 33–73.

Hermes MG, Melo GAR, Carpenter JM (2014) The higher-level phylogenetic relationships of the Eumeninae (Insecta, Hymenoptera, Vespidae), with emphasis on *Eumenes* sensu lato. Cladistics 30: 453–484. https://doi.org/10.1111/cla.12059

Hunt JH (2007) The Evolution of Social Wasps. Oxford Univ. Press, New York. https://doi.org/10.1093/acprof:oso/9780195307979.001.0001

Iwata K (1971) Evolution of Instinct. Comparative Ethology of Hymenoptera. Mono-shoten, Kanagawa-ken, 503 pp.

Krombein KV (1979) Catalog of Hymenoptera in America North of Mexico. Smithsonian Institution Press. https://doi.org/10.5962/bhl.title.5074

Pickett KM, Carpenter JM (2010) Simultaneous analysis and the origin of eusociality in the Vespidae (Insecta: Hymenoptera). Arthropod Syst Phylogeny 68: 3–33.

Piekarski PK (2017) Advanced castes at the outset of eusociality in wasps (Vespidae). MS Thesis, University of Central Florida, Orlando.

Richards OW (1978) The social wasps of the Americas excluding the Vespinae. British Museum (Natural History), London, 580 pp.

Vernier R (1997) Essai d'analyse cladistique des genres d'Eumeninae (Vespidae, Hymenoptera) représentés en Europe septentrionale, occidentale et centrale. Bulletin de la Société Neuchâteloise des Sciences Naturelles 120: 87–98.

Yamane S (1990) A revision of the Japanese Eumenidae (Hymenoptera: Vespoidea). Insecta Matsumurana (NS) 43: 1–189.

You J, Chen B, Li T-j (2013) Two new species of the genus *Ancistrocerus* Wesmael (Hymenoptera, Vespidae, Eumeninae) from China, with a key to the Oriental species. ZooKeys 303: 77–86. https://doi.org/10.3897/zookeys.303.4922